

**Importance of Sulfide, Polysulfides, and Elemental Sulfur for
Abiotic and Biotic Redox Processes in Sulfur-Metal(loid) Systems**

Dissertation

zur Erlangung des Doktorgrades der Naturwissenschaften (Dr. rer. nat.)

an der Graduiertenschule für Mathematik und Naturwissenschaften

der Universität Bayreuth

vorgelegt von

Regina Lohmayer

Bayreuth, Mai 2015

Die vorliegende Arbeit wurde in der Zeit von März 2011 bis Mai 2015 in Bayreuth am Lehrstuhl Umweltgeochemie unter Betreuung von Frau Professorin Dr. Britta Planer-Friedrich angefertigt.

Vollständiger Abdruck der von der Bayreuther Graduiertenschule für Mathematik und Naturwissenschaften (BayNAT) der Universität Bayreuth genehmigten Dissertation zur Erlangung des akademischen Grades eines Doktors der Naturwissenschaften (Dr. rer. nat.).

Dissertation eingereicht am: 26.05.2015

Zulassung durch das Leitungsgremium: 19.06.2015

Wissenschaftliches Kolloquium: 30.10.2015

Amtierender Direktor: Prof. Dr. Stephan Kümmel

Prüfungsausschuss:

Prof. Dr. Britta Planer-Friedrich (Erstgutachterin)

Prof. Dr. Ruben Kretschmar (Zweitgutachter)

Prof. Dr. Egbert Matzner (Vorsitz)

Prof. Dr. Stefan Peiffer

ACKNOWLEDGEMENTS

I would like to express my sincere thanks to all people, who supported me during my PhD.

First of all, I would like to thank Prof. Dr. Britta Planer-Friedrich for her supervisorship and her constant and intense scientific support on the work in the laboratory or in the field and on the presentation of results of my research in publications and presentations. I am especially thankful for numerous productive discussions, critical comments, and valuable suggestions.

I would like to thank Prof. Dr. Stefan Peiffer, Prof. Dr. Andreas Kappler, and all members of the DFG research group e-TraP for many valuable discussions. Thanks to Dr. Alexey Kamyshny for his helpfulness concerning questions regarding polysulfide chemistry and to Prof. Dr. Ralf Steudel and Dr. Joachim Weiss for valuable hints in the field of chromatographic analysis. My acknowledgements to Dr. Elvira Bura-Nakić for her help during sampling at Lake Rogoznica in Croatia and various instructive conversations about fundamental principles of chemistry. I would like to acknowledge the valuable scientific cooperation with all authors of the publications to which I contributed.

For laboratory assistance on the analysis by HPLC in the early phase of my PhD I would like to thank Dr. Sasan Rabieh and Dr. Sophie Fortenfant. Thanks to Prof. Dr. Andreas Kappler and his Geomicrobiology Group at the University of Tübingen for laboratory training and helpful advice in the field of microbiology. My acknowledgements to Stefan Will and Dr. Frank Thomas for support in the analysis by IC-ICP-MS.

Special thanks to all current and former members of the Environmental Geochemistry Group and especially to Sinikka Hinrichsen, Maria Ullrich, Julia Arndt, Judith Mehlhorn, Cornelia Härtig, Dr. Elke Süß, Dr. Frank Thomas, and Dr. Jörg Schaller for their helpfulness, their interest in my work, and numerous encouraging discussions. I would like to thank my supervised bachelor and master students Anja Schnell, Gloria Reithmaier, Axel Müller, and Carolin Kerl for the good cooperation.

I would like to acknowledge financial support by the State of Bavaria for a 2.5-years PhD scholarship and by the University of Bayreuth Graduate School for a travel grant to the EuCheMS conference 2014 in Istanbul.

Sincere thanks to my family and my partner for their unlimited support.

ABSTRACT

Sulfur, an ubiquitous element in the environment, occurs in different oxidation states from +6 to -2. Between the thermodynamically stable end members sulfate and sulfide, a variety of intermediate sulfur species exist, examples of which are sulfite, polythionates, thiosulfate, elemental sulfur, and polysulfides. Polysulfides are highly reducing and nucleophilic sulfur chains of the general structure S_n^{2-} ($n \geq 2$). Due to their high reactivity and instability, inorganic polysulfide analysis is challenging. Currently, the most reliable analytical approach is derivatization of inorganic polysulfides to form more stable organic polysulfanes, which can be analyzed chromatographically. Intermediate sulfur species in general and polysulfides in particular are assumed to be decisive for a variety of redox transformation processes of metal(loid)s but are only rarely analyzed.

The aim of the present study was to investigate the role of sulfide, elemental sulfur, and especially polysulfides for abiotic and biotic redox processes in sulfur-metal(loid) systems. Open questions resulting from previous investigations concerning the interaction of different sulfur species with iron, arsenic, and molybdenum were addressed with special focus on the sulfur speciation.

Elemental sulfur disproportionation is among the oldest metabolic pathways in earth's history and still raises many questions. Growth of microorganisms by elemental sulfur disproportionation was found to depend on the presence of a sulfide scavenger such as ferric iron. In the present study, growth of haloalkaliphilic bacteria by elemental sulfur disproportionation was shown for the first time and was observed both, in the presence of iron, which is in accordance to previous studies, but also in the absence of iron. This was possible due to substantial formation of polysulfides under anoxic and alkaline conditions, which decreased free sulfide concentrations in solution and consequently rendered elemental sulfur disproportionation thermodynamically favorable.

The reaction of dissolved sulfide with ferric (oxyhydr)oxides can result in the formation of thermodynamically stable pyrite, the most commonly occurring sulfide-bearing mineral. In former studies, different reaction pathways of pyrite formation were determined to occur in the aqueous phase. In the present study, polysulfides were found at the mineral surface during sulfidation of ferric (oxyhydr)oxides. Concentrations of disulfide, the dominating polysulfide species, increased with the reactivity of the iron minerals, which is also positively correlated to the kinetics of pyrite formation. Overall, it was concluded that surface-associated polysulfides play a decisive role as pyrite precursors.

The reductive dissolution of ferric (oxyhydr)oxides is crucial with regard to the release of adsorbed nutrients or contaminants. It can be mediated indirectly by sulfur-reducing bacteria. Previously, thiosulfate, elemental sulfur, or polysulfides were proposed to serve as electron shuttles between bacteria and ferric minerals. We found elemental sulfur, attached to the mineral surface, as predominant sulfur oxidation product. Besides thiosulfate, tetrathionate, sulfite, and sulfide, polysulfides could initiate the electron shuttling process but were of minor importance for the shuttling

process itself. Overall, the present study revealed a detailed insight into the role of different sulfur species during microbially mediated ferric mineral reduction.

Soluble arsenic-sulfur species are crucial for the cycling of arsenic under sulfidic conditions. In former studies, trivalent thioarsenites were found to form by the reaction of arsenite with sulfide and to rapidly oxidize to pentavalent thioarsenates. The latter were suggested to form directly by the reaction of arsenite with polysulfides. In the present study, polysulfides were found to react with arsenite to form monothioarsenate. Moreover, the higher nucleophilicity of polysulfides in comparison to sulfide seemed to accelerate the formation of higher thiolated arsenates. The formation of polysulfides and monothioarsenate was also observed in biotic systems during growth of an anaerobic haloalkaliphile, which couples arsenate reduction with sulfide oxidation. Additionally, monothioarsenate was microbially disproportionated to arsenite and polysulfides. Confirming previous suggestions, polysulfides were found to play a crucial role for thioarsenate formation.

Evidence for substantial microbial acceleration of thioarsenate transformation processes was found earlier. In the present study, monothioarsenate transformation was considerably faster in the presence of a hyperthermophile bacterium in comparison to abiotic conditions. Abiotically, monothioarsenate was determined to be desulfidized to form arsenate and sulfide, which in turn was oxidized to elemental sulfur and thiosulfate under high temperature and oxic conditions. The bacteria accelerated monothioarsenate transformation mainly by oxidizing the abiotically formed intermediate sulfur species to sulfate. In general, sulfur redox chemistry was found to be decisive for thioarsenate transformation processes.

The formation of soluble thiomolybdate species was assumed to be crucial for molybdenum burial in sediments, an important indicator for reconstructing paleoredox conditions. However, up to now there is no evidence about thiomolybdate occurrence in the environment. In the laboratory, we found that rate and extent of thiomolybdate formation increased with increasing sulfide to molybdate excess and a pH of 7 was determined to be most favorable for the nucleophilic substitution reaction. Polysulfides did not have any influence on thiomolybdate formation. We optimized ion-pair chromatographic separation of thiomolybdates for coupling to an inductively coupled plasma-mass spectrometer to be able to analyze nanomolar thiomolybdate concentrations. Using this new method, spontaneous formation of thiomolybdates could be observed in euxinic marine waters after addition of a molybdate spike. Moreover, natural occurrence of thiomolybdates was detected for the first time in sulfidic geothermal waters.

Overall, sulfide, elemental sulfur, and especially polysulfides were found to be a significant factor for a variety of abiotic and biotic transformation processes of the metal(loid)s iron, arsenic, and molybdenum. In general, sulfur speciation has a large impact on the speciation, reactivity, and mobility of the respective metal(loid)s. Extensive knowledge about the occurrence of different sulfur species and sulfur redox processes thus helps to understand the biogeochemical cycling of metal(loid)s in the environment.

ZUSAMMENFASSUNG

Schwefel ist ein Element, das ubiquitär in der Umwelt vorkommt und Oxidationsstufen zwischen +6 und -2 annehmen kann. Zwischen den thermodynamisch stabilen Endgliedern Sulfat und Sulfid gibt es eine Reihe intermediärer Schwefelspezies, wie beispielsweise Sulfit, Polythionate, Thiosulfat, elementaren Schwefel und Polysulfide. Polysulfide sind reduzierende und nukleophile Schwefelketten der Form S_n^{2-} ($n \geq 2$). Aufgrund ihrer hohen Reaktivität und Instabilität stellt die Bestimmung von Polysulfiden eine analytische Herausforderung dar. Der verlässlichste analytische Ansatz ist zum gegenwärtigen Zeitpunkt die Derivatisierung anorganischer Polysulfide zur Bildung stabilerer organischer Polysulfane, die chromatographisch analysiert werden können. Generell wird angenommen, dass intermediäre Schwefelspezies im Allgemeinen und Polysulfide im Besonderen entscheidend sind für eine Reihe von Redox- und Transformationsprozessen von Metall(oid)en. Allerdings gibt es dazu bisher kaum analytische Daten.

Das Ziel der vorliegenden Studie war, die Rolle von Sulfid, elementarem Schwefel und insbesondere Polysulfiden für abiotische und biotische Redoxprozesse in Schwefel-Metal(loid)-Systemen zu untersuchen. Offene Fragen, die aus früheren Arbeiten zur Interaktion von verschiedenen Schwefelspezies mit Eisen, Arsen und Molybdän resultierten, wurden aufgegriffen und mit besonderem Schwerpunkt auf der Schwefelspeziesuntersuchung untersucht.

Die Disproportionierung von elementarem Schwefel zählt zu den ältesten Stoffwechselwegen in der Erdgeschichte und wirft noch immer viele Fragen auf. Bislang wurde festgestellt, dass das Wachstum von Mikroorganismen durch Disproportionierung von elementarem Schwefel von der Anwesenheit eines Sulfidfängers wie Eisen abhängt. In der vorliegenden Studie wurde erstmals das Wachstum von haloalkaliphilen Bakterien durch Disproportionierung von elementarem Schwefel gezeigt und sowohl in An- als auch in Abwesenheit von Eisen beobachtet. Dies wurde durch die substantielle Bildung von Polysulfiden unter anoxischen und alkalischen Bedingungen ermöglicht, was zur Abnahme von freiem Sulfid in Lösung führte und damit die Disproportionierung von elementarem Schwefel thermodynamisch begünstigte.

Die Reaktion von gelöstem Sulfid mit Eisen(III)-(oxyhydr)oxiden kann zur Bildung von thermodynamisch stabilem Pyrit, dem am häufigsten vorkommenden sulfidhaltigen Mineral, führen. In früheren Studien wurden verschiedene Reaktionswege der Pyritbildung in der wässrigen Phase bestimmt. In der vorliegenden Arbeit wurden im Zuge der Sulfidierung von Eisen(III)-(oxyhydr)oxiden Polysulfide auf den Mineraloberflächen gefunden. Die Konzentration von Disulfid, der dominierenden Polysulfidspezies, stieg mit der Reaktivität der Eisenminerale an, die auch positiv mit der Kinetik der Pyritbildung korreliert. Insgesamt wurde der Schluss gezogen, dass Oberflächen-assoziierte Polysulfide eine entscheidende Rolle als Vorläufer von Pyrit spielen.

Die reduktive Auflösung von Eisen(III)-(oxyhydr)oxiden ist entscheidend im Hinblick auf die Freisetzung von adsorbierten Nähr- oder Schadstoffen. Der Auflösungsprozess kann indirekt durch

Schwefel-reduzierende Bakterien beeinflusst werden. In einer früheren Studie wurden Thiosulfat, elementarer Schwefel oder Polysulfide als mögliche Elektronen-Shuttles zwischen Bakterien und Eisen(III)-Mineralen vorgeschlagen. Wir fanden elementaren Schwefel an der Mineraloberfläche als dominierendes Schwefel-Oxidationsprodukt. Neben Thiosulfat, Tetrathionat, Sulfit und Sulfid konnten Polysulfide den Elektronen-Shuttle-Prozess initiieren, waren aber von geringerer Bedeutung für den Shuttle-Prozess an sich. Insgesamt gelang es, einen detaillierten Einblick in die Rolle verschiedener Schwefelspezies für die mikrobiell vermittelte Reduktion von Eisen(III)-Mineralen zu erhalten.

Lösliche Arsen-Schwefel-Spezies sind wesentlich für den Kreislauf von Arsen unter sulfidischen Bedingungen. In früheren Studien wurde die Bildung dreiwertiger Thioarsenite durch die Reaktion von Arsenit mit Sulfid und die schnelle Oxidation zu fünfwertigen Thioarsenaten beobachtet. Es wurde vermutet, dass Letztere sich auch direkt durch die Reaktion von Arsenit mit Polysulfiden bilden. In vorliegender Studie wurde beobachtet, dass Polysulfide mit Arsenit zu Monothioarsenat reagieren. Außerdem schien die im Vergleich zu Sulfid höhere Nukleophilie von Polysulfiden die Bildung höher thiolierter Arsenate zu beschleunigen. Die Bildung von Polysulfiden und Monothioarsenat wurde auch in biotischen Systemen während des Wachstums eines anaeroben haloalkaliphilen Bakteriums gefunden, das die Reduktion von Arsenat mit der Oxidation von Sulfid koppelt. Zusätzlich wurde Monothioarsenat mikrobiell zu Arsenit und Polysulfiden disproportioniert. Frühere Annahmen bestätigend, spielten Polysulfide eine entscheidende Rolle bei der Bildung von Thioarsenaten.

Nachweise für eine substanzielle mikrobielle Beschleunigung von Thioarsenat-Transformationsprozessen wurden bereits in früheren Arbeiten gefunden. In der vorliegenden Studie war die Umwandlung von Monothioarsenat in Anwesenheit eines hyperthermophilen Bakteriums deutlich schneller als unter abiotischen Bedingungen. Abiotisch fand eine Desulfidierung von Monothioarsenat zu Arsenat und Sulfid statt. Sulfid wiederum wurde bei hoher Temperatur und unter oxidischen Bedingungen zu elementarem Schwefel und Thiosulfat oxidiert. Die Bakterien beschleunigten die Umwandlung von Monothioarsenat hauptsächlich durch die Oxidation der abiotisch gebildeten intermediären Schwefelspezies zu Sulfat. Insgesamt wurde ein entscheidender Einfluss der Schwefel-Redoxchemie auf Thioarsenat-Transformationsprozesse festgestellt.

Für Thiomolybdatspezies wird angenommen, dass ihre Bildung entscheidend ist für die Ablagerung von Molybdän in Sedimenten, was als wichtiger Indikator zur Rekonstruktion von Paläoredoxbedingungen dient. Allerdings wurden Thiomolybdate bisher nicht in der Umwelt nachgewiesen. In Laborversuchen stellten wir fest, dass Rate und Ausmaß der Thiomolybdatbildung mit steigendem Sulfid zu Molybdat Überschuss anstiegen und dass ein pH-Wert von 7 am günstigsten für die nukleophile Substitutionsreaktion war. Polysulfide hatten keinen Einfluss auf die Thiomolybdatbildung. Wir optimierten die Trennung von Thiomolybdaten mittels Ionenpaar-Chromatographie zur Kopplung mit einem induktiv gekoppelten Plasma-Massenspektrometer, um nanomolare Thiomolybdat-Konzentrationen analysieren zu können. Mit dieser neuen Methode konnte

die spontane Bildung von Thiomolybdaten in euxinischen Salzwasserproben nach Zugabe eines Molybdat-Spikes beobachtet werden. Darüber hinaus wurde erstmals das natürliche Vorkommen von Thiomolybdaten in sulfidischen Geothermalwässern nachgewiesen.

Insgesamt konnte gezeigt werden, dass Sulfid, elementarer Schwefel und besonders Polysulfide eine entscheidende Rolle für eine Reihe von abiotischen und biotischen Umwandlungsprozessen der Metall(oid)e Eisen, Arsen und Molybdän spielen. Die Schwefelspezierung hat damit allgemein einen großen Einfluss auf die Speziierung, Reaktivität und Mobilität der jeweiligen Metall(oid)e. Umfassendes Wissen über das Vorkommen der verschiedenen Schwefelspezies und über Schwefel-Redoxprozesse trägt demzufolge maßgeblich zum Verständnis der biogeochemischen Kreisläufe von Metall(oid)en in der Umwelt bei.

TABLE OF CONTENTS

Acknowledgements	IV
Abstract	V
Zusammenfassung	VII
Table of Contents	X
List of Abbreviations	XII
List of Figures	XIII
Extended Summary	1
1 Introduction	1
1.1 Overview on sulfur chemistry with sulfate and sulfide as end members of the sulfur redox cycle	1
1.2 The intermediate sulfur species sulfite, polythionates, thiosulfate, and elemental sulfur	3
1.3 The intermediate sulfur species polysulfides	4
1.3.1 Properties, relevance, and speciation of polysulfides	4
1.3.2 Analysis of polysulfides	6
1.4 Interaction of inorganic reduced sulfur species with metal(loid)s	8
1.4.1 Sulfur and iron	8
1.4.2 Sulfur and arsenic	10
1.4.3 Sulfur and molybdenum	12
1.5 Objectives	14
2 Methods	15
2.1 Analysis of different sulfur species	15
2.2 Analysis of polysulfides	15
3 Results and Discussion	17
3.1 Interaction of sulfur and iron	17
3.1.1 Sulfur speciation during elemental sulfur disproportionation in the presence and absence of iron (study 1)	17

3.1.2	Role of polysulfides as pyrite precursors (study 2).....	19
3.1.3	Role of intermediate sulfur species for biogeochemical iron transformations (study 3).....	21
3.2	Interaction of sulfur and arsenic	23
3.2.1	Role of sulfide and polysulfides for thioarsenate formation in the presence and absence of haloalkaliphilic anaerobic bacteria (study 4).....	23
3.2.2	Impact of sulfur redox chemistry on thioarsenate transformation reactions in the presence and absence of aerobic hyperthermophile bacteria (study 5)	27
3.3	Interaction of sulfur and molybdenum – Formation and natural occurrence of thiomolybdates (study 6)	29
4	Conclusions	33
	References	37
	Contribution to the different studies.....	44
	Appendix – Publications	47
	Study 1: Disproportionation of elemental sulfur by haloalkaliphilic bacteria from soda lakes	48
	Study 2: Occurrence of Surface Polysulfides during the Interaction between Ferric (Hydr)Oxides and Aqueous Sulfide.....	59
	Study 3: Sulfur Species as Redox Partners and Electron Shuttles for Ferrihydrite Reduction by <i>Sulfurospirillum deleyianum</i>	78
	Study 4: Anaerobic chemolithotrophic growth of the haloalkaliphilic bacterium strain MLMS-1 by disproportionation of monothioarsenate	92
	Study 5: Chemolithotrophic growth of the aerobic hyperthermophilic bacterium <i>Thermocrinis ruber</i> OC 14/7/2 on monothioarsenate and arsenite.....	114
	Study 6: Ion-Pair Chromatography Coupled to Inductively Coupled Plasma-Mass Spectrometry (IPC-ICP-MS) as a Method for Thiomolybdate Speciation in Natural Waters	148
	(Eidesstattliche) Versicherungen und Erklärungen.....	157

LIST OF ABBREVIATIONS

HPLC	high performance liquid chromatography
IC	ion chromatography
ICP	inductively coupled plasma
IPC	ion-pair chromatography
MES	methanol-extractable sulfur
MQ-water	Milli-Q (purified and deionized water)
MS	mass spectrometry
UV	ultraviolet
Vis	visible
XANES	X-ray absorption near edge structure
XAS	X-ray absorption spectroscopy
XPS	X-ray photoelectron spectroscopy

LIST OF FIGURES

Fig. 1. Stable sulfur species in aqueous solution as a function of pH and Eh (25 °C, 1 bar total pressure, $\Sigma\{S\} = 10^{-3}$) according to Rickard and Luther (2007).	1
Fig. 2. Distribution of polysulfides as a function of pH and Eh according to Rickard and Luther (2007).	5
Fig. 3. Formation of thioarsenates in mixtures of 0.1 mM arsenite or monothioarsenate and 1 mM sulfide or ~0.5 mM sulfur in form of polysulfides, sulfide, and elemental sulfur at different pH values over time. Solutions were prepared either in MQ-water or in 0.5 M NaNO ₃ . Analysis was done by IC-ICP-MS (As(III) = arsenite, As(V) = arsenate, MonoTAs(V) = monothioarsenate, DiTAs(V) = dithioarsenate, TriTAs(V) = trithioarsenate, TetraTAs(V) = tetrathioarsenate).	25

EXTENDED SUMMARY

1 INTRODUCTION

1.1 Overview on sulfur chemistry with sulfate and sulfide as end members of the sulfur redox cycle

Sulfur, which is known since ancient times and was given the element symbol S in 1814 by J. J. Berzelius, has the atomic number 16 and belongs to the group of non-metallic chalcogens. Sulfur is ubiquitous in the environment. In the atmosphere, sulfur mainly occurs as sulfur dioxide, in volcanic or geothermal areas also as hydrogen sulfide. In the earth's crust, it is the fourteenth most abundant element. About 400 sulfur minerals exist, among which pyrite (FeS_2) and gypsum ($\text{CaSO}_4 \cdot 2\text{H}_2\text{O}$) are the two most commonly occurring sulfide- and sulfate-bearing minerals (Wedepohl, 1984). Sulfur is an essential element for living cells, as it is a component of the amino acids methionine and cysteine. Plants and microorganisms are able to form these organic compounds from inorganic sulfur species taken up from the environment. Sulfur serves as energy source for various sulfur-oxidizing or -reducing microorganisms and plays an important role for many abiotic redox processes. Sulfur occurs in different oxidation states from +6 to -2. Under ambient conditions, the thermodynamically stable aqueous sulfur species are mainly the end members sulfate (SO_4^{2-} , oxidation state +6) and sulfide (H_2S or HS^- , oxidation state -2) (Fig. 1). Countless studies were conducted about sulfate and sulfide concerning, e.g., their physical and chemical properties, environmental occurrence, analysis, biological relevance, and participation in various biotic and abiotic redox processes. In the following, only a short overview will be given for sulfate and sulfide, since the main focus will be on intermediate sulfur species and specifically polysulfides.

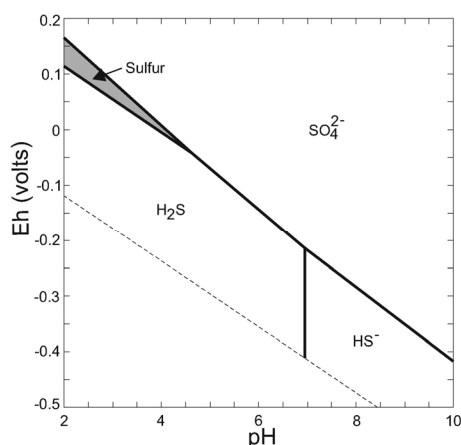


Fig. 1. Stable sulfur species in aqueous solution as a function of pH and Eh (25 °C, 1 bar total pressure, $\Sigma\{\text{S}\} = 10^{-3}$) according to Rickard and Luther (2007).

Sulfate is one of the most abundant anions in natural waters. The sulfur isotopic signature of seawater sulfate is used to reconstruct changes in the global sulfur cycle on geologic time scales (Strauss, 2004).

Due to the high symmetry of the sulfate ion, its abiotic reduction below 150 °C is extremely slow (Rickard and Luther, 2007). However, it is readily reduced by an enormous variety of sulfate-reducing bacteria. In general, microbial sulfate reduction is one major pathway in the biogeochemical sulfur cycle and closely related to the mineralization of organic matter. Sulfate-reducing bacteria are ubiquitous in anoxic environments and also occur under extreme conditions, e.g., in acid mine drainage areas or in soda lakes (Muyzer and Stams, 2008). Sulfate reduction is geochemically important because in the course of sulfate reduction, hydrogen ions are consumed, which leads to an increase in pH, and sulfide is produced, which is, e.g., important for metal attenuation (Church et al., 2007).

Free sulfide in aqueous solutions is mainly present as H_2S and HS^- with minor amounts of S^{2-} . In the following, the term “sulfide” will be used to refer to all these species for reasons of simplification. Sulfide is the end product of microbial sulfate reduction, and in the environment, only a small part of it is buried as pyrite in sediments (Berner, 1982). The largest fraction is subject to abiotic or microbial oxidation. Sulfide can be oxidized by oxygen (Chen and Morris, 1972) or, e.g., metals such as iron (Poulton et al., 2004). The reaction of sulfide with different metals and metalloids will be discussed in detail below. The strong nucleophile sulfide is toxic for many aerobic organisms due to the inhibition of specific enzymes (Nicholls and Kim, 1982). However, sulfide can be oxidized by a variety of microorganisms using, e.g., oxygen or nitrate as oxidants. A recent study concerning thermodynamics and kinetics of sulfide oxidation revealed that, with oxygen as the oxidant, microbial sulfide oxidation rates are over three orders of magnitude higher in comparison to the abiotic process (Luther et al., 2011).

Redox reactions between the end members sulfide and sulfate lead to formation of various intermediate sulfur species such as – from oxidizing to reducing – sulfite, polythionates, thiosulfate, elemental sulfur, and polysulfides. Except for elemental sulfur (oxidation state 0), which is thermodynamically stable in the low-pH range (Fig. 1), most of the intermediate sulfur species are not stable. Nevertheless, intermediate sulfur species can exist for long times due to kinetic reasons and are supposedly decisive for stepwise electron shuttling processes in the course of a variety of redox processes. Since intermediate sulfur species are less stable than sulfide or sulfate, their analysis is usually more challenging in comparison to routine analytical methods applied for sulfate or sulfide. This is the reason why intermediate sulfur species are often not measured explicitly but deficiencies in sulfur mass and redox balances are simply attributed to the occurrence of intermediate sulfur species. Hence, the aim of the present study was to elucidate the role of intermediate sulfur species and specifically polysulfides for a variety of redox processes.

In the following, chemical properties, importance, formation and transformation processes of intermediate sulfur species will be described briefly. A special focus will be laid on the chemistry and analysis of polysulfides, which will be presented in a separate section. In a further section, the

importance of different sulfur species for various abiotic and biotic redox reactions of selected metal(loid)s will be described.

1.2 The intermediate sulfur species sulfite, polythionates, thiosulfate, and elemental sulfur

Sulfite (SO_3^{2-}) with sulfur in the oxidation state +4 is a highly nucleophilic sulfur species, which occurs, e.g., during acidic decomposition of thiosulfate (Moses et al., 1984) or aqueous sulfide oxidation by oxygen (Chen and Morris, 1972). Sulfite in turn is rapidly oxidized to sulfate by oxygen. Autoxidation of sulfite can be catalyzed by different metal ions such as Cu^{2+} , Fe^{2+} , or Fe^{3+} (Roy and Trudinger, 1970). Sulfite can react with elemental sulfur, which leads to the formation of thiosulfate. Despite, or rather due to its toxic effect on cells, sulfite can be reduced or oxidized by various microorganisms (Simon and Kroneck, 2013).

Polythionates ($\text{S}_n\text{O}_6^{2-}$) are sulfur chains with a SO_3^- group at each end. Hence, the terminal sulfur atoms are in the oxidation state +5 and the inner sulfur atoms are in the oxidation state 0. Chain lengths of up to 80 sulfur atoms are possible but mainly the occurrence of tri-, tetra-, penta-, or hexathionate is observed (Druschel et al., 2003). Tetrathionate can be formed by the oxidation of thiosulfate by an oxidant such as Fe(III) or Cu(II) (Lyons and Nickless, 1968), by oxygen with the aid of a catalyst such as pyrite (Xu and Schoonen, 1995), or as an intermediate in microbial thiosulfate oxidation (Wentzien et al., 1994). Polythionates can be reduced microbially since many bacteria possess an enzyme for tetrathionate reduction (Liu et al., 2013). Moreover, a hydrolase enzyme has been found which transforms tetrathionate to sulfate, thiosulfate, and elemental sulfur (Kletzin, 2008). In the alkaline pH range, the reaction of polythionates with hydrogen sulfide results in the formation of thiosulfate and polysulfides (Klimmek et al., 1991).

Thiosulfate ($\text{S}_2\text{O}_3^{2-}$) contains two sulfur atoms in different oxidation states, which for a long time were assumed to be +6 and -2. Based on XANES spectroscopy analyses, Vairavamurthy et al. (1993) concluded that one sulfur atom is in the oxidation state +5, the other in the oxidation state -1. Thiosulfate is, e.g., formed by aqueous sulfide oxidation (Chen and Morris, 1972) or autoxidation of polysulfides (Steudel et al., 1986) and is rather stable under neutral pH conditions. In acidic or alkaline solutions, thiosulfate can be decomposed to various sulfur species such as sulfide, sulfate, sulfite, or polythionates (Roy and Trudinger, 1970). Bacteria can use thiosulfate in various ways. It can be reduced, oxidized, or disproportionated to sulfate and sulfide (Jorgensen, 1990). In general, thiosulfate is an important intermediate in the sulfur cycle both for oxidation and reduction processes.

Elemental sulfur exists in more than 30 allotropes (Meyer, 1964). The thermodynamically most stable form is cyclooctasulfur S_8 , which can be cleaved by nucleophiles such as sulfite or sulfide (Roy and Trudinger, 1970). The solubility of elemental sulfur in water is very low (19 ± 6 nM S_8) (Boulegue, 1978). Elemental sulfur can be oxidized or reduced microbially. It was found for a purple sulfur bacterium that only the polymeric, chain-like molecules of elemental sulfur and no sulfur rings were

taken up by the cells (Franz et al., 2007). Globules of water-insoluble polymeric sulfur were also found to form intra- and extracellularly in the course of microbial thiosulfate oxidation (Grimm et al., 2008). Elemental sulfur can also be disproportionated by certain microorganisms and hence is used simultaneously as electron donor and electron acceptor (Thamdrup et al., 1993). Up to now, only a small number of bacterial strains are known to grow on elemental sulfur disproportionation. The products of elemental sulfur disproportionation are sulfate and sulfide. Under standard conditions the disproportionation is endergonic unless free sulfide is removed from solution, e.g., by oxidation or precipitation (Finster, 2008).

1.3 The intermediate sulfur species polysulfides

1.3.1 Properties, relevance, and speciation of polysulfides

Inorganic polysulfides are sulfur chains of the general structure S_n^{2-} ($n \geq 2$). Therefore, the oxidation state of the individual sulfur atoms lies between -2 of sulfide and 0 of elemental sulfur. Formally, the structure of polysulfides can also be written as $(S_{n-1}^0 S^{II})^{2-}$, which means that one sulfur atom is in the oxidation state -2 and (n-1) sulfur atoms are in the oxidation state 0 (Kamyshny et al., 2004). In his review about the chemistry of organic polysulfanes, Steudel (2002) emphasizes that the term polysulfides should only be used for ionic compounds and that covalent compounds of the structure $X-S_n-X$ are named depending on the identity of X; e.g., $H-S_n-H$ are called (poly)sulfanes and $CH_3-S_n-CH_3$ are called dimethylpolysulfanes.

Polysulfides form by the reaction of sulfide with elemental sulfur (Hartler et al., 1967), are highly reducing and nucleophilic. The degree of nucleophilicity increases with increasing chain length (LaLonde et al., 1987). In solution, polysulfides are rapidly oxidized by oxygen to form elemental sulfur and thiosulfate (Steudel et al., 1986). Disproportionation of polysulfides in the course of a change of pH was found to occur in the time span of 10 s, which means that equilibrium conditions in aqueous polysulfide solutions are reached very fast (Kamyshny et al., 2003).

Polysulfides are of industrial and technical use. They are important electron shuttles in lithium-sulfur batteries (Hofmann et al., 2014), help to increase pulp yields (Li et al., 1998), or are used as electrolytes in solar cells (Jovanovski et al., 2011).

Polysulfides play an important role for numerous environmental processes. They occur as intermediates during aqueous sulfide oxidation (Chen and Morris, 1972; Kamyshny et al., 2006; Steudel, 1996). They were found in an oxygen rich freshwater lake as precursors of volatile sulfur compounds (Gun et al., 2000) and in a meromictic salt lake as important intermediates in the sulfur cycle (Overmann et al., 1996). Polysulfides can also be used by various microorganisms. The fact that polysulfides contain zero-valent sulfur in a water soluble state is of significant importance in this context. In fact, a specific bacterial enzyme for polysulfide reduction could be identified (Jormakka et al., 2008). Bacteria were found to use polysulfides as electron acceptors and polysulfides were

supposed to be intermediates during microbial growth on elemental sulfur (Klimmek et al., 1991). Disulfide can be microbially disproportionated to sulfate and sulfide and in this context plays an important role in marine methane oxidation (Milucka et al., 2012).

The concentration and chain length of polysulfide species in solution depend on many different parameters, such as pH, elemental sulfur concentration, redox potential, and temperature. In general, the maximum polysulfide concentration in solution increases with increasing pH (Schauder and Müller, 1993). Below pH 6, elemental sulfur precipitates from polysulfide solutions (Steudel, 2003). According to titration experiments, penta- or hexasulfide were determined as dominating species below pH 12, tetrasulfide above pH 12, and tri- and disulfide were assumed to be stable at pH 13 or 14 (Schwarzenbach and Fischer, 1960). Giggenbach (1972) measured optical absorption spectra in solutions from pH 6.8 to 17.5 and identified di-, tri-, tetra-, and pentasulfide. In his experiments, the polysulfide chain length also decreased with increasing pH.

In sulfide solutions saturated with elemental sulfur, Teder (1971) determined an increase of polysulfide chain length with pH and an average length of 5.4. Furthermore, Cloke (1963) determined tetra- and pentasulfide as dominating species in solutions with high sulfur concentrations. For sulfur over-saturated solutions, Kamyshny et al. (2004) showed that pentasulfide is the dominating polysulfide species above pH 7 and HS_2^- is dominating below pH 7. Rickard and Luther (2007) adapted the data from Kamyshny et al. (2004) and presented a pH-Eh diagram without rhombic sulfur and stable sulfide species (Fig. 2). This diagram shows clearly that H_2S_2 , HS_2^- , and S_2^{2-} are the dominating species over a wide pH-Eh range. Rickard and Luther (2007) emphasize that at the redox boundary between SO_4^{2-} and S(-II) from pH 5 to 9, which is relevant for many environmental systems, S_8^{2-} , S_6^{2-} , and HS_2^- are dominating.

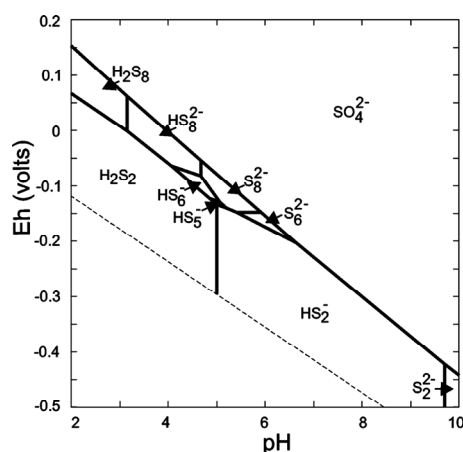


Fig. 2. Distribution of polysulfides as a function of pH and Eh according to Rickard and Luther (2007).

According to calculations concerning polysulfane (H_2S_n), hydropolysulfide (HS_n^-), and polysulfide (S_n^{2-}) speciation as a function of the total amount of dissolved reduced sulfur species at pH 8,

pentasulfur species dominate at saturated conditions, whereas with decreasing sulfur concentrations the relative contribution of disulfur species increases until reaching 100 % (Gun et al., 2000).

Moreover, temperature was found to have a significant influence on polysulfide speciation in solution. In general, polysulfide concentration was found to increase with increasing temperature (Kamyshny et al., 2007; Schauder and Müller, 1993). Teder (1971) already determined an increase of polysulfide average chain length by 0.6 from 5.4 at 25 °C to 6.0 at 80 °C. Kamyshny et al. (2007) also determined an increase of polysulfide chain length with increasing temperature, which in turn was dependent on pH. At pH 8.2, the increase of temperature from 25 °C to 80 °C led to a chain length increase by 0.25 sulfur atoms, above pH 10, chain length increased by 0.2.

1.3.2 Analysis of polysulfides

Since the first observations of polysulfides by Carl Wilhelm Scheele in the 18th century (Scheele, 1777), many different attempts were made for their analytical determination. The instability and high reactivity of polysulfides is challenging for any kind of analytical method. For quantification of total amounts and polysulfide speciation, a variety of methods such as measurement of UV-Vis spectra (Chen and Morris, 1972; Schwarzenbach and Fischer, 1960), electrochemical methods such as polarography (Kariuki et al., 2001; Umiker et al., 2002) and cyclic or linear sweep voltammetry (Rozan et al., 2000), or ion-pair chromatography (Studel et al., 1989) were applied. In particular, the different attempts to determine individual polysulfide species had to struggle with various problems. This can explain the fact that for a long time, the maximum chain length of polysulfides was subject of controversial debates. Based on the deconvolution of absorption spectra, Giggenbach (1972) concluded that the maximum length of polysulfide chains is given by 5 sulfur atoms. However, pure polysulfide standards do not exist, which makes it impossible to obtain pure spectra of the individual species. Moreover, absorption spectra were concluded to get more and more similar with increasing polysulfide chain length (Kamyshny et al., 2004). The attempt to separate a polysulfide mixture by anion-exchange chromatography was found to lead to dissociation of polysulfides in sulfide and elemental sulfur (Uddin et al., 1987). By ion-pair chromatography under alkaline conditions, a semi-quantitative analysis of a polysulfide mixture could be achieved, where the separation of the individual species was not possible (Studel et al., 1989). Detection of different polysulfide species was possible by electrospray ionization-mass spectrometry, but a lack of reference material made quantification difficult and long chain polysulfides were assumed to be overestimated (Gun et al., 2004). However, qualitative evidence for the existence of polysulfides up to a chain length of 8 or 9 sulfur atoms could be achieved. Based on considerations concerning the dissolution of elemental sulfur in sulfide or polysulfide solutions, Studel (2003) predicted the occurrence of polysulfide chains of 9 or even 10 sulfur atoms. In general, the high reactivity of polysulfides presents a serious challenge for any analytical method.

In an attempt to stabilize the highly reactive polysulfides for analysis, different derivatization techniques were tested. Their aim is to convert labile inorganic polysulfides into more stable organic polysulfanes. Due to the high reactivity of polysulfides, it is essential that the derivatization is faster than any change of speciation. The predominant yield of disubstituted disulfides after derivatization with pentafluorophenyl bromide (Kage et al., 1991) is according to Kamyshny et al. (2004) a clear indication of disintegration of long chain polysulfides during the derivatization process. The derivatization with methyl iodide can lead to an overestimation of polysulfides because polysulfides were found to form during the methylation process (Goifman et al., 2004). Moreover, this analytical method also seems to be biased as mainly short chain polysulfides were found (Kamyshny et al., 2006).

The currently most reliable method for derivatization and analysis of polysulfides was published by Kamyshny et al. (2004) and Kamyshny et al. (2006). Derivatization is done by addition of methyl trifluoromethanesulfonate (methyl triflate). In order to accelerate the rate determining step of the phase transfer of the hydrophobic methyl triflate to the aqueous solution, the derivatization is carried out in a water-methanol mixture, which would as such lead to a disproportionation of polysulfides. The same effect can be attributed to the hydrolysis of methyl triflate, which leads to a decrease of pH. Hence, to avoid a change of species distribution by derivatization, methylation has to be much faster than disproportionation reactions. This issue was investigated by performing kinetic and isotope dilution tests, which showed 95 to 97 % species preservation during derivatization. Polysulfides with chain lengths from 2 to 8 sulfur atoms could be quantified by analysis with high performance liquid chromatography coupled to UV detection (HPLC-UV). However, the method was not validated for disulfide. This was mostly ascribed to the fact that disulfide starts to protonate below pH 10. Hydrodisulfide, which is the dominant form below pH 9.6, is less nucleophilic than disulfide and therefore, the methylation rate is slower.

Disproportionation of derivatized polysulfides was found to decrease with decreasing pH, which implies that sample acidification by methyl triflate hydrolysis contributes to the stabilization of dimethylpolysulfanes. Over 12 h, no change in speciation of dimethylpolysulfanes stored at 4 °C was observed (Kamyshny et al., 2004). Commercial standards are only available for dimethyldisulfide and dimethyltrisulfide. Kamyshny et al. (2004) used synthesized reference material for the quantification from dimethyldisulfide to dimethylheptasulfide. For calibration of dimethyloctasulfide, the correlation between molar absorptivity and chain length was used. The reference material was prepared according to Rizkov et al. (2004), who synthesized a dimethylpolysulfane mixture and separated it by preparative chromatography by elution with acetonitrile and formic acid. In this solvent, the fractions containing the individual dimethylpolysulfanes were stable for 3 weeks under storage at 5 °C. The identification from dimethyldisulfane to dimethyloctasulfane was based on nuclear magnetic resonance spectroscopy and the correlation of the number of sulfur atoms in dimethylpolysulfane molecules with the chromatographic retention time.

In general, derivatization of polysulfides by methyl triflate, analysis of derivatized polysulfides by HPLC-UV, and quantification based on synthesized dimethylpolysulfane reference material were reported to be suitable for analysis of polysulfides in natural samples.

1.4 Interaction of inorganic reduced sulfur species with metal(loid)s

The general aim of the present study was to elucidate the importance of sulfide, polysulfides, and elemental sulfur for abiotic and biotic redox processes in sulfur-metal(loid) systems. Especially polysulfides are assumed to be decisive for a variety of processes, but are only rarely analyzed. To investigate the supposedly important role of polysulfides in detail, the three elements iron, arsenic, and molybdenum were chosen, for which diverse interactions with sulfur are known. Within 6 studies, still open questions resulting from previous investigations concerning different sulfur-metal(loid) interactions were addressed. The topics were widely spread and covered different pH, redox, and temperature conditions, sulfur-saturated and sulfur-limited environments, biotic and abiotic systems, and speciation in the aqueous phase and associated to the solid phase. As the main interest was to investigate the interaction of sulfur with the selected metal(loid)s iron, arsenic, and molybdenum, they determine the overall structure of the present thesis and divide it in three major parts with subsections for the 6 research questions that were addressed.

1.4.1 Sulfur and iron

The transition metal iron is the fourth most abundant element in the earth's crust and exists in oxidation states from -2 to +6. In the environment, iron occurs mainly as poorly soluble ferric iron in the oxidation state +3 or as readily soluble ferrous iron in the oxidation state +2. Numerous minerals exist which contain ferrous, ferric, or a mixture of ferrous and ferric iron. One group of iron minerals are ferric (oxyhydr)oxides, representatives of which are ferrihydrite, lepidocrocite, or goethite. Iron is essential for almost all living organisms as it is involved in various important metabolic processes. Iron redox transformations can proceed abiotically or be mediated or accelerated by a variety of microorganisms and play a crucial role for biogeochemical cycles of other elements, such as carbon, oxygen, nitrogen, and sulfur (Melton et al., 2014).

1.4.1.1 Sulfur speciation during microbial elemental sulfur disproportionation

In particular at the oxic-anoxic interface, iron was shown to catalyze sulfide oxidation to elemental sulfur (Ma et al., 2006). The presence of ferrihydrite was also found to enable growth of certain bacteria by elemental sulfur disproportionation (Finster et al., 1998). Elemental sulfur disproportionation might be among the oldest metabolic pathways in earth's history (Finster, 2008). However, up to now only few bacterial strains are known to be able to grow on elemental sulfur disproportionation and exact reaction mechanisms remain to be elucidated. Since elemental sulfur disproportionation is an endergonic process under standard conditions, it requires the presence of a

sulfide scavenger to reduce concentrations of free sulfide in solution and hence render the reaction thermodynamically favorable. Under neutral conditions, growth of microorganisms by elemental sulfur disproportionation was only observed in the presence of metals such as iron or manganese (Thamdrup et al., 1993). The reaction products of elemental sulfur disproportionation are sulfide and sulfate. Hence, especially under alkaline conditions the formation of polysulfides from elemental sulfur and sulfide can be expected and consequently might influence the thermodynamics of the process. However, up to now microbial elemental sulfur disproportionation under alkaline conditions was not yet investigated and the question whether metal sulfide scavengers are also necessary under alkaline conditions is still open. These questions were addressed in study 1.

1.4.1.2 Role of polysulfides as pyrite precursors

In the environment, the occurrence of ferric (oxyhydr)oxides is extremely important because they offer adsorption sites for toxic trace elements such as arsenic (Bennett and Dudas, 2003) or nutrients such as phosphorus (Wang et al., 2013). Consequently, the reduction and dissolution of ferric (oxyhydr)oxides lead to the release of adsorbed substances. One element especially important in this context is sulfur. The reaction with sulfide causes reductive dissolution of ferric (oxyhydr)oxides (Afonso and Stumm, 1992). However, the reaction mechanisms, the kind of oxidized sulfur species, and the distribution of iron and sulfur species between the solid and aqueous phase were found to vary greatly (Peiffer and Gade, 2007; Poulton, 2003; Saalfield and Bostick, 2009).

In the course of ferric (oxyhydr)oxide reduction under sulfidic conditions, the generated ferrous iron can react to form iron sulfides. A variety of also metastable iron sulfide phases exists. Pyrite (FeS_2) is the thermodynamically stable and most commonly occurring iron sulfide mineral. The yearly pyrite production in the oceans comes to 5 million tons (Rickard and Luther, 2007). However, pyrite formation is often prevented because of kinetic reasons. Different reaction mechanisms for pyrite formation were established over many years of research and are summarized by Rickard and Luther (2007). These mechanisms include pyrite nucleation and crystal growth as well as the reaction of ferrous monosulfides (FeS) with sulfide or polysulfides in the aqueous phase. Based on recent experiments concerning the sulfidation of lepidocrocite, polysulfides were proposed to play a crucial role not in the aqueous phase but as surface-bound sulfur species in the process of pyrite formation (Hellige et al., 2012). However, up to now analytical evidence for the occurrence of polysulfides on iron mineral surfaces is missing and the role of polysulfides in the course of pyrite formation remains to be elucidated. These questions were addressed in study 2.

1.4.1.3 Intermediate sulfur species as electron shuttles

The ferric mineral dissolution can also be influenced indirectly by sulfur-reducing microorganisms, which are not able to reduce ferric iron itself but can use oxidized sulfur species as electron acceptors and hence are responsible for the formation of sulfide. In experiments with thiosulfate, the sulfur-reducing bacterium *Sulfurospirillum deleyianum*, and ferrihydrite, sulfur was found to shuttle electrons

between the bacteria and the iron mineral and seemed to be recycled up to 60 times (Straub and Schink, 2004). As the bacteria cannot use sulfate as electron acceptor, thiosulfate, elemental sulfur, or polysulfides were proposed as reoxidized sulfur species to complete the electron shuttling process. The iron reduction process was also found to proceed when the iron mineral and the bacteria were spatially separated. Hence, it was concluded that the sulfur species had to be present in the aqueous phase. However, sulfur species were not determined in this study. Therefore, at the moment it can only be speculated about the supposedly decisive role of intermediate sulfur species for the process of microbially mediated ferric (oxyhydr)oxide dissolution. These questions were addressed in study 3.

In general, intermediate sulfur species and especially polysulfides are assumed to be key reactants for various iron redox processes. There, they are proposed to be important both in the aqueous phase and associated to the solid phase. However, details concerning polysulfide occurrence in the process of ferric (oxyhydr)oxide reduction and pyrite formation remain to be elucidated.

1.4.2 Sulfur and arsenic

The toxic metalloid arsenic exists in the four oxidation states -3, 0, +3, and +5. In aqueous environments, arsenic is mainly present as oxyanions of trivalent arsenite ($\text{H}_x\text{As}^{\text{III}}\text{O}_3^{x-3}$, $x=1-3$) or pentavalent arsenate ($\text{H}_x\text{As}^{\text{V}}\text{O}_4^{x-3}$, $x=1-3$) (Cullen and Reimer, 1989). Arsenic has a high affinity for sulfur. Over the last 150 years, numerous studies concerning precipitation of arsenic sulfur minerals, formation, synthesis, and stability of soluble thioarsenic species were conducted (Brauner and Tomíček, 1887; McCay, 1888; McCay and Foster, 1904; Schwedt and Rieckhoff, 1996; Thilo et al., 1970).

1.4.2.1 Role of sulfide and polysulfides for abiotic thioarsenate formation

With the development and application of highly sophisticated analytical methods especially since the 1990s, a controversial debate began about the identification of soluble thioarsenic species as trivalent thioarsenites ($\text{H}_x\text{As}^{\text{III}}\text{S}_n\text{O}_{3-n}^{x-3}$, with $n=1-3$ and $x=1-3$) or pentavalent thioarsenates ($\text{H}_x\text{As}^{\text{V}}\text{S}_n\text{O}_{4-n}^{x-3}$, with $n=1-4$ and $x=1-3$). A method for determination of thioarsenic species at low concentrations is ion chromatography (IC) coupled to inductively coupled plasma-mass spectrometry (ICP-MS). As the occurrence of thioarsenic species was observed in mixtures of arsenite and sulfide under reducing conditions, they were identified as thioarsenites in an initial study (Wilkin et al., 2003). In the course of later investigations, this conclusion was proven to be wrong and the respective thioarsenic species were identified as thioarsenates (Stauder et al., 2005; Wallschläger and Stadey, 2007). In highly concentrated solutions, thioarsenates could be structurally characterized by X-ray absorption spectroscopy (XAS) and differentiated from thioarsenites (Suess et al., 2009). Furthermore, it could be shown by XAS that thioarsenites are formed by the reaction of arsenite and sulfide under completely anoxic conditions (Planer-Friedrich et al., 2010). Planer-Friedrich et al. (2010) discussed the seemingly contradictory results of thioarsenite determination by XAS and thioarsenate determination by IC-ICP-MS. This discrepancy could be explained by the chemical properties of thioarsenites.

Thioarsenites are extremely sensitive towards pH changes and changes of the ratio of OH^- and SH^- in solution. Consequently, alkaline elution in the course of IC-ICP-MS analyses leads to transformation of thioarsenites to arsenite. Moreover, the exposure of capped sample vials to atmospheric oxygen on an IC autosampler results in immediate oxidation of thioarsenites to thioarsenates. To date, the occurrence of thioarsenites can only be proven by XAS.

The observation of oxidation of thioarsenites to thioarsenates is important for the discussion concerning thioarsenate formation pathways. It shows that thioarsenites are intermediates in the process of thioarsenate formation and contradicts Helz and Tossell (2008), who assumed that thioarsenates are formed exclusively by ligand exchange of SH^- versus OH^- starting from arsenate. At pH 4, monothioarsenate was found to form in a solution containing arsenate and sulfide (Rochette et al., 2000). Another way of thioarsenate formation is the reaction of elemental sulfur with arsenite under alkaline conditions (Schwedt and Rieckhoff, 1996). However, the exact pathways of thioarsenate formation remain to be clarified also with special focus on the role of different sulfur species.

In contrast to thioarsenites, thioarsenates are stable under alkaline conditions. Indeed, tetrathioarsenate is only stable at pH 13, tri- and dithioarsenate start to decompose to arsenite below pH 7 and pH 5, respectively, and monothioarsenate is stable from pH 1 to 13 (Planer-Friedrich and Wallschläger, 2009). Monothioarsenate stability is also not influenced by aeration, while trithioarsenate was found to transform partially to arsenite (Planer-Friedrich et al., 2009). This oxidative transformation of trithioarsenate was found to be highly influenced by sulfur redox chemistry, as the formation of thiosulfate and a loss of sulfur from solution were observed. This sulfur loss was assumed to be due to volatilization of H_2S or the formation of colloidal elemental sulfur or polysulfides.

For natural samples, analysis by XAS is not possible as arsenic concentrations in the millimolar range are required. Therefore, the only way of analyzing natural samples is by using IC-ICP-MS. For completely anoxic systems, the report of thioarsenates by IC-ICP-MS might be an analytical artifact. For all systems with trace levels of oxygen, thioarsenites are immediately oxidized to thioarsenates and then determined correctly as naturally occurring arsenic species.

1.4.2.2 Role of sulfide and polysulfides for thioarsenate formation in the presence of haloalkaliphilic anaerobic bacteria

An example of an environment, where microbially driven redox processes of arsenic and sulfur were found, is the alkaline, hypersaline Mono Lake in California, USA. During periods of stratification, thioarsenic species were found to dominate arsenic speciation in sulfidic waters (Hollibaugh et al., 2005). In experiments with enrichment cultures, arsenite oxidation was found to be accelerated by addition of the strong reductant sulfide (Fisher et al., 2008). The formation of thioarsenic species was detected and was attributed to the reaction of arsenite with, e.g., polysulfides, as possible products of microbial sulfide oxidation. It was assumed that microorganisms can also oxidize sulfur bound to

arsenic. Hence, direct or indirect microbial transformation of arsenite and thioarsenates to arsenate may be possible. However, analytical data concerning the supposedly important role of polysulfides for thioarsenate formation are missing until now. These questions were addressed in study 4.

1.4.2.3 Impact of sulfur redox chemistry on thioarsenate transformation reactions in the presence and absence of aerobic hyperthermophile bacteria

Thioarsenates were also detected in geothermal hot springs of Yellowstone National Park. There, they were found over a pH range from 2.1 to 9.3 and as dominating arsenic species under alkaline conditions (Planer-Friedrich et al., 2007). Formation and transformation of arsenic species in Yellowstone National Park are highly influenced by microbial activity. The transformation of trithioarsenate was found to be microbially accelerated 40 to 500 times in comparison to the abiotic process (Planer-Friedrich et al., 2009). On-site incubation experiments with filamentous microbial mats at a geothermal hot spring revealed different possible thioarsenate transformation pathways (Härtig and Planer-Friedrich, 2012). Abiotic thioarsenate transformation processes can be triggered indirectly by microorganisms by oxidation or reduction of abiotic reaction products. Another possibility is direct microbial transformation of arsenic and sulfur contained in thioarsenates. For all transformation processes, also intermediate sulfur species such as thiosulfate or elemental sulfur as sulfide oxidation products are supposed to play a key role but were not measured in detail up to now. These questions were addressed in study 5.

In summary, the redox chemistry of arsenic and sulfur are closely linked together. Abiotic and biotic conversion of sulfur species is of extreme importance for formation and transformation of soluble thioarsenic species. In these processes, a special role is also attributed to intermediate sulfur species such as polysulfides. However, details of the related reaction pathways remain to be elucidated.

1.4.3 Sulfur and molybdenum

The transition metal molybdenum exists in oxidation states from -2 to +6, with +4 and +6 being most stable. Molybdenum is part of a variety of minerals, such as wulfenite (PbMoO_4) or molybdenite (MoS_2). Molybdenum is essential for life because it is a component of numerous enzymes and cofactors (Schwarz et al., 2009) and therefore, e.g., required for bacterial nitrogen fixation (Williams and da Silva, 2002). Molybdenum has 35 isotopes, 7 of which are naturally occurring, and has a high affinity for forming compounds with oxygen and sulfur. Under oxic conditions, dissolved molybdenum is mainly present as the highly stable and inert molybdate anion ($\text{Mo}^{\text{VI}}\text{O}_4^{2-}$). In sea water, molybdenum concentrations are around 100 nM (Collier, 1985), in rivers around 10 nM, and in lakes and wetlands variations from picomoles to hundreds of nanomoles are possible (Pizarro et al., 2014).

1.4.3.1 Formation of thiomolybdates from molybdate and sulfide or polysulfides

Under sulfidic conditions, precipitation of molybdenum leads to an enrichment in sediments. Hence, accumulation of molybdenum provides important information about paleoredox conditions (Crusius et

al., 1996). A decisive step for molybdenum deposition is supposed to be the reaction of molybdate with aqueous sulfide to form thiomolybdates ($\text{Mo}^{\text{VI}}\text{O}_{4-x}\text{S}_x^{2-}$, with $x = 1-4$). In synthetic solutions of molybdate and sulfide, thiomolybdates were found to form without oxidation state changes by a stepwise ligand exchange of sulfur versus oxygen groups (Erickson and Helz, 2000). Reaction kinetics was found to decrease with each sulfidation step and tetrathiomolybdate was determined as the thermodynamically stable end product. Thiomolybdate formation was described as an acid-catalyzed process and pH 7.3 was determined to be most favorable for the nucleophilic attack by HS^- (Harmer and Sykes, 1980). Thiomolybdates were assumed to be stable under alkaline conditions (Weiss et al., 1988). Under acidic conditions, the precipitation of amorphous molybdenum trisulfide was observed (Wildervanck and Jellinek, 1964). For natural systems, different theories exist concerning the processes which lead from thiomolybdate formation to molybdenum burial. One scenario includes the reaction of elemental sulfur with trithiomolybdate, subsequent reduction of molybdenum, and formation of highly reactive molybdenum-polysulfide compounds, which are scavenged from the aqueous phase (Dahl et al., 2013; Vorlicek et al., 2004). For Lake Rogoznica, a stratified sea water lake in Croatia, the precipitation of an iron-molybdenum-sulfur mineral was postulated to explain molybdenum scavenging after thiomolybdate formation (Helz et al., 2011). In the course of this study, aqueous molybdenum speciation was also predicted by modeling and revealed a predominance of tetrathiomolybdate as thermodynamically stable species in euxinic bottom waters. Thiomolybdates also were predicted to occur in geothermal waters of Iceland (Kaasalainen and Stefansson, 2012).

1.4.3.2 Analysis of thiomolybdates

Although thiomolybdates are supposed to play an important role for different geochemical processes, they have never been determined in natural samples. This can be explained by the fact that no analytical method, which is sensitive enough to measure nanomolar thiomolybdenum concentrations, is available at the moment. One possibility is to determine thiomolybdates by UV-Vis spectroscopy (Müller et al., 1969; Reid et al., 2007). However, this method is unsuitable for determining nanomolar concentrations in natural samples due to low sensitivity, overlapping spectra, and possible interferences of matrix components. Another possibility for thiomolybdate determination is ion-pair chromatographic (IPC) separation with acetonitrile eluent and suppressed conductivity or UV detection (Weiss et al., 1988). Again, the method is not sufficiently sensitive for the analysis of natural samples. A highly sensitive detection method for determination of trace levels of elements is ICP-MS. However, the published chromatographic method for thiomolybdate separation cannot just be coupled to ICP-MS detection because the acetonitrile eluent concentrations would extinguish the ICP plasma. Hence, the prerequisite for the determination of thiomolybdates in natural samples is the adaptation of the IPC method to be able to use ICP-MS as detection system. Subsequently, data concerning natural occurrence of different thiomolybdenum species could help to answer remaining questions concerning the behavior of molybdenum in the environment. Aspects regarding thiomolybdate formation and analysis in natural samples were addressed in study 6.

1.5 Objectives

The central aim of the present study was to elucidate the role of intermediate sulfur species, in particular the role of polysulfides, for various formation, transformation, and redox processes of different metal(loid) species. To be able to investigate the occurrence of polysulfides in detail, a reliable analytical method was necessary. Hence, the first and fundamental goal was to *establish a method for polysulfide analysis* in our laboratory. Polysulfide determination was accomplished by derivatization of polysulfides with methyl triflate, analysis by HPLC-UV, and quantification based on synthesized and fractionated reference material according to already published methods.

In summary, the objectives of the 6 different studies based on the open questions explained in the previous sections were to

- (1) analyze the *sulfur speciation during microbial elemental sulfur disproportionation* in the presence and absence of iron and conclude whether the presence of metals is absolutely necessary to enable elemental sulfur disproportionation (study 1).
- (2) investigate the abiotic reaction of ferric (oxyhydr)oxides with dissolved sulfide focussing on the sulfur speciation in solution and at the mineral surface and elucidate the *role of polysulfides as pyrite precursors* (study 2).
- (3) elucidate the supposedly important role of *intermediate sulfur species as electron shuttles* in the process of microbially mediated ferric (oxyhydr)oxide reduction (study 3).
- (4) investigate the *role of sulfide and polysulfides for thioarsenate formation* both abiotically and in the presence of haloalkaliphilic anaerobic bacteria and investigate a possible direct microbial use of arsenic-bound sulfur (study 4).
- (5) determine the *impact of sulfur redox chemistry on thioarsenate transformation reactions* in the presence and absence of aerobic hyperthermophile bacteria (study 5).
- (6) investigate *thiomolybdate formation and stability under different parameters*, establish an *analytical method for thiomolybdate determination* at environmentally relevant concentrations, and prove the *occurrence of thiomolybdates in natural samples* (study 6).

2 METHODS

2.1 Analysis of different sulfur species

In the course of the individual studies, various sulfur species were measured. Sulfide was determined photometrically, elemental sulfur, thiosulfate, and sulfate were determined chromatographically. Descriptions concerning the analytical methods can be found in the respective studies.

Thioarsenates were determined by IC-ICP-MS according to the method published by Planer-Friedrich et al. (2007) and as described in study 4 and study 5. The development of a method for thiomolybdate analysis in natural samples was central aspect of study 6 and details concerning the newly developed IPC-ICP-MS method can be found therein.

2.2 Analysis of polysulfides

Routinely, analysis of inorganic polysulfides was performed according to the method published by Kamyshny et al. (2004) and Kamyshny et al. (2006). The basis of the method is the conversion of labile inorganic polysulfides to more stable organic dimethylpolysulfanes by derivatization with methyl triflate. Organic dimethylpolysulfanes can then be analyzed chromatographically.

Due to the hydrophobicity of methyl triflate, derivatization was carried out in a water-methanol mixture. For this purpose, methanol was placed in a suitable vial, to which the sample and methyl triflate were added simultaneously. The simultaneous addition of sample and methyl triflate prevented hydrolysis of methyl triflate before the derivatization reaction, which would lead to a decrease in pH and accordingly to disproportionation of polysulfides. A ratio of methanol to sample volume of 80:20 was selected, since this was the ratio at which Kamyshny et al. (2006) got optimum results. The volume of methyl triflate was also chosen according to the recommendations of Kamyshny et al. (2006). At neutral pH values, 6 μ L methyl triflate per 1 mL of methanol-sample mixture were used. At higher pH values, the methyl triflate amount was increased to 15 μ L per 1 mL of methanol-sample mixture. Derivatization was performed with filtered samples to determine polysulfide speciation in solution and with unfiltered samples to determine polysulfides associated with particulate substances, such as bacterial cells or iron minerals.

Dimethylpolysulfanes were analyzed by HPLC (Merck Hitachi L-2130 pump, L-2200 autosampler, and L-2420 UV-Vis detector) using a reversed phase C18 column (Bischoff Waters Spherisorb, ODS2, 5 μ m, 250 x 4.6 mm). To achieve good peak resolution especially at the beginning of the chromatograms, where the peaks of the lower dimethylpolysulfanes elute closely together, not isocratic elution as described by Kamyshny et al. (2004) and Kamyshny et al. (2006) but gradient elution according to the method of Rizkov et al. (2004) was applied. The flow rate was set to 1 mL/min and the initial solvent composition consisted of 70 % methanol and 30 % MQ-water. The concentration of methanol was increased linearly to 80 % within 10 min, maintained for 15 min,

increased linearly to 100 % within 10 min, maintained for 10 min, returned linearly to 70 % within 5 min, and maintained for 10 min. The injection volume was 100 μ L and detection was performed at 230 nm.

Concentrations of dimethyldisulfane and dimethyltrisulfane were quantified by using commercially available standards ($C_2H_6S_2$, Acros Organics; $C_2H_6S_3$, Acros Organics). For quantification of dimethyltetrasulfane to dimethyloctasulfane, a dimethylpolysulfane mixture was synthesized according to the method of Rizkov et al. (2004). Separation of the mixture was achieved by preparative chromatography in a modification of the method described by Rizkov et al. (2004). A reversed phase C18 column (Phenomenex SphereClone, ODS2, 5 μ m, 250 x 10 mm) and an eluent of 50 % acetonitrile and 50 % formic acid were used. The flow rate was set to 5 mL/min and the injection volume of the mixture was 20 μ L. Starting 3 min after injection, fractions were collected every 20 s over a time span of 20 min. The fractions were analyzed by the method described above to identify the ones containing the highest portions of the different dimethylpolysulfanes. The identification from dimethyltetrasulfane to dimethyloctasulfane was done using the correlation of the number of sulfur atoms in dimethylpolysulfane molecules with the chromatographic retention time (Rizkov et al., 2004). The fractions with the respectively highest concentrations of the individual dimethylpolysulfanes were chosen for calibration. For determination of the total sulfur concentrations, 125 μ L of each fraction were mixed with 1.5 mL concentrated hydrochloric acid and 5 mL concentrated nitric acid and heated in a microwave (MarsXpress, CEM) at 200 $^{\circ}$ C for 10 min. The concentrations of produced sulfate were determined by ICP-MS (XSeries2, Thermo Fisher) and used for quantification.

In addition to polysulfide determination by derivatization and chromatographic analysis, the occurrence of polysulfides attached to mineral surfaces was determined by X-ray photoelectron spectroscopy (XPS) in study 2. Details concerning the analysis are provided in study 2.

3 RESULTS AND DISCUSSION

3.1 Interaction of sulfur and iron

3.1.1 Sulfur speciation during elemental sulfur disproportionation in the presence and absence of iron (study 1)

Recently, sulfate-reducing bacteria isolated from soda lakes were found to be able to disproportionate sulfite and thiosulfate (Sorokin et al., 2008a). Soda lakes are characterized by pH values up to 11 and salt concentrations up to saturation. Up to now, no haloalkaliphilic bacterium was found to be able to disproportionate elemental sulfur. Hence, the questions were pursued whether haloalkaliphiles are able to disproportionate elemental sulfur and whether iron as sulfide scavenger is necessary to enable bacterial growth (study 1). Special focus was laid on the sulfur speciation. It was investigated if sulfide reacts with elemental sulfur to form polysulfides, which can be expected under anoxic conditions and at pH 10.

Intriguingly, growth of *Desulfurivibrio alkaliphilus*, *Desulfurivibrio* sp. AMeS2, and *Dethiobacter alkaliphilus*, three bacterial strains isolated from soda lakes, was observed both in the presence and absence of goethite. This is in clear contrast to former studies with neutrophilic bacteria, which only grew in the presence of ferrihydrite (Finster et al., 1998). Moreover, doubling times were shorter than for neutrophilic bacteria, which reveals a higher energy gain under alkaline conditions.

In cultures with iron, the precipitation of iron sulfides was observed. The precipitates were identified as iron monosulfide (FeS) and mackinawite (FeS₂), but no pyrite formation could be detected. This is in contrast to microbial elemental sulfur disproportionation in the presence of iron in neutral solutions, where the formation of pyrite was observed (Thamdrup et al., 1993). Elemental sulfur disproportionating bacteria were even found to accelerate pyrite formation 10⁴ to 10⁵ times compared to rates expected from kinetic studies of abiotic pyrite formation (Canfield et al., 1998). A thin film of FeS precursor molecules was found on the outside of bacterial cell walls (Stanton and Goldhaber, 1991), which elucidates the supposedly important role of surface reactions in the process of pyrite formation. Under alkaline conditions, the field of thermodynamic pyrite stability is limited by mackinawite (Schoonen, 2004) and experimental studies concerning goethite sulfidation showed that pyrite did not form under alkaline conditions (Stanton and Goldhaber, 1991). This can explain why in the reported experiments with haloalkaliphiles no pyrite formation was observed. However, as expected, the scavenging of free sulfide by precipitation with iron seemed to have enabled elemental sulfur disproportionation.

In addition, another process was found to decrease free sulfide concentrations in solution and this was as expected the formation of polysulfides. In the experiments with iron, up to 0.85 mM polysulfides were detected, which is equivalent to 3.4 % of the originally applied elemental sulfur concentration. In cultures without iron, up to 30 % of the applied elemental sulfur was transformed to polysulfides.

Hence, without iron, the formation of polysulfides was the key process for decreasing free sulfide concentrations in solution and therefore enabled bacterial growth on elemental sulfur disproportionation.

The rate of sulfide, sulfate, and polysulfide formation turned out to be much faster in experiments without iron. However, bacterial cell growth began much later and cellular growth yields were lower in comparison to the experiments with iron. This leads to the conclusion that the formation of iron sulfides was more efficient in scavenging free sulfide from solution than the formation of polysulfides. However, the fact that experiments with iron were carried out with two and a half times the amount of elemental sulfur in comparison to the experiments without iron might also have played a role for kinetics and bacterial energy gain of elemental sulfur disproportionation.

Polysulfide speciation was dominated by tri- and tetrasulfide in experiments with iron and by tetra- to hexasulfide in experiments without iron. Despite the difference in initial elemental sulfur amounts, both systems were saturated with respect to elemental sulfur at least at the beginning of the experiments. This allows for a comparison with the study of Kamyshny et al. (2004), which predicted a dominance of tetra- to hexasulfide at alkaline pH values. This is in perfect agreement with the polysulfide speciation observed in the experiments without iron. A decrease of polysulfide chain length, as seen in the experiments with iron, could be caused by a decrease of pH. However, this effect can be excluded because the solutions were buffered and the bacteria are obligate alkaliphiles, which cannot grow at pH values below 8.5 (Sorokin et al., 2008b). Another possibility might be that the presence of iron had an effect on polysulfide speciation. Sulfur was removed from the aqueous phase by precipitation with iron. Calculations from Gun et al. (2000) revealed that with decreasing concentrations of total reduced sulfur species in solution, short chain polysulfides become more and more important.

Desulfurivibrio alkaliphilus and *Dethiobacter alkaliphilus* were found to be able to use polysulfides as electron acceptors (Sorokin et al., 2008b). Hence, the question arose whether they can also disproportionate zero-valent sulfur contained in polysulfides. The water solubility of polysulfides contributes to their easy availability to microorganisms. The probability of direct polysulfide disproportionation is also supported by the fact that bacteria were found to preferentially take up sulfur chains in comparison to sulfur rings (Franz et al., 2007). In the course of microbial elemental sulfur disproportionation, Milucka et al. (2012) detected the production of sulfide and sulfate in a ratio of 7:1, which corresponds exactly to the theoretical value of disulfide disproportionation. The dominating polysulfide species in the present experiments with haloalkaliphiles were tetrasulfide, pentasulfide, and hexasulfide. Their disproportionation should yield sulfide to sulfate ratios of 4.33:1, 4:1, or 3.8:1, respectively (Milucka et al., 2012). The observed ratio of sulfide to sulfate was around 3:1. Hence, it cannot be decided ultimately whether polysulfides were also disproportionated microbially.

In general, it can be concluded that the presence of metals such as iron is not necessary in the alkaline pH range to enable microbial growth on elemental sulfur disproportionation. Instead, polysulfides were found to play a decisive role for elemental sulfur disproportionation under alkaline conditions.

3.1.2 Role of polysulfides as pyrite precursors (study 2)

In order to elucidate reaction pathways of abiotic pyrite formation, sulfidation of ferric (oxyhydr)oxides was investigated with a special focus on the occurrence of different sulfur species not only in the aqueous phase but also associated to mineral surfaces ([study 2](#)). The reaction of lepidocrocite and goethite with aqueous sulfide was studied under anaerobic conditions and at neutral pH. Experiments were conducted either with excess iron or excess sulfide. Under excess iron conditions, sulfide disappeared from solution within 10 min and 1.5 h in the presence of lepidocrocite and goethite, respectively. Under excess sulfide conditions, the initially applied ferric iron was almost completely reduced within 3 h, while aqueous sulfide concentrations decreased and remained constant at low levels.

Sulfate and thiosulfate were below detection limit in all experiments. Only trace amounts of polysulfides were detected in solution, which came to 5 % of the initially applied sulfur concentration at maximum. The sulfur fraction, which increased during sulfidation, was methanol-extractable sulfur (MES). MES included elemental sulfur and zero-valent sulfur bound in polysulfides both in the aqueous phase and associated to the mineral surface. The amount of solid phase-bound MES came to 80 % and was investigated in detail by cryogenic X-ray photoelectron spectroscopy (XPS). These analyses showed that significant amounts of polysulfides were formed at the surface of the minerals. Disulfide accounted for 10.7 % to 14.4 % of total sulfur detected at the mineral surfaces. The higher polysulfides could not be distinguished by XPS and made up 6.8 % to 30.1 % of total sulfur. A reaction mechanism of sulfide oxidation by metal ions such as ferric iron with intermediate occurrence of polysulfides was described in detail by Steudel (1996). In the first one-electron oxidation step, sulfur radicals $S^{\cdot-}$ are formed, which react spontaneously to form disulfide. Further oxidation of disulfide leads to the formation of higher polysulfides, which can serve as precursors of elemental sulfur molecules.

In the present study, also elemental sulfur was detected at the mineral surfaces, where the relative share of elemental sulfur was higher in the experiments with excess sulfide in comparison to the experiments with excess iron. For the relative amount of polysulfides, the opposite was the case. There, the relative increase of polysulfide concentrations was mainly due to an increase of the sum of higher polysulfides.

In general, a higher reactivity of lepidocrocite was detected, which became also obvious in the higher amounts of elemental sulfur and polysulfides at the mineral surface in comparison to goethite. Influence of different surface areas can be excluded because the concentration of surface sites was approximately the same for the two minerals. Poulton et al. (2004) also found huge differences in the

reaction of different iron (oxyhydr)oxides with dissolved sulfide and attributed this to mineral properties such as electron mobility and bond strength. A general distinction was made between highly reactive minerals of low crystallinity, such as lepidocrocite, and less reactive minerals of high crystallinity, such as goethite.

In light of the newly discovered occurrence of surface polysulfides, considerations concerning the nature of polysulfide surface associations were made. On the basis of iron and sulfur mass balance calculations, it was assumed that polysulfides might be associated with the generated ferrous iron on the ferric iron mineral surface. In particular, surface-associated disulfide was identified as key precursor for pyrite formation. Accordingly, pyrite can be formed directly from surface Fe(II)-disulfide associations or by reaction of surface-bound disulfide with FeS from solution. Up to now, the possible occurrence of surface-bound polysulfides was not taken into account and pyrite formation was considered as reaction of ferrous iron and polysulfides in solution (Luther, 1991; Rickard, 1975).

In the time scale and under the conditions of the present study no pyrite formation was observed. In the course of investigations concerning the reaction kinetics of sulfide with ferrihydrite, lepidocrocite, and goethite, pyrite formation was observed within the period of days (Hellige et al., 2012; Peiffer et al., 2015). In this context, the authors elucidated the importance of excess Fe(II) in the course of pyrite formation. Excess Fe(II) is solid Fe(II) which cannot be recovered as FeS and was therefore interpreted – according to Gorski and Scherer (2011) – as a transfer of electrons to the bulk mineral phase. These electrons are assumed to be decisive for surface-bound polysulfide and consequently pyrite formation. In the case of excess sulfide, FeS formation dominates over excess Fe(II) formation, which leads to a great delay in pyrite formation. This finding concerning the influence of excess sulfide concentrations is in contrast to earlier observations, where a positive correlation between sulfide concentration and pyrite formation rate was determined (Rickard, 1975). Formation of excess Fe(II) was also found to differ between the particular minerals and was highest for ferrihydrite, followed by lepidocrocite and goethite (Peiffer et al., 2015). This was attributed to varying capabilities of electron transfer within the minerals. In general, the authors showed that the pathways and kinetics of pyrite formation strongly depend on the sulfide concentration and specific mineral properties.

In the course of the present study it became obvious that not only parameters such as pH or absolute elemental sulfur and sulfide concentrations but also factors such as iron mineral reactivity or the ratio of sulfide and iron concentrations influence polysulfide concentration and speciation. This was the first study that reported the occurrence of polysulfides attached to mineral surfaces during sulfidation of ferric (oxyhydr)oxides. Up to now, surface-bound polysulfides were not considered but certainly are of high relevance for numerous environmental processes apart from pyrite formation.

3.1.3 Role of intermediate sulfur species for biogeochemical iron transformations (study 3)

Besides the abiotic sulfidation of ferric (oxyhydr)oxides ([study 2](#)), we investigated the microbially mediated anoxic reductive dissolution of ferrihydrite ([study 3](#)). Straub and Schink (2004) found that thiosulfate initiated electron shuttling via sulfur species between the sulfur-reducing bacterium *Sulfurospirillum deleyianum* and ferrihydrite. The present study was conducted to examine the electron shuttling process in more detail with special focus on the role of intermediate sulfur species.

Therefore, the microbial reductive and the abiotic oxidative part of the electron shuttling process were investigated separately in a first step. In accordance with the literature (Schumacher et al., 1992; Wolfe and Pfennig, 1977), sulfide was observed as final product of microbial thiosulfate reduction. Intermediately, elemental sulfur and hexasulfide, presumably occurring inside or attached to bacterial cells, were detected. Previously, evidence was found that polysulfides occur as intermediates during bacterial growth on elemental sulfur (Klimmek et al., 1991). Our results suggest that this is also the case during bacterial growth on thiosulfate. The abiotic reaction of sulfide and ferrihydrite in a molar ratio of 1:50 yielded mainly elemental sulfur attached to the mineral surface followed by thiosulfate in solution. It is known that elemental sulfur can be used as electron acceptor by *S. deleyianum* (Straub and Schink, 2004). The fact that the main product of abiotic sulfide oxidation was found attached to the mineral surface implies that direct physical contact of microorganisms and iron mineral phase is necessary to enable electron shuttling via sulfur species. This is in contrast to the finding of Straub and Schink (2004) that iron reduction was possible when *S. deleyianum* was spatially separated from ferrihydrite.

Elemental sulfur was also found in former studies as main oxidation product from the reaction of sulfide with ferrihydrite (e.g., Poulton, 2003; Saalfield and Bostick, 2009). In contrast to the previously described study concerning abiotic sulfidation of lepidocrocite and goethite ([study 2](#)), polysulfide occurrence was insignificant ([study 3](#)). This might be due to intrinsic mineral properties. The relative amount of polysulfides but also elemental sulfur was found to be higher in the case of lepidocrocite in comparison to the less reactive goethite ([study 2](#)). As ferrihydrite is known to be even more reactive than lepidocrocite (Peiffer et al., 2015), oxidation of sulfide to elemental sulfur at the surface of ferrihydrite might have been too fast for detection of polysulfides.

In experiments with bacteria, thiosulfate, and ferrihydrite with an initial molar sulfur:iron ratio of 1:2.5, small amounts of polysulfides were detected besides elemental sulfur associated with the solid phase, which could have been both, microorganisms and/or iron mineral phase. Polysulfide speciation was dominated by hexa- to octasulfide. The prevalence of long-chain polysulfides at pH 7 is in accordance with studies of sulfur-unsaturated solutions, where an increase of chain length with decreasing pH was predicted (Giggenbach, 1972; Schwarzenbach and Fischer, 1960). However, for the abiotic sulfidation of lepidocrocite and goethite at identical pH and redox conditions, the predominance of disulfide was shown by XPS analysis ([study 2](#)). The fact that no disulfide was

detected in the biotic experiments ([study 3](#)) might be due to methodological reasons. On the one hand, disulfide concentrations simply might have been too low, as the sensitivity of the UV detection decreases with decreasing chain length (Kamyshny et al., 2004). On the other hand, disulfide is already protonated at pH 7, which leads to slower and consequently incomplete methylation during polysulfide derivatization (Kamyshny et al., 2004). The dominance of disulfide determined by XPS ([study 2](#)) and the occurrence of hexa- to octasulfide determined after derivatization by HPLC-UV ([study 3](#)) comes close to polysulfide speciation predicted by Rickard and Luther (2007) (Fig. 2).

In accordance with Straub and Schink (2004), minor amounts of thiosulfate enabled iron reduction in fifty-fold stoichiometric excess. In addition, other sulfur species were found to enable ferrihydrite reduction to the same extent. The use of sulfite as electron acceptor by *S. deleyianum* is in agreement with the results of Eisenmann et al. (1995), but in contrast to the findings of Straub and Schink (2004). To the best of our knowledge, we were the first to show the reduction of tetrathionate by *S. deleyianum*. The addition of polysulfides showed the fastest reaction kinetics of iron reduction. Cystine, as oxidized form of cysteine, was also tested since cysteine – following the experiments of Straub and Schink (2004) – was added to the experimental solutions as sulfur source and reducing agent. The addition of cystine enabled complete ferrihydrite reduction but yielded the lowest reduction rate. Since the rate of ferrihydrite reduction was the same when applying sulfide as completely reduced sulfur species or thiosulfate, polythionates, or sulfite as intermediate sulfur species, it can be concluded that microbial sulfur reduction was extremely fast and that the abiotic reaction of sulfide and ferrihydrite was rate-determining for the overall electron shuttling process.

As indicated by the experiments with cystine, cysteine, which ideally should only protect reduced sulfur species from oxidation as assumed by Straub and Schink (2004), might also have a certain influence on the sulfur electron shuttling process. Cysteine was already shown to abiotically reduce different iron (oxyhydr)oxides (Amirbahman et al., 1997). Additionally, electron shuttling via cysteine and cystine between microorganisms and iron was observed (Doong and Schink, 2002; Liu et al., 2013). We also found that the addition of cysteine substantially increased iron reduction in both, abiotic and biotic experiments. Since cysteine is also known to reduce inorganic sulfur species such as thiosulfate (Szczepkowski, 1958), it was not possible to determine whether iron was reduced directly or indirectly by cysteine. Due to the considerable influence of cysteine on iron reduction and the fact that *S. deleyianum* also grew with thiosulfate as only sulfur source, we strongly recommend to eliminate cysteine from experiments where sulfur redox processes are investigated.

In the process of microbially driven ferrihydrite reduction in the presence of minor amounts of different sulfur species, almost no aqueous sulfide and no accumulation of re-oxidized sulfur species were detected. However, black precipitates of FeS were observed in the beginning of the experiments, which dissolved over time. This supports the assumption of FeS serving as sulfur reservoir, which was recycled in the course of ongoing iron reduction. Released ferrous iron was found to precipitate from the bicarbonate rich medium as siderite. In the course of abiotic sulfidation of ferrihydrite, also black

FeS precipitates were observed, which remained in suspension, while for goethite and lepidocrocite black FeS precipitates disappeared over time (Peiffer et al., 2015). Within the same experiment, the transformation of ferrihydrite into a mixture of hematite, goethite, and magnetite was observed. A detailed study on magnetite formation during iron reduction showed that magnetite formation increased with increasing ferrihydrite concentrations (Piepenbrock et al., 2011). In our study we chose – according to Straub and Schink (2004) – sufficiently low ferrihydrite concentrations to avoid the formation of black magnetite, which would possibly mask other iron transformation processes such as precipitation and dissolution of FeS.

Overall, polysulfides did – contrary to previous speculations – not dominate the electron shuttling process between *S. deleyianum* and ferrihydrite. However, a more detailed picture of various sulfur redox processes in the course of microbially mediated iron reduction could be achieved. These findings can contribute to the understanding of complex redox interactions between sulfur and iron in anoxic environments.

3.2 Interaction of sulfur and arsenic

3.2.1 Role of sulfide and polysulfides for thioarsenate formation in the presence and absence of haloalkaliphilic anaerobic bacteria (study 4)

In the past, different pathways of thioarsenate formation were discussed. In experiments with haloalkaliphilic anaerobes, thioarsenates were suggested to form via the reaction of arsenite and polysulfides (Fisher et al., 2008). By repeating and extending the reported experiments, we investigated the role of sulfide and polysulfides for thioarsenate formation ([study 4](#)).

The first question, which was addressed, was the identification of the thioarsenic species, which occurred intermediately during arsenate respiration by the anaerobic haloalkaliphile MLMS-1, isolated from Mono Lake (Hoefl et al., 2004). Analysis by XAS unequivocally identified the questionable species as monothioarsenate and not as monothioarsenite as was suggested previously (Hoefl et al., 2004). Since microbial arsenate reduction is coupled to sulfide oxidation to elemental sulfur, different arsenic and sulfur species might have been possible reaction partners for monothioarsenate formation. Reaction of arsenate and sulfide could be excluded at alkaline conditions as it was shown earlier to occur only at pH values below 4 (Rochette et al., 2000).

To elucidate monothioarsenate formation pathways, different abiotic experiments with arsenite were performed. Analysis was done by IC-ICP-MS. Previously, it was shown that IC-ICP-MS is not suitable for thioarsenite detection and that thioarsenites are intermediates for thioarsenate formation to which they transform during analysis by IC-ICP-MS (Planer-Friedrich et al., 2010). In the course of the present study, mixtures of arsenite and sulfide yielded only minor amounts of monothioarsenate. With increasing sulfide excess, the total amount of thioarsenic species increased, which were dominated by tri- and tetrathioarsenate. Hence, the speciation of thioarsenites as precursors for

thioarsenate formation also had to be dominated by higher thiolated species. This finding is in accordance with previous studies. Monothioarsenite never became the dominant species in earlier reported arsenite-sulfide mixing experiments, whereas trithioarsenite always was the prevailing thioarsenic species at different As:S ratios (Planer-Friedrich et al., 2010). Consequently, sulfidation of arsenite under anaerobic conditions seems to be too fast for longer and exclusive existence of the intermediate species monothioarsenite, which also prevents the predominant formation of monothioarsenate by this reaction pathway.

The next step was to test the reaction of arsenite with polysulfides as possible intermediates in the course of microbial arsenate respiration or products of the reaction of microbially produced elemental sulfur with initially applied sulfide. Indeed, the dominant occurrence of monothioarsenate was found at an arsenite:polysulfide ratio of 1:3. Consequently, monothioarsenite as precursor for monothioarsenate formation is not necessary when sulfur is not present as completely reduced species but as zero-valent sulfur. A tenfold polysulfide to arsenite excess led again to the formation of higher thiolated arsenates. This was assumed to be due to generally higher sulfide concentrations in solution and the consequent predominant formation of thioarsenites. Hence, the kinetic of thioarsenite formation, which depends strongly on the ratio of SH^- and OH^- in solution, seems to determine whether the addition of zero-valent sulfur to arsenite and consequently monothioarsenate formation takes place.

Another possible reaction pathway for the occurrence of higher thiolated arsenates might be that monothioarsenate was formed in any case by the initial reaction of arsenite with zero-valent sulfur and that subsequent ligand exchange of SH^- versus OH^- led to the formation of higher thiolated arsenates. However, there are some arguments which contradict this theory. Sulfidation of arsenic might occur via nucleophilic attack as was shown for the formation of thiomolybdates (Erickson and Helz, 2000; Harmer and Sykes, 1980). In this process, protonation of the oxygen atoms is decisive. However, monothioarsenate is supposed to react comparably to arsenate as both substances are chemically quite similar, e.g., with respect to pKa values (Thilo et al., 1970) and arsenate was shown to react with sulfide only at pH values below 4 (Rochette et al., 2000). Additionally, one could assume that ligand exchange of SH^- versus OH^- works in both directions, which would imply instability of thioarsenates at excess OH^- as was for example seen for thioarsenites. This is definitely not the case for thioarsenates since, e.g., tetrathioarsenate only is stable under highly alkaline conditions (Planer-Friedrich and Wallschläger, 2009).

Additional abiotic experiments, not included in study 4, were conducted to investigate thioarsenate formation in more detail (Fig. 3). Solutions of arsenic and sulfur were prepared inside an anoxic glovebox and kept there until analysis by IC-ICP-MS. In mixtures of arsenite and sulfide at a ratio of 1:10, substantial thioarsenate formation was observed at pH 8 and 11. The degree of thiolation was higher at the lower pH. At pH 13, almost no thioarsenates were observed. Hence, the pH value and the

ratio of SH^- to OH^- determined thioarsenite and consequently also thioarsenate formation, which was seen before and is in accordance with earlier observations (Planer-Friedrich et al., 2010).

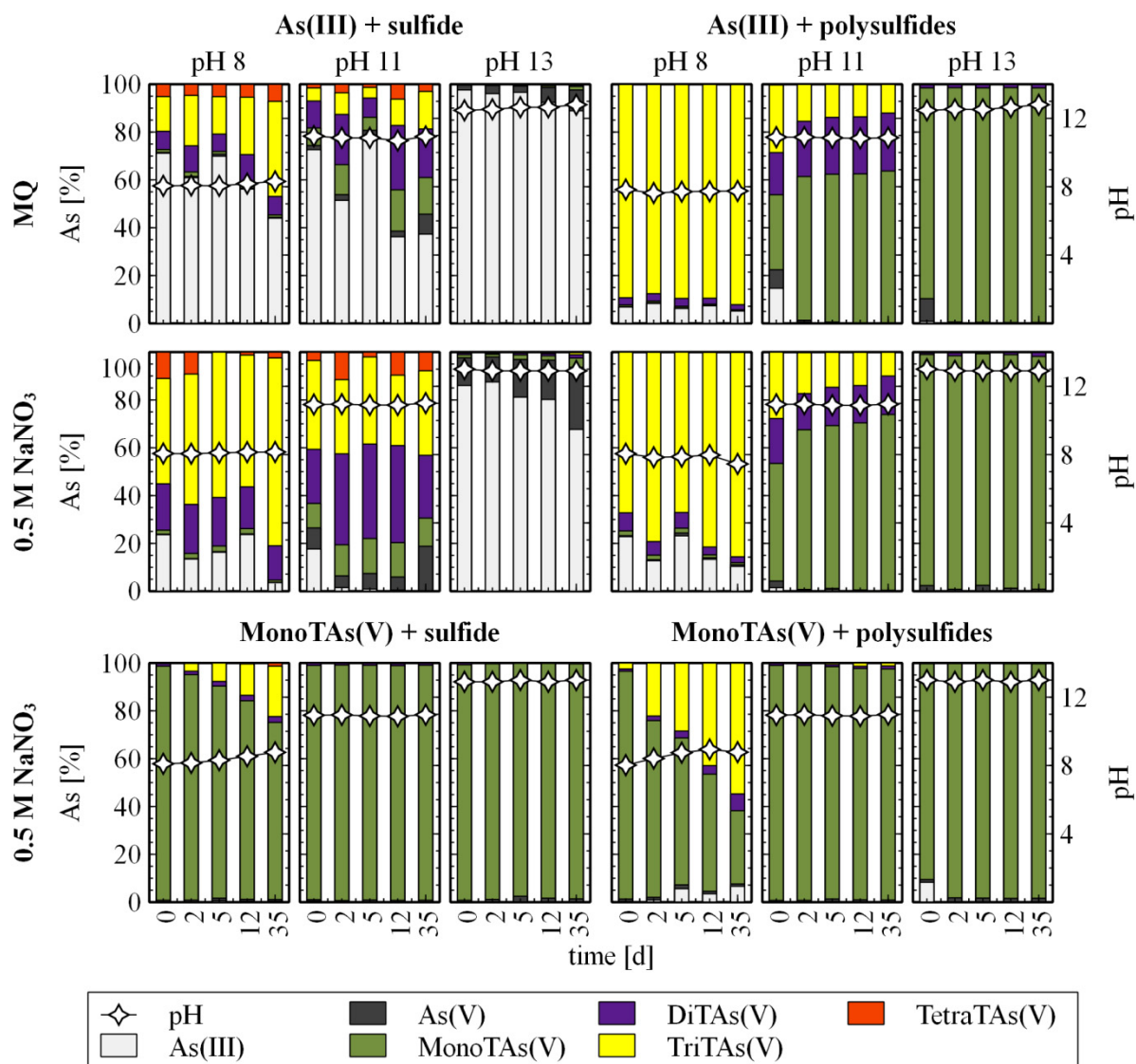


Fig. 3. Formation of thioarsenates in mixtures of 0.1 mM arsenite or monothioarsenate and 1 mM sulfide or ~ 0.5 mM sulfur in form of polysulfides, sulfide, and elemental sulfur at different pH values over time. Solutions were prepared either in MQ-water or in 0.5 M NaNO_3 . Analysis was done by IC-ICP-MS (As(III) = arsenite, As(V) = arsenate, MonoTAs(V) = monothioarsenate, DiTAs(V) = dithioarsenate, TriTAs(V) = trithioarsenate, TetraTAs(V) = tetrathioarsenate).

Conducting the experiments at higher ionic strength led to a substantial increase of thioarsenate formation rates. The effect of ionic strength on reaction kinetics depends, among others, on the charge of the reacting ions; if they are equally charged, reaction rates increase, if they are oppositely charged, reaction rates decrease at high ionic strength (Brönsted, 1928; Castaneda-Agullo et al., 1961). As thioarsenate formation was also accelerated at pH 8, where arsenite is fully protonated and sulfide is present as HS^- , the effect of ionic strength on dissociation equilibria in solution (Brönsted, 1928; Castaneda-Agullo et al., 1961) also might have played a role.

In mixtures of arsenite and polysulfides, with an average sulfur to arsenite excess of about 5, complete transformation of arsenite to monothioarsenate was observed at pH 13, which is a pH at which no thioarsenites are formed. Additionally, the reaction of arsenite and zero-valent sulfur is supposed to be favored at high pH values, since the amount of polysulfides and thus zero-valent sulfur present in solution increases with increasing pH (Schauder and Müller, 1993). At pH 11, monothioarsenate was the dominating species followed by tri- and dithioarsenate. At pH 8, the formation of monothioarsenate was presumably prevented by the fast formation of thioarsenites. Trithioarsenate was the dominant species as also found for mixtures of arsenite with tenfold sulfide excess. However, trithioarsenate formation was much faster in the presence of polysulfides, even though the total sulfide to arsenite excess was only about threefold. This effect might be due to specific properties of polysulfides. In general, the increase of chain lengths was observed with decreasing pH. As described earlier, the nucleophilicity of polysulfides increases with chain length (LaLonde et al., 1987) and starting from tetrasulfide, polysulfides are more nucleophilic than sulfide (Luther, 1990). Hence, kinetic of thioarsenite formation seems to be determined not only by the absolute amount of sulfide but also by the kind of sulfide species present in solution.

When adding sulfide or polysulfides to monothioarsenate, no speciation changes were observed at pH 11 and pH 13. At pH 8, the gradual formation of trithioarsenate was observed over time. Again, trithioarsenate formation was faster in mixtures with polysulfides. In general, higher thiolated arsenates only formed at pH 8, at which thioarsenite formation is possible. However, based on the present experiments, it can just be assumed that ligand exchange of SH^- versus OH^- is improbable in the case of thioarsenates but cannot be excluded completely.

Thioarsenate and polysulfide speciation was also determined in biotic experiments in the presence of the anaerobic haloalkaliphile MLMS-1 ([study 4](#)). In the course of arsenate respiration, the formation of polysulfides and subsequently monothioarsenate could indeed be observed. This finding demonstrates again that monothioarsenate is formed by the reaction of arsenite with zero-valent sulfur. Since approximately equimolar concentrations of arsenate and sulfide were applied, sulfide concentrations were too low for the formation of higher thiolated arsenates. In contrast to the process of elemental sulfur disproportionation by haloalkaliphilic bacteria ([study 1](#)), where tetra- to hexasulfide were the dominating polysulfide species, mainly disulfide followed by tri- and tetrasulfide were found in the course of arsenate respiration by haloalkaliphilic bacteria. This can be attributed to the fact that in the first study elemental sulfur was applied in excess, whereas in the latter study elemental sulfur was gradually produced by the activity of the bacteria and apparently reacted with the initially applied sulfide to form polysulfides.

Moreover, direct microbial use of arsenic-bound sulfur was studied by initially applying monothioarsenate instead of arsenate in biotic experiments. In the course of microbial growth, monothioarsenate concentrations decreased and concentrations of arsenite and polysulfides, mainly consisting of disulfide, increased. An exact mass balance could not be calculated due to already

described uncertainties in disulfide determination and due to a polysulfide signal from synthesized monothioarsenate. It could not be determined whether this polysulfide signal resulted from residuals of monothioarsenate synthesis, which is performed by the reaction of As_2O_3 with elemental sulfur, or from possible transformation processes during derivatization. However, actual polysulfide formation in the course of the experiment became obvious in a yellow coloring of the solution. Finally, it was concluded that microbial disproportionation of monothioarsenate resulted in the formation of arsenite and polysulfides.

Overall, it could be shown that polysulfides play a key role for monothioarsenate formation and are possibly also relevant for the formation of higher thiolated species. However, kinetics were found to be slower for the reaction of arsenite with zero-valent sulfur in comparison to the reaction with sulfide. Additionally, polysulfides were identified as products of microbial thioarsenate transformation reactions.

3.2.2 Impact of sulfur redox chemistry on thioarsenate transformation reactions in the presence and absence of aerobic hyperthermophile bacteria (study 5)

Microbially mediated transformation reactions of thioarsenic species in geothermal waters of Yellowstone National Park have been observed in previous studies (Härtig and Planer-Friedrich, 2012; Planer-Friedrich et al., 2009). However, details concerning thioarsenate transformation processes remained to be elucidated. Therefore, the aim of the reported study was to systematically investigate thioarsenate transformation processes under laboratory conditions in the presence and absence of *Thermocrinis ruber*. Special focus was laid on the role of sulfur redox chemistry. *T. ruber* is an aerobic hyperthermophile, which was isolated from a hot spring in Yellowstone National Park, uses oxygen as electron acceptor, and grows under neutral to alkaline pH conditions and optimally at 80 °C (Huber et al., 1998). Experiments were conducted with 3 or 8 % oxygen in the gas headspace.

Abiotically, a substantial decrease of initially applied monothioarsenate concentrations was observed. After 7 days, 70 % monothioarsenate had mainly transformed to arsenate, followed by 10 % arsenite. Since a separate abiotic experiment revealed that arsenite was completely stable under the respective conditions, it can be excluded that monothioarsenate first transformed exclusively to arsenite, which subsequently may have been oxidized to arsenate. In a former study, trithioarsenate aeration yielded arsenite and not arsenate as transformation product (Planer-Friedrich et al., 2009). The same was observed when adding small amounts of hydrogen peroxide to a trithioarsenate solution. With increasing hydrogen peroxide concentrations, subsequent formation of dithioarsenate, monothioarsenate, and arsenate was detected. This comparison of thioarsenic transformation products reveals again the exceptional position of monothioarsenate in the series of thioarsenate species.

The observed abiotic instability of monothioarsenate is in contrast to previous studies, where monothioarsenate was completely stable after aeration for 24 hours or heating to 80 °C for 2 hours

(Planer-Friedrich et al., 2009). Also, in the course of abiotic on-site incubation experiments in Yellowstone National Park, monothioarsenate was completely stable for several hours (Härtig and Planer-Friedrich, 2012). Hence, the long time frame of the laboratory experiments over several days under high temperature and oxic conditions seems to have triggered abiotic monothioarsenate transformation processes.

With regard to the observed changes in arsenic speciation, it can be assumed that the initial monothioarsenate transformation reaction was desulfidation resulting in the formation of arsenate and sulfide. However, no increase of sulfide concentrations was observed. This can be explained by extremely rapid sulfide oxidation, which was also observed in a separate experiment. The fast disappearance of sulfide was supported by the experimental pH, since at pH 8, a maximum of sulfide oxidation rates was observed previously (Chen and Morris, 1972).

The main final sulfur oxidation product of abiotic monothioarsenate transformation was thiosulfate. Polysulfides were detectable already at the beginning of the experiment. As described before, it is not clear whether polysulfides in monothioarsenate solutions originate from residuals of monothioarsenate synthesis or transformation reactions during derivatization. In general, the intermediate occurrence of polysulfides in the course of sulfide oxygenation was found to account for 15 % at maximum within the time frame of several hours (Chen and Morris, 1972), which may explain that no increase in polysulfide concentrations was detectable during the decrease of monothioarsenate concentrations. In contrast, an increase in the deficit of the sulfur mass balance, i.e., the difference between applied sulfur concentration and sum of measured dissolved sulfur species, was observed especially during the initial decrease of monothioarsenate concentrations. This was attributed to the formation of elemental sulfur colloids or precipitates. In the reaction of sulfide with oxygen, the transfer of two electrons is favorable because with zero-valent sulfur and peroxide stable products are formed (Luther, 2010). However, the reaction was described to be kinetically slow and to be accelerated by the presence of metals in solution. This might also have played a role in the reported study, since the bacterial growth medium, in which also the abiotic experiments were performed, contained small amounts of iron and manganese.

From the previous study ([study 4](#)), it could be expected that monothioarsenate decomposition proceeds in the opposite way of monothioarsenate formation and hence yields arsenite and zero-valent sulfur in the course of a disproportionation reaction. However, under the reported experimental conditions, this reaction pathway seems to have been of minor importance and a fast desulfidation and oxidation of sulfur contained in monothioarsenate appears to have been decisive for the transformation processes. In the previously reported experiments with haloalkaliphilic bacteria ([study 4](#)), monothioarsenate disproportionation was triggered by microbial activity as the bacteria could simultaneously use arsenic as electron acceptor and sulfur as electron donor.

In biotic experiments with *T. ruber*, growth was observed in the presence of monothioarsenate and was attributed to different possible transformation pathways. Biotically, complete and in comparison

to the abiotic experiment much faster monothioarsenate transformation was observed. The main reaction products were arsenate and sulfate. It is known that *T. ruber* can grow on elemental sulfur and thiosulfate (Huber et al., 1998). Microbial oxidation of thiosulfate to sulfate was also proven in a separate experiment. Hence, it can be concluded that *T. ruber* mainly grew on elemental sulfur and thiosulfate as abiotic products of monothioarsenate decomposition and thereby accelerated transformation processes due to a shift in chemical equilibrium. Additionally, it could be shown for the first time that *T. ruber* can use arsenite as electron donor. Hence, also small amounts of abiotically produced arsenite, which disappeared completely in the course of the biotic experiment, seemed to have been used for bacterial growth.

Moreover, concentrations of initially present polysulfides decreased biotically much faster than abiotically. Consequently, it could be assumed that also polysulfides were used for microbial growth. In the course of the previously mentioned microbial polysulfide disproportionation ([study 1](#)), the easy accessibility of water soluble polysulfide chains for microorganisms was already discussed. In the present experiments, polysulfides were clearly dominated by tetrasulfide. In general, high temperatures favor – as described before – the occurrence of polysulfides (Kamyshny et al., 2007; Schauder and Müller, 1993). Different factors with partially opposing effects might have influenced polysulfide speciation in the present experiment. A low pH causes high polysulfide chain lengths in systems not saturated with elemental sulfur (Giggenbach, 1972), a low amount of total reduced sulfur species causes low chain lengths (Gun et al., 2000), and a high temperature leads to an increase in polysulfide chain lengths (Kamyshny et al., 2007). In general, it has to be considered that the occurrence of polysulfides was related to the presence of monothioarsenate, while details concerning the exact origin of polysulfides could not be clarified.

Apart from the obvious microbial use of abiotic monothioarsenate transformation products, also direct microbial growth on sulfur bound in monothioarsenate was taken into account. This hypothesis was supported by the fact that biotic monothioarsenate decomposition proceeded faster than expected from the occurrence of its abiotic transformation products elemental sulfur and thiosulfate. Overall, a complex interaction of different abiotic and biotic sulfur redox processes was found to be decisive for the rate and extent of monothioarsenate transformation. The role of polysulfides for monothioarsenate transformation under high temperature and oxic conditions was less pronounced than observed previously for monothioarsenate formation and microbial disproportionation processes.

3.3 Interaction of sulfur and molybdenum – Formation and natural occurrence of thiomolybdates (study 6)

Previously, the formation of thiomolybdates was found to proceed from molybdate and sulfide by an acid catalyzed nucleophilic substitution reaction (Erickson and Helz, 2000) and their formation was supposed to play a crucial role for the burial of molybdenum in sediments (Helz et al., 2011). The aim of the present study was to investigate formation of thiomolybdates under varying conditions, to

elucidate the potential relevance of polysulfides for formation and transformation processes, to develop an analytical method for thiomolybdate determination in natural samples, and to prove their occurrence in the environment.

We conducted experiments with different sulfide:molybdate ratios at an initial pH of 7.3. An increase in sulfide:molybdate excess led to an increase of rate and extent of thiomolybdate formation. This is in accordance with previous experiments (Erickson and Helz, 2000). The observed decrease of sulfidation rates with each step might be due to an increasing steric hindrance by an increasing number of large sulfur ligands and different protonation constants of the individual thiomolybdates (Harmer and Sykes, 1980). The process of thiomolybdate formation by ligand exchange of SH^- versus OH^- is comparable to thioarsenite formation. The extent of thioarsenite formation was also found to increase with increasing sulfide to arsenite excess (Planer-Friedrich et al., 2010). However, the process of thioarsenite formation seems to proceed faster than thiomolybdate formation, since in the first case an immediate dominance of trithioarsenite always was found (Planer-Friedrich et al., 2010), whereas in the latter case tetrathiomolybdate concentrations increased slowly over time and a concurrent occurrence of all four thiomolybdates in solution was observed ([study 6](#)).

In experiments with molybdate and polysulfides, the rate and extent of thiomolybdate formation seem to have been determined only by the amount of sulfide in solution. Hence, the presence of – in comparison to sulfide – higher nucleophilic polysulfides did not lead to an acceleration of thiomolybdate formation by nucleophilic substitution of SH^- versus OH^- . This is in contrast to the previously observed effect of polysulfides for thioarsenate formation ([study 4](#)) and might, at least partly, be due to a generally lower polysulfide concentration in solution at pH 7.3 in comparison to pH 8. The presence of zero-valent sulfur did not have any observable effect on thiomolybdate formation in the present study. Previously, the reaction of especially trithiomolybdate with zero-valent sulfur with subsequent reduction of molybdenum was determined (Vorlicek et al., 2004). However, those experiments were performed at a higher pH of 8.2, starting initially with a trithiomolybdate solution, and mostly a higher sulfur to molybdenum excess than used in our experiments. Consequently, no effect of polysulfides on thiomolybdate formation might have been observable, at least partly, due to the chosen experimental conditions of the present study.

In terms of pH, a pH value of 7 was most favorable for thiomolybdate formation. This is in accordance with the literature, where a pH slightly above 7 was described as the best compromise between proton availability and dominance of HS^- over H_2S (Harmer and Sykes, 1980). In experiments at pH 11, where a twofold excess of SH^- versus OH^- was present in solution, no thiomolybdates formed at all over a period of two weeks. Consequently, either a higher excess of SH^- versus OH^- is necessary for thiomolybdate formation or the excess of SH^- versus OH^- is not as decisive as was seen for the formation of thioarsenites and thioarsenates, respectively, and instead the pH plays a more crucial role for thiomolybdate formation.

Tetrathiomolybdate was determined to be the thermodynamically stable thiomolybdate species (Erickson and Helz, 2000; Helz et al., 2011). Stability of tetrathiomolybdate was tested in different experiments ([study 6](#)). In contrast to previous assumptions (Weiss et al., 1988), tetrathiomolybdate was not stable under alkaline conditions and mainly transformed back to molybdate. This is comparable to observations for thioarsenites, where an excess of OH⁻ versus SH⁻ led to a transformation to arsenite (Planer-Friedrich et al., 2010), and is in contrast to the findings concerning thioarsenates since tetrathioarsenate only is stable under highly alkaline conditions (Planer-Friedrich and Wallschläger, 2009).

In order to be able to determine thiomolybdates in natural samples, we adapted the previously published method of thiomolybdate determination by IPC separation with acetonitrile eluent and suppressed conductivity or UV detection (Weiss et al., 1988). Replacement of acetonitrile by 2-propanol and modification of the gradient conditions allowed the use of ICP-MS as detection system and detection limits of approximately 10 nM could be achieved.

The predicted natural occurrence of thiomolybdates in Lake Rogoznica (Helz et al., 2011) could not be verified due to disturbing effects of high ionic strengths matrices and total molybdenum concentrations close to the detection limit of the IPC-ICP-MS method. However, after adding a molybdate spike to a euxinic bottom water sample of the lake, which resulted in a sulfide to molybdate excess of 6600, the formation of all four thiomolybdates could be observed. This observation supports the assumption that not only the thermodynamically stable tetrathiomolybdate but also intermediate thiomolybdates might occur in the lake. Especially seasonal variations might be important for intermediate thiomolybdate formation. Vertical mixing usually occurs in autumn and leads to disturbance of equilibrium conditions. After the mixing event, only the water sample directly at the bottom of the lake was found to be sulfidic, whereas during the rest of the year abundant sulfide concentrations were found from 10 to 13 m (Helz et al., 2011). Particularly in summer, elevated microbial sulfate reduction was noticed, which led to an increase of sulfide concentrations and a decrease of pH around the neutral range (Helz et al., 2011), both of which are favorable conditions for thiomolybdate formation. Additionally, at the chemocline between the upper oxic and the lower sulfidic zone, a dense population of purple phototrophic sulfur bacteria is responsible for sulfide oxidation to zero-valent sulfur (Kamyshny et al., 2011). In general, microbial sulfur oxidation might lead to direct or indirect thiomolybdate transformation processes comparable to observations in the case of thioarsenates ([study 4 and 5](#)). Diurnal or annual variations of the position of the chemocline might also be important in this context. However, optimization of the method, such as separation of matrix components or sample preconcentration, is necessary before details concerning thiomolybdate formation and transformation processes in Lake Rogoznica can be elucidated.

The actual natural occurrence of thiomolybdates could be shown for approximately 20 geothermal hot springs in Yellowstone National Park. The most dominant and sometimes exclusive thiomolybdate species was tetrathiomolybdate, which is in accordance with the thermodynamic stability of

tetrathiomolybdate (Erickson and Helz, 2000; Helz et al., 2011). For two springs, the simultaneous occurrence of all four thiomolybdates was observed. However, molybdate always was the dominant species. This is in contrast to what was observed for arsenic in geothermal hot springs of Yellowstone National Park, where thioarsenates constituted up to 83 % of total arsenic (Planer-Friedrich et al., 2007). Comparing the chemistry of the hot springs with the respective thiomolybdate speciation revealed that not the absolute sulfide to molybdenum excess but rather the pH or ratio of SH^- to OH^- seems to have determined the extent of thiomolybdate formation. Additionally, parameters such as the achievement of equilibrium conditions or the competition between molybdenum and other metals or metalloids for the reaction with sulfide have to be considered.

Overall, the present study provides the first evidence of thiomolybdate occurrence in the environment. After further optimization, the newly developed method is supposed to be applicable to a large number of natural systems. Hence, the basis was laid for thiomolybdate analysis in natural samples and consequently an increasing understanding of the role of thiomolybdates for molybdenum burial in sediments.

4 CONCLUSIONS

The aim of the present study was to investigate the role of sulfide, polysulfides, and elemental sulfur for abiotic and biotic redox processes in sulfur-metal(loid) systems. In the literature, polysulfides in particular were supposed to play a crucial role for numerous redox processes but were analyzed only rarely. Therefore, special focus was laid on the importance of polysulfides in the interaction of different sulfur species with iron, arsenic, and molybdenum.

The process of elemental sulfur disproportionation was previously found to enable growth of bacteria only in the presence of metals functioning as sulfide scavengers. In the reported study (study 1: Poser et al., 2013), growth of haloalkaliphilic bacteria by elemental sulfur disproportionation, which was reported for the first time, was observed both, in the presence and absence of iron. In the latter case, the formation of polysulfides was found to decrease the concentration of free sulfide in solution and therefore enable growth of bacteria also in the absence of iron. In the reported study, the process of sulfide scavenging from solution by formation of iron sulfides seemed to be more efficient than scavenging by formation of polysulfides, but growth rates in the experiments without iron might have been underestimated due to differing elemental sulfur amounts. In the absence of iron, also indications of direct microbial disproportionation of polysulfides were found. Overall, the evidence of microbial elemental sulfur disproportionation under alkaline conditions in the absence of metals allows for a reevaluation of sulfur cycling in alkaline environments such as soda lakes and brings new insights in one of the oldest metabolic pathways in earth's history.

The reaction of dissolved sulfide with ferric (oxyhydr)oxides leads to a variety of sulfur and mineral transformation reactions, which finally may result in the formation of thermodynamically stable pyrite. Up to now, pyrite formation was considered as process proceeding in the aqueous phase. Nevertheless, in the present study (study 2: Wan et al., 2014) the occurrence of polysulfides as possible pyrite precursors was observed almost exclusively at iron mineral surfaces. Polysulfide concentrations were higher in solutions with excess iron in comparison to solutions with excess sulfide, and polysulfide and elemental sulfur concentrations increased with the reactivity of the iron mineral. It was concluded that pyrite formation proceeds directly from surface Fe(II)-disulfide associations or by reaction of surface-bound disulfide with FeS from solution. The reported findings might be of relevance for a variety of processes in the sulfur cycle. Fe(II)-polysulfides as pyrite precursors might for example be important in the course of denitrification processes in systems where thermodynamically stable pyrite did not yet form. Additionally, surface-associated polysulfides might be more stable than polysulfides in solution and therefore could serve as reservoir for microorganisms. In general, it can be concluded that the occurrence of polysulfides has to be considered not only in the aqueous phase but also associated to mineral surfaces.

In the process of indirect ferrihydrite reduction by the sulfur-reducing bacterium *S. deleyianum*, thiosulfate, elemental sulfur, or polysulfides were assumed to serve as electron shuttling compounds

but were not identified in a previous study. In our experiments (study 3: Lohmayer et al., 2014), elemental sulfur attached to the mineral surface was found to be the major sulfur oxidation product and consequently was supposed to be primarily responsible for the electron shuttling process between the bacteria and the iron mineral. For the entire process, direct physical contact between the bacteria and the iron mineral seemed to be necessary, which is in contrast to earlier findings. Small amounts of polysulfides were detected in the course of microbial thiosulfate reduction and in experiments with low iron to sulfur excess. Polysulfides were found, apart from thiosulfate, tetrathionate, sulfite, and sulfide, to be able to initiate the electron shuttling process but obviously were not dominating the shuttling process itself. However, this also might have been due to specific iron mineral properties since the reactivity of iron minerals was found to influence sulfur oxidation products in the previously described study. In general, our study provides details concerning sulfur redox processes in the course of microbially mediated ferric mineral reduction, which is of major importance for the biogeochemical iron cycle and consequently also for the availability and mobility of different nutrients and contaminants in the environment.

The formation of soluble arsenic-sulfur species has been studied for more than one hundred years. Previously, arsenite and sulfide were found to react to thioarsenites, which in turn were oxidized to thioarsenates. Moreover, thioarsenates were suggested to form from the reaction of arsenite with polysulfides. At conditions, where thioarsenite formation was prevented due to excess of OH^- versus SH^- , we found that arsenite and polysulfides reacted almost exclusively to monothioarsenate (study 4: Planer-Friedrich et al., 2015). The formation of higher thiolated arsenates was accelerated in the presence of polysulfides in comparison to the presence of sulfide probably because of faster thioarsenite formation due to the higher nucleophilicity of polysulfides. Whether the formation of higher thiolated arsenates also is possible by ligand exchange starting from monothioarsenate could not be determined. In the course of arsenate reduction coupled to sulfide oxidation by the anaerobic haloalkaliphile MLMS-1, the subsequent formation of polysulfides and monothioarsenate was observed. This confirms the results of the abiotic experiment also for biotic systems. Moreover, monothioarsenate could be disproportionated microbially, which resulted in the formation of arsenite and polysulfides. Overall, polysulfides were found to play a crucial role especially for monothioarsenate formation. In general, thioarsenates are not only relevant in extreme environments, such as soda lakes, but may also be formed under sulfate-reducing conditions in the groundwater. Since, e.g., the extent of sorption to iron minerals varies between the different arsenic species, extensive knowledge about processes of thioarsenate formation is extremely important for evaluating arsenic mobility in the environment.

Previously, thioarsenate transformation processes were found to be influenced by sulfur redox chemistry and to be accelerated substantially in the presence of microorganisms, however, details concerning reaction pathways remained to be elucidated. In the present study (study 5: Härtig et al., 2014), we found evidence that under high temperature and oxic conditions desulfidation of

monothioarsenate took place resulting in the formation of arsenate and sulfide, which subsequently was oxidized to elemental sulfur and thiosulfate. The presence of the hyperthermophile bacterium *T. ruber* led to a considerable increase in rate and extent of monothioarsenate transformation. This was attributed mainly to a shift in chemical equilibrium by microbial oxidation of abiotically produced intermediate sulfur species to sulfate. Polysulfides did not play a crucial role for monothioarsenate transformation under the chosen experimental conditions. Furthermore, evidence for direct microbial use of sulfur bound in monothioarsenate was found. Overall, it can be concluded that thioarsenates themselves or a variety of arsenic or sulfur transformation products can serve as electron donors or acceptors for microorganisms. Thioarsenate transformation kinetics seems to depend strongly on the rate and extent of sulfur oxidation processes. Finally, sulfur redox processes are decisive for arsenic speciation and consequently also for arsenic mobility in the environment.

The formation of thio-species is also crucial for the mobility of molybdenum in the environment, since thiomolybdates were assumed to play a key role for molybdenum precipitation under euxinic conditions. However, thiomolybdates have so far never been determined in natural samples. In our study (study 6: Lohmayer et al., 2015), we found that, in the laboratory, rate and extent of molybdate thiolation increased with increasing sulfide to molybdate excess and that a neutral pH was most favorable for the ligand exchange of SH^- versus OH^- by nucleophilic substitution. The presence of polysulfides did not have any effect on thiomolybdate formation and evidence for a previously determined reaction of trithiomolybdate with zero-valent sulfur could not be found. In order to analyze thiomolybdates in natural samples, a previously published analytical method was adapted so that IPC-ICP-MS could be used for determination of nanomolar thiomolybdate concentrations. In natural samples, matrix components were found to have a disturbing effect on analysis and further method optimization is necessary. However, the spontaneous formation of mono- to tetrathiomolybdate was observed in a molybdate spiked euxinic bottom water sample of Lake Rogoznica, for which the natural predominance of thermodynamic stable tetrathiomolybdate was predicted. For geothermal hot springs in Yellowstone National Park, the first evidence of thiomolybdate occurrence in the environment could be provided. Tetrathiomolybdate was by far the most dominant thiomolybdate species but also the intermediate thiomolybdates could be observed. Especially in systems not in equilibrium or underlying seasonal variations, the occurrence of intermediate thiomolybdates might be of importance. The newly developed method is the basis for thiomolybdate determination in the environment. Detailed information about natural thiomolybdate occurrence will help to elucidate reaction pathways of molybdenum burial in sediments and therefore is important for reconstructing paleoenvironmental conditions. Moreover, increasing knowledge about the formation and transformation of thiomolybdates in the environment is decisive for understanding the molybdenum-sulfur cycle in nature.

Overall, polysulfides were found to occur in the aqueous phase and to be decisive for microbial growth and sulfur redox processes. Moreover, polysulfides were seen to influence the speciation of

Conclusions

metal(loid)s, to occur on mineral surfaces and therefore play an important role for mineral transformation processes. Different sulfur species were detected to serve as electron shuttling compounds, to influence species transformation processes and consequently be decisive for the reactivity and mobility of metal(loid)s. As sulfur exists in a wide variety of oxidation states and occurs ubiquitously in nature, it is a major factor of influence for the occurrence and speciation of metal(loid)s. Therefore, extensive knowledge about sulfur speciation and redox processes helps to understand the biogeochemical cycling of metal(loid)s in the environment.

REFERENCES

- Afonso, M.D., Stumm, W. (1992): Reductive dissolution of iron(III) (hydr)oxides by hydrogen sulfide. *Langmuir* 8, 1671-1675.
- Amirbahman, A., Sigg, L., vonGunten, U. (1997): Reductive dissolution of Fe(III) (hydr)oxides by cysteine: Kinetics and mechanism. *Journal of Colloid and Interface Science* 194, 194-206.
- Bennett, B., Dudas, M.J. (2003): Release of arsenic and molybdenum by reductive dissolution of iron oxides in a soil with enriched levels of native arsenic. *Journal of Environmental Engineering and Science* 2, 265-272.
- Berner, R.A. (1982): Burial of organic carbon and pyrite sulfur in the modern ocean: Its geochemical and environmental significance. *American Journal of Science* 282, 451-473.
- Boulegue, J. (1978): Solubility of Elemental Sulfur in Water at 298 K. *Phosphorus Sulfur and Silicon and the Related Elements* 5, 127-128.
- Brauner, B., Tomíček, F. (1887): Über die Einwirkung von Schwefelwasserstoff auf Arsensäure. *Monatshefte für Chemie und verwandte Teile anderer Wissenschaften* 8, 607-625.
- Brønsted, J.N. (1928): Acid and Basic Catalysis. *Chemical Reviews* 5, 231-338.
- Canfield, D.E., Thamdrup, B., Fleischer, S. (1998): Isotope fractionation and sulfur metabolism by pure and enrichment cultures of elemental sulfur-disproportionating bacteria. *Limnology and Oceanography* 43, 253-264.
- Castaneda-Agullo, M., Del Castillo, L.M., Whitaker, J.R., Tappel, A.L. (1961): Effect of Ionic Strength on Kinetics of Trypsin and Alpha Chymotrypsin. *Journal of General Physiology* 44, 1103-1120.
- Chen, K.Y., Morris, J.C. (1972): Kinetics of Oxidation of Aqueous Sulfide by O₂. *Environmental Science & Technology* 6, 529-537.
- Church, C.D., Wilkin, R.T., Alpers, C.N., Rye, R.O., McCleskey, R.B. (2007): Microbial sulfate reduction and metal attenuation in pH 4 acid mine water. *Geochemical Transactions* 8, 1-14.
- Cloke, P.L. (1963): The geologic role of polysulfides – Part I. The distribution of ionic species in aqueous sodium polysulfide solutions. *Geochimica et Cosmochimica Acta* 27, 1265-1298.
- Collier, R.W. (1985): Molybdenum in the Northeast Pacific Ocean. *Limnology and Oceanography* 30, 1351-1354.
- Crusius, J., Calvert, S., Pedersen, T., Sage, D. (1996): Rhenium and molybdenum enrichments in sediments as indicators of oxic, suboxic and sulfidic conditions of deposition. *Earth and Planetary Science Letters* 145, 65-78.
- Cullen, W.R., Reimer, K.J. (1989): Arsenic speciation in the environment. *Chemical Reviews* 89, 713-764.
- Dahl, T.W., Chappaz, A., Fitts, J.P., Lyons, T.W. (2013): Molybdenum reduction in a sulfidic lake: Evidence from X-ray absorption fine-structure spectroscopy and implications for the Mo paleoproxy. *Geochimica et Cosmochimica Acta* 103, 213-231.
- Doong, R.A., Schink, B. (2002): Cysteine-mediated reductive dissolution of poorly crystalline iron(III) oxides by *Geobacter sulfurreducens*. *Environmental Science & Technology* 36, 2939-2945.
- Druschel, G.K., Hamers, R.J., Banfield, J.F. (2003): Kinetics and mechanism of polythionate oxidation to sulfate at low pH by O₂ and Fe³⁺. *Geochimica et Cosmochimica Acta* 67, 4457-4469.
- Eisenmann, E., Beuerle, J., Sulger, K., Kroneck, P.M.H., Schumacher, W. (1995): Lithotrophic growth of *Sulfurospirillum deleyianum* with sulfide as electron donor coupled to respiratory reduction of nitrate to ammonia. *Archives of Microbiology* 164, 180-185.
- Erickson, B.E., Helz, G.R. (2000): Molybdenum(VI) speciation in sulfidic waters: Stability and lability of thiomolybdates. *Geochimica et Cosmochimica Acta* 64, 1149-1158.
- Finster, K. (2008): Microbiological disproportionation of inorganic sulfur compounds. *Journal of Sulfur Chemistry* 29, 281-292.
- Finster, K., Liesack, W., Thamdrup, B. (1998): Elemental sulfur and thiosulfate disproportionation by *Desulfocapsa sulfoexigens* sp nov, a new anaerobic bacterium isolated from marine surface sediment. *Applied and Environmental Microbiology* 64, 119-125.
- Fisher, J.C., Wallschläger, D., Planer-Friedrich, B., Hollibaugh, J.T. (2008): A new role for sulfur in arsenic cycling. *Environmental Science & Technology* 42, 81-85.

- Franz, B., Lichtenberg, H., Hormes, J., Modrow, H., Dahl, C., Prange, A. (2007): Utilization of solid 'elemental' sulfur by the phototrophic purple sulfur bacterium *Allochromatium vinosum*: a sulfur K-edge X-ray absorption spectroscopy study. *Microbiology-Sgm* 153, 1268-1274.
- Giggenbach, W.F. (1972): Optical Spectra and Equilibrium Distribution of Polysulfide Ions in Aqueous Solution at 20 Degrees. *Inorganic Chemistry* 11, 1201-1207.
- Goifman, A., Ryzkov, D., Gun, J., Kamyshny, A., Jr., Modestov, A.D., Lev, O. (2004): Inorganic polysulfides' quantitation by methyl iodide derivatization: dimethylpolysulfide formation potential. *Water Science and Technology* 49, 179-184.
- Gorski, C.A., Scherer, M.M. (2011): Fe²⁺ sorption at the Fe oxide-water interface: a revised conceptual framework, In: *Aquatic Redox Chemistry*. American Chemical Society, pp. 315-343.
- Grimm, F., Franz, B., Dahl, C. (2008): Thiosulfate and Sulfur Oxidation in Purple Sulfur Bacteria, In: Dahl, C., Friedrich, C. (Eds.) *Microbial Sulfur Metabolism*. Springer Berlin Heidelberg, pp. 101-116.
- Gun, J., Goifman, A., Shkrob, I., Kamyshny, A., Ginzburg, B., Hadas, O., Dor, I., Modestov, A.D., Lev, O. (2000): Formation of polysulfides in an oxygen rich freshwater lake and their role in the production of volatile sulfur compounds in aquatic systems. *Environmental Science & Technology* 34, 4741-4746.
- Gun, J., Modestov, A.D., Kamyshny, A., Ryzkov, D., Gitis, V., Goifman, A., Lev, O., Hultsch, V., Grischek, T., Worch, E. (2004): Electrospray ionization mass spectrometric analysis of aqueous polysulfide solutions. *Microchimica Acta* 146, 229-237.
- Harmer, M.A., Sykes, A.G. (1980): Kinetics of the Interconversion of Sulfido- and Oxomolybdate(VI) Species MoO_xS_{4-x}²⁻ in Aqueous Solutions. *Inorganic Chemistry* 19, 2881-2885.
- Härtig, C., Lohmayer, R., Kolb, S., Horn, M.A., Inskeep, W.P., Planer-Friedrich, B. (2014): Chemolithotrophic growth of the aerobic hyperthermophilic bacterium *Thermocrinis ruber* OC 14/7/2 on monothioarsenate and arsenite. *FEMS Microbiology Ecology* 90, 747-760.
- Härtig, C., Planer-Friedrich, B. (2012): Thioarsenate Transformation by Filamentous Microbial Mats Thriving in an Alkaline, Sulfidic Hot Spring. *Environmental Science & Technology* 46, 4348-4356.
- Hartler, N., Libert, J., Teder, A. (1967): Rate of sulfur dissolution in aqueous sodium sulfide. *Industrial & Engineering Chemistry Process Design and Development* 6, 398-406.
- Hellige, K., Pollok, K., Larese-Casanova, P., Behrends, T., Peiffer, S. (2012): Pathways of ferrous iron mineral formation upon sulfidation of lepidocrocite surfaces. *Geochimica et Cosmochimica Acta* 81, 69-81.
- Helz, G.R., Bura-Nakić, E., Mikac, N., Ciglencić, I. (2011): New model for molybdenum behavior in euxinic waters. *Chemical Geology* 284, 323-332.
- Helz, G.R., Tossell, J.A. (2008): Thermodynamic model for arsenic speciation in sulfidic waters: A novel use of ab initio computations. *Geochimica et Cosmochimica Acta* 72, 4457-4468.
- Hoelt, S.E., Kulp, T.R., Stolz, J.F., Hollibaugh, J.T., Oremland, R.S. (2004): Dissimilatory arsenate reduction with sulfide as electron donor: Experiments with mono lake water and isolation of strain MLMS-1, a chemoautotrophic arsenate respirer. *Applied and Environmental Microbiology* 70, 2741-2747.
- Hofmann, A.F., Fronczek, D.N., Bessler, W.G. (2014): Mechanistic modeling of polysulfide shuttle and capacity loss in lithium-sulfur batteries. *Journal of Power Sources* 259, 300-310.
- Hollibaugh, J.T., Carini, S., Gurleyuk, H., Jellison, R., Joye, S.B., LeClerc, G., Meile, C., Vasquez, L., Wallschlager, D. (2005): Arsenic speciation in Mono lake, California: Response to seasonal stratification and anoxia. *Geochimica et Cosmochimica Acta* 69, 1925-1937.
- Huber, R., Eder, W., Heldwein, S., Wanner, G., Huber, H., Rachel, R., Stetter, K.O. (1998): *Thermocrinis ruber* gen. nov., sp. nov., a Pink-Filament-Forming Hyperthermophilic Bacterium Isolated from Yellowstone National Park. *Applied and Environmental Microbiology* 64, 3576-3583.
- Jorgensen, B.B. (1990): The sulfur cycle of freshwater sediments: Role of thiosulfate. *Limnology and Oceanography* 35, 1329-1342.
- Jormakka, M., Yokoyama, K., Yano, T., Tamakoshi, M., Akimoto, S., Shimamura, T., Curmi, P., Iwata, S. (2008): Molecular mechanism of energy conservation in polysulfide respiration. *Nature Structural & Molecular Biology* 15, 730-737.

- Jovanovski, V., Gonzalez-Pedro, V., Gimenez, S., Azaceta, E., Cabanero, G., Grande, H., Tena-Zaera, R., Mora-Sero, I., Bisquert, J. (2011): A Sulfide/Polysulfide-Based Ionic Liquid Electrolyte for Quantum Dot-Sensitized Solar Cells. *Journal of the American Chemical Society* 133, 20156-20159.
- Kaasalainen, H., Stefansson, A. (2012): The chemistry of trace elements in surface geothermal waters and steam, Iceland. *Chemical Geology* 330, 60-85.
- Kage, S., Nagata, T., Kudo, K. (1991): Determination of polysulphides in blood by gas chromatography and gas chromatography-mass spectrometry *Journal of Chromatography-Biomedical Applications* 564, 163-169.
- Kamyshny, A., Ekel'tchik, I., Gun, J., Lev, O. (2006): Method for the determination of inorganic polysulfide distribution in aquatic systems. *Analytical Chemistry* 78, 2631-2639.
- Kamyshny, A., Goifman, A., Gun, J., Rizkov, D., Lev, O. (2004): Equilibrium distribution of polysulfide ions in aqueous solutions at 25 degrees C: A new approach for the study of polysulfides equilibria. *Environmental Science & Technology* 38, 6633-6644.
- Kamyshny, A., Goifman, A., Rizkov, D., Lev, O. (2003): Kinetics of disproportionation of inorganic polysulfides in undersaturated aqueous solutions at environmentally relevant conditions. *Aquatic Geochemistry* 9, 291-304.
- Kamyshny, A., Gun, J., Rizkov, D., Voitsekovski, T., Lev, O. (2007): Equilibrium distribution of polysulfide ions in aqueous solutions at different temperatures by rapid single phase derivatization. *Environmental Science & Technology* 41, 2395-2400.
- Kamyshny, A., Zerkle, A.L., Mansaray, Z.F., Ciglencečki, I., Bura-Nakić, E., Farquhar, J., Ferdelman, T.G. (2011): Biogeochemical sulfur cycling in the water column of a shallow stratified sea-water lake: Speciation and quadruple sulfur isotope composition. *Marine Chemistry* 127, 144-154.
- Kariuki, S., Morra, M.J., Umiker, K.J., Cheng, I.F. (2001): Determination of total ionic polysulfides by differential pulse polarography. *Analytica Chimica Acta* 442, 277-285.
- Kletzin, A. (2008): Oxidation of Sulfur and Inorganic Sulfur Compounds in *Acidianus ambivalens*, In: Dahl, C., Friedrich, C.G. (Eds.) *Microbial Sulfur Metabolism*. Springer Berlin Heidelberg, pp. 184-201.
- Klimmek, O., Kroger, A., Steudel, R., Holdt, G. (1991): Growth of *Wolinella succinogenes* with polysulfide as terminal acceptor of phosphorylative electron transport. *Archives of Microbiology* 155, 177-182.
- LaLonde, R.T., Ferrara, L.M., Hayes, M.P. (1987): Low-temperature, polysulfide reactions of conjugated ene carbonyls: A reaction model for the geologic origin of S-heterocycles. *Organic Geochemistry* 11, 563-571.
- Li, Z., Ma, H., Kubes, G.J., Li, J. (1998): Synergistic effect of kraft pulping with polysulphide and anthraquinone on pulp-yield improvement. *Journal of Pulp and Paper Science* 24, 237-241.
- Liu, Y.W., Denkmann, K., Kosciow, K., Dahl, C., Kelly, D.J. (2013): Tetrathionate stimulated growth of *Campylobacter jejuni* identifies a new type of bi-functional tetrathionate reductase (TsdA) that is widely distributed in bacteria. *Molecular Microbiology* 88, 173-188.
- Lohmayer, R., Kappler, A., Lösekann-Behrens, T., Planer-Friedrich, B. (2014): Sulfur Species as Redox Partners and Electron Shuttles for Ferrihydrite Reduction by *Sulfurospirillum deleyianum*. *Applied and Environmental Microbiology* 80, 3141-3149.
- Lohmayer, R., Reithmaier, G.M.S., Bura-Nakić, E., Planer-Friedrich, B. (2015): Ion-Pair Chromatography Coupled to Inductively Coupled Plasma-Mass Spectrometry (IPC-ICP-MS) as a Method for Thiomolybdate Speciation in Natural Waters. *Analytical Chemistry* 87, 3388-3395.
- Luther, G.W. (1990): The frontier-molecular-orbital theory approach in geochemical processes, In: Stumm, W. (Ed.) *Aquatic Chemical Kinetics*. John Wiley & Sons, New York, pp. 173-198.
- Luther, G.W. (1991): Pyrite synthesis via polysulfide compounds. *Geochimica et Cosmochimica Acta* 55, 2839-2849.
- Luther, G.W. (2010): The Role of One- and Two-Electron Transfer Reactions in Forming Thermodynamically Unstable Intermediates as Barriers in Multi-Electron Redox Reactions. *Aquatic Geochemistry* 16, 395-420.
- Luther, G.W., Findlay, A.J., MacDonald, D.J., Owings, S.M., Hanson, T.E., Beinart, R.A., Girguis, P.R. (2011): Thermodynamics and kinetics of sulfide oxidation by oxygen: a look at

- inorganically controlled reactions and biologically mediated processes in the environment. *Frontiers in Microbiology* 2, 1-9.
- Lyons, D., Nickless, G. (1968): The lower oxy-acids of sulphur, In: Nickless, G. (Ed.) *Inorganic Sulphur Chemistry*. Elsevier, New York, pp. 509-534.
- Ma, S.F., Noble, A., Butcher, D., Trouwborst, R.E., Luther, G.W. (2006): Removal of H₂S via an iron catalytic cycle and iron sulfide precipitation in the water column of dead end tributaries. *Estuarine Coastal and Shelf Science* 70, 461-472.
- McCay, L.W. (1888): Die Einwirkung von Schwefelwasserstoff auf Arsensäure. *Zeitschrift für analytische Chemie* 27, 632-634.
- McCay, L.W., Foster, W. (1904): Über die Trisulfoxyarsensäure. *Zeitschrift für anorganische Chemie* 41, 452-473.
- Melton, E.D., Swanner, E.D., Behrens, S., Schmidt, C., Kappler, A. (2014): The interplay of microbially mediated and abiotic reactions in the biogeochemical Fe cycle. *Nature Reviews Microbiology* 12, 797-808.
- Meyer, B. (1964): Solid allotropes of sulfur. *Chemical Reviews* 64, 429-451.
- Milucka, J., Ferdelman, T.G., Polerecky, L., Franzke, D., Wegener, G., Schmid, M., Lieberwirth, I., Wagner, M., Widdel, F., Kuypers, M.M.M. (2012): Zero-valent sulphur is a key intermediate in marine methane oxidation. *Nature* 491, 541-546.
- Moses, C.O., Nordstrom, D.K., Mills, A.L. (1984): Sampling and analysing mixtures of sulphate, sulphite, thiosulphate and polythionate. *Talanta* 31, 331-339.
- Müller, A., Glemser, O., Diemann, E., Hofmeister, H. (1969): Transition metal chalcogen compounds. Formation and decomposition of transition metal chalcogen anions in aqueous solution. *Zeitschrift für Anorganische und Allgemeine Chemie* 371, 74-80.
- Muyzer, G., Stams, A.J.M. (2008): The ecology and biotechnology of sulphate-reducing bacteria. *Nature Reviews Microbiology* 6, 441-454.
- Nicholls, P., Kim, J.K. (1982): Sulfide as an inhibitor and electron donor for the cytochrome c oxidase system. *Canadian Journal of Biochemistry* 60, 613-623.
- Overmann, J., Beatty, J.T., Krouse, H.R., Hall, K.J. (1996): The sulfur cycle in the chemocline of a meromictic salt lake. *Limnology and Oceanography* 41, 147-156.
- Peiffer, S., Behrends, T., Hellige, K., Larese-Casanova, P., Wan, M., Pollok, K. (2015): Pyrite formation and mineral transformation pathways upon sulfidation of ferric hydroxides depend on mineral type and sulfide concentration. *Chemical Geology* 400, 44-55.
- Peiffer, S., Gade, W. (2007): Reactivity of ferric oxides toward H₂S at low pH. *Environmental Science & Technology* 41, 3159-3164.
- Piepenbrock, A., Dippon, U., Porsch, K., Appel, E., Kappler, A. (2011): Dependence of microbial magnetite formation on humic substance and ferrihydrite concentrations. *Geochimica et Cosmochimica Acta* 75, 6844-6858.
- Pizarro, J., Rubio, M.A., Rios, E., Vila, I. (2014): Concentration level of molybdenum in aquatic systems. *Fresenius Environmental Bulletin* 23, 159-168.
- Planer-Friedrich, B., Fisher, J.C., Hollibaugh, J.T., Suss, E., Wallschläger, D. (2009): Oxidative Transformation of Trithioarsenate Along Alkaline Geothermal Drainages: Abiotic versus Microbially Mediated Processes. *Geomicrobiology Journal* 26, 339-350.
- Planer-Friedrich, B., Härtig, C., Lohmayer, R., Suess, E., McCann, S.H., Oremland, R. (2015): Anaerobic Chemolithotrophic Growth of the Haloalkaliphilic Bacterium Strain MLMS-1 by Disproportionation of Monothioarsenate. *Environmental Science & Technology*.
- Planer-Friedrich, B., London, J., McCleskey, R.B., Nordstrom, D.K., Wallschläger, D. (2007): Thioarsenates in geothermal waters of Yellowstone National Park: Determination, preservation, and geochemical importance. *Environmental Science & Technology* 41, 5245-5251.
- Planer-Friedrich, B., Suess, E., Scheinost, A.C., Wallschläger, D. (2010): Arsenic Speciation in Sulfidic Waters: Reconciling Contradictory Spectroscopic and Chromatographic Evidence. *Analytical Chemistry* 82, 10228-10235.
- Planer-Friedrich, B., Wallschläger, D. (2009): A Critical Investigation of Hydride Generation-Based Arsenic Speciation in Sulfidic Waters. *Environmental Science & Technology* 43, 5007-5013.

- Poser, A., Lohmayer, R., Vogt, C., Knoeller, K., Planer-Friedrich, B., Sorokin, D., Richnow, H.-H., Finster, K. (2013): Disproportionation of elemental sulfur by haloalkaliphilic bacteria from soda lakes. *Extremophiles* 17, 1003-1012.
- Poulton, S.W. (2003): Sulfide oxidation and iron dissolution kinetics during the reaction of dissolved sulfide with ferrihydrite. *Chemical Geology* 202, 79-94.
- Poulton, S.W., Krom, M.D., Raiswell, R. (2004): A revised scheme for the reactivity of iron (oxyhydr)oxide minerals towards dissolved sulfide. *Geochimica et Cosmochimica Acta* 68, 3703-3715.
- Reid, R.S., Clark, R.J., Quagraine, E.K. (2007): Accurate UV-visible spectral analysis of thiomolybdates. *Canadian Journal of Chemistry* 85, 1083-1089.
- Rickard, D., Luther, G.W. (2007): Chemistry of iron sulfides. *Chemical Reviews* 107, 514-562.
- Rickard, D.T. (1975): Kinetics and mechanism of pyrite formation at low temperatures. *American Journal of Science* 275, 636-652.
- Rizkov, D., Lev, O., Gun, J., Anisimov, B., Kuselman, I. (2004): Development of in-house reference materials for determination of inorganic polysulfides in water. *Accreditation and Quality Assurance* 9, 399-403.
- Rochette, E.A., Bostick, B.C., Li, G.C., Fendorf, S. (2000): Kinetics of arsenate reduction by dissolved sulfide. *Environmental Science & Technology* 34, 4714-4720.
- Roy, A.B., Trudinger, P.A. (1970): *The Biochemistry of Inorganic Compounds of Sulphur*. Cambridge University Press, London and New York.
- Rozan, T.F., Theberge, S.M., Luther, G.W. (2000): Quantifying elemental sulfur (S⁰), bisulfide (HS⁻) and polysulfides (S_x²⁻) using a voltammetric method. *Analytica Chimica Acta* 415, 175-184.
- Saalfeld, S.L., Bostick, B.C. (2009): Changes in iron, sulfur, and arsenic speciation associated with bacterial sulfate reduction in ferrihydrite-rich systems. *Environmental Science & Technology* 43, 8787-8793.
- Schauder, R., Müller, E. (1993): Polysulfide as a possible substrate for sulfur-reducing bacteria. *Archives of Microbiology* 160, 377-382.
- Scheele, C.W. (1777): *Chemische Abhandlung von der Luft und dem Feuer*. Swederus, Crusius, Upsala, Leipzig.
- Schoonen, M.A.A. (2004): Mechanisms of sedimentary pyrite formation. *Geological Society of America Special Papers* 379, 117-134.
- Schumacher, W., Kroneck, P.M.H., Pfennig, N. (1992): Comparative systematic study on "Spirillum" 5175, *Campylobacter* and *Wolinella* species - Description of "Spirillum" 5175 as *Sulfurospirillum deleyianum* gen. nov., spec. nov. *Archives of Microbiology* 158, 287-293.
- Schwarz, G., Mendel, R.R., Ribbe, M.W. (2009): Molybdenum cofactors, enzymes and pathways. *Nature* 460, 839-847.
- Schwarzenbach, G., Fischer, A. (1960): Die Acidität der Sulfane und die Zusammensetzung wässriger Polysulfidlösungen. *Helvetica Chimica Acta* 43, 1365-1390.
- Schwedt, G., Rieckhoff, M. (1996): Separation of thio- and oxothioarsenates by capillary zone electrophoresis and ion chromatography. *Journal of Chromatography A* 736, 341-350.
- Simon, J., Kroneck, P.M.H. (2013): Microbial Sulfite Respiration, In: Poole, R.K. (Ed.) *Advances in Microbial Physiology*, Vol 62. Academic Press Ltd-Elsevier Science Ltd, London, pp. 45-117.
- Sorokin, D.Y., Tourova, T.P., Henstra, A.M., Stams, A.J.M., Galinski, E.A., Muyzer, G. (2008a): Sulfidogenesis under extremely haloalkaline conditions by *Desulfonatronospira thiodismutans* gen. nov., sp nov., and *Desulfonatronospira delicata* sp. nov. - a novel lineage of *Deltaproteobacteria* from hypersaline soda lakes. *Microbiology-Sgm* 154, 1444-1453.
- Sorokin, D.Y., Tourova, T.P., Mussmann, M., Muyzer, G. (2008b): *Dethiobacter alkaliphilus* gen. nov sp nov., and *Desulfurivibrio alkaliphilus* gen. nov sp nov.: two novel representatives of reductive sulfur cycle from soda lakes. *Extremophiles* 12, 431-439.
- Stanton, M.R., Goldhaber, M.B. (1991): An Experimental Study of Goethite Sulfidization: Relationships to the Diagenesis of Iron and Sulfur, In: Tuttle, M.L. (Ed.) *Geochemical, Biogeochemical, and Sedimentological Studies of the Green River Formation, Wyoming, Utah, and Colorado*. U.S. Geological Survey, Denver, Colorado.
- Stauder, S., Raue, B., Sacher, F. (2005): Thioarsenates in sulfidic waters. *Environmental Science & Technology* 39, 5933-5939.

- Steudel, R. (1996): Mechanism for the formation of elemental sulfur from aqueous sulfide in chemical and microbiological desulfurization processes. *Industrial & Engineering Chemistry Research* 35, 1417-1423.
- Steudel, R. (2002): The chemistry of organic polysulfanes R-S_n-R (n > 2). *Chemical Reviews* 102, 3905-3945.
- Steudel, R. (2003): Inorganic Polysulfides S_n²⁻ and Radical Anions S_n^{·-}. *Elemental Sulfur and Sulfur-Rich Compounds II* 231, 127-152.
- Steudel, R., Holdt, G., Gobel, T. (1989): Ion-pair chromatographic-separation of inorganic sulphur anions including polysulphide. *Journal of Chromatography* 475, 442-446.
- Steudel, R., Holdt, G., Nagorka, R. (1986): Sulfur-compounds.104. On the autoxidation of aqueous sodium polysulfide. *Zeitschrift Fur Naturforschung Section B-a Journal of Chemical Sciences* 41, 1519-1522.
- Straub, K.L., Schink, B. (2004): Ferrihydrite-dependent growth of *Sulfurospirillum deleyianum* through electron transfer via sulfur cycling. *Applied and Environmental Microbiology* 70, 5744-5749.
- Strauss, H. (2004): 4 Ga of seawater evolution: Evidence from the sulfur isotopic composition of sulfate. *Geological Society of America Special Papers* 379, 195-205.
- Suess, E., Scheinost, A.C., Bostick, B.C., Merkel, B.J., Wallschläger, D., Planer-Friedrich, B. (2009): Discrimination of Thioarsenites and Thioarsenates by X-ray Absorption Spectroscopy. *Analytical Chemistry* 81, 8318-8326.
- Szczepkowski, T.W. (1958): Reactions of thiosulphate with cysteine. *Nature* 182, 934-935.
- Teder, A. (1971): The Equilibrium Between Elementary Sulfur and Aqueous Polysulfide Solutions. *Acta Chemica Scandinavica* 25, 1722-1728.
- Thamdrup, B., Finster, K., Hansen, J.W., Bak, F. (1993): Bacterial Disproportionation of Elemental Sulfur Coupled to Chemical-Reduction of Iron or Manganese. *Applied and Environmental Microbiology* 59, 101-108.
- Thilo, E., Hertzog, K., Winkler, A. (1970): Über Vorgänge bei der Bildung des Arsen(V)-sulfids beim Ansäuern von Tetrathioarsenatlösungen. *Zeitschrift für Anorganische und Allgemeine Chemie* 373, 111-121.
- Uddin, Z., Markuszewski, R., Johnson, D.C. (1987): Determination of Inorganic Sulfur Species in Highly Alkaline Solutions by Liquid Chromatography with Polarographic Detection. *Analytica Chimica Acta* 200, 115-129.
- Umiker, K.J., Morra, M.J., Cheng, I.F. (2002): Aqueous sulfur species determination using differential pulse polarography. *Microchemical Journal* 73, 287-297.
- Vairavamurthy, A., Manowitz, B., Luther, G.W., Jeon, Y. (1993): Oxidation state of sulfur in thiosulfate and implications for anaerobic energy metabolism. *Geochimica et Cosmochimica Acta* 57, 1619-1623.
- Vorliceck, T.P., Kahn, M.D., Kasuya, Y., Helz, G.R. (2004): Capture of molybdenum in pyrite-forming sediments: Role of ligand-induced reduction by polysulfides. *Geochimica et Cosmochimica Acta* 68, 547-556.
- Wallschläger, D., Staley, C.J. (2007): Determination of (oxy)thioarsenates in sulfidic waters. *Analytical Chemistry* 79, 3873-3880.
- Wan, M.L., Shchukarev, A., Lohmayer, R., Planer-Friedrich, B., Peiffer, S. (2014): Occurrence of Surface Polysulfides during the Interaction between Ferric (Hydr)Oxides and Aqueous Sulfide. *Environmental Science & Technology* 48, 5076-5084.
- Wang, X.M., Liu, F., Tan, W.F., Li, W., Feng, X.H., Sparks, D.L. (2013): Characteristics of phosphate adsorption-desorption onto ferrihydrite: Comparison with well-crystalline Fe (hydr)oxides. *Soil Science* 178, 1-11.
- Wedepohl, K.H. (1984): Sulfur in the Earth's Crust, Its Origin and Natural Cycle, In: Müller, A., Krebs, B. (Eds.) *Sulfur, its Significance for Chemistry, for the Geo-, Bio-, and Cosmosphere and Technology*. Elsevier, Amsterdam, pp. 39-54.
- Weiss, J., Möckel, H.J., Müller, A., Diemann, E., Walberg, H.J. (1988): Retention of thiometalates and selenometalates in mobile-phase ion chromatography. *Journal of Chromatography* 439, 93-108.
- Wentzien, S., Sand, W., Albertsen, A., Steudel, R. (1994): Thiosulfate and tetrathionate degradation as well as biofilm generation by *Thiobacillus intermedius* and *Thiobacillus versutus* studied by

- microcalorimetry, HPLC, and ion-pair chromatography. *Archives of Microbiology* 161, 116-125.
- Wildervanck, J.C., Jellinek, F. (1964): Preparation and Crystallinity of Molybdenum and Tungsten Sulfides. *Zeitschrift für Anorganische und Allgemeine Chemie* 328, 309-318.
- Wilkin, R.T., Wallschläger, D., Ford, R.G. (2003): Speciation of arsenic in sulfidic waters. *Geochemical Transactions* 4, 1-7.
- Williams, R.J.P., da Silva, J.J.R.F. (2002): The involvement of molybdenum in life. *Biochemical and Biophysical Research Communications* 292, 293-299.
- Wolfe, R.S., Pfennig, N. (1977): Reduction of sulfur by *Spirillum* 5175 and syntrophism with *Chlorobium*. *Applied and Environmental Microbiology* 33, 427-433.
- Xu, Y., Schoonen, M.A.A. (1995): The stability of thiosulfate in the presence of pyrite in low-temperature aqueous solutions. *Geochimica et Cosmochimica Acta* 59, 4605-4622.

CONTRIBUTION TO THE DIFFERENT STUDIES

Study 1

Disproportionation of elemental sulfur by haloalkaliphilic bacteria from soda lakes

A. Poser	50 %	concepts, laboratory work, manuscript preparation
R. Lohmayer	20 %	polysulfide analysis, discussion of results, comments on manuscript
C. Vogt	10 %	concepts, discussion of results, comments on manuscript
K. Knoeller	5 %	discussion of results, comments on manuscript
B. Planer-Friedrich	2.5 %	discussion of results, comments on manuscript
D. Sorokin	2.5 %	provision of bacterial strains, discussion of results, comments on manuscript
H.-H. Richnow	5 %	concepts, discussion of results, comments on manuscript
K. Finster	5 %	provision of bacterial strains, discussion of results, comments on manuscript

Study 2

Occurrence of Surface Polysulfides during the Interaction between Ferric (Hydr)Oxides and Aqueous Sulfide

M. Wan	55 %	concepts, laboratory work, manuscript preparation
A. Shchukarev	10 %	XPS analysis, discussion of results, comments on manuscript
R. Lohmayer	10 %	HPLC polysulfide analysis, discussion of results
B. Planer-Friedrich	10 %	concepts, comments on manuscript
S. Peiffer	15 %	concepts, discussion of results, comments on manuscript

Study 3

Sulfur Species as Redox Partners and Electron Shuttles for Ferrihydrite Reduction by *Sulfurospirillum deleyianum*

R. Lohmayer	80 %	concepts, laboratory work, manuscript preparation
A. Kappler	5 %	concepts, provision of bacterial strain, discussion of results, comments on manuscript
T. Lösekann-Behrens	5 %	genome sequence analysis, comments on manuscript
B. Planer-Friedrich	10 %	concepts, discussion of results, comments on manuscript

Study 4**Anaerobic chemolithotrophic growth of the haloalkaliphilic bacterium strain MLMS-1 by disproportionation of monothioarsenate**

B. Planer-Friedrich	30 %	concepts, manuscript preparation
C. Härtig	30 %	concepts, laboratory work, cultivation of MLMS-1, IC-ICP-MS analysis, interpretation of data, discussion of results, manuscript preparation
R. Lohmayer	30 %	polysulfide analysis, monothioarsenate synthesis, interpretation of data, discussion of results, comments on manuscript
E. Suess	5 %	XAS analysis, interpretation of data, discussion of results, comments on manuscript
S. H. McCann	2.5 %	provision of bacterial strain, comments on manuscript
R. Oremland	2.5 %	discussion of results, comments on manuscript

Study 5**Chemolithotrophic growth of the aerobic hyperthermophilic bacterium *Thermocrinis ruber* OC 14/7/2 on monothioarsenate and arsenite**

C. Härtig	55 %	concepts, laboratory work, cultivation of <i>Thermocrinis ruber</i> , IC-ICP-MS analysis, interpretation of data, discussion of results, manuscript preparation
R. Lohmayer	20 %	polysulfide analysis, monothioarsenate synthesis, interpretation of data, discussion of results, comments on manuscript
S. Kolb	5 %	discussion of results, comments on manuscript
M. A. Horn	5 %	discussion of results, comments on manuscript
W. P. Inskeep	5 %	discussion of results, comments on manuscript
B. Planer-Friedrich	10 %	concepts, discussion of results, comments on manuscript

Study 6**Ion-Pair Chromatography Coupled to Inductively Coupled Plasma-Mass Spectrometry (IPC-ICP-MS) as a Method for Thiomolybdate Speciation in Natural Waters**

R. Lohmayer	85 %	concepts, laboratory work, manuscript preparation
G. M. S. Reithmaier	5 %	laboratory work, discussion of results
E. Bura-Nakić	5 %	discussion of results, comments on manuscript
B. Planer-Friedrich	5 %	concepts, discussion of results, comments on manuscript

APPENDIX – PUBLICATIONS

Study 1: Poser et al., 2013

Poser, A., Lohmayer, R., Vogt, C., Knoeller, K., Planer-Friedrich, B., Sorokin, D., Richnow, H.-H., Finster, K. (2013): Disproportionation of elemental sulfur by haloalkaliphilic bacteria from soda lakes. *Extremophiles* 17, 1003-1012.

Study 2: Wan et al., 2014

Wan, M.L., Shchukarev, A., Lohmayer, R., Planer-Friedrich, B., Peiffer, S. (2014): Occurrence of Surface Polysulfides during the Interaction between Ferric (Hydr)Oxides and Aqueous Sulfide. *Environmental Science & Technology* 48, 5076-5084.

Study 3: Lohmayer et al., 2014

Lohmayer, R., Kappler, A., Lösekann-Behrens, T., Planer-Friedrich, B. (2014): Sulfur Species as Redox Partners and Electron Shuttles for Ferrihydrite Reduction by *Sulfurospirillum deleyianum*. *Applied and Environmental Microbiology* 80, 3141-3149.

Study 4: Planer-Friedrich et al., 2015

Planer-Friedrich, B., Härtig, C., Lohmayer, R., Suess, E., McCann, S.H., Oremland, R. (2015): Anaerobic chemolithotrophic growth of the haloalkaliphilic bacterium strain MLMS-1 by disproportionation of monothioarsenate. *Environmental Science & Technology*.

Study 5: Härtig et al., 2014

Härtig, C., Lohmayer, R., Kolb, S., Horn, M.A., Inskeep, W.P., Planer-Friedrich, B. (2014): Chemolithotrophic growth of the aerobic hyperthermophilic bacterium *Thermocrinis ruber* OC 14/7/2 on monothioarsenate and arsenite. *FEMS Microbiology Ecology* 90, 747-760.

Study 6: Lohmayer et al., 2015

Lohmayer, R., Reithmaier, G.M.S., Bura-Nakić, E., Planer-Friedrich, B. (2015): Ion-Pair Chromatography Coupled to Inductively Coupled Plasma-Mass Spectrometry (IPC-ICP-MS) as a Method for Thiomolybdate Speciation in Natural Waters. *Analytical Chemistry* 87, 3388-3395.

Study 1

Reproduced with permission from

Disproportionation of elemental sulfur by haloalkaliphilic bacteria from soda lakes

Alexander Poser, Regina Lohmayer, Carsten Vogt, Kay Knoeller, Britta Planer-Friedrich,
Dimitry Sorokin, Hans-H. Richnow, Kai Finster

Extremophiles, 2013, 17, pp 1003-1012

Copyright 2013 American Chemical Society

Disproportionation of elemental sulfur by haloalkaliphilic bacteria from soda lakes

Alexander Poser · Regina Lohmayer · Carsten Vogt ·
Kay Knoeller · Britta Planer-Friedrich · Dimitry Sorokin ·
Hans-H. Richnow · Kai Finster

Received: 18 June 2013 / Accepted: 26 August 2013 / Published online: 13 September 2013
© Springer Japan 2013

Abstract Microbial disproportionation of elemental sulfur to sulfide and sulfate is a poorly characterized part of the anoxic sulfur cycle. So far, only a few bacterial strains have been described that can couple this reaction to cell growth. Continuous removal of the produced sulfide, for instance by oxidation and/or precipitation with metal ions such as iron, is essential to keep the reaction exergonic. Hitherto, the process has exclusively been reported for neutrophilic anaerobic bacteria. Here, we report for the first time disproportionation of elemental sulfur by three pure

cultures of haloalkaliphilic bacteria isolated from soda lakes: the Deltaproteobacteria *Desulfurivibrio alkaliphilus* and *Desulfurivibrio* sp. AMeS2, and a member of the Clostridia, *Dethiobacter alkaliphilus*. All cultures grew in saline media at pH 10 by sulfur disproportionation in the absence of metals as sulfide scavengers. Our data indicate that polysulfides are the dominant sulfur species under highly alkaline conditions and that they might be disproportionated. Furthermore, we report the first organism (*Dt. alkaliphilus*) from the class Clostridia that is able to grow by sulfur disproportionation.

Communicated by A. Oren.

A. Poser · C. Vogt (✉) · H.-H. Richnow
Department of Isotope Biogeochemistry, Helmholtz Centre
for Environmental Research UFZ, Permoserstraße 15,
04318 Leipzig, Germany
e-mail: carsten.vogt@ufz.de

R. Lohmayer · B. Planer-Friedrich
University of Bayreuth, Environmental Geochemistry,
Universitätsstraße 30, 95440 Bayreuth, Germany

K. Knoeller
Department Catchment Hydrology, Helmholtz Centre for
Environmental Research UFZ, Theodor-Lieser-Straße 4,
06120 Halle, Germany

D. Sorokin
Winogradsky Institute of Microbiology, Russian Academy
of Sciences, Prospect 60-let Otyabrya 7/2, 117312 Moscow,
Russia

D. Sorokin
Department of Biotechnology, Delft University of Technology,
Julianalaan 67, 2628 BC Delft, The Netherlands

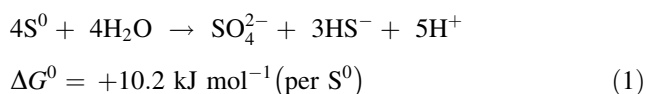
K. Finster
Microbiology Section, Department of Bioscience, Aarhus
University, Ny Munkegade 114–116, 8000 Aarhus C, Denmark

Keywords Elemental sulfur · Disproportionation ·
Soda lakes · Alkaliphilic · Polysulfides ·
Desulfurivibrio

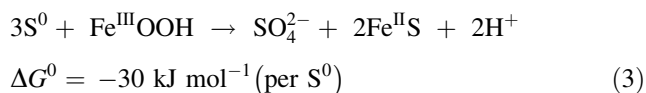
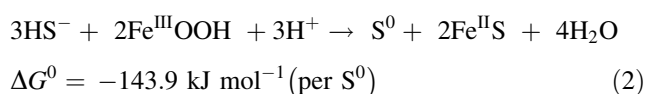
Introduction

There is increasing evidence that the disproportionation of partially oxidized sulfur compounds such as elemental sulfur, thiosulfate and sulfite is a quantitatively important, ancient and ecologically relevant process in the sulfur cycle (Bak and Cypionka 1987; Bak and Pfennig 1987; Thamdrup et al. 1993; Janssen et al. 1996; Finster et al. 1998; Philippot et al. 2007; Finster 2008). During disproportionation the sulfur compound is acting simultaneously as electron donor and electron acceptor and is transformed into a more oxidized and a more reduced species (Bak and Cypionka 1987; Finster 2008), similar to organic fermentation. While the disproportionation of thiosulfate and sulfite is a relatively common metabolic trait among the deltaproteobacterial sulfate reducers (Krämer and Cypionka 1989), only a few bacterial strains have been isolated that can disproportionate elemental sulfur in a growth

sustaining process. Under standard conditions, the disproportionation of elemental sulfur to sulfate and sulfide (Eq. 1) is an endergonic process (Bak and Cypionka 1987; Finster 2008) as the concentration of free sulfide affects the ΔG of the reaction (Frederiksen and Finster 2004).



Reoxidation and/or precipitation of sulfide with metal ions, e.g., iron or manganese will shift the reaction towards a negative Gibbs free energy. In the presence of Fe(III), the ratio of the produced sulfide and sulfate will be 2:1 instead of 3:1 as part of the sulfide is chemically oxidized to elemental sulfur by Fe(III) (Eqs. 2, 3) (Thamdrup et al. 1993; Frederiksen and Finster 2004; Finster 2008).



The pathway of elemental sulfur disproportionation has only been partly resolved (Frederiksen and Finster 2003, 2004; Finster 2008). Based on enzyme assays, it has been proposed that sulfite is the key intermediate and that it could be further oxidized to sulfate by the reversed sulfate reduction pathway. However, the initial reaction steps leading to the formation of sulfite are not understood.

So far the ability to grow by disproportionation of elemental sulfur has been restricted to members of the *Desulfobulbaceae* (Finster 2008). Recently, Sorokin et al. (2008a, 2011a) and Pikuta et al. (2003) enriched and isolated sulfate-reducing bacteria from soda lakes capable of sulfite and thiosulfate disproportionation. Soda lakes are extreme environments for two main reasons: they are highly alkaline showing pH values of up to 11 and they contain salt concentrations up to saturation (Sorokin et al. 2011b, 2013). Due to high concentrations of sodium sulfate and high primary production, soda lakes are generally characterized by intensive sulfur transformations. Sulfate reduction is supposed to be the dominating part of the sulfur cycle, although only a few sulfate reducers have been enriched from soda lakes (Sorokin et al. 2011b). This might be due to general energetic limitations caused by highly alkaline and salty conditions (Oren 2011), as sulfate needs to be activated by ATP consumption prior to reduction (Sorokin et al. 2008a). Therefore, microorganisms that can use thiosulfate or elemental sulfur/polysulfides as electron acceptors might be selectively enriched compared to sulfate reducers, as the metabolization of

these compounds can proceed without ATP loss (Sorokin et al. 2011a, b, c). The question arises if alkaline soda lakes, which are characterized by a high microbial diversity (Melack and Kilham 1974; Duckworth et al. 1996; Jones et al. 1996; Foti et al. 2008; Sorokin et al. 2010), harbor microorganisms that are able to disproportionate elemental sulfur. Elemental sulfur at high pH is, contrastingly to neutral or acidic habitats, not only present as colloids or in true solution (Zamana and Borzenko 2011), but also as soluble polysulfides with different chain lengths after reacting with sulfide (Eq. 4).



Sulfide that is produced during the disproportionation of elemental sulfur might therefore be rapidly converted into polysulfides resulting in favorable conditions for sulfur disproportionating microorganisms. The ΔG^0 value of this reaction strongly depends on the length of the polysulfides, ranging between +66 kJ/mol (for pentasulfide S_5^{2-}) and +77.4 kJ/mol (for disulfide S_2^{2-}) (Kamysny et al. 2007).

However, the ability of elemental sulfur disproportionation has not yet been reported for any haloalkaliphilic microorganism. To close this gap of knowledge, we tested strains isolated from soda lakes for their ability to couple the disproportionation of elemental sulfur to growth. Special emphasis was put on the question if metals (e.g., in the form of FeOOH) are required as sulfide scavengers to conserve sufficient energy for growth. We also investigated if polysulfides only represent intermediates along the disproportionation pathway, or if they directly can undergo disproportionation as it has been shown in studies by Kamysny et al. (2004) who reported abiotic disproportionation of inorganic polysulfides in aqueous solution and Milucka et al. (2012) who discovered disproportionation of disulfide by members of the Deltaproteobacteria.

Methods

Bacterial strains and culture conditions

Both *Dethiobacter alkaliphilus* (class Clostridia) and *Desulfurivibrio alkaliphilus* (class Deltaproteobacteria) were enriched as anaerobic chemoautotrophs with hydrogen as electron donor and thiosulfate or elemental sulfur/polysulfides as electron acceptors (see Sorokin et al. 2008b for a complete description). *Desulfurivibrio* sp. AMeS2 was enriched and isolated from soda lake sediments under anaerobic conditions with elemental sulfur as a single substrate and has 97 % 16S rRNA sequence similarity with *Desulfurivibrio alkaliphilus*. The microorganisms were cultivated under strictly anaerobic conditions, by flushing

the headspace with N₂, in a mineral medium (modified DSMZ medium DSM 1104) at pH 10 and at 37 °C. The carbonate/bicarbonate-buffered medium contained 0.1 M NaHCO₃, 0.2 M Na₂CO₃, 0.1 M NaCl, 2.9 mM K₂HPO₄, 3.7 mM NH₄Cl and 1 mM MgCl₂·6 H₂O. After sterilization, the medium was amended with 1 mL of trace element solution SL-10 with 0.5 g/L Na₂-EDTA (DSMZ medium 320), 1 mL of a selenite/tungstate solution (DSMZ medium 385), 10 mL of a vitamin solution (DSMZ medium 141) and 4.9 mM sodium acetate. All solutions were sterilized separately to prevent precipitation with mineral salts during the process. Elemental sulfur was sterilized separately as described in Sorokin et al. (2008a) and added as the only sulfur substrate to a final concentration of 25 mM to cultures supplemented with iron and to 10 mM to iron-free cultures.

Iron cultures were supplemented with heat-sterilized goethite (α-FeOOH) to a final concentration of 10 mg/L. The pH remained stable after addition of iron throughout the experimental incubation times. Doubling times were calculated from the growth phase data. For all cultures without Fe(III), the doubling times were calculated between 144 and 192 h of incubation. The values for cultures with Fe(III) were calculated between 48–96 h (DSV and DTB) and 24–48 h (AMeS2) of incubation.

Experimental set up

The experiments were performed in triplicate including duplicate autoclaved controls with 5 % inoculum. Cells of pre-grown cultures, which served as an inoculum, were centrifuged (4,000 rpm, 10 min) twice and re-suspended in fresh medium to avoid a transfer of sulfide and sulfate.

All experiments were carried out in 120 ml serum bottles containing 100 ml medium and 20 ml gas phase. The bottles were sealed with Teflon-coated butyl rubber stoppers and aluminum crimps. As the samples were prepared inside an anaerobic glove box (Coy Type A Vinyl Anaerobic Chamber) under nitrogen/hydrogen atmosphere, the bottles were afterwards flushed with pure nitrogen gas to remove hydrogen that can act as an electron donor.

Analytical procedure

For the different analytical procedures, samples were taken by a syringe flushed with nitrogen prior to sampling. In cultures in which Fe(III) was present, sulfide was precipitated and analyzed as Fe-sulfides. The chemical analysis of all sulfides was performed spectrophotometrically by the methylene blue method according to Cline (1969), modified as described by Herrmann et al. (2008). Sulfate was analyzed in

samples that were filtered through 0.2 μm pore size cellulose acetate filters and sulfate concentrations were determined by ion chromatography (DX 500 Dionex) after separation on a IonPacAS18/AG18 column and KOH (23 mM) as eluent. Polysulfides were quantified after a modified method of Kamyshny et al. (2006), which is based on derivatization of polysulfides to produce dimethylpolysulfanes. Derivatization was achieved in 1.5 mL HPLC vials by filtering 100 μL sample aliquots into 800 μL of methanol containing 15 μL methyl triflate (Sigma Aldrich). The derivatization with methyl triflate transforms the relatively unstable polysulfides into more stable dimethylpolysulfanes. Dimethylpolysulfanes were analyzed on a Merck Hitachi HPLC system equipped with a L-2130 pump, a L-2200 autosampler and a L-2420 UV-VIS detector. For separation, a Bischoff reversed phase C18 column (Waters-Spherisorb, ODS2, 5 μm, 250 × 4.6 mm) and gradient elution according to Rizkov et al. (2004) were used. Dimethylpolysulfanes measurements were performed at a wavelength of 230 nm. Concentrations of Me₂S₂ and Me₂S₃ were determined using commercially available standards (methyl disulfide, C₂H₆S₂, 99 %, 94.19 g/mol, Acros Organics, Geel, Belgium; dimethyl trisulfide, C₂H₆S₃, ≥98 %, 126.25 g/mol, Acros Organics, Geel, Belgium). For quantification of Me₂S₄ to Me₂S₈ sulfanes, calibration curves of synthesized dimethylpolysulfane reference materials were used. Synthesis of a dimethylpolysulfane mixture was performed following the method described by Rizkov et al. (2004). The constituents of the dimethylpolysulfane mixture were separated by preparative chromatography using a Phenomenex reversed phase C18 column (Sphereclone, ODS(2) 5 μm, 250 × 10 mm) and an eluent consisting of 50 % acetonitrile and 50 % formic acid. The flow rate was 5 ml/min. Collected fractions containing the individual dimethylpolysulfanes were oxidized with hydrochloric and nitric acid in a microwave (MarsXpress, CEM) for 10 min. The resulting sulfate were analyzed by ICP-MS (XSeries2, Thermo-Fisher) and used for calculation of the concentrations of the dimethylpolysulfanes in the different fractions.

Mössbauer spectroscopy

Mössbauer spectroscopy was performed to detect the mineral form of the added FeOOH and the formed Fe-sulfides. The samples were analyzed with a WissEl Mössbauer gamma-ray spectrometer using Co-57 as a gamma-ray source. See Gütlich and Schröder (2012) and Gütlich et al. (2012) for further information about Mössbauer spectroscopy.

Cell counts

Direct microscopy was used for cell counting (Adrian et al. 2007). Eighteen μL of well-suspended cell suspension were mixed and incubated with 1 μL SYBR Green (Bio Rad) for staining and stored for 15 min in the dark. This mixture was immobilized on agarose-coated slides and sealed with cover glass. Counting of the cells was performed by epifluorescence microscopy (Nikon Eclipse TE300). To guarantee accurate counting, each sample/slide was scanned in a z -pattern and at least 10 pictures were taken with a Nikon DXM 1200F digital camera (fixed focus and aperture). Subsequently, the pictures were processed with the ImageJ software, and cells were counted using the ImageJ cell counter. There was no interference of the solid phases

of FeOOH/FeS and the size of the cells, which were counted, could be adjusted by the ImageJ software.

Results and discussion

Growth yields in the presence and absence of Fe(III)

Supplemented with elemental sulfur and iron, *Dt. alkaliphilus* and *Dv. sp.* AMeS2 started to grow immediately, while *Dv. alkaliphilus* started growth after a lag phase of 48 h (Fig. 1). All strains reached cell densities of around 1.8×10^8 cells/ml and showed doubling times of 6–7 h, which is significantly faster than the doubling times of 2 days obtained for the neutrophilic strain *Desulfocapsa*

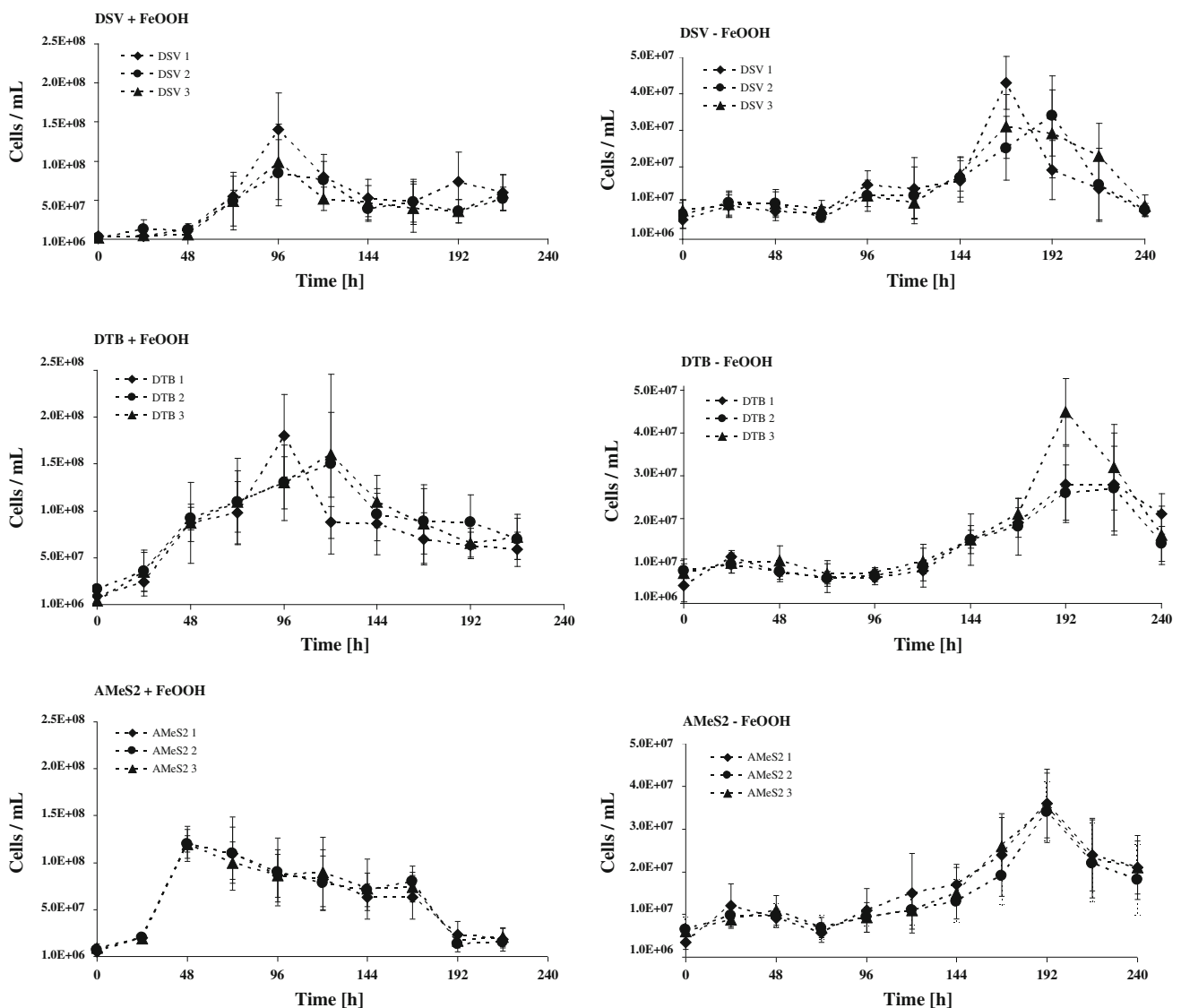


Fig. 1 Growth yields and characteristics of *Desulfurivibrio alkaliphilus*, *Dethiobacter alkaliphilus* and *Desulfurivibrio sp.* AMeS2 by sulfur disproportionation. Shown are the cells/ml of 3 parallel cultures

over time in the presence and absence of Fe(III) . Cultures without added sulfur did not grow (data not shown). Note different scales between 1 and 2

sulfexigens when grown on elemental sulfur disproportionation (Finster et al. 1998). None of our cultures grew without elemental sulfur (data not shown). Cell growth was accompanied by production of sulfate and sulfide. Interestingly, all strains grew by elemental sulfur disproportionation in the absence of iron (Fig. 1) in contrast to neutrophilic disproportionating strains (Finster et al. 1998). In the absence of iron oxides, growth started after a lag phase of approximately 120 h and the final cell density was 4.5×10^7 cells/ml. The doubling time of all strains was between 6 and 7 h and, therefore, consistent with the values obtained in the iron-amended cultures. This indicates that the energy gain of elemental sulfur disproportionation is higher under alkaline than under neutral conditions. However, the cellular growth yield was one order of magnitude lower in the absence of iron than in its presence. We link this difference to the fact that despite an equally high energy gain under alkaliphilic conditions, precipitation of the produced sulfide with iron (Eq. 2) (Grant 1992; Peiffer et al. 1992; Nielsen et al. 2008) is more efficient in keeping the concentrations of free sulfide at very low levels than the formation of polysulfides. It could also be speculated that the higher concentrations of free sulfide in the cultures without FeOOH have a toxic effect on the microorganisms. However, it is well known that H_2S is the most toxic sulfide species (Koschorreck 2008) and at pH 10 almost the entire sulfide is present as HS^- .

Production of sulfide and sulfate during elemental sulfur disproportionation

In the presence of Fe(III), the disproportionation of elemental sulfur theoretically results in the formation of sulfide (present as Fe-sulfides) and sulfate at a 2:1 ratio (Thamdrup et al. 1993; Frederiksen and Finster 2004; Finster 2008). We measured ratios of 1.8:1, 2.1:1 and 2.0:1 for *Dv. alkaliphilus*, *Dt. alkaliphilus* and *Dv. sp. AMeS2*, respectively, at the end of the experiment after the sulfide and sulfate concentrations remained stable. These values are in good agreement with the theoretical values.

Notably, at the beginning of culture growth the production of sulfate prevailed over the production of sulfides (Fig. 2). This was also reported by Thamdrup et al. (1993). Deviations from the theoretical ratio of 2:1 at the beginning of sulfur disproportionation are most likely a result of the chemical oxidation of the formed free sulfide to elemental sulfur or sulfate by iron oxides (Peiffer et al. 1992; Sullivan et al. 1988; Stumm and Morgan 1996). Thus Fe(III), which was added in the form of FeOOH in excess could change the observed ratio by lowering the sulfide concentration. During a later phase of growth more sulfide is produced and Fe(III) is reduced and precipitated as iron sulfides, evident by a blackening color of the culture, thus resulting

in lower abiotic oxidation rates. We found that FeS was the dominant iron sulfide species, traces of FeS_2 were found by Mössbauer Spectroscopy and identified as mackinawite and not pyrite as it was reported in Thamdrup et al. (1993) and Canfield and Thamdrup (1996).

In the absence of iron, we calculated sulfide:sulfate ratios of 2.2:1 (*Dv. alkaliphilus*), 3.4:1 (*Dt. alkaliphilus*) and 2.7:1 (*Dv. sp. AMeS2*) at the end of incubation (Fig. 2). Here, sulfide was measured as free sulfide and sulfane sulfur in polysulfides. These values are in the range of the theoretical ratios of 3:1 (Thamdrup et al. 1993; Finster 2008) for elemental sulfur disproportionation without iron. However, we observed a slight decrease of the sulfate concentration in all cultures after 96 h of incubation. This is surprising as none of the strains is able to use sulfate as an electron acceptor (Sorokin et al. 2008a). We currently have no explanation for the observed decrease in sulfate concentrations in these cultures.

Presence of polysulfides

The concentrations of polysulfides were measured in cultures with and without iron. Interestingly, polysulfide concentrations of up to 0.85 mM (sum of all polysulfides) (Fig. 3) were found in cultures supplemented with iron. This indicates that despite the chemical reaction of sulfide with iron a considerable amount of sulfide must have reacted with the residual elemental sulfur and resulted in the formation of polysulfides. In cultures without iron, polysulfide production was significantly enhanced and concentrations of up to 3 mM (sum of all polysulfides) were measured (Fig. 4). We found polysulfides with different chain lengths ranging from S_2^{2-} to S_8^{2-} . While S_3^{2-} and S_4^{2-} were dominant in the cultures with iron, S_4^{2-} to S_6^{2-} prevailed in cultures without iron. These results are in good agreement with reports of Boulegue and Michard (1978) and Kamyshny et al. (2004) who showed that S_3^{2-} , S_5^{2-} and S_6^{2-} are the dominant polysulfides between pH 7 and 12.5. The possible role of polysulfides and their positive effect on the disproportionation process are discussed in the following chapters.

Polysulfides as intermediates along the disproportionation pathway

Polysulfides could be intermediates in the reaction pathway of elemental sulfur disproportionation and in addition function as sulfide scavengers. As shown in Table 1, a fraction of the sulfide is trapped in polysulfides, keeping concentrations of free sulfide below 4–5 mM. As long as the concentration of free sulfide is <10 mM disproportionation is an exergonic process but more energy can be conserved with decreasing free sulfide concentrations (Finster 2008). The observed

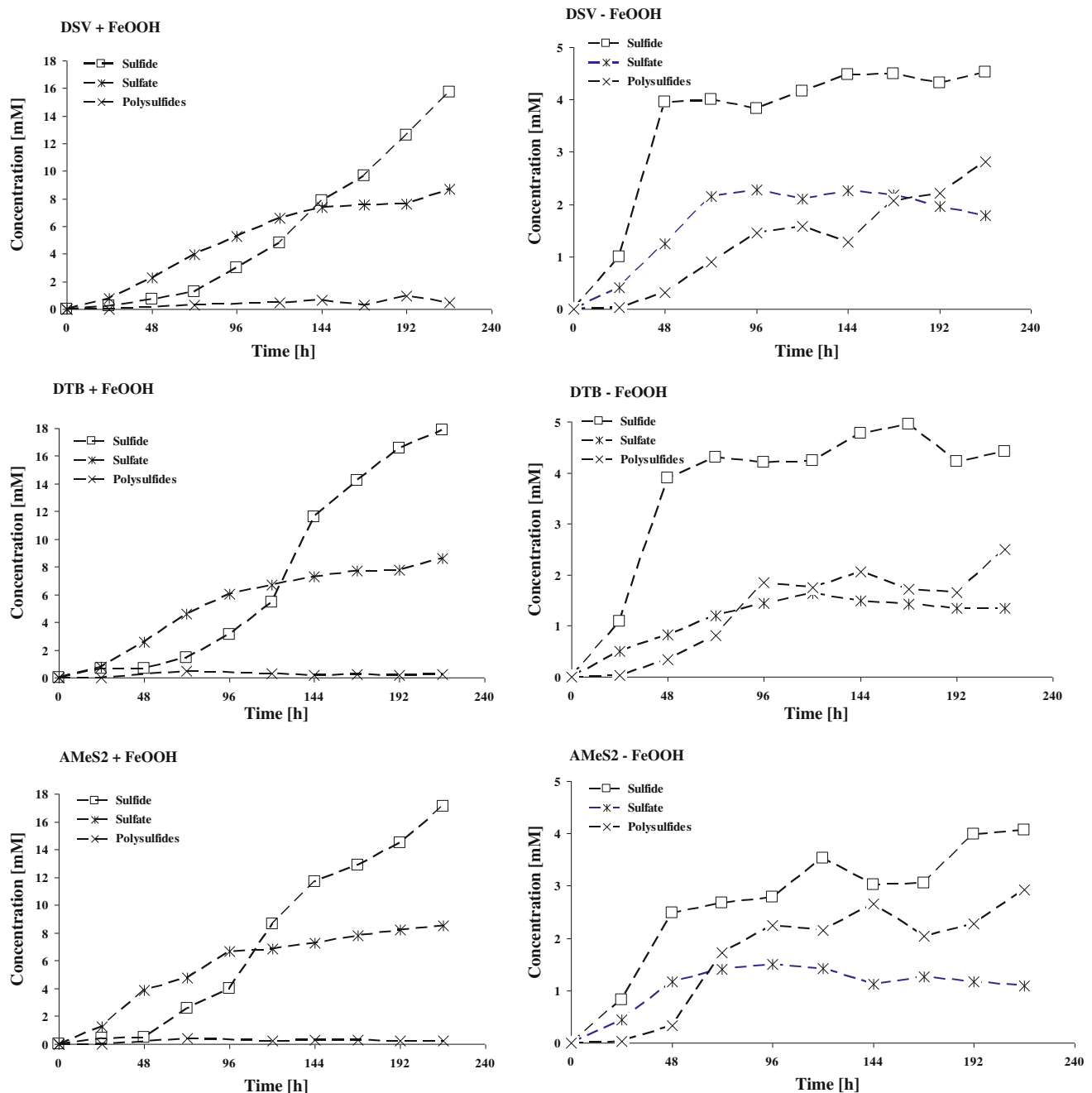


Fig. 2 Concentration of sulfide (*open square*), sulfate (*asterisk*) and polysulfides (*cross symbol*) as products/intermediates during sulfur disproportionation by *Desulfurivibrio alkaliphilus*, *Dethiobacter*

alkaliphilus and *Desulfurivibrio* sp. AMeS2 with or without FeOOH addition. Note that in the presence of FeOOH all sulfide was precipitated as Fe-sulfides

delayed cell growth compared to sulfide, sulfate and polysulfide production might indicate that the energy which is gained by sulfur disproportionation is also used for the formation of more/other polysulfides (Kamyshny et al. 2007). Only when the concentrations of sulfide, sulfate and polysulfides attain certain equilibrium more energy can be used for substantial bacterial growth and polysulfides might then act as sulfide scavengers, similar to iron, and pull the overall

disproportionation reaction towards more negative ΔG^0 values. In contrast to sulfide/sulfate production in the presence of iron, sulfide/sulfate/polysulfide formation in the absence of iron was much faster and cellular production was one order of magnitude lower. In conclusion, the results show that polysulfides as sulfide scavengers are not as efficient as FeOOH (Kamyshny et al. 2004; Peiffer et al. 1992; Nielsen et al. 2008).

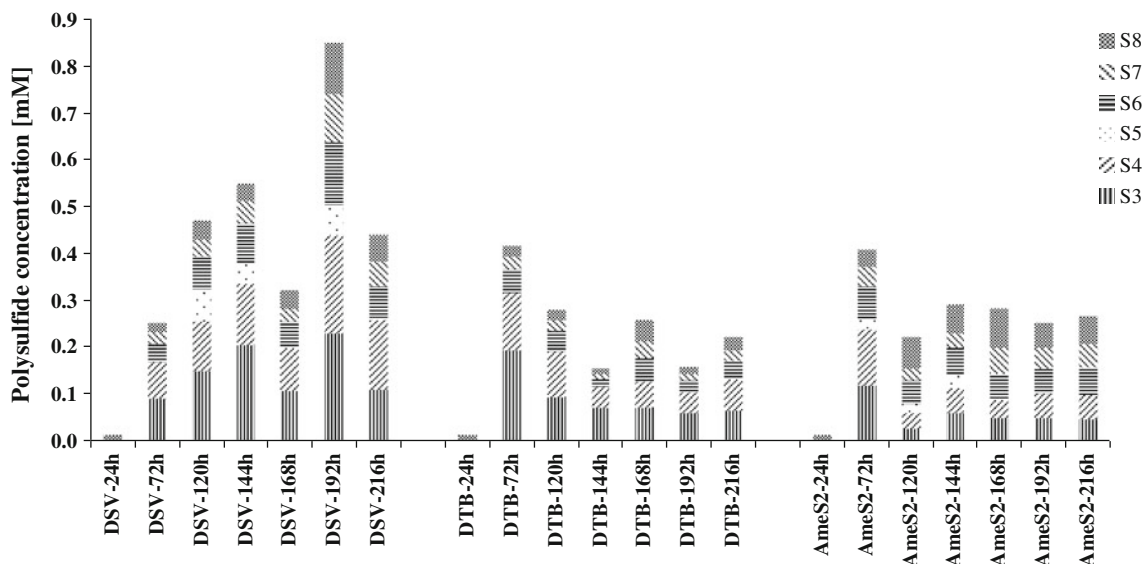


Fig. 3 Concentration in mM of the formed single polysulfide species (S_3^{2-} to S_8^{2-}) during disproportionation and growth by *Desulfurivibrio alkaliphilus* (DSV), *Dethiobacter alkaliphilus* (DTB) and

Desulfurivibrio sp. AMeS2 (AMeS2) after 24–216 h. All cultures were prepared with iron (FeOOH)

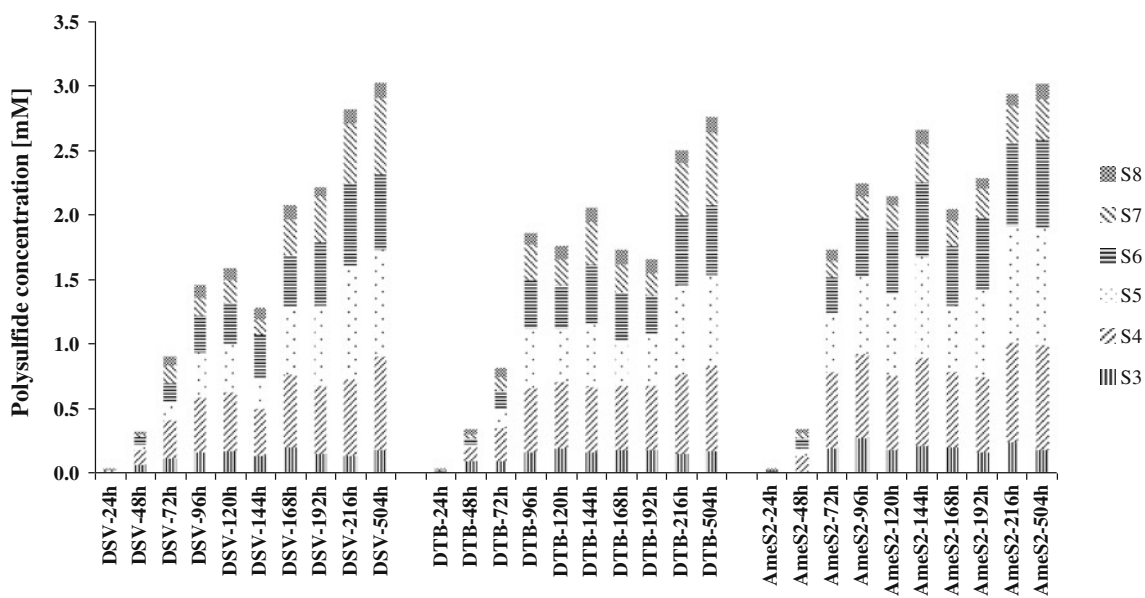


Fig. 4 Concentration in mM of the formed single polysulfide species (S_3^{2-} to S_8^{2-}) during disproportionation and growth by *Desulfurivibrio alkaliphilus* (DSV), *Dethiobacter alkaliphilus* (DTB) and *Desulfurivibrio* sp. AMeS2 (AMeS2) after 24–216 h without the

addition of iron (FeOOH). The analysis of S_2^{2-} was interfered by overlapping peaks and therefore no quantitative assessment was possible

Polysulfides as substrates for disproportionation

Direct polysulfide disproportionation is plausible as the uptake of linear sulfur molecules by cells is much easier than the uptake of ring-like sulfur (Franz et al. 2007). So far, several mechanisms for the uptake of elemental sulfur have been suggested. They are involving an increase in hydrophobicity of the cell surface or blebbing of vesicles

off the outer cell membrane to reduce the hydrophobic character of elemental sulfur (Knickerbocker et al. 2000). It would also facilitate the adhesion of elemental sulfur particles to cell membrane by glycocalyx or by a reaction with thiol groups (Franz et al. 2007). Polysulfides on the other hand are water soluble and might therefore more easily pass the outer cell membrane than elemental sulfur, requiring less time and energy. Usually, polysulfides are

Table 1 The concentrations of total sulfide, sulfide embedded in polysulfides (sulfane sulfur) and free sulfide [mM] in cultures of *Desulfurivibrio alkaliphilus* (DSV), *Dethiobacter alkaliphilus* (DTB) and *Desulfurivibrio* sp. AMeS2 (AMeS2) over a time span of 216 h

Strain/time	Total sulfides [mM]	Sulfide in polysulfides [mM]	Free sulfide [mM]
DSV-24 h	1.00	0.01	0.99
DSV-48 h	3.95	0.07	3.88
DSV-72 h	4.00	0.19	3.81
DSV-96 h	3.83	0.31	3.52
DSV-120 h	4.16	0.33	3.83
DSV-144 h	4.47	0.27	4.20
DSV-168 h	4.50	0.43	4.07
DSV-192 h	4.32	0.45	3.87
DSV-216 h	4.53	0.55	3.98
DTB-24 h	1.09	0.00	1.09
DTB-48 h	3.90	0.08	3.82
DTB-72 h	4.30	0.17	4.13
DTB-96 h	4.21	0.38	3.83
DTB-120h	4.24	0.37	3.87
DTB-144 h	4.78	0.42	4.36
DTB-168 h	4.95	0.36	4.59
DTB-192 h	4.22	0.35	3.87
DTB-216 h	4.42	0.50	3.92
AmeS2-24 h	0.82	0.00	0.82
AmeS2-48 h	2.48	0.07	2.41
AmeS2-72 h	2.68	0.38	2.30
AmeS2-96 h	2.79	0.48	2.31
AmeS2-120 h	3.53	0.45	3.08
AmeS2-144 h	3.03	0.55	2.48
AmeS2-168 h	3.06	0.43	2.63
AmeS2-192 h	3.98	0.47	3.51
AmeS2-216 h	4.07	0.61	3.45

attached to carriers such as Sud (sulfide dehydrogenase) or rhodanese-like proteins (Hedderich et al. 1999) because they are unstable at neutral pH conditions (cysteine-bound organic polysulfides). These carriers are not necessary at high pH as anoxic, alkaline conditions ensure chemical polysulfide stability (inorganic polysulfides). Hence, the question arises if polysulfides instead of elemental sulfur were disproportionated. If so, the sulfide:sulfate ratio would be in the range of 3.8:1 and 4.3:1 for S_4^{2-} to S_6^{2-} polysulfides, respectively (Milucka et al. 2012). Our data do not rule out polysulfide disproportionation as the calculated ratios are in some cases close to the theoretical values (*Dt. alkaliphilus*). It might also take a while until enough sulfide is produced to reach the equilibrium reaction between sulfide and elemental sulfur to form polysulfides and maintain the equilibrium polysulfide pool. Polysulfide disproportionation has only

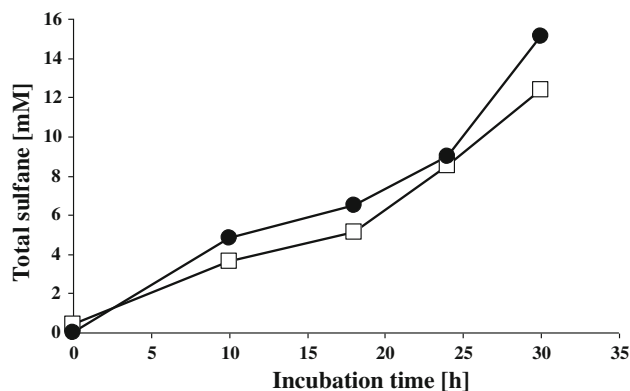


Fig. 5 Formation of sulfane sulfur by reduction of elemental sulfur (open square) or internal sulfur of polysulfide (S_5^{2-}) (filled circle) during their disproportionation by washed cells of strain *Desulfurivibrio* sp. AMeS2 at pH 10 and 0.6 M total Na^+ . S_8 was used in excess together with 0.5 mM HS^- . Starting concentration of internal sulfur was 30 mM. Concentration of cell protein was 0.1 mg/ml, incubation temperature = 30 °C. In abiotic controls (with boiled cells) sulfur was not metabolized

been reported in two studies. Milucka et al. (2012) showed that disulfide disproportionation is associated with anaerobic methane oxidation (ANME), to remove the produced elemental sulfur formed by sulfate reduction. The occurrence of abiotic disproportionation of inorganic polysulfides has been reported by Kamyshny et al. (2004). As shown in Fig. 5 polysulfide disproportionation under alkaline conditions, as it is indicated by the sulfide:sulfate ratio of 4.5:1, is much faster than elemental sulfur disproportionation.

In conclusion, we describe the first bacterium from the class Clostridia that grows by sulfur disproportionation. Furthermore, we demonstrated that in contrast to neutrophilic organisms, haloalkaliphilic bacteria grow by elemental sulfur disproportionation also in the absence of iron oxides as sulfide scavenger. Polysulfides were shown to be important intermediate compounds during this reaction, indicating that microbial sulfur disproportionation at high pH benefits from the unique conditions for sulfur chemistry that ensures stability of polysulfides. We show furthermore that polysulfides might not only form as sulfur intermediates along the disproportionation pathway under alkaline conditions, but could be also used as a substrate for disproportionation similar to elemental sulfur. Thus, polysulfides play a major role during sulfur disproportionation at high pH, although their exact role during this process—especially in the presence of elemental sulfur—remains unclear at the moment.

Acknowledgments Alexander Poser was supported by the German Research Foundation within the FOR 580 e-TraP project (Grant FOR 580 RIC). Britta Planer-Friedrich and Regina Lohmayer acknowledge funding by the German Research Foundation within project PL 302/5-

1. Kai Finster acknowledges support by the Danish agency for science technology and innovation (Ref. no. 272-08-0497). This work was also supported by the RFBR Grant 13-04-40205 Comfi to Dmitry Y. Sorokin. We thank Christian Schröder (University Tübingen) for the Mössbauer analyses and Stephanie Hinke for valuable technical assistance.

References

- Adrian L, Hansen SK, Fung JM, Görisch H, Zinder SH (2007) Growth of *Dehalococcoides* strains with chlorophenols as electron acceptors. *Environm Sci Technol* 41:2318–2323
- Bak F, Cypionka H (1987) A novel type of energy-metabolism involving fermentation of inorganic sulfur-compounds. *Nature* 326:891–892
- Bak F, Pfennig N (1987) Chemolithotrophic growth of *Desulfovibrio sulfodismutans* sp. nov. by disproportionation of inorganic sulfur-compounds. *Arch Microbiol* 147:184–189
- Boulegue J, Michard G (1978) Constantes de formation des ions polysulfures S_6^{2-} , S_5^{2-} et S_4^{2-} en phase aqueuse. *J F Hydrol* 9:27–33
- Canfield DE, Thamdrup B (1996) Fate of elemental sulfur in an intertidal sediment. *FEMS Microbiol Ecol* 19:95–103
- Cline JD (1969) Spectrophotometric determination of hydrogen sulfide in natural waters. *Limnol Oceanogr* 14:454–458
- Duckworth AW, Grant WD, Jones BE, van Steenberg R (1996) Phylogenetic diversity of soda lake alkaliphiles. *FEMS Microbiol Ecol* 19:181–191
- Finster K (2008) Microbiological disproportionation of inorganic sulfur compounds. *J Sulfur Chem* 29:281–292
- Finster K, Liesack W, Thamdrup B (1998) Elemental sulfur and thiosulfate disproportionation by *Desulfocapsa sulfoexigens* sp. nov., a new anaerobic bacterium isolated from marine surface sediment. *Appl Environ Microbiol* 64:119–125
- Foti MJ, Sorokin DY, Zacharova EE, Pimenov NV, Kuenen JG, Muyzer G (2008) Bacterial diversity and activity along a salinity gradient in soda lakes of the Kulunda Steppe (Altai, Russia). *Extremophiles* 12:133–145
- Franz B, Lichtenberg H, Hormes J, Modrow H, Dahl C, Prange A (2007) Utilization of solid ‘elemental’ sulfur by the phototrophic purple sulfur bacterium *Allochromatium vinosum*: a sulfur K-edge X-ray absorption spectroscopy study. *Microbiology* 153:1268–1274
- Frederiksen TM, Finster K (2003) Sulfite-oxido-reductase is involved in the oxidation of sulfite in *Desulfocapsa sulfoexigens* during disproportionation of thiosulfate and elemental sulfur. *Biodegradation* 14:189–198
- Frederiksen TM, Finster K (2004) The transformation of inorganic sulfur compounds and the assimilation of organic and inorganic carbon by the sulfur disproportionating bacterium *Desulfocapsa sulfoexigens*. *Antonie Van Leeuwenhoek* 85:141–149
- Grant WD (1992) Alkaline Environments. In: Lederberg J (ed) *Encyclopedia of microbiology*, vol 1. Academic Press, San Diego, pp 73–80
- Gütlich P, Schröder C (2012) Mössbauer Spectroscopy. In: Schäfer R, Schmidt PC (eds) *Methods in Physical Chemistry*. Wiley-VCH, New York, pp 351–389
- Gütlich P, Schröder C, Schünemann V (2012) Mössbauer spectroscopy—an indispensable tool in solid state research. *Spectrosc Eur* 24(4):21–32
- Hedderich R, Klimmek O, Kröger A, Dirmeier R, Keller M, Stetter KO (1999) Anaerobic respiration with elemental sulfur and with disulfides. *FEMS Microbiol Rev* 22:353–381
- Herrmann S, Kleinstüber S, Neu TU, Richnow HH, Vogt C (2008) Enrichment of anaerobic benzene degrading microorganisms by in situ microcosms. *FEMS Microbiol Ecol* 63:94–106
- Janssen PH, Schuhmann A, Bak F, Liesack W (1996) Disproportionation of inorganic sulfur compounds by the sulfate-reducing bacterium *Desulfocapsa thiozymogenes* gen. nov., sp. nov. *Arch Microbiol* 166:184–192
- Jones BE, Grant WD, Duckworth AW, Owenson GG (1996) Microbial diversity of soda lakes. *Extremophiles* 2:191–200
- Kamyshny A, Goifman A, Rizkov D, Lev O (2004) Kinetics of disproportionation of inorganic polysulfides in undersaturated aqueous solutions at environmentally relevant conditions. *Aquat Geochem* 9:291–304
- Kamyshny A, Ekelchik I, Gun J, Lev O (2006) Method for the determination of inorganic polysulfide distribution in aquatic systems. *Anal Chem* 78:2631–2639
- Kamyshny A, Gun J, Rizkov D, Voitsekovski T, Lev O (2007) Equilibrium distribution of polysulfide ions in aqueous solutions at different temperatures by rapid single phase derivatization. *Environ Sci Technol* 41:2395–2400
- Knickerbocker C, Nordstrom DK, Southam G (2000) The role of “blebbing” in overcoming the hydrophobic barrier during biooxidation of elemental sulfur by *Thiobacillus thiooxidans*. *Chem Geol* 169:425–433
- Koschorreck M (2008) Microbial sulphate reduction at a low pH. *FEMS Microbiol Ecol* 64:329–342
- Krämer M, Cypionka H (1989) Sulfate formation via ATP sulfurylase in thiosulfate-disproportionating and sulfite-disproportionating bacteria. *Arch Microbiol* 151:232–237
- Melack JM, Kilham P (1974) Photosynthetic rates of phytoplankton in East African alkaline, saline lakes. *Limnol Oceanogr* 19:743–755
- Milucka J, Ferdelman TG, Polerecky L, Franzke D, Wegener G, Schmid M, Lieberwirth I, Wagner M, Widdel F, Kuypers MMM (2012) Zero-valent sulphur is a key intermediate in marine methane oxidation. *Nature* 491:541–546
- Nielsen AH, Hvitved-Jacobsen T, Vollertson J (2008) Effects of pH and iron concentrations on sulfide precipitation in wastewater collection systems. *Water Environ Res* 80:380–384
- Oren A (2011) Thermodynamic limits to microbial life at high salt concentration. *Environ Microbiol* 13:1908–1923
- Peiffer S, dos Santos Afonso M, Wehrl B, Gächter R (1992) Kinetics and mechanism of the reaction of H_2S with lepidocrocite. *Environm Sci Technol* 26:2408–2413
- Philippot P, van Zuilen M, Lepot K, Thomazo C, Farquhar J, van Kranendonk MJ (2007) Early archaen microorganisms preferred elemental sulfur, not sulfate. *Science* 317:1534–1537
- Pikuta EV, Hoover RB, Bej AK, Marsic D, Whitman WB, Cleland D, Krader P (2003) *Desulfonatronum thiodismutans* sp. nov., a novel alkaliphilic, sulfate-reducing bacterium capable of lithoautotrophic growth. *Int J Syst Evol Microbiol* 53:1327–1332
- Rizkov D, Lev O, Gun J, Anisimov B, Kuselman I (2004) Development of in-house reference materials for determination of inorganic polysulfides in water. *Accred Qual Assur* 9:399–403
- Sorokin DY, Tourova TP, Henstra AM, Stams AJM, Galinski EA, Muyzer G (2008a) Sulfidogenesis under extremely haloalkaline conditions by *Desulfonatronospira thiodismutans* gen. nov., sp. nov., and *Desulfonatronospira delicata* sp. nov. - a novel lineage of *Deltaproteobacteria* from hypersaline soda lakes. *Microbiology* 154:1444–1453
- Sorokin DY, Tourova T, Mußmann M, Muyzer G (2008b) *Dethiobacter alkaliphilus* gen. nov. sp. nov., and *Desulfurivibrio alkaliphilus* gen. nov. sp. nov.: two novel representatives of reductive sulfur cycle from soda lakes. *Extremophiles* 12:431–439

- Sorokin DY, Rusanov II, Pimenov NV, Tourova TP, Abbas B, Muyzer G (2010) Sulfidogenesis under extremely haloalkaline conditions in soda lakes of Kulunda Steppe (Altai, Russia). *FEMS Microbiol Ecol* 73:273–290
- Sorokin DY, Tourova TP, Detkova EN, Kolganova TV, Galinski EA, Muyzer G (2011a) Culturable diversity of lithotrophic haloalkaliphilic sulfate-reducing bacteria in soda lakes and the description of *Desulfonatronum thioautotrophicum* sp. nov., *Desulfonatronum thiosulfatophilum* sp. nov., *Desulfonatronovibrio thiodismutans* sp. nov., and *Desulfonatronovibrio magnus* sp. nov. *Extremophiles* 15:391–401
- Sorokin DY, Kuenen JG, Muyzer G (2011b) The microbial sulfur cycle at extremely haloalkaline conditions of soda lakes. *Front Microbiol* 2:44
- Sorokin DY, Detkova EN, Muyzer G (2011c) Sulfur-dependent respiration under extremely haloalkaline conditions in soda-lake acetogens and the description of *Natronella sulfidigena* sp. nov. *FEMS Microbiol Lett* 319:88–95
- Sorokin DY, Banciu H, Robertson LA, Kuenen JG, Muyzer G (2013) Halophilic and haloalkaliphilic sulfur-oxidizing bacteria from habitats and soda lakes. In: Rosenberg E et al (eds) *The prokaryotes—prokaryotic physiology and biochemistry*. Springer-Verlag, Berlin-Heidelberg, pp 530–551
- Stumm W, Morgan JJ (1996) *Aquatic chemistry: chemical equilibria and rates in natural water*. Wiley-Interscience, New York
- Sullivan PJ, Reddy KJ, Yelton JL (1988) Iron sulfide oxidation and the chemistry of acid generation. *Environ Geol Water Sci* 11:289–295
- Thamdrup B, Finster K, Hansen JW, Bak F (1993) Bacterial disproportionation of elemental sulfur coupled to chemical reduction of iron or manganese. *Appl Environ Microbiol* 59:101–108
- Zamana LV, Borzenko SV (2011) Elemental sulfur in the brine of Lake Droninskoe (Eastern Transbaikalia). *Dokl Earth Sci* 438:775–778

Study 2

Reproduced with permission from

Occurrence of Surface Polysulfides during the Interaction between Ferric (Hydr)Oxides and Aqueous Sulfide

Moli Wan, Andrey Shchukarev, Regina Lohmayer, Britta Planer-Friedrich, Stefan Peiffer

Environmental Science & Technology, 2014, 48, pp 5076-5084

Copyright 2014 American Chemical Society

Occurrence of Surface Polysulfides during the Interaction between Ferric (Hydr)Oxides and Aqueous Sulfide

Moli Wan,^{*,†} Andrey Shchukarev,[‡] Regina Lohmayer,[§] Britta Planer-Friedrich,[§] and Stefan Peiffer[†]

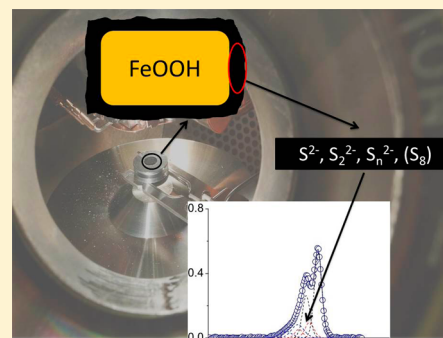
[†]BayCEER, Department of Hydrology, University of Bayreuth, D-95440, Bayreuth, Germany

[‡]Environmental and Biogeochemistry, Department of Chemistry, Umeå University, SE-901 87 Umeå, Sweden

[§]Environmental Geochemistry, University of Bayreuth, D-95440 Bayreuth, Germany

Supporting Information

ABSTRACT: Polysulfides are often referred to as key reactants in the sulfur cycle, especially during the interaction of ferric (hydr)oxides and sulfide, forming ferrous-sulfide minerals. Despite their potential relevance, the extent of polysulfide formation and its relevance for product formation pathways remains enigmatic. We applied cryogenic X-ray Photoelectron Spectroscopy and wet chemical analysis to study sulfur oxidation products during the reaction of goethite and lepidocrocite with aqueous sulfide at different initial Fe/S molar ratios under anoxic conditions at neutral pH. The higher reactivity of lepidocrocite leads to faster and higher electron turnover compared to goethite. We were able to demonstrate for the first time the occurrence of surface-associated polysulfides being the main oxidation products in the presence of both minerals, with a predominance of disulfide ($S_2^{2-}(\text{surf})$), and elemental sulfur. Concentrations of aqueous polysulfide species were negligible (<1%). With prior sulfide fixation by zinc acetate, the surface-associated polysulfides could be precipitated as zerovalent sulfur (S^0), which was extracted by methanol thereafter. Of the generated S^0 , 20–34% were associated with $S_2^{2-}(\text{surf})$. Varying the Fe/S ratio revealed that surface polysulfide formation only becomes dominant when the remaining aqueous sulfide concentration is low (<0.03 mmol L⁻¹). We hypothesize these novel surface sulfur species, particularly surface disulfide, to act as pyrite precursors. We further propose that these species play an overlooked role in the sulfur cycle.



INTRODUCTION

The interaction between ferric (hydr)oxides and sulfide has been widely studied^{1–4} due to its fundamental relevance for the cycling of sulfur in many anaerobic environments, such as marine or lake sediments and aquifers and due to its potential link with sedimentary pyrite formation.^{5–9} It is generally observed that in addition to an iron sulfide phase, elemental sulfur also forms during this reaction.^{2,3,10,11} It has been suggested that the oxidation of HS^- by ferric iron occurs via a single electron step to generate sulfur radicals $S^{\bullet-}$.^{4,12} This reaction allows for the generation of polysulfides and subsequently of elemental sulfur.¹² Alternatively, it has been proposed that two electrons are transferred simultaneously and $S(-II)$ is directly oxidized to $S(0)$,¹³ which then rapidly equilibrates with aqueous sulfide to form polysulfides under environmentally relevant conditions.¹⁴ In either case, polysulfides are regarded as essential intermediates.

Some evidence exists for the occurrence of aqueous polysulfides at low concentration levels during reaction of dissolved sulfide with ferric (hydr)oxides.^{2,11} Unfortunately, these measurements are based on indirect methods, such as converting polysulfide species into thiosulfate and its subsequent determination² or optical spectroscopy combined with thermodynamic calculations.¹¹ Recently developed selective and specific analytical tools (e.g., the single-phase

derivatization technique¹⁵) have not yet been applied, to study these interactions.

Hellige et al. investigated the sulfidation of lepidocrocite under conditions where aqueous sulfide was completely consumed within a short time (15 min).³ They found a large deficit in the sulfur mass balance, which they attributed to unknown solid phase-bound sulfur species. High resolution transmission electron microscope (HRTEM) images revealed that a large fraction of surface-associated sulfur had formed in these experiments which they could not further identify. They also observed rapid pyrite formation (after several days), a process that is regarded to require polysulfides as precursor substances.¹⁶ Surface-associated polysulfides have been observed at the surface of iron sulfide minerals after surface sulfide oxidation using surface-sensitive techniques such as X-ray photoelectron spectroscopy (XPS).^{17–20} Comparable studies about their occurrence during oxidation of dissolved sulfides at ferric mineral surfaces have not been performed yet, although strong indications for the formation of surface associated sulfur exist. The extent of polysulfide formation and its relevance for

Received: January 7, 2014

Revised: April 16, 2014

Accepted: April 16, 2014

Published: April 16, 2014

Table 1. Initial Experimental Conditions^a

mineral	initial Fe content (g/L)	c(Fe) (mmol L ⁻¹)	c(Fe)/c(S)	SS(Fe)/c(S) ^b
goethite (Gt)	3.6	40.4	5.05 (HR)	0.11
	0.28	3.0	0.37 (LR)	0.01
lepidocrocite (Lp)	2	22.5	2.8 (HR)	0.10
	0.38	3.9	0.5 (LR)	0.02

^aAll runs were conducted at pH 7. ^bConcentration of surface sites (SS) was calculated based on a value of 6.3×10^{-6} mol/m² for both ferric (hydr)oxides.⁴³

product formation pathways during the reaction remains enigmatic.

This study therefore aims at resolving the fate of sulfur during the reaction between ferric (hydr)oxides and dissolved sulfide. To these ends, we applied wet chemical methods in combination with XPS to determine sulfur oxidation products both in solution and at the surface of ferric (hydr)oxides. Since XPS analyzes the surface under vacuum and elemental sulfur is volatile under ultra vacuum, we performed the whole analytical procedure at cryogenic temperature (-155 °C).

MATERIALS AND METHODS

All solutions were prepared in a glovebox system (Inert Lab 4GB Glovebox Systems, Innovative Technology, U.S.A.) with a O₂ level in a range of 0–1 ppm. The working gas in the glovebox is N₂ (99.99%). The deionized water was purged with N₂ (99.99%) for at least 1 h to remove O₂ before the transfer into the glovebox. All reagents were of analytical grade.

Ferric (Hydr)Oxides. Synthetic ferric oxides were prepared after Schwertmann and Cornell.²¹ To synthesize goethite, 100 mL Fe(NO₃)₃ ($c = 1$ mol L⁻¹) and 180 mL KOH ($c = 5$ mol L⁻¹) were mixed rapidly in a 2 L polyethylene flask. Red-brown ferrihydrite precipitated immediately. The suspension was then diluted to 2 L with deionized water and kept at 70 °C for 60 h. To synthesize lepidocrocite, a FeCl₂ ($c = 0.06$ mol L⁻¹) solution was oxidized by air which was pumped through the solution at a controlled flow rate of 100 mL min⁻¹. The pH was maintained at 6.8 by addition of NaOH ($c = 0.5$ mol L⁻¹) with a pH-stat device (Titrino, Metrohm). The oxidation was carried out at room temperature with sufficient stirring for 3 h. The synthetic goethite and lepidocrocite were washed with deionized water and freeze-dried.

The mineral characterization with Mößbauer spectroscopy demonstrated that no other Fe containing phases were present in goethite and around 4% goethite in lepidocrocite. Multipoint BET (Brunauer, Emmett, and Teller) gas adsorption with N₂ (Gemini 2375 analyzer) gave a surface area of 39.33 m² g⁻¹ and 70.24 m² g⁻¹ for goethite and lepidocrocite, respectively.

Experimental Setup. The experimental setup was similar to that used in a previous study.³ In a closed vessel, 450 mL aqueous sulfide solution (approximately 8 mmol L⁻¹ Na₂S solution, concentration (S(-II))_{ini} determined prior to each experiment) was adjusted to pH 7.0 in the glovebox by addition of HCl ($c = 1$ mol L⁻¹), to which 50 mL of a suspension containing a preselected amount of synthetic ferric (hydr)oxides (goethite or lepidocrocite) was added. The pH was kept constant at pH = 7.00 ± 0.05 with HCl ($c = 0.1$ mol L⁻¹) using the pH-Stat device (Titrino, Metrohm). The solution was gently stirred with a Teflon-coated magnetic stirring bar during the whole experiment. Initial molar ratios of Fe/S were adjusted to be “high”, with iron concentrations being in excess to sulfide (HR runs, cf. Table 1) and “low” with excess aqueous sulfide (LR runs). The runs with high Fe/S ratio are comparable to

previous experiments that were performed under comparable conditions with regard to pH, anoxic atmosphere, and mineral application.³ The same concentration of surface area was used for the two minerals in HR runs. Blank experiments with pure sulfide solution were performed in order to quantify sulfide loss in the low Fe/S ratio runs due to degassing. The 168 h-experiments yielded a linear sulfide loss with time at a rate of 0.014 mmol L⁻¹ h⁻¹ ($R^2 = 0.914$).

Aqueous samples were removed regularly for wet chemical analysis. Samples for XPS analysis were taken after 3 h in HR runs and after 168 h in LR runs by removing 40 mL of the suspension from the reactor, centrifuging, decanting, then resuspending it in deionized water and centrifuging it again. The concentration of the residual Fe and S species was calculated as the difference between the species concentration in the suspension before centrifugation and in the supernatant after centrifugation.

All steps were done in the glovebox except centrifugation. The black precipitates in HR runs were dried overnight under anoxic conditions in the glovebox. LR samples contained volatile sulfide which might damage the purification system of the glovebox. Samples from LR runs were therefore freeze-dried. After drying, all samples were stored under a N₂ atmosphere in sealed crimp vials.

Wet Chemical Analysis. Aqueous sulfide was determined after filtration (0.2 μm, Nylon) by the methylene blue method.²² However, this method can determine not only hydrogen sulfide and sulfide ions, but also sulfide associated with aqueous polysulfide.²³ We therefore refer to this fraction as methylene-blue-detectable sulfur (MBS). Sulfate was determined after filtration (0.2 μm, Nylon) following the turbidimetric method based on the BaSO₄ precipitation described by Tabatabai.²⁴ Thiosulfate was determined immediately after filtration (0.2 μm, Nylon) by ion-pair chromatography following the method described by Steudel et al.²⁵

Aqueous polysulfides (S_n²⁻(aq)) were determined following the method developed by Kamyshtny et al.¹⁵ Due to their instability toward oxygen and pH-changes, inorganic polysulfides were derivatized with methyl trifluoromethanesulfonate (methyl triflate) to form dimethylpolysulfanes. To this end, 200 μL of the filtered samples and 8 μL triflate ($c = 8.7$ mol L⁻¹) were added simultaneously into 1200 μL methanol previously buffered with 100 μL phosphate buffer ($c = 50$ mmol L⁻¹) at pH 7 and shaken intensely for 10 s. Dimethylpolysulfanes were determined by HPLC (Merck Hitachi, L-2130 pump, L-2200 autosampler, L-2420 UV-vis detector) after separation on a C18 column (Waters-Spherisorb, ODS2, 5 μm, 250 × 4.6 mm²) and gradient elution according to Rizkov et al.²⁶ The detection was performed at a wavelength of 230 nm. The total polysulfide concentration was calculated as the sum of individual polysulfide fractions.

Methanol-extractable sulfur (MES) was extracted after pretreatment of 500 μL of unfiltered sample with 250 μL of

ZnAc ($c = 0.1 \text{ mol L}^{-1}$) to precipitate free sulfide following a procedure modified after Kamyshny et al.¹⁴ After 10 min, 6 mL methanol were injected into the suspension. The sample was shaken for 3 h and then filtered ($0.2 \mu\text{m}$, Nylon). The prior sulfide fixation allows ZnAc to react with S^{2-} as well as S_n^{2-} ($n \geq 2$) to precipitate ZnS and $(n - 1) \text{ S}^0$ atoms, which are extracted later with methanol. MES therefore comprises elemental sulfur and aqueous polysulfide-bound sulfur ($\text{S}_n^{2-} - \text{S}^0$ with $n \geq 2$), as pointed out by Kamyshny et al.¹⁴ Since samples for MES determination were unfiltered, MES includes also sulfur associated at the mineral surface. The samples were determined by HPLC (PerkinElmer 2000 pump and autosampler, Fa. linear-UV-vis detector and software peak-sample 409) after separation on a C18 column (Nucleosil 100-5 PAH) and isocratic elution by pure methanol with a flow rate of 0.4 mL min^{-1} . The detection was performed at a wavelength of 265 nm.

Acid-extractable Fe(II) ($\text{Fe(II)}_{\text{HCl}}$) was determined after extraction of both the precipitate and the suspension with HCl ($c = 0.5 \text{ mol L}^{-1}$) and filtration using the phenanthroline method.²⁷

Samples for HPLC measurements were stored in the freezer at around $-18 \text{ }^\circ\text{C}$ and analyzed within 1 week. Photometric measurements were performed within 1–2 h after sampling.

Cryogenic XPS. Sample loading for XPS measurements was performed in an argon atmosphere to protect the samples, due to their oxygen sensitivity. Vials were opened under argon flow, samples were placed on the molybdenum holder, gently pressed to create a flat surface, and immediately placed on the claw of the transfer rod that was precooled at $-170 \text{ }^\circ\text{C}$. The sample was frozen in the spectrometer air-lock under dry N_2 (g) for 45 s prior to a vacuum activation of 10^{-7} Torr. The frozen sample was then transferred to the precooled manipulator in the analysis chamber. During the whole analysis, the pressure and the sample temperature were maintained at 10^{-9} Torr and $-155 \text{ }^\circ\text{C}$, respectively. All XPS spectra were collected with Kratos Axis Ultra DLD electron spectrometer using monochromatized Al $K\alpha$ (1486.6 eV) radiation. Survey spectra were collected from 1000 to 0 eV at a pass energy of 160 eV. High resolution spectra for Fe 2p, S 2p, O 1s, C 1s, Cl 2p, and Na 1s were collected at a pass energy of 20 eV with a scan step of 0.1 eV. In order to verify the occurrence of elemental sulfur, selected samples were measured once under liquid N_2 temperature and then left in the analysis chamber at the same position under vacuum overnight without cooling and measured again the next day at room temperature. Processing of the spectra was accomplished by Kratos software. High-resolution XPS spectra were fitted using linear combinations of 70:30 G-Lorentz functions on Shirley background-subtracted spectra. The O 1s peak at 529.8 eV corresponding to the Fe–O bond of goethite/lepidocrocite was used as the internal standard for binding energy (BE) scale calibration. In the absence of the Fe–O bond, peak positions were referred to the aliphatic C 1s component, set at 285.0 eV.

RESULTS AND DISCUSSION

Reaction Progress As Derived from Wet Chemical Analysis. Ferric (hydr)oxides reacted in a different way with aqueous sulfide in runs with excess iron over sulfide (HR) compared to those with excess sulfide over iron (LR) runs. In the HR runs, the concentration of MBS decreased along with the increase of MES. Only trace amount of MBS ($<0.03 \text{ mmol L}^{-1}$, detection limit of MBS was $0.0009 \text{ mmol L}^{-1}$) could be

determined after 1.5 h in the HR_Gt run (Figure 1) and after 10 min in the HR_Lp run (S1). After 3 h, a significant fraction

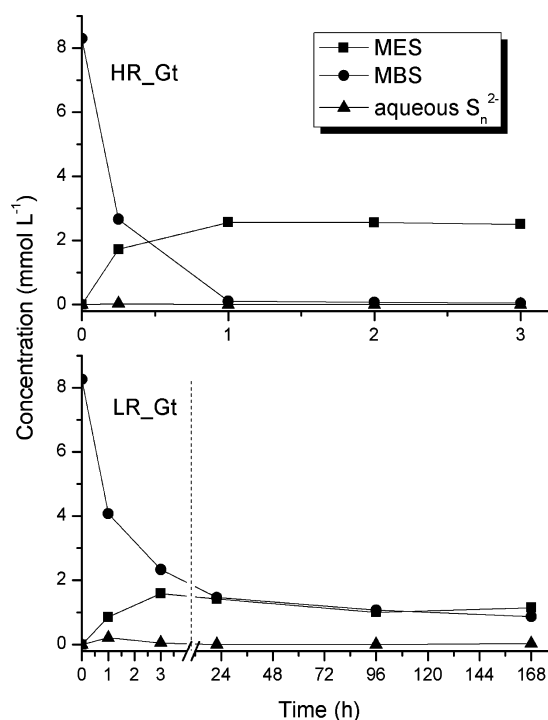


Figure 1. Sulfur speciation during reaction between aqueous sulfide and goethite for iron excess (HR) and sulfide excess (LR) conditions. Note the different time scales between HR_Gt and LR_Gt.

of the initially added S was recovered as MES (31.3% in HR_Gt run and 25.6% in HR_Lp run). Within this time, more $\text{Fe(II)}_{\text{HCl}}$ had formed in the presence of lepidocrocite (7.0 mmol L^{-1}) than in the presence of goethite (5.5 mmol L^{-1}) (Figure 2). $\text{S}_n^{2-}(\text{aq})$ was detected in the first 15 min of the HR_Gt run, the concentration of which made up 5% of the initially added S (in a replicate run only 2%). No $\text{S}_n^{2-}(\text{aq})$ could be detected in HR runs after 3 h.

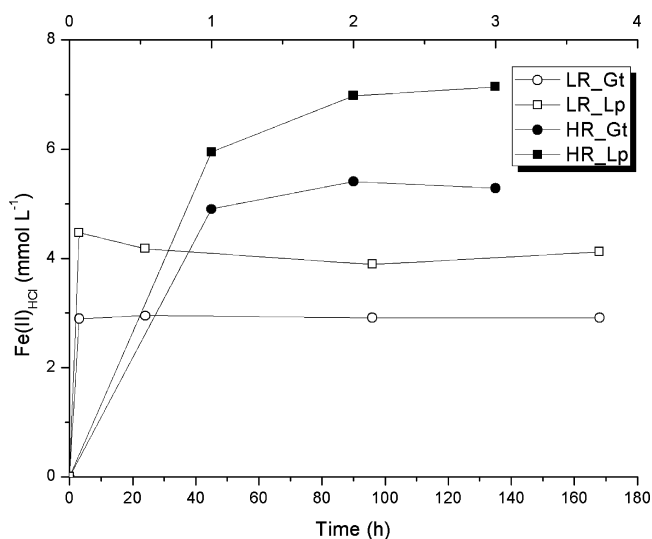


Figure 2. Concentrations of $\text{Fe(II)}_{\text{HCl}}$ of all runs. Note the two different time scales. The data with closed symbols refer to the top x axis.

In LR runs, the concentration of MBS decreased after 3 h to 29.2% of the initially added S in the LR_Gt run and to 6.5% in the LR_Lp run, respectively, along with which the ferric (hydr)oxides was almost completely consumed (Figure 2). MES increased to 16.7% and 19.3% of the initially added S, respectively. $S_n^{2-}(\text{aq})$ remained at a low concentration, with around 2.2% of the initially added S after 3 h and a decrease to 0.9% after 168 h. Thiosulfate and sulfate were undetectable in all runs (data not shown, detection limits were $6 \mu\text{mol L}^{-1}$ and $28 \mu\text{mol L}^{-1}$ for thiosulfate and sulfate, respectively).

Most of the MBS as well as 18.5% of the generated MES and 20.4% of the generated $\text{Fe(II)}_{\text{HCl}}$ were removed with the supernatant after centrifugation. Hence, around 80% of the MES and $\text{Fe(II)}_{\text{HCl}}$ remained in the residual solid phase.

Sulfur Surface-Speciation As Detected by Cryogenic XPS. The survey spectra clearly demonstrate the occurrence of sulfur at the ferric (hydr)oxide's surface after reaction with sulfide (Figure 3 for goethite, Supporting Information (SI),

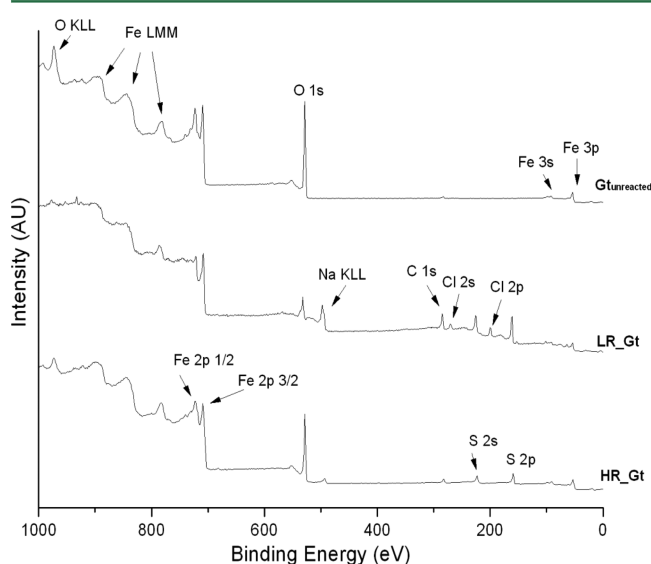


Figure 3. Survey XPS spectra of samples in experiments with goethite.

Figure S2 for lepidocrocite). Spectra also revealed impurities of remaining Na and Cl and contamination with organic carbon from sampling handling mainly in the LR runs.

The high resolution of Fe 2p spectra were fitted following the principle of minimal number of components. The binding energies of $\text{Fe(III)} 2p_{3/2}$ of goethite and lepidocrocite are located at 711.5 and 711.2 eV, respectively, and $\text{Fe(III)} 2p_{1/2}$, both at 724.3 eV. After having reacted with sulfide, a new iron signal with a $\text{Fe} 2p_{3/2}$ binding energy of 707.6 ± 0.2 eV appeared which we interpret as a sulfide-bound ferrous iron species (Fe(II)-S).^{17,19,28} Because of a negligible concentration of the Fe-OH and the Fe-O group in the O 1s spectra (SI, Figure S3 & S4), the Fe 2p spectra of LR runs can be assumed to reflect only Fe(II) species. The concentration of Fe(II) in the LR run was therefore 100% (Figure 4, SI, Figure S5). The Fe(II) concentration in the spectrum of HR run was calculated to be 16.7% (Figure 4) and 8.7% (SI, Figure S5) in the HR_Gt and HR_Lp run, respectively.

S 2p spectra obtained after the reaction and the species concentrations are shown in Figure 5, the corresponding fitting parameters of which are listed in Table 2. Each species in the S 2p spectrum was fitted with a doublet due to spin-orbit splitting

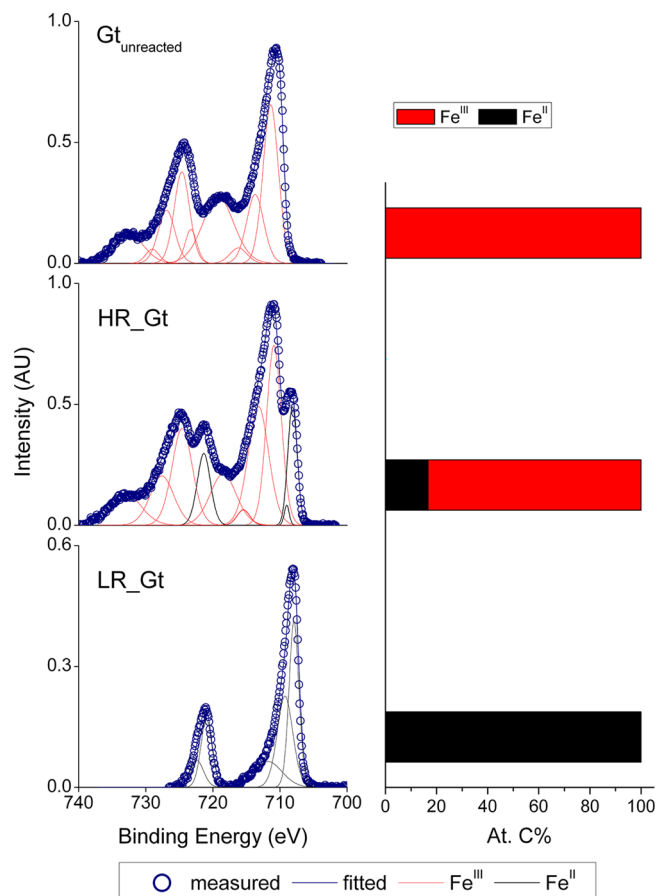


Figure 4. High resolution Fe 2p spectra of goethite and corresponding spectral area concentration of each species before and after reaction. Compound colors in bar chart are the same as in the spectra.

of S $2p_{1/2}$ and S $2p_{3/2}$. It is reasonable to assume that a fraction of the initial sulfide was bound to Fe(II) generated from Fe(III) reduction. Hence, a species with a S $2p_{3/2}$ binding energy characteristic for the Fe(II)-S bond ($S^{2-}(\text{surf})$, 161.2 ± 0.3 eV)^{17,19,29} is regarded to be present in all runs, contributing to 68.1%, 50.2%, 73.3%, and 66.4% of the S 2p spectral area in the HR_Gt, HR_Lp, LR_Gt and LR_Lp run, respectively (Table 2, Figure 5). Proper fitting of the spectra could, however, not be achieved by considering sulfide only. A reasonable fitting of the spectrum of the HR_Gt run was obtained with two additional species, which contributed to 14.4% and 17.5% of the spectral area. S $2p_{3/2}$ binding energies were 162.1 ± 0.2 eV and 163.2 ± 0.3 eV, which can be attributed to disulfide ($S_2^{2-}(\text{surf})$) and polysulfide ($S_n^{2-}(\text{surf})$, with $n > 2$), respectively (cf. Table 2, and references therein). Three other spectra were possible to fit considering only additional species besides the three species discussed above. The HR_Lp spectrum required two species with a S $2p_{3/2}$ binding energy of 164.5 eV (2.7%) corresponding to elemental sulfur ($S_8(\text{surf})$) and 167.5 eV (3.8%) corresponding to sulfite³⁰ ($\text{SO}_3^{2-}(\text{surf})$, Table 2 and Figure 5). The LR_Gt and LR_Lp spectra also required consideration of the S_8 species with a binding energy of 164.4 ± 0.5 eV (4.2% and 15.7%, respectively) (Table 2). The fraction of $S_8(\text{surf})$ was higher in the LR_Lp run compared with the LR_Gt run after 168 h. No $S_8(\text{surf})$ was observed in the HR_Gt run.

There are several indications that the higher reactivity of lepidocrocite has induced a higher electron turnover in the

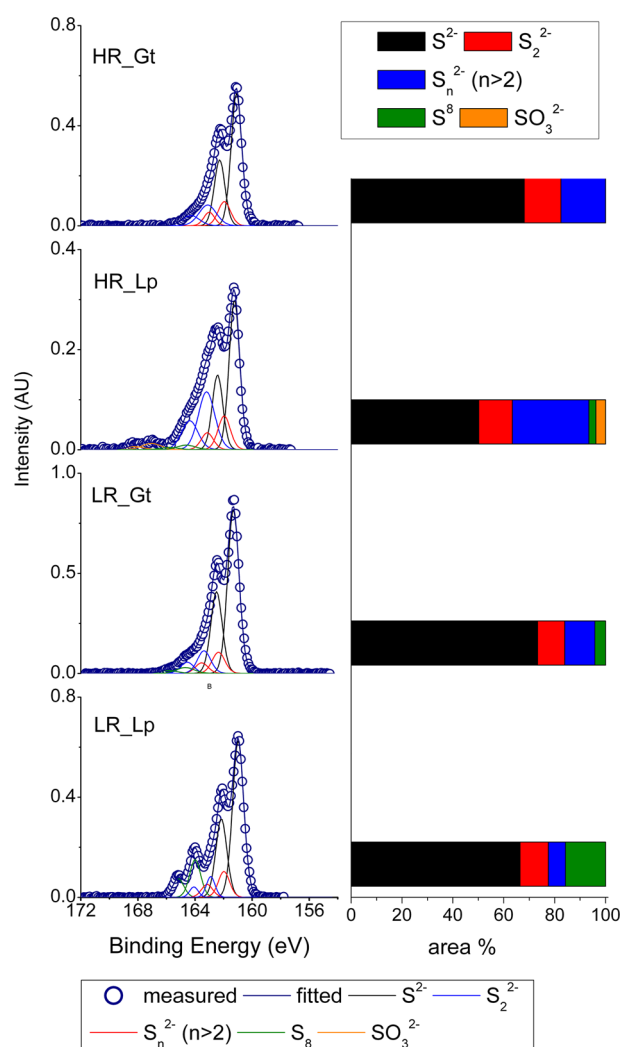


Figure 5. High-resolution S 2p spectra and corresponding spectral area concentration of each species in all runs. Compound colors in the bar chart are the same as in the spectra.

HR_Lp run compared to the HR_Gt run.³¹ The fraction of $S_2^{2-}(\text{surf})$ and $S_n^{2-}(\text{surf})$ ($n > 2$) was higher in the HR_Lp run as well as the yield of $\text{Fe(II)}_{\text{HCl}}$. Additionally, products detected by XPS had a higher oxidation state ($S_8(\text{surf})$ and $\text{SO}_3^{2-}(\text{surf})$) in the presence of lepidocrocite. However, formation of $\text{SO}_3^{2-}(\text{surf})$ from oxidation of reduced sulfur species during sample handling cannot be excluded. $\text{SO}_3^{2-}(\text{surf})$ was detected only in the HR_Lp run and has not been observed in previous studies on $\text{Fe(III)}-\text{S}(-\text{II})$ interaction. We did not analyze for dissolved SO_3^{2-} as an independent verification and sulfate and thiosulfate could not be detected in any sample from this study, which excludes $\text{SO}_3^{2-}(\text{surf})$ formation from disproportionation of thiosulfate.³²

Sulfur Mass Balance. In contrast to the bulk concentration values obtained from wet chemistry data, XPS quantifies the mass percentage of surface-bound species. Hence, the question arises whether these surface species need to be considered in the overall mass balance of the reaction between aqueous sulfide and ferric (hydr)oxides and whether they affect its stoichiometry. To these ends, we will in a first step test whether the mass balance for sulfur detected by wet chemistry methods is complete. In a second approach, we will analyze to what extent the quantitative measurements made by XPS can be related to the bulk measurements.

Characteristic products of the reaction between aqueous sulfide and ferric (hydr)oxides are regarded to consist of elemental sulfur and FeS (amorphous FeS or mackinawite).^{3,10} Elemental sulfur is typically determined using the MES technique which indeed makes up a large fraction of total sulfur recovered from the experiments. Methanol extraction, however, also allows for the determination of surface-associated zerovalent sulfur,¹⁴ a fraction which seems to be relevant according to the XPS results. Hence, application of the bulk techniques MBS and MES considers the concentration of the species aqueous sulfide, $\text{S}(-\text{II})$ associated with aqueous polysulfides ($S_n^{2-}(\text{aq})$), and the concentration of total zerovalent sulfur, including S^0 in the form of colloidal elemental sulfur in the suspension ($S_8(\text{coll})$) and the sulfur associated at

Table 2. XPS Fitting Parameters of Fe and S Species

	Gt _{unreacted}		Lp _{unreacted}		HR_Gt		HR_Lp		LR_Gt		LR_Lp		ref. data ^a
	BE ^b (eV)	FWHM ^c	BE (eV)	FWHM	BE (eV)	FWHM	BE (eV)	FWHM	BE (eV)	FWHM	BE (eV)	FWHM	
S 2p _{3/2}													
S ²⁻	n.d. ^d	n.d.	n.d.	n.d.	161.1	0.85	161.2	0.85	161.3	0.9	161.0	0.9	161.2 ²⁹ 161.3 ^{17,19}
S ₂ ²⁻	n.d.	n.d.	n.d.	n.d.	162.0	1	161.9	1	162.3	1.05	162.0	0.9	162.1 ¹⁹ 162.6 ²⁸
S _n ²⁻	n.d.	n.d.	n.d.	n.d.	163.1	1.4	163.1	1.35	163.4	1.1	162.9	0.7	163.3 ^{2,19} 163.2 ¹⁷ 163.4 ²⁰
S ⁸	n.d.	n.d.	n.d.	n.d.	n.d.	n.d.	164.5	1.5	164.7	1.45	164.0	0.9	165.3 ¹⁷ 164 ²⁰
SO ₃ ²⁻	n.d.	n.d.	n.d.	n.d.	n.d.	n.d.	167.5	1.55	n.d.	n.d.	n.d.	n.d.	166.5 ³⁰
Fe 2p _{3/2}													
Fe(II)-S	n.d.	n.d.	n.d.	n.d.	711.4	2.55	711.0	2.9	n.d.	n.d.	n.d.	n.d.	707.8 ¹⁹ 707.2 ¹⁷ 707.4 ²⁸
Fe(III)-O	711.5	2.6	711.2	2.3	707.6	1.55	707.7	1.65	707.8	1.7	707.4	1.85	711.5 ²⁰

^aAll reference data were recalibrated with the internal standard of Fe-O bond at binding energy of 529.8 eV. ^bBinding energy. ^cFull width at half maximum. ^dNot detected.

the surface ($S_8(\text{surf})$), S° bound to $S_n^{2-}(\text{aq})$ and S° bound to surface associated polysulfides ($S_2^{2-}(\text{surf})$ and $S_n^{2-}(\text{surf})$).

A critical fraction in the sulfur mass balance is sulfur associated with Fe(II). This fraction can comprise crystalline pyrite, mackinawite (FeS), but also species of weak crystallinity with variable stoichiometries. Using HRTEM, Hellige et al. identified nanomackinawite with a large amount of an amorphous phase rich in both iron and sulfur within the first 3 days of experiments comparable to the HR_LP experiment (cf., Figure 8a in Hellige et al.³). Pyrite crystals were observed only after 1 week. Given that experimental conditions in this study were similar to the previous study, we conclude that pyrite did not form in the HR runs. Moreover, the absence of crystalline (i.e., not HCl extractable) pyrite in our experiments at the given reaction time scale of 3 h in the HR runs and 168 h in the LR runs can be also inferred from our wet chemical analysis of $\text{Fe(II)}_{\text{HCl}}$ and MES. Both analytical fractions remained relatively constant after their built-up (e.g., Figure 2 for $\text{Fe(II)}_{\text{HCl}}$). We therefore exclude the formation of pyrite in both HR and LR runs.

The sulfide sulfur associated with Fe(II) is typically determined as acid volatile sulfide (AVS) but it apparently consists also of S(-II) bound in the polysulfide sulfur species e.g. noncrystalline surface disulfide ($S_2^{2-}(\text{surf})$). The S° atom in such species may be analyzed with the MES technique. AVS was not analyzed in this study due to the large uncertainties inherent to this methodology.³³ A good proxy for Fe(II)-S associations, however, would be the amount of HCl-extractable Fe(II), provided a 1:1 stoichiometry exists. Magnetite, which would be extractable with HCl and which had been observed in a previous study with lepidocrocite as an intermediate, was estimated to make up <7% of the generated $\text{Fe(II)}_{\text{HCl}}$ in our experiments (cf., SI) and seems therefore negligible. We therefore calculated the recovery of sulfur by wet chemical analysis using the concentrations measured with the bulk techniques MES, MBS, and $\text{Fe(II)}_{\text{HCl}}$ (eq 1). In LR runs, the degassing rate was considered.

$$S_{\text{recovery}} = \frac{c(\text{MES}) + c(\text{MBS}) + c(\text{Fe(II)}_{\text{HCl}})}{c(\text{S(-II)}_{\text{ini}})} \quad (1)$$

S_{recovery} was found to be 100.8%, 103.9%, 95.7%, and 97.0% for HR_Gt, HR_LP, LR_Gt and LR_LP, respectively. Given the errors inherent to this mass balance approach (we estimated a total error of $\pm 10\%$ based on propagation of errors of the individual methods), recovery seems to be complete.

XPS is a surface-sensitive technique which is able to detect surface coverage up to a thickness of 10 nm.³⁴ A previous HRTEM study demonstrated that during the time the experiments were performed, sulfur was clearly associated with the surface of the ferric minerals.³ We therefore assume that all solid phase-bound S quantified by wet chemical analysis is detectable by XPS and use the area percentage of the S 2p spectra to quantify surface sulfur speciation and to compare these data with the bulk concentration.

The amount of S° detected as polysulfide sulfur by XPS analysis was estimated using eq 2. The chain length of surface-associated polysulfides ($S_n^{2-}(\text{surf})$ with $n = 3-8$) other than disulfide cannot be identified by XPS. We assumed an average chain length of such polysulfides to be 5, in order to simplify the calculation. The total amount of S° bound as polysulfides was 21.2%, 30.7%, 14.8%, and 11.0% in the HR_Gt (3 h),

HR_LP (3 h), LR_Gt (168 h), and LR_LP run (168 h), respectively (Table 3).

$$c(S_{\text{polysulfide}}^\circ) = \frac{1}{2}c(S_2^{2-}(\text{surf})) + \frac{4}{5}c(S_5^{2-}(\text{surf})) \quad (2)$$

Table 3. S° Obtained as MES and from XPS Calculation

	%	HR_Gt	HR_LP	LR_Gt	LR_LP
wet chemical analysis	MES	30.5	25.6	16.7	19.3
XPS	S_{xps}°	21.2	33.4	19.1	26.8
	S_8	0	2.7	4.2	15.7
	S° associated with S_2^{2-}	7.2	6.6	5.4	5.6
	S° bound to S_n^{2-} ($n = 5$)	14.0	24.1	9.5	5.5

Thus, the total amount of S° detected by XPS (S_{xps}°), which is the sum of S_8 and polysulfide-bound S° , was 21.2%, 33.4%, 19.1% and 26.8%, respectively (Table 3). These values can be compared to the MES fractions of the total initial sulfur determined at the time when also the XPS samples were taken, which were 30.5%, 25.6%, 16.7% and 19.3%, respectively (Table 3). The match between the amount of S° derived from XPS measurements and the amount obtained from HPLC measurements is not perfect, but the values are at least in the same order of magnitude.

This analysis clearly indicates that surface polysulfides plus S_8 are a significant fraction of the MES pool. MES is commonly regarded to consist of S_8 sulfur (colloidal and solid phase), aqueous polysulfides,¹⁴ and surface-associated S° . The absence of aqueous polysulfide in HR runs and the low concentration in LR runs (0.9% of the initially added S) imply that MES in our experiments comprised mainly S_8 and surface-associated S° . S_8 concentrations detected by XPS were rather low while concentrations of surface-associated polysulfides were high. We therefore conclude that the S° extracted by methanol with ZnAc pretreatment (MES) comprised the surface polysulfide species.

This conclusion raises the question about the nature of such surface associations. XPS indicates a large quantity of S to be $S_2^{2-}(\text{surf})$, which is either adsorbed to the mineral surface or bound to the generated Fe(II) (e.g., as FeS). Potentially, Fe(II) could be also associated with the surface polysulfides, e.g., as an amorphous Fe(II)-polysulfide phase. This assumption does not conflict with the 1:1 stoichiometry for Fe(II)-S associations inherent to the calculation of the S recovery in eq 1. If sulfur associated with Fe(II) contains methanol-extractable S° and solid phase-bound sulfide, as would be the case with Fe(II)-polysulfide associations, then the S mass balance would still remain complete. In the presence of an amorphous phase of the stoichiometry FeS_n , our wet chemical analysis would extract such species as $\text{Fe(II)}_{\text{HCl}}$ and $(n - 1)$ S° atoms as MES and the S recovery of FeS_n would be the sum of $\text{Fe(II)}_{\text{HCl}}$ and MES.

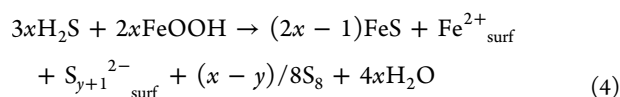
Unfortunately, a direct proof for the occurrence of Fe(II)-polysulfide associations was not possible with the analytical methods used in this study. We therefore tested the possibility for their occurrence based on a mass balance approach. To this end, we compared the fraction $f_{\text{Fe(II),HCl}}$ of $\text{Fe(II)}_{\text{HCl}}$ formed per mol of initial S(-II)

$$f_{\text{Fe(II),HCl}} = \text{Fe(II)}_{\text{HCl}} / \text{S(-II)}_{\text{ini}} \quad (3)$$

with the fraction $f_{S_{2-}, XPS}$ of the spectral area of surface S^{2-} determined with XPS in the HR runs. Inherent to this approach is the assumption that precipitated FeS can be extracted with HCl as $Fe(II)_{HCl}$ and detected with XPS as $S^{2-}(surf)$ (LR runs contain excess initial aqueous sulfide so that these experiments cannot be used for this comparison). Hence, in the absence of any $Fe(II)$ -polysulfide associations the two fractions $f_{Fe(II), HCl}$ and $f_{S_{2-}, XPS}$ would match each other. This was indeed the case in the HR_Gt run ($f_{Fe(II), HCl} = 66.8\%$ and $f_{S_{2-}, XPS} = 68.1\%$).

However, in the HR_Lp run a distinctly higher $Fe(II)_{HCl}$ fraction was observed ($f_{Fe(II), HCl} = 78.7\%$, $f_{S_{2-}, XPS} = 50.2\%$) indicating that sufficient $Fe(II)$ was available to bind surface $S_2^{2-}(surf)$ and $S_n^{2-}(surf)$ ($n > 2$) species besides $S^{2-}(surf)$ and that the occurrence of $Fe(II)$ -polysulfide associations seems possible in this experiment.

This finding has implications for the initial reaction stoichiometry of the interaction between ferric (hydr)oxides and dissolved sulfide, in which a significant fraction of surface-bound polysulfides associated with $Fe(II)$ should be considered, in addition to S_8 and FeS . A generalized stoichiometry matching the recovery can thus be formulated (eq 4)



where $S_{y+1}^{2-}_{surf}$ denotes surface polysulfide and Fe^{2+}_{surf} surface-bound $Fe(II)$. The coefficient x reflects the number of generated S^0 atoms and y ($0 \leq y \leq x$) is the number of S^0 atoms associated with surface polysulfides. Note that under conditions where $y = 0$, we obtain the idealized stoichiometry:

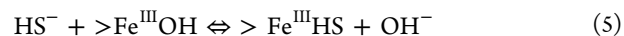


Implication for Sulfur Biogeochemistry. Polysulfides are regarded to be the key reactants for pyrite formation.^{9,16} Pyrite occurrence has been demonstrated in solutions either rich in aqueous polysulfides^{8,9,35} or rich in aqueous $S(-II)$ and S_8 ,^{8,36} in which aqueous polysulfides can rapidly form.¹⁴ Hellige et al. have postulated the contribution of surface bound polysulfides to pyrite formation based on HRTEM measurements and on theoretical considerations.³ They demonstrated that pyrite formation occurred as precipitation of new a phase after 1 week following the reaction between aqueous sulfide and lepidocrocite and disaggregation of iron sulfur associations under experimental conditions comparable to this study. However, they could not further resolve the nature of these species.

Our study supports this hypothesis, showing that a large fraction of S can be recovered as polysulfides at the surface of the iron minerals at a low residual concentration of aqueous sulfide ($<0.03 \text{ mmol L}^{-1}$, LR runs) or after aqueous sulfide has been consumed (HR runs). This finding conflicts with previous studies in which polysulfides are generally assumed to be present in the aqueous phase only or, at least, the existence of polysulfides at the solid phase was not taken into consideration.^{15,16,35,37,38} Solid-phase sulfur forming during the initial interaction between dissolved sulfide and ferric (hydr)oxides is commonly regarded to consist of elemental sulfur, S^{2-} , bound as FeS and S_2^{2-} bound to crystalline pyrite.^{3,10}

Of particular relevance for pyrite formation may be the discovery of surface-associated disulfide. The cause for their formation can be related to the reaction between aqueous sulfide and the ferric (hydr)oxidés mineral surface. Electron transfer between sulfide and ferric iron is regarded to be

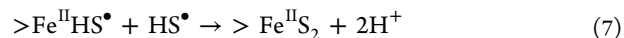
preceded by an adsorption step of sulfide onto the ferric (hydr)oxidés surface.⁴



It has been postulated that the one-electron transfer between surface-associated sulfide and ferric iron (eq 6) generates sulfide radicals HS^\bullet .

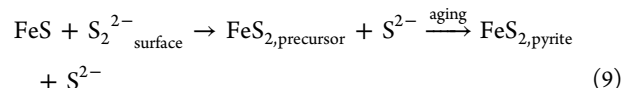
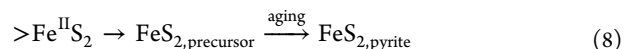


This species may spontaneously react with an additional HS^\bullet radical to form a surface disulfide¹² (eq 7),



which may tend to further react to form polysulfides with longer chain (S_n^{2-} , $n > 2$) and to elemental sulfur depending on pH.¹² Note that $>Fe^{III}OH$, $>Fe^{III}HS$, $>Fe^{II}HS^\bullet$ and $>Fe^{II}S_2$ are surface species.

Surface disulfide species can be regarded to be the precursor required for pyrite formation, which will trigger pyrite formation in the presence of abundant surface-associated $Fe(II)$ either through direct combination (eq 8) or through reaction with FeS (eq 9).



Note that the $FeS_{2,precursor}$ is a noncrystalline form. Reaction 8 leads to FeS dissolution and subsequent reprecipitation as pyrite. HRTEM images discussed in the study of Hellige et al. support this model.³ They observed after 2 h a sulfur-rich rim coating the crystals of lepidocrocite containing domains of nano mackinawite. The coating disintegrated after 72 h of reaction and precipitated as an amorphous phase rich in Fe and S, marking the onset of the formation of pyrite. The S^{2-} released from reaction 8 may be reabsorbed at the surface and react with remaining ferric (hydr)oxides.

Moreover, surface associated polysulfides may play an overlooked role in the sulfur cycle. Polysulfides are generally regarded to exert a high reactivity and to be involved in both abiotic and biotic reactions. For instance, polysulfide species were detected as intermediates during microbial sulfur disproportionation and might even be disproportionated themselves.³⁹ They can serve as electron acceptors for specific bacteria such as *Deltaproteobacteria* from soda lakes.⁴⁰ Polysulfide pathway is regarded to be the important pathway of biotic oxidation of metal sulfides such as arsenopyrite.⁴¹ The chemical bonds between the metal and sulfur are broken by proton attachment, and the sulfur is then liberated as hydrogen sulfide, which could be oxidized in a one-electron step to form polysulfide species.^{12,41} However, only aqueous polysulfide species have been determined to date.^{15,16,35,37,38} This study clearly demonstrates that a large amount ($>50\%$ of generated S^0) and previously unknown fraction of the oxidized sulfur is stabilized as polysulfides at the mineral surface. The question arises as to what extent the occurrence of these species may help to decipher unexplained observations, such as the cryptic sulfur cycle driven by iron in the methane zone of a marine sediment.⁴² Our findings therefore call for a revisiting of the role of polysulfide species in abiotic and biotic sulfur cycling.

■ ASSOCIATED CONTENT

5 Supporting Information

The reaction pattern, the Fe 2p spectra, and the calculation process of minor iron minerals in the runs with lepidocrocite as well as the O 1s spectra after reaction with sulfide in all of the runs. The S 2p spectrum without cooling showed significant elemental sulfur decrease. This material is available free of charge via the Internet at <http://pubs.acs.org>.

■ AUTHOR INFORMATION

Corresponding Author

*Phone: ++49-921-553500; fax: ++49-921-552366; e-mail: moli.wan@uni-bayreuth.de.

Notes

The authors declare no competing financial interest.

■ ACKNOWLEDGMENTS

This study was financially supported by the German Research Foundation (DFG) for the research group “etrap” (electron transfer processes in anoxic aquifers) (FOR 580, PE 438/11-3, und PLA 302/7-1) and by the European Science Foundation (ESF) for the research networking programme “FIMIN” (The Functionality of Iron Minerals in Environmental Processes). We thank Professor Per Persson for granting access to the XPS analysis, and Dr. Thilo Behrends for his valuable comments and discussions. Finally, we thank the editor and the anonymous reviewers for their constructive comments.

■ REFERENCES

- (1) Peiffer, S.; Dos Santos Afonso, M.; Wehrli, B.; Gaechter, R. Kinetics and mechanism of the reaction of hydrogen sulfide with lepidocrocite. *Environ. Sci. Technol.* **1992**, *26* (12), 2408–2413.
- (2) Poulton, S. W. Sulfide oxidation and iron dissolution kinetics during the reaction of dissolved sulfide with ferrihydrite. *Chem. Geol.* **2003**, *202* (1–2), 79–94.
- (3) Hellige, K.; Pollok, K.; Larese-Casanova, P.; Behrends, T.; Peiffer, S. Pathways of ferrous iron mineral formation upon sulfidation of lepidocrocite surfaces. *Geochim. Cosmochim. Acta* **2012**, *81* (0), 69–81.
- (4) Dos Santos Afonso, M.; Stumm, W. Reductive dissolution of iron(III) (hydr)oxides by hydrogen sulfide. *Langmuir* **1992**, *8* (6), 1671–1675.
- (5) Berner, R. A. Sedimentary pyrite formation. *Am. J. Sci.* **1970**, *268* (1), 1–23.
- (6) Raiswell, R.; Berner, R. A. Pyrite formation in euxinic and semi-euxinic sediments. *Am. J. Sci.* **1985**, *285* (8), 710–724.
- (7) Morse, J. W. Sulfides in sandy sediments: New insights on the reactions responsible for sedimentary pyrite formation. *Aquat. Geochem.* **1999**, *5* (1), 75–85.
- (8) Wang, Q.; Morse, J. W. Pyrite formation under conditions approximating those in anoxic sediments I. Pathway and morphology. *Mar. Chem.* **1996**, *52* (2), 99–121.
- (9) Schoonen, M.; Barnes, H. Reactions forming pyrite and marcasite from solution: II. Via FeS precursors below 100 °C. *Geochim. Cosmochim. Acta* **1991**, *55* (6), 1505–1514.
- (10) Yao, W.; Millero, F. J. Oxidation of hydrogen sulfide by hydrous Fe(III) oxides in seawater. *Mar. Chem.* **1996**, *52* (1), 1–16.
- (11) Pyzik, A. J.; Sommer, S. E. Sedimentary iron monosulfides: Kinetics and mechanism of formation. *Geochim. Cosmochim. Acta* **1981**, *45* (5), 687–698.
- (12) Steudel, R. Mechanism for the Formation of Elemental Sulfur from Aqueous Sulfide in Chemical and Microbiological Desulfurization Processes. *Ind. Eng. Chem. Res.* **1996**, *35* (4), 1417–1423.
- (13) Luther, G. W. The role of one- and two-electron transfer reactions in forming thermodynamically unstable intermediates as

barriers in multi-electron redox reactions. *Aquat. Geochem.* **2010**, *16* (3), 395–420.

(14) Kamyshny, A.; Borkenstein, C. G.; Ferdelman, T. G. Protocol for quantitative detection of elemental sulfur and polysulfide zero-valent sulfur distribution in natural aquatic samples. *Geostand. Geoanal. Res.* **2009**, *33* (3), 415–435.

(15) Kamyshny, A.; Ekeltchik, I.; Gun, J.; Lev, O. Method for the determination of inorganic polysulfide distribution in aquatic systems. *Anal. Chem.* **2006**, *78* (8), 2631–2639.

(16) Rickard, D.; Luther, G. I. Chemistry of iron sulfides. *Chem. Rev.* **2007**, *107* (2), 514–562.

(17) Mullet, M.; Boursiquot, S.; Abdelmoula, M.; Génin, J.-M.; Ehrhardt, J.-J. Surface chemistry and structural properties of mackinawite prepared by reaction of sulfide ions with metallic iron. *Geochim. Cosmochim. Acta* **2002**, *66* (5), 829–836.

(18) Eggleston, C. M.; Ehrhardt, J. J.; Stumm, W. Surface structural controls on pyrite oxidation kinetics: An XPS-UPS, STM, and modeling study. *Am. Mineral.* **1996**, *81* (9), 1036–1056.

(19) Nesbitt, H.; Muir, I. X-ray photoelectron spectroscopic study of a pristine pyrite surface reacted with water vapour and air. *Geochim. Cosmochim. Acta* **1994**, *58* (21), 4667–4679.

(20) Thomas, J. E.; Jones, C. F.; Skinner, W. M.; Smart, R. S. C. The role of surface sulfur species in the inhibition of pyrrhotite dissolution in acid conditions. *Geochim. Cosmochim. Acta* **1998**, *62* (9), 1555–1565.

(21) Schwertmann, U.; Cornell, R. M. *Iron Oxides in the Laboratory*; Wiley-VCH: Weinheim, Germany, 2008.

(22) Fonselius, S.; Dyrssen, D.; Yhlen, B. Determination of hydrogen sulphide. In *Methods Seawater Analysis*, 3rd ed.; Wiley Online Library: Weinheim, Germany, 2007; Chapter 5, pp 91100.

(23) Mylon, S. E.; Benoit, G. Subnanomolar Detection of Acid-Labile Sulfides by the Classical Methylene Blue Method Coupled to HPLC. *Environ. Sci. Technol.* **2001**, *35* (22), 4544–4548.

(24) Tabatabai, M. A rapid method for determination of sulfate in water samples. *Environ. Lett.* **1974**, *7* (3), 237–243.

(25) Steudel, R.; Holdt, G.; Göbel, T.; Hazeu, W. Chromatographic separation of higher polythionates SnO_6^{2-} ($n = 3 \dots 22$) and their detection in cultures of *Thiobacillus ferrooxidans*; Molecular composition of bacterial sulfur secretions. *Angew. Chem. Int. Ed.* **1987**, *26* (2), 151–153.

(26) Rizkov, D.; Lev, O.; Gun, J.; Anisimov, B.; Kuselman, I. Development of in-house reference materials for determination of inorganic polysulfides in water. *Accredit. Qual. Assur.* **2004**, *9* (7), 399–403.

(27) Tamura, H.; Goto, K.; Yotsuyanagi, T.; Nagayama, M. Spectrophotometric determination of iron (II) with 1, 10-phenanthroline in the presence of large amounts of iron (III). *Talanta* **1974**, *21* (4), 314–318.

(28) Karthe, S.; Szargan, R.; Suoninen, E. Oxidation of pyrite surfaces: A photoelectron spectroscopic study. *Appl. Surf. Sci.* **1993**, *72* (2), 157–170.

(29) Nesbitt, H.; Scaini, M.; Höchst, H.; Bancroft, G.; Schaufuss, A.; Szargan, R. Synchrotron XPS evidence for Fe^{2+} -S and Fe^{3+} -S surface species on pyrite fracture-surfaces, and their 3D electronic states. *Am. Mineral.* **2000**, *85* (5–6), 850–857.

(30) Baltrusaitis, J.; Cwiertny, D. M.; Grassian, V. H. Adsorption of sulfur dioxide on hematite and goethite particle surfaces. *Phys. Chem. Chem. Phys.* **2007**, *9* (41), 5542–5554.

(31) Poulton, S. W.; Krom, M. D.; Raiswell, R. A revised scheme for the reactivity of iron (oxyhydr)oxide minerals towards dissolved sulfide. *Geochim. Cosmochim. Acta* **2004**, *68* (18), 3703–3715.

(32) Moses, C. O.; Nordstrom, D. K.; Mills, A. L. Sampling and analysing mixtures of sulphate, sulphite, thiosulphate and polythionate. *Talanta* **1984**, *31* (5), 331–339.

(33) Rickard, D.; Morse, J. W. Acid volatile sulfide (AVS). *Mar. Chem.* **2005**, *97* (3), 141–197.

(34) Vickerman, J. C.; Gilmore, I. S. *Surface Analysis: The Principal Techniques*. Wiley Online Library: Weinheim, Germany, 2009; Vol. 2.

(35) Luther, G. W. Pyrite synthesis via polysulfide compounds. *Geochim. Cosmochim. Acta* **1991**, 2839–2849.

(36) Benning, L. G.; Wilkin, R. T.; Barnes, H. Reaction pathways in the Fe–S system below 100 C. *Chem. Geol.* **2000**, 167 (1), 25–51.

(37) Lichtschlag, A.; Kamyshny, A., Jr; Ferdelman, T. G.; deBeer, D. Intermediate sulfur oxidation state compounds in the euxinic surface sediments of the Dvurechenskii mud volcano (Black Sea). *Geochim. Cosmochim. Acta* **2013**, 105 (0), 130–145.

(38) Giggenbach, W. Optical spectra and equilibrium distribution of polysulfide ions in aqueous solution at 20. deg. *Inorg. Chem.* **1972**, 11 (6), 1201–1207.

(39) Poser, A.; Lohmayer, R.; Vogt, C.; Knoeller, K.; Planer-Friedrich, B.; Sorokin, D.; Richnow, H.-H.; Finster, K. Disproportionation of elemental sulfur by haloalkaliphilic bacteria from soda lakes. *Extremophiles* **2013**, 17 (6), 1003–1012.

(40) Sorokin, D. Y.; Tourova, T. P.; Mußmann, M.; Muyzer, G. *Dethiobacter alkaliphilus* gen. nov. sp. nov., and *Desulfurivibrio alkaliphilus* gen. nov. sp. nov.: Two novel representatives of reductive sulfur cycle from soda lakes. *Extremophiles* **2008**, 12 (3), 431–439.

(41) Rohwerder, T.; Gehrke, T.; Kinzler, K.; Sand, W. Bioleaching review part A. *Appl. Microbiol. Biotechnol.* **2003**, 63 (3), 239–248.

(42) Holmkvist, L.; Ferdelman, T. G.; Jørgensen, B. B. A cryptic sulfur cycle driven by iron in the methane zone of marine sediment (Aarhus Bay, Denmark). *Geochim. Cosmochim. Acta* **2011**, 75 (12), 3581–3599.

(43) Peiffer, S.; Gade, W. Reactivity of ferric oxides toward H₂S at low pH. *Environ. Sci. Technol.* **2007**, 41 (9), 3159–3164.

■ NOTE ADDED AFTER ASAP PUBLICATION

Britta Planer-Friedrich's name was misspelled in the version of this paper published April 23, 2014. The correct version published April 25, 2014.

Correction to Occurrence of Surface Polysulfides during the Interaction between Ferric (Hydr)Oxides and Aqueous Sulfide

Moli Wan,* Andrey Shchukarev, Regina Lohmayer, Britta Planer-Friedrich, and Stefan Peiffer

Environ. Sci. Technol., 2014, 48 (9), 5076–5084 DOI: 10.1021/es405612f

In Table 2 the X-ray photoelectron spectroscopy (XPS) parameters, binding energy (BE) and full width at half-maximum (fwhm), of the species Fe(II)-S and Fe(III)-O for HR_Gt, HR_Lp, LR_Gt and LR_Lp were reverted and should be interchanged.

In Table 2 the reference of the data 163.3^{2,19} should be 163.3¹⁹.

Published: May 20, 2014



The occurrence of surface polysulphides during the interaction between ferric (hydr)oxides and aqueous sulphide

Moli Wan¹, Andrey Shchukarev², Regina Lohmayer³, Britta Planer-Friedrich³, Stefan Peiffer¹

¹ Department of Hydrology, University of Bayreuth, D-95440, Bayreuth, Germany

² Biogeochemistry, Department of Chemistry, Umeå Iniversity, SE-901 87 Umeå, Sweden

³ Environmental Geochemistry, University of Bayreuth, D-95440 Bayreuth, Germany

8 pages and 6 figures are presented in this supporting information.

Sulphur mass balance

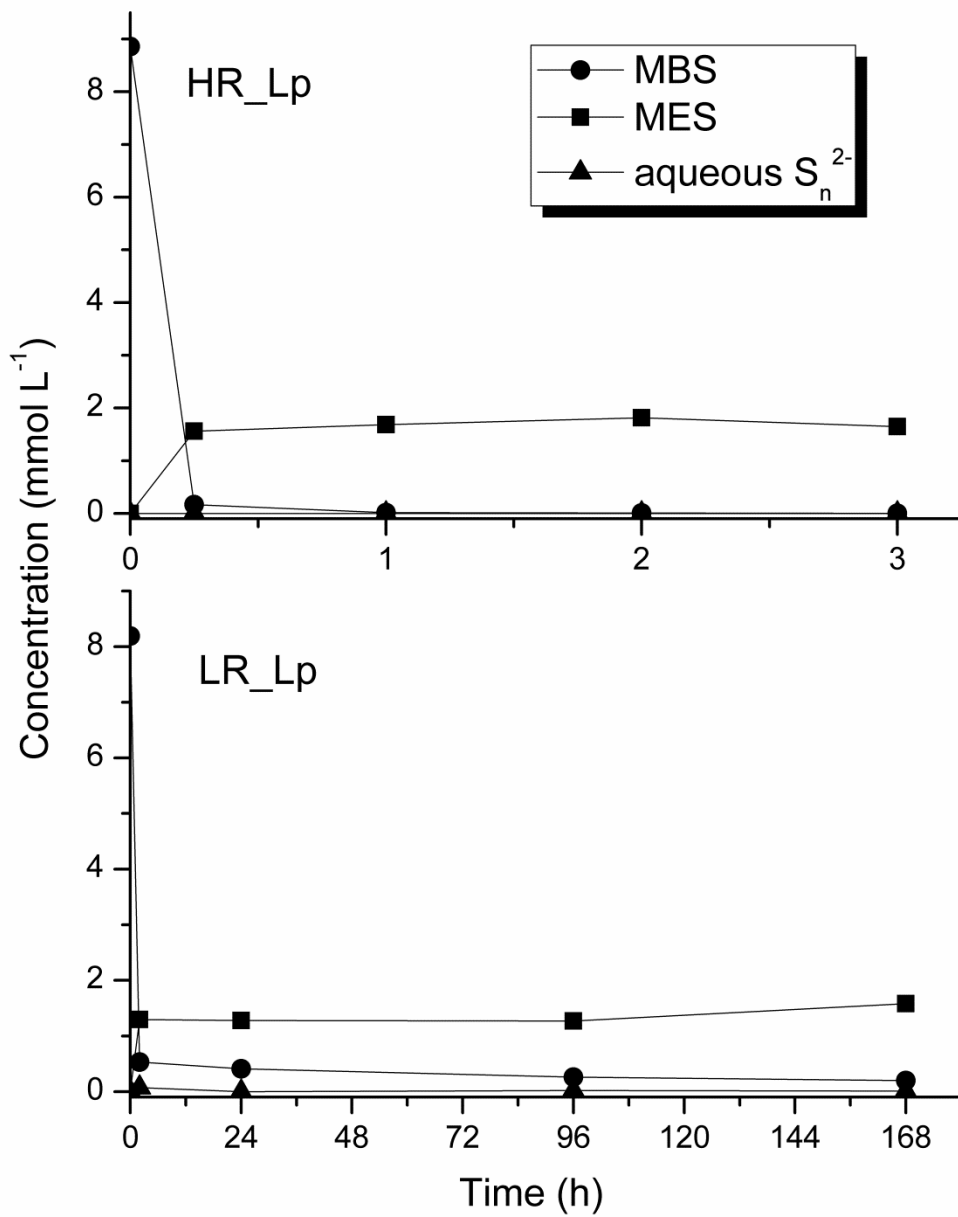
Magnetite was regarded to be an intermediate of minor relevance in the previous paper¹. The concentration of magnetite was not given but it may be attributed to the fraction of $\text{Fe(II)}_{\text{excess}}$ which was calculated as:

$$\text{Fe(II)}_{\text{excess}} = \text{Fe(II)}_{\text{HCl}} - \text{FeS} = \text{Fe(II)}_{\text{HCl}} - (\text{S(-II)}_{\text{ini}} - \text{S}^{\circ}) \quad (1)$$

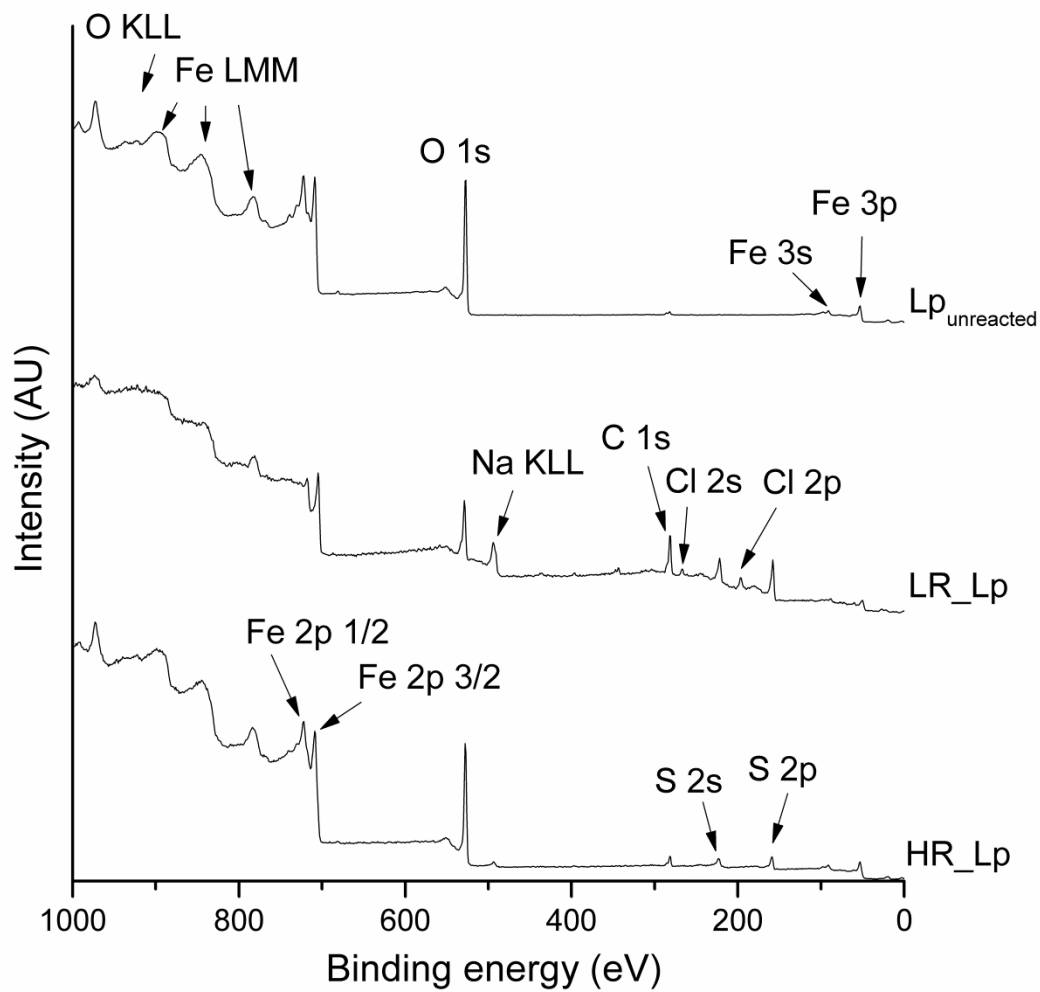
Although their S° is extracted without ZnAc pretreatment, we can in a first approximation apply this equation for our experiments

$$\text{Fe(II)}_{\text{excess}} = \text{Fe(II)}_{\text{HCl}} - \text{FeS} = \text{Fe(II)}_{\text{HCl}} - (\text{S(-II)}_{\text{ini}} - \text{MES}) \quad (2)$$

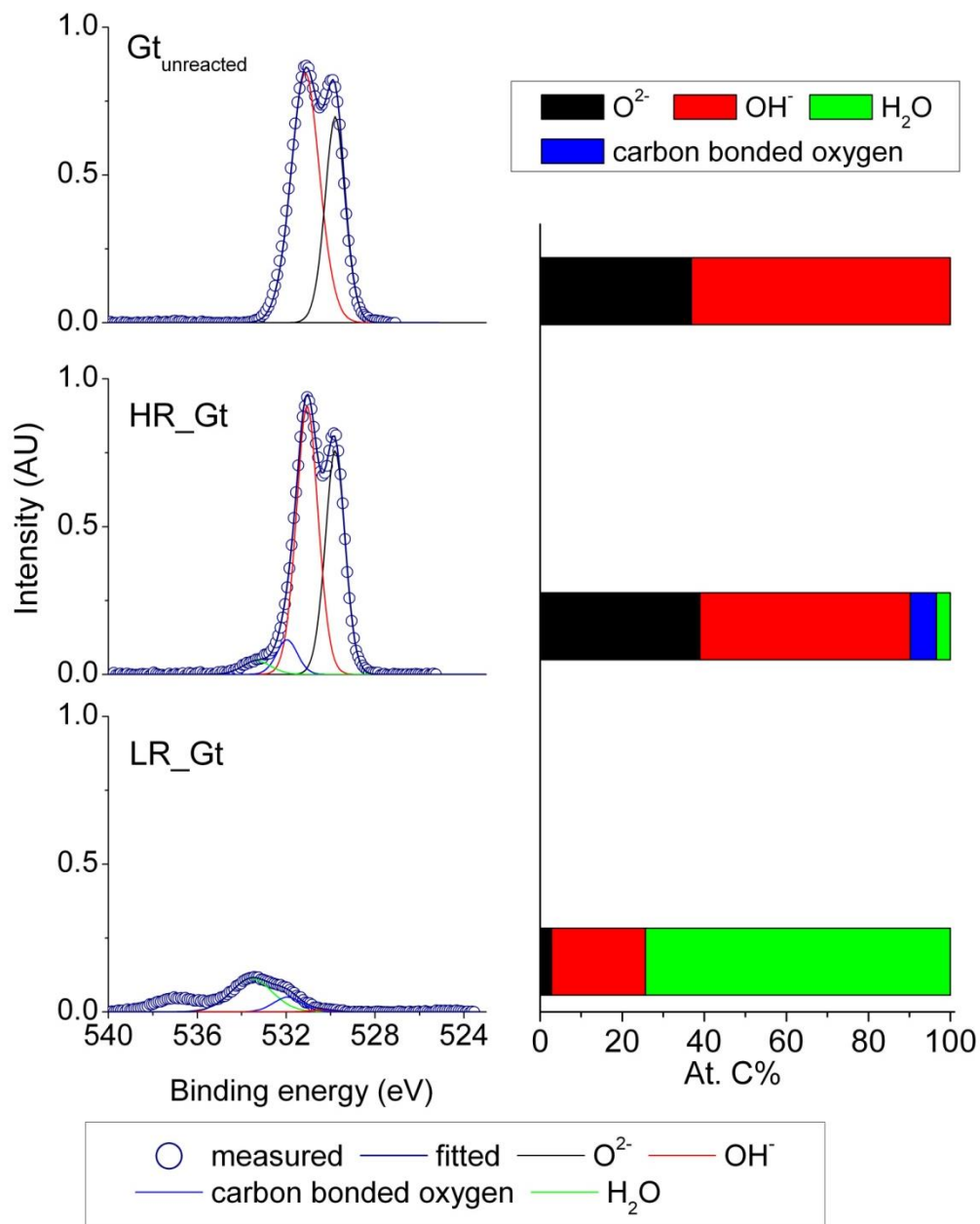
The calculation shows that $\text{Fe(II)}_{\text{excess}}$ would be a minor fraction in the HR_Lp run (7%) and absent in the other three runs (negative values in HR_Gt (-2%), LR_Gt (-33%) and LR_Lp (-3%) runs, respectively). Hence magnetite should be a minor component in our experiments.



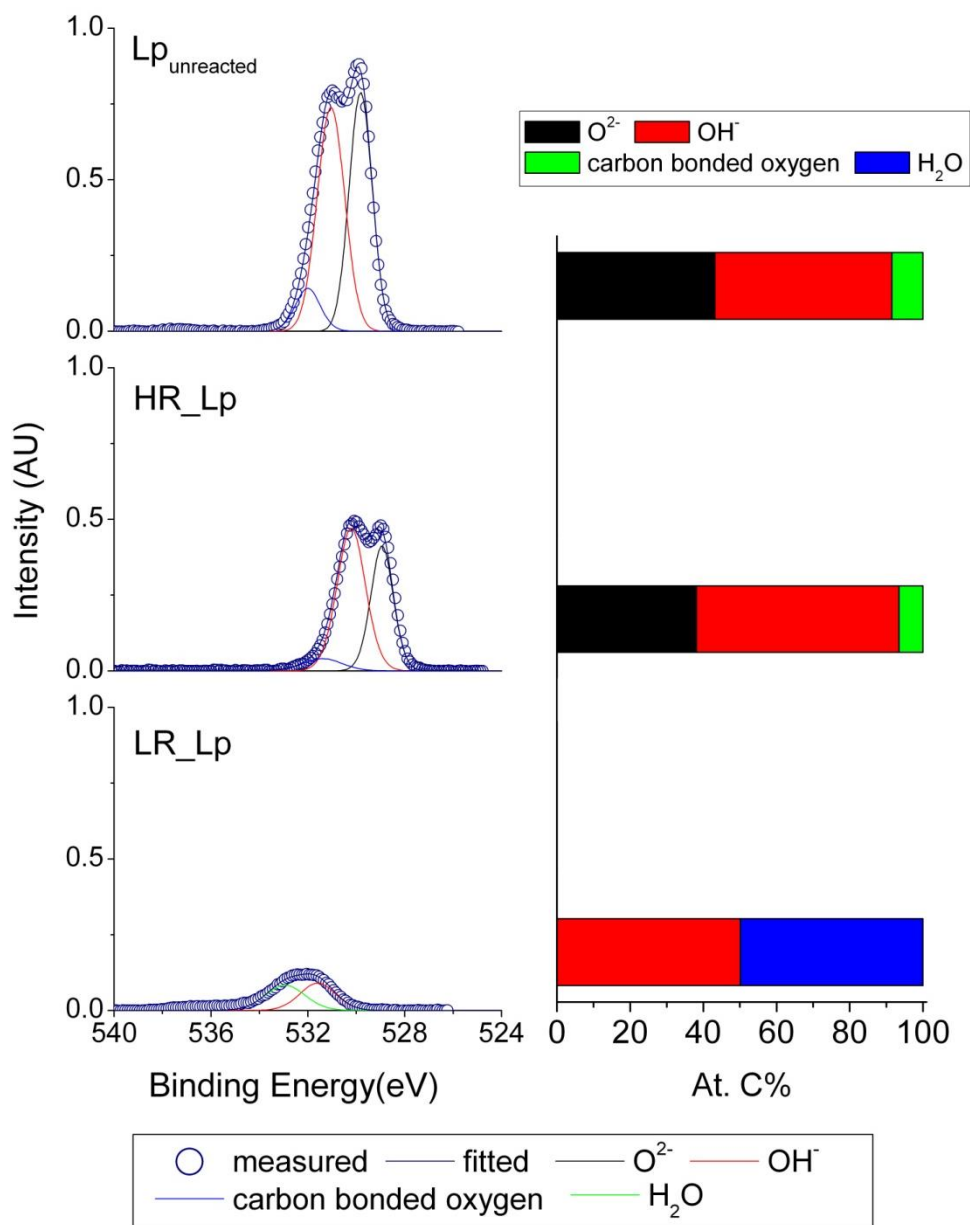
S 1. Sulphur speciation during reaction between aqueous sulphide and lepidocrocite for iron excess (HR) and sulfide excess (LR) conditions. Note the different time scales between HR_Lp and LR_Lp.



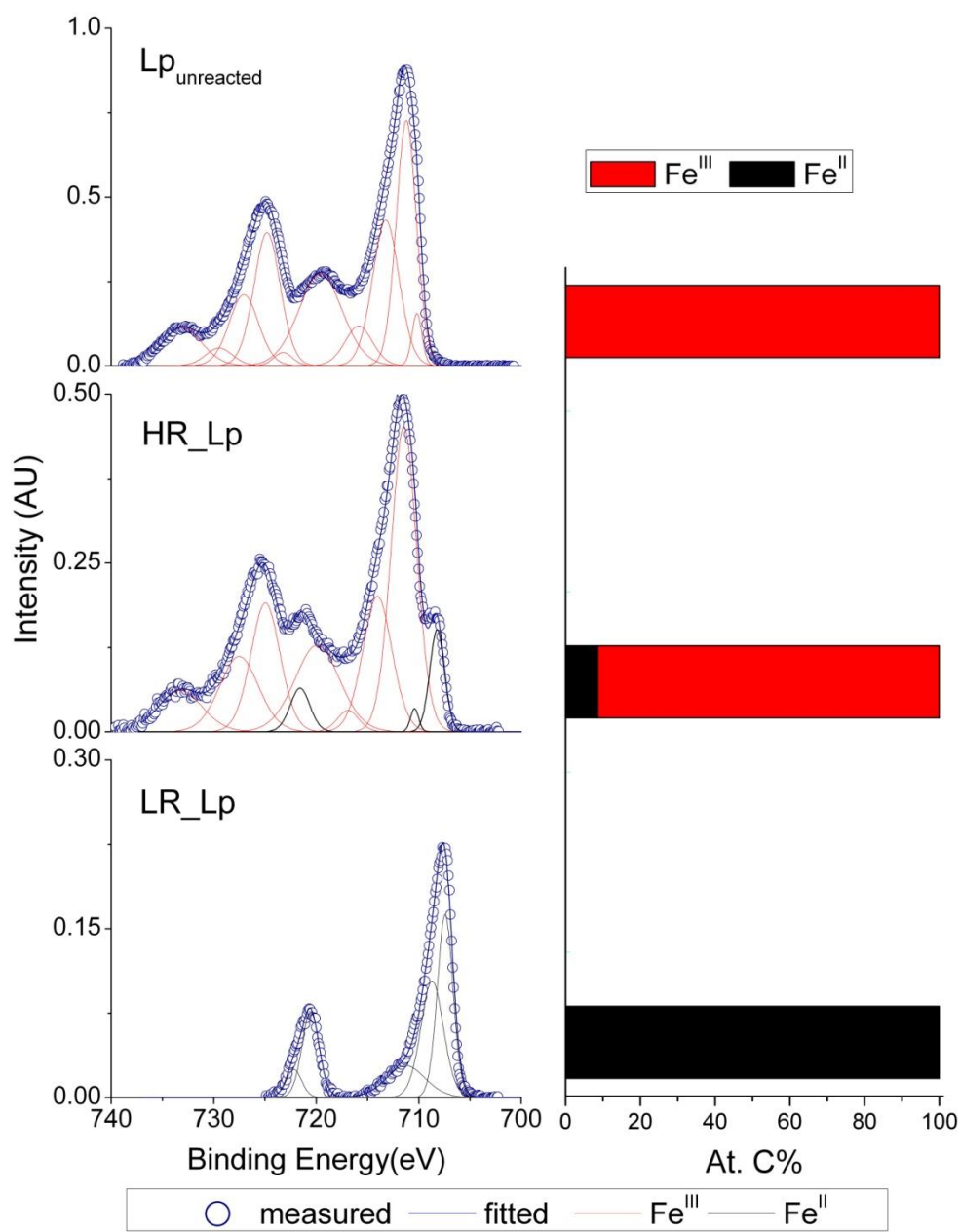
S 2. Survey XPS spectra of samples in experiments with lepidocrocite.



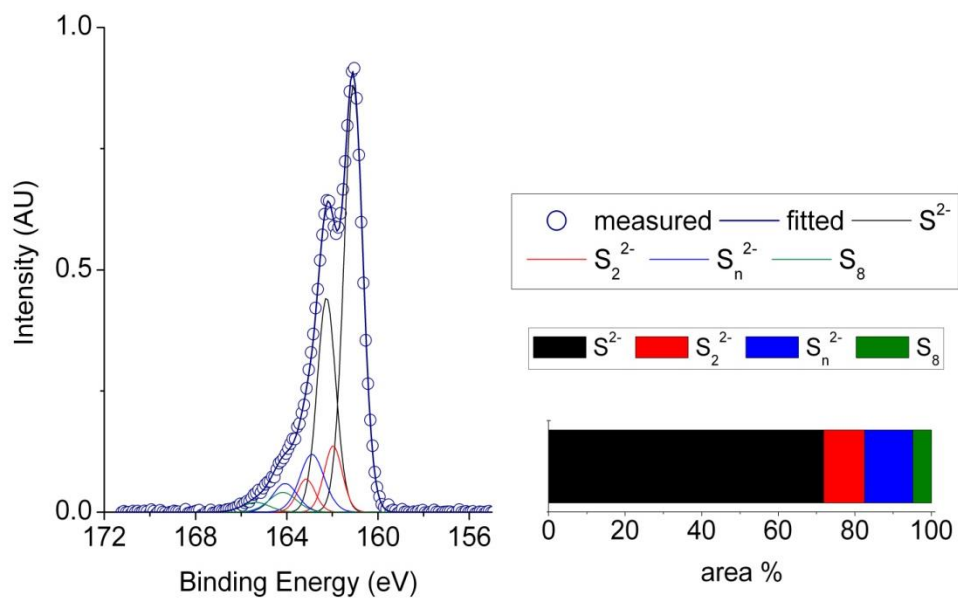
S 3. High resolution O 1s spectra of goethite and corresponding spectral area concentration of each species before and after reaction. Compound colours in bar chart are the same as in the spectra.



S 4. High resolution O 1s spectra of lepidocrocite and corresponding spectral area concentration of each species before and after reaction. Compound colours in bar chart are the same as in the spectra.



S 5. High resolution Fe 2p spectra of lepidocrocite and corresponding spectral area concentration of each species before and after reaction. Compound colours in bar chart are the same as in the spectra.



S 6. High resolution S 2p spectra of LR_Lp after leaving in the analysis chamber overnight without cooling. The corresponding spectral area concentration of each species has the same color as in the spectra.

Reference

1. Hellige, K.; Pollok, K.; Larese-Casanova, P.; Behrends, T.; Peiffer, S., Pathways of ferrous iron mineral formation upon sulfidation of lepidocrocite surfaces. *Geochim. Cosmochim. Acta* **2012**, *81*, (0), 69-81.

Study 3

Reproduced with permission from

**Sulfur Species as Redox Partners and Electron Shuttles for Ferrihydrite
Reduction by *Sulfurospirillum deleyianum***

Regina Lohmayer, Andreas Kappler, Tina Lösekann-Behrens, Britta Planer-Friedrich

Applied and Environmental Microbiology, 2014, 80, pp 3141-3149

Copyright 2014 American Society for Microbiology

Sulfur Species as Redox Partners and Electron Shuttles for Ferrihydrite Reduction by *Sulfurospirillum deleyianum*

Regina Lohmayer,^a Andreas Kappler,^b Tina Lösekann-Behrens,^b Britta Planer-Friedrich^a

Environmental Geochemistry Group, Bayreuth Center for Ecology and Environmental Research (BayCEER), University of Bayreuth, Bayreuth, Germany^a; Geomicrobiology, Center for Applied Geosciences, University of Tuebingen, Tuebingen, Germany^b

Iron(III) (oxyhydr)oxides can represent the dominant microbial electron acceptors under anoxic conditions in many aquatic environments, which makes understanding the mechanisms and processes regulating their dissolution and transformation particularly important. In a previous laboratory-based study, it has been shown that 0.05 mM thiosulfate can reduce 6 mM ferrihydrite indirectly via enzymatic reduction of thiosulfate to sulfide by the sulfur-reducing bacterium *Sulfurospirillum deleyianum*, followed by abiotic reduction of ferrihydrite coupled to reoxidation of sulfide. Thiosulfate, elemental sulfur, and polysulfides were proposed as reoxidized sulfur species functioning as electron shuttles. However, the exact electron transfer pathway remained unknown. Here, we present a detailed analysis of the sulfur species involved. Apart from thiosulfate, substoichiometric amounts of sulfite, tetrathionate, sulfide, or polysulfides also initiated ferrihydrite reduction. The portion of thiosulfate produced during abiotic ferrihydrite-dependent reoxidation of sulfide was about 10% of the total sulfur at maximum. The main abiotic oxidation product was elemental sulfur attached to the iron mineral surface, which indicates that direct contact between microorganisms and ferrihydrite is necessary to maintain the iron reduction process. Polysulfides were not detected in the liquid phase. Minor amounts were found associated either with microorganisms or the mineral phase. The abiotic oxidation of sulfide in the reaction with ferrihydrite was identified as rate determining. Cysteine, added as a sulfur source and a reducing agent, also led to abiotic ferrihydrite reduction and therefore should be eliminated when sulfur redox reactions are investigated. Overall, we could demonstrate the large impact of intermediate sulfur species on biogeochemical iron transformations.

Iron(III) (oxyhydr)oxides are important for various processes in the environment. Potentially toxic trace metalloids and metals such as arsenic, lead, and cadmium sorb to the surface of iron(III) (oxyhydr)oxides and are removed from the aqueous phase (1–5). Also, the availability of nutrients such as phosphate can be limited by adsorption (6, 7). During reductive dissolution, substances adsorbed to the surface of iron(III) (oxyhydr)oxides are released.

Microorganisms play an important role in the reduction of iron(III) (oxyhydr)oxides. Several bacterial species, such as *Geobacter* and *Shewanella* spp., can grow by using iron(III) minerals as electron acceptors. Either the bacteria are in direct contact with poorly soluble iron(III) (oxyhydr)oxides and transfer electrons directly to the minerals (8) or different electron-shuttling compounds such as flavins, humic substances, or quinones can transfer electrons from the cells to the iron(III) (oxyhydr)oxides (9–12).

The occurrence of sulfur is another factor that is of importance for biogeochemical redox processes related to iron. Especially in its reduced state, sulfur is highly reactive with iron. Hydrogen sulfide (H₂S) can lead to the abiotic reductive dissolution of iron oxides (13) with the consequent release of adsorbed substances. However, sulfur does not necessarily have to be present as sulfide to lead to the reduction of iron oxides. A wide range of sulfur-reducing bacteria exist that can use the different oxidized sulfur species as electron acceptors and therefore contribute to the formation of sulfide, which can then react abiotically with iron oxides (14). Sulfidogenesis by sulfate-reducing bacteria was found to lead to iron mineral transformation and arsenic mobilization (15, 16). Straub and Schink (17) also investigated this reaction pathway of sulfur-mediated iron(III) mineral reduction in experiments with *Sulfurospirillum deleyianum* and ferrihydrite. The sulfur-reducing bacterium *S. deleyianum* is not able to use ferric iron as an electron

acceptor (18) but can reduce thiosulfate (S₂O₃²⁻), elemental sulfur (S⁰), and sulfite (SO₃²⁻). Sulfate (SO₄²⁻) cannot be reduced (19, 20). When offering the bacteria 0.05 mM thiosulfate as an electron acceptor, Straub and Schink (17) observed a reduction of 6 mM ferrihydrite. On the basis of this finding, they proposed a shuttling mechanism whereby thiosulfate is microbially reduced to sulfide, which is then reoxidized by ferrihydrite reduction. Their data suggested that sulfur had cycled between the bacteria and iron up to 60 times. Thiosulfate, elemental sulfur, or polysulfides (S_n²⁻) were proposed by Straub and Schink (17) to complete the sulfur cycle, but the identity of the reoxidized sulfur species was not revealed until now.

In the present study, we therefore investigated the process of electron shuttling between *S. deleyianum* and ferrihydrite in more detail with a focus on sulfur speciation. The main goal was to identify the reoxidized sulfur species that are produced by the abiotic reaction of sulfide and ferrihydrite. To this end, the experiment was split into its reductive (microbial) and oxidative (abiotic) reactions. We then repeated the experiments done by Straub

Received 19 December 2013 Accepted 2 March 2014

Published ahead of print 14 March 2014

Editor: S.-J. Liu

Address correspondence to Britta Planer-Friedrich, b.planer-friedrich@uni-bayreuth.de.

Supplemental material for this article may be found at <http://dx.doi.org/10.1128/AEM.04220-13>.

Copyright © 2014, American Society for Microbiology. All Rights Reserved.

doi:10.1128/AEM.04220-13

and Schink (17) but also tested sulfur species other than thiosulfate and analyzed the sulfur species present.

MATERIALS AND METHODS

Bacterial cultivation. A culture of *S. deleyianum* (DSM 6946) was obtained from the Deutsche Sammlung von Mikroorganismen und Zellkulturen. Freshwater medium, which contained 4.4 mM KH_2PO_4 , 5.6 mM NH_4Cl , 0.7 mM $\text{CaCl}_2 \cdot 2\text{H}_2\text{O}$, and 2.0 mM $\text{MgSO}_4 \cdot 7\text{H}_2\text{O}$ or, for a sulfate-free medium, 2.0 mM $\text{MgCl}_2 \cdot 6\text{H}_2\text{O}$, was prepared in a Widdel flask and autoclaved. After cooling under an atmosphere of $\text{N}_2\text{-CO}_2$ (90/10 [vol/vol]), the medium was supplied with bicarbonate buffer, autoclaved under $\text{N}_2\text{-CO}_2$ (90/10 [vol/vol]) to a final concentration of 30 mM, and 1 ml/liter each of a sterile vitamin, a trace element (SL-10), and a selenite tungstate solution was added (21). The pH was adjusted to 7 by the addition of anoxic and sterile 1 M HCl. The medium was used to fill serum bottles that had been washed with 1 M HCl and distilled water prior to autoclaving. The headspace was flushed with $\text{N}_2\text{-CO}_2$ (90/10 [vol/vol]), and the bottles were sealed with butyl rubber stoppers and aluminum crimps. For standard cultivation, the medium was supplied with 20 mM fumarate ($\text{C}_4\text{H}_2\text{Na}_2\text{O}_4$; Merck) as an electron acceptor, 20 mM formate (CHNaO_2 ; Merck) as an electron donor, 20 mM acetate ($\text{C}_2\text{H}_3\text{NaO}_2$; Sigma-Aldrich) as a carbon source, and 0.5 mM L-cysteine ($\text{C}_3\text{H}_7\text{NO}_2\text{S}$; Roth) as both a sulfur source and a reducing agent. All solutions were prepared in ultrapure water (Merck Millipore, 18.2 m Ω /cm, 3 ppb total organic carbon at 25°C), either autoclaved or sterilely filtered with 0.2- μm cellulose acetate filters (MembraPure; membraPure), and stored in serum bottles under N_2 . The cultures were incubated at 28°C in the dark.

Preparation of ferrihydrite suspensions. Ferrihydrite was synthesized as described by Schwertmann and Cornell (22) and Raven et al. (23). A total of 20 g of iron(III) nitrate nonahydrate [$\text{Fe}(\text{NO}_3)_3 \cdot 9\text{H}_2\text{O}$; Acros Organics] was suspended in ultrapure water. The pH was adjusted to 7.3 by adding 1 M KOH. The suspension was centrifuged and washed with ultrapure water four times. The wet pellet was resuspended in ultrapure water to a final concentration of about 0.5 M ferric iron [Fe(III)], transferred to a serum bottle, which was deoxygenized by flushing with N_2 , and stored at 8°C in the dark. Ferrihydrite suspensions were used for experiments within 2 months after preparation.

Experimental setup and sampling. All experiments were carried out with serum bottles (30, 50, or 100 ml), which were standing upright for the whole duration of the experiment and were filled with medium (30, 25, or 100 ml). For the experiments, the standard concentrations of thiosulfate, cysteine, acetate, and formate, at 0.1, 2, 5, and 10 mM, respectively, were the same as in the study of Straub and Schink (17). Experimental variations included different thiosulfate and cysteine concentrations, as well as replacement of thiosulfate with other sulfur compounds. Note that the concentrations of sulfur-containing substances are referred to as moles equivalent of S, in contrast to the paper of Straub and Schink (17). Stock solutions were either autoclaved or sterilely filtered and stored in serum bottles under N_2 . Solutions of sodium thiosulfate pentahydrate ($\text{Na}_2\text{O}_3\text{S}_2 \cdot 5\text{H}_2\text{O}$), sodium sulfite (Na_2SO_3 [anhydrous]; Fluka), potassium tetrathionate ($\text{K}_2\text{S}_4\text{O}_6$; Sigma-Aldrich), sodium sulfide nonahydrate ($\text{Na}_2\text{S} \cdot 9\text{H}_2\text{O}$; Sigma-Aldrich), and potassium polysulfide (K_2S_x ; Sigma-Aldrich) were prepared in ultrapure water. The latter two were prepared inside a Coy anoxic glove box ($\text{N}_2\text{-H}_2$ [95/5, vol/vol]). The solution of L-cystine ($\text{C}_6\text{H}_{12}\text{N}_2\text{O}_4\text{S}_2$; Applichem) used first was also prepared in ultrapure water. As cystine is not very soluble in water, the solution for a further experiment was prepared by dissolving cystine in 5 M NaOH, diluting it with ultrapure water, and adjusting the pH to 9 by adding 1 M HCl.

The standard nominal ferrihydrite concentration was 5 mM, as described by Straub and Schink (17), to avoid the formation of magnetite, which was observed at higher concentrations (24). As particles settled very fast in ferrihydrite suspension, it was difficult to add exactly the same amount of ferrihydrite to each serum bottle. Therefore, the initial ferrihydrite concentrations varied from approximately 3 to 5 mM. A standard inoculum size of 1% was chosen instead of the 0.01% used by Straub and

Schink (17) to shorten the initial lag phase and to observe mineral transformations in shorter times. Comparative experiments were also done with a 0.01% inoculum.

Samples were taken from the serum bottles inside the glove box with a needle and a syringe, which was flushed and filled with $\text{N}_2\text{-CO}_2$ (90/10 [vol/vol]) to replace the volume of liquid removed with the same volume of gas. Also inside the glove box, samples were filtered with 0.2- μm cellulose-acetate filters (MembraPure; membraPure), acidified for iron analysis, derivatized for polysulfide analysis, and mixed with 2% (wt/vol) zinc acetate dihydrate [$\text{Zn}(\text{CH}_3\text{COO})_2 \cdot 2\text{H}_2\text{O}$; Grüssing] to precipitate dissolved sulfide.

Analytical methods. (i) Iron. Ferrous iron [Fe(II)] and total iron [Fe(tot)] were determined photometrically by the ferrozine assay (25). Therefore, unfiltered samples were diluted in 1 M HCl 2-fold for Fe(II) determination and 20-fold for Fe(tot) determination. After Fe mineral dissolution, samples were centrifuged for 5 min at 15,000 rpm and hydroxylamine hydrochloride ($\text{NH}_2\text{OH} \cdot \text{HCl}$ [Acros Organics], 10% [wt/vol] in 1 M HCl) was added to Fe(tot) samples to reduce all iron to Fe(II) before adding the ferrozine reagent (0.1% [wt/vol] ferrozine [$\text{C}_{20}\text{H}_{13}\text{N}_4\text{NaO}_6\text{S}_2 \cdot \text{H}_2\text{O}$; Acros Organics]–50% ammonium acetate [$\text{C}_2\text{H}_7\text{NO}_2$; Acros Organics]). The absorbance at 570 nm of the purple ferrozine-Fe(II) complex was measured with a microplate reader (Infinite 200 PRO; TECAN). Fe(III) concentrations were calculated by subtracting Fe(II) concentrations from Fe(tot) concentrations.

Over the course of ferrihydrite reduction, we observed significant color changes of the suspensions from brown to black. These black suspended particles immediately dissolved in 1 M HCl and had a characteristic hydrogen sulfide smell, suggesting that they were ferrous sulfides and not magnetite. As iron concentrations were quantified from unfiltered samples, such suspended iron precipitates were codetermined with truly dissolved iron species. However, we observed that in most experimental setups with ferrihydrite and bacteria, the Fe(tot) concentration in the samples taken decreased over time (data not shown) and whitish-gray precipitates were sticking to the bottoms of the serum bottles. These precipitates were soluble in 1 M HCl, and test measurements showed that they contained 93 to 101% Fe(II) (data not shown). Straub and Schink (17) also observed white to gray precipitates, which were assumed to be precipitates of Fe(II) and carbonate (siderite) or phosphate (vivianite). Overall, this means that Fe(II) concentrations determined in solution accounted only for aqueous iron and ferrous sulfides and not for ferrous carbonates or phosphates. To quantify the total amount of ferrous iron [Fe(II) total] formed, the missing amount of Fe(tot), i.e., the difference between the initial and actually measured values of Fe(tot), was added to the respective values of Fe(II) determined in solution, assuming that the missing Fe was precipitated as Fe(II) carbonates and phosphates at the glass wall.

(ii) Sulfide. The analysis of sulfide in filtered samples was performed photometrically by the methylene blue method (26). Absorption at 660 nm was measured (Hach Lange DR 3800).

(iii) Polysulfides and elemental sulfur. Polysulfide analysis was performed by the method of Kamyshny et al. (27), which is based on the conversion of labile inorganic polysulfides into more stable dimethylpolysulfanes. This is achieved by derivatization with methyl trifluoromethanesulfonate (methyl triflate, $\text{CF}_3\text{SO}_2\text{OCH}_3$; Sigma-Aldrich) in a water-methanol (H_3COH , high-performance liquid chromatography [HPLC] gradient grade; VWR) mixture. In the present study, derivatization was done with both unfiltered and filtered samples. For the filtered samples, 800 μl of methanol was placed in a 1.5-ml HPLC vial to which 200 μl of filtered sample and 6 μl of methyl triflate were added simultaneously. For the unfiltered samples, derivatization was performed in 2-ml Eppendorf centrifuge tubes with 1.5 times the amount of each reagent. After derivatization, these solutions were also filtered into 1.5-ml HPLC vials. Samples were stored in a freezer until analysis. Dimethylpolysulfanes were analyzed by HPLC (Merck Hitachi L-2130 pump, L-2200 autosampler, and L-2420 UV-VIS detector) and separated by gradient elution over a C_{18}

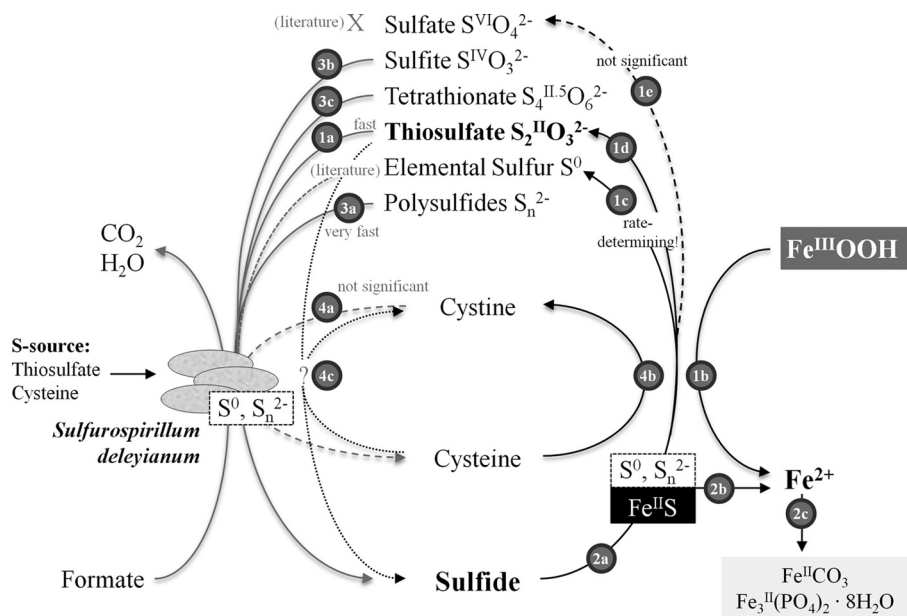


FIG 1 Proposed mechanisms of sulfur cycle-mediated ferrihydrite reduction by *S. deleyianum*. Thiosulfate, sulfide, and iron are in bold because they are the main reactants in the cycle. The numbered processes are discussed in the text.

column (Bischoff Waters Spherisorb, ODS2, 5 μm , 250 by 4.6 mm) by a modification of the method of Rizkov et al. (28). Initially, the solvent consisted of 70% methanol and 30% ultrapure water at a flow rate of 1 ml/min. The methanol concentration was increased to 80% for 10 min, kept constant for 15 min, increased to 100% for 10 min, kept constant for 10 min, decreased to 70% for 5 min, and kept constant for the last 10 min. The injection volume was 100 μl , and detection was performed at a wavelength of 230 nm. Concentrations of dimethyl disulfide and dimethyl trisulfide were determined by the use of commercially available standards ($\text{C}_2\text{H}_6\text{S}_2$ [Acros Organics], $\text{C}_2\text{H}_6\text{S}_3$ [Acros Organics]). For quantification of polysulfides from dimethyl tetrasulfide to dimethyl octasulfide, a dimethylpolysulfane mixture was synthesized as described by Rizkov et al. (28). Separation of the mixture was performed by preparative chromatography with a reversed-phase C_{18} column [Phenomenex SphereClone ODS(2), 5 μm , 250 by 10 mm], an eluent of 50% acetonitrile ($\text{C}_2\text{H}_3\text{N}$, HPLC gradient grade; Roth) and 50% formic acid (CH_2O_2 ; Grüssing), and a flow rate of 5 ml/min. The individual dimethylpolysulfanes in the collected fractions were oxidized to sulfate in a microwave (MarsXpress; CEM) with hydrochloric and nitric acids at 200°C for 10 min. The resulting sulfate concentrations were analyzed by inductively coupled plasma mass spectrometry (ICPMS, XSeries2; Thermo Fisher) and used for quantification.

The method of polysulfide derivatization in methanol with subsequent HPLC analysis was also suitable for the detection of elemental sulfur. For preparation of calibration standards, elemental sulfur powder (S, reagent grade, purified by sublimation, up to a 100-mesh particle size, powder; Sigma-Aldrich) was dissolved in dichloromethane (CH_2Cl_2 ; Sigma-Aldrich) and diluted in the same methanol-water mixture (5:1 ratio) that was used for derivatization.

(iv) **Thiosulfate.** Filtered samples for thiosulfate measurement were flash frozen in liquid nitrogen and stored in a freezer until analysis, which was performed with the above-mentioned HPLC system by a modification of the protocol published by Steudel et al. (29). For separation, a reversed-phase C_{18} column (Grace GraceSmart, RP18, 5 μm , 150 by 4.6 mm) was used. Elution was performed with two alternative eluent compositions, once with 0.002 M tetra-*n*-butylammonium hydroxide [$(\text{CH}_3\text{CH}_2\text{CH}_2\text{CH}_2)_4\text{N}(\text{OH})$; Fluka] and 0.001 M sodium carbonate (Na_2CO_3 ; Merck) in 85% ultrapure water and 15% acetonitrile ($\text{C}_2\text{H}_3\text{N}$, HPLC gradient grade; Roth), with the pH adjusted

to 7.7 by the addition of 1 M HCl and once—to achieve more reliable eluent preparation and hence more stable analytical conditions—with 0.002 M tetrabutylammonium dihydrogen phosphate [$(\text{CH}_3\text{CH}_2\text{CH}_2\text{CH}_2)_4\text{N}[\text{OP}(\text{OH})_2\text{O}]$; Sigma-Aldrich] in 85% ultrapure water and 15% acetonitrile. The flow rate was 1 ml/min, the injection volume was 10 μl , and the detection wavelength was 215 nm.

(v) **Sulfate.** Sulfate was measured by anion-exchange chromatography-ICPMS in filtered samples, which were flash frozen in liquid nitrogen and kept in a freezer until analysis (30). The injection volume was 100 μl , and separation was achieved with an anion-exchange column (Dionex IonPac, AG-16/AS-16, 4 mm) and elution with a gradient of 0.02 to 0.1 M NaOH at a flow rate of 1.2 ml/min. Sulfate was detected by ICPMS (XSeries2, Thermo-Fisher) as SO^+ (m/z 48).

Genome sequence analysis. Comparative analysis of the finished *S. deleyianum* genome was performed with the integrated microbial genomes (IMG) platform and the tools provided therein (31).

RESULTS AND DISCUSSION

As a summary of our studies we propose a revised model for the involvement of different sulfur species in electron shuttling between *S. deleyianum* and ferrihydrite compared to the model previously published by Straub and Schink (17). Our model is shown in Fig. 1, and the individual reactions will be discussed in the following sections.

Separating the reduction of thiosulfate to sulfide by *S. deleyianum* from the abiotic oxidation of sulfide by ferrihydrite. To gain insights into the electron-shuttling processes in the ferrihydrite-*S. deleyianum* cultures, the experiment was split into reductive (microbial) and oxidative (abiotic) reactions. The first set of experiments was conducted with *S. deleyianum* but without the addition of iron(III) minerals, and the second was conducted abiotically with ferrihydrite.

Microbial reduction of thiosulfate by *S. deleyianum*. In the absence of ferrihydrite, *S. deleyianum* reduced 2 and 0.1 mM thiosulfate completely to sulfide (see Fig. SI-1 in the supplemental material; reaction 1a in Fig. 1), which is in accordance with the

literature (19, 20). According to IMG genome annotation (31), thiosulfate reduction to sulfide is mediated by a Phs-like thiosulfate reductase complex (gene loci *Sdel_0269*, *Sdel_0270*, and *Sdel_0271*) via the non-thiol-dependent thiosulfate disproportionation pathway. Elemental sulfur was measurable between days 2 and 7 in unfiltered and filtered samples (see Table SI-1 in the supplemental material), which means that in the absence of iron(III) minerals, elemental sulfur seems to be stable in solution. From days 2 to 7, thiosulfate was completely reduced to sulfide by *S. deleyianum*. Elemental sulfur concentrations were highest on day 2 but accounted for less than 1% of the initial thiosulfate concentrations and decreased until day 7. From day 7 on, polysulfides were detectable as S_6^{2-} in unfiltered samples of both experiments with 2 and 0.1 mM thiosulfate (see Table SI-1). With concentrations of ≤ 0.012 mM in the experiment with 2 mM thiosulfate, the amount of S_6^{2-} came to 0.6% of the initial thiosulfate concentration. In the experiment with 0.1 mM thiosulfate, the respective percentage of S_6^{2-} was 17% at maximum.

Polysulfides can form from the reaction between elemental sulfur and sulfide, which was shown to be the end product of thiosulfate reduction by *S. deleyianum*. Hedderich et al. (32) came to the conclusion that polysulfides occur as intermediate species in the process of sulfur respiration. This seems to be the case not only with elemental sulfur but also with thiosulfate as an electron acceptor. Finding polysulfides only in unfiltered and not in filtered samples indicates that polysulfides are associated with the microorganisms, either bound to the cell surface or occurring inside the cells. To sum up, elemental sulfur and polysulfides do form as intermediate sulfur species in the microbial thiosulfate reduction process, but the final product in solution is sulfide exclusively.

Abiotic oxidation of sulfide coupled to ferrihydrite reduction. In the absence of *S. deleyianum*, sulfide, which was added to a 5 mM ferrihydrite suspension in 10 steps of 0.01 mM at intervals of 1 h, reduced ferrihydrite (reaction 1b in Fig. 1) and was itself oxidized mainly to elemental sulfur (Fig. 2; reaction 1c in Fig. 1). We hypothesize that elemental sulfur was bound to the surface of the iron minerals, as it was detectable only in unfiltered samples. Without the addition of cysteine (Fig. 2A), elemental sulfur was detected after 4.9 h and the concentration increased continuously to 0.037 mM. The thiosulfate concentration also increased after 6.2 h but to a lesser extent than the elemental sulfur concentration (reaction 1d in Fig. 1). Polysulfides occurred in only insignificant amounts in unfiltered samples. As no darkening of the suspension was observed, the formation of FeS could be excluded. Sulfate was detectable in minor amounts over the whole course of the experiment. The oxidation of sulfide to sulfate stops the process of electron shuttling between the microorganisms and ferrihydrite (reaction 1e, Fig. 1). Genome analysis shows that a sulfate adenylyltransferase mediating the conversion of sulfate to adenylylsulfate is encoded in the *S. deleyianum* genome (gene locus *Sdel_1709*) but an adenylylsulfate reductase is absent. Thus, *S. deleyianum* is unable to perform dissimilatory sulfate reduction, which is also in accordance with previous reports (19, 20). In this experiment, the addition of 0.1 mM sulfide led to the reduction of 0.14 mM ferrihydrite.

In the second abiotic experiment, where sulfide was added in the presence of 2 mM cysteine to a 5 mM ferrihydrite suspension (Fig. 2B), 0.93 mM Fe(II) was produced. The suspension gradually turned black, suggesting that FeS was formed and sulfide was removed from solution (reaction 2a in Fig. 1). This process was also

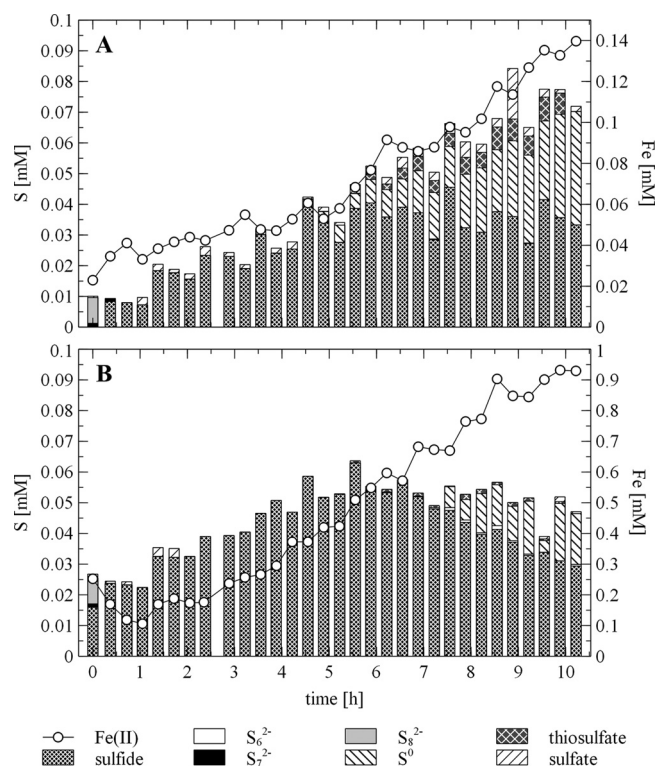


FIG 2 Abiotic Fe(II) production from ferrihydrite and sulfur speciation in freshwater medium to which 0.1 mM sulfide was added in 10 steps at intervals of 1 h beginning at 0.4 h. Concentrations of polysulfides and elemental sulfur (S^0) were detectable only in unfiltered samples. Experiment A was conducted without cysteine, and experiment B was conducted with 2 mM cysteine. Note the different scales for Fe(II) on the secondary y axes. Sulfate data for experiment B from 2.1 to 4.2 h and from 5.6 to 9.2 h are missing.

obvious from the sum of all of the sulfur species, which increased until 5.6 h and then decreased and at the end was two-thirds of the sum of the sulfur species in the experiment without cysteine. Cysteine seemed to enforce the precipitation of FeS by keeping sulfide in the reduced state. The production of elemental sulfur began later and occurred to a lesser extent than in the experiment without cysteine. Polysulfides, thiosulfate, and sulfate occurred in insignificant amounts. Sulfide was already measurable at the beginning of the experiment, i.e., before the first addition of sulfide. This is an analytical artifact because cysteine also yields a sulfide signal in the methylene blue measurement. A comparison of literature data shows that the identity of oxidized sulfur species produced by the reaction of sulfide and ferrihydrite seems to differ, depending on the experimental conditions. In experiments with ferrihydrite-coated sand and gaseous H_2S , FeS (ca. 67%) and elemental sulfur (ca. 33%) were found as main products detected under anoxic conditions (33). In artificial seawater, Poulton (34) found that in the reaction with ferrihydrite, dissolved sulfide was oxidized mainly to elemental sulfur and that reduced Fe(II) was associated with the oxide surface to a large extent. Up to 15% of the total Fe(II) was found as FeS at pH 7.5. Under estuarine conditions, the reaction of hydrous ferric iron oxides and aqueous sulfide produced 86% elemental sulfur, including polysulfide sulfur, and 14% thiosulfate (35). In experiments with ferrihydrite, sulfate, and sulfate-reducing bacteria, elemental sulfur was also found as a major oxidation product attached to the iron mineral

TABLE 1 Reduction of Fe(III) in ferrihydrite in incubations of *S. deleyianum*

Thiosulfate concn (mM)	% inoculum	% Fe(III) reduction in expt 1, 2 ^a
2	1	100, 95
0.1	1	91, 86
2	0.01	76, 62
0.1	0.01	38, 32

^a Bacteria were supplied with 2 mM cysteine as a sulfur source and a reductant, 5 mM acetate as a carbon source, and 10 mM formate as an electron donor. Results obtained in duplicate experiments after 14 days are presented.

surface. However, sulfur speciation in solution was dominated by sulfate (36). In all of these studies, elemental sulfur was analyzed directly at the surface or after extraction of unfiltered samples or the filter itself. Nevertheless, elemental sulfur could also be detected in solution as a product of the reaction between ferrihydrite and H₂S at low pH (37). In the present study, elemental sulfur was found as a major oxidation product but only in unfiltered samples. Straub and Schink (17) postulated that elemental sulfur, polysulfides, and/or thiosulfate could serve as electron shuttles between *S. deleyianum* and ferrihydrite, but they did not identify the oxidized sulfur species. Since they also observed ferrihydrite reduction when the iron mineral and the microorganisms were spatially separated, the electron-shuttling compound would have to be present in the aqueous phase. In contrast, our finding that elemental sulfur was attached to the mineral surface indicates that iron reduction is possible only with direct contact of the microorganisms and the iron mineral.

The roles of individual sulfur species in iron(III) mineral reduction by *S. deleyianum*. (i) **The role of thiosulfate as an electron acceptor for *S. deleyianum*.** Straub and Schink (17) showed that 5 mM ferrihydrite was reduced within 35 days in an experiment with 0.05 mM thiosulfate (equivalent to 0.1 mM S), 2 mM cysteine, and a 0.01% *S. deleyianum* inoculum. For comparison, we conducted experiments with different concentrations of thiosulfate and different inoculum amounts (Table 1). Ferrihydrite reduction was fastest with 2 mM thiosulfate and a 1% inoculum. The inoculum amount had a greater influence than the thiosulfate concentration on the rate of iron(III) mineral reduction. In all of the experiments, complete reduction of ferrihydrite within 29 days was observed. In the experiments with 2 mM thiosulfate, black mineral particles formed that did not disappear until the end of the experiment. In the experiment with 0.1 mM thiosulfate and a 1% inoculum, the suspension also turned darker in the beginning and then gradually became clearer until complete colorlessness in the end. With 0.1 mM thiosulfate and a 0.01% inoculum, it took longer until the suspension was completely clear. As processes of iron reduction seemed to be qualitatively similar in systems with 0.1 mM thiosulfate and a 1 or 0.01% inoculum, the greater inoculum amount was chosen for further experiments to accelerate the reactions observable in the experiments.

(ii) **Kinetics of thiosulfate consumption.** After the addition of 2 mM thiosulfate to suspensions with 5 mM ferrihydrite and a 1% inoculum, parallel reduction of Fe(III) and thiosulfate was observable (Fig. 3A). In the first phase, up to day 3, only small amounts of Fe(II) were produced. Up to day 6, thiosulfate and Fe(III) were depleted more rapidly, while the suspension turned completely black, indicating the formation of FeS (reaction 2a, Fig. 1). Almost no free sulfide

was detectable in filtered samples, which means that precipitation of FeS or oxidation of sulfide by the reaction with ferrihydrite must have been faster than reduction of thiosulfate by the microorganisms. Small amounts of polysulfides were found in unfiltered samples, suggesting that they are associated with the microorganisms or are attached to the mineral. We have recently found evidence that polysulfides attached to the surface of iron(III) (oxyhydr)oxides are precursors of pyrite formation (51)—a similar process might have occurred in the present experiment. Simultaneously with polysulfides, elemental sulfur concentrations increased rapidly between days 5 and 6 and then were stable until the end. As already seen in the abiotic experiment, elemental sulfur was the main oxidation product of sulfide but accounted for only 10% of the initial thiosulfate concentration. For complete ferrihydrite reduction, polysulfides, elemental sulfur, or sulfide from FeS precipitations (reaction 2b, Fig. 1) had to act as a recyclable sulfur reservoir. When polysulfides and elemental sulfur had reached maximum concentrations (at day 5.7, Fig. 3A), the process of Fe removal from suspension started, as the amount of Fe(II) in suspension remained stable while the calculated amount of total Fe(II) increased. At the bottoms of the bottles, whitish gray precipitations formed, which we assume were siderite or vivianite (reaction 2c in Fig. 1). At that time point, no sulfide seemed to have been left to precipitate with Fe(II). Apparently, an equilibrium between Fe(II) in suspension and surface-bound polysulfides and elemental sulfur had been established.

When only 0.1 mM thiosulfate was used (Fig. 3B), the thiosulfate was consumed almost completely within 5 days, whereas

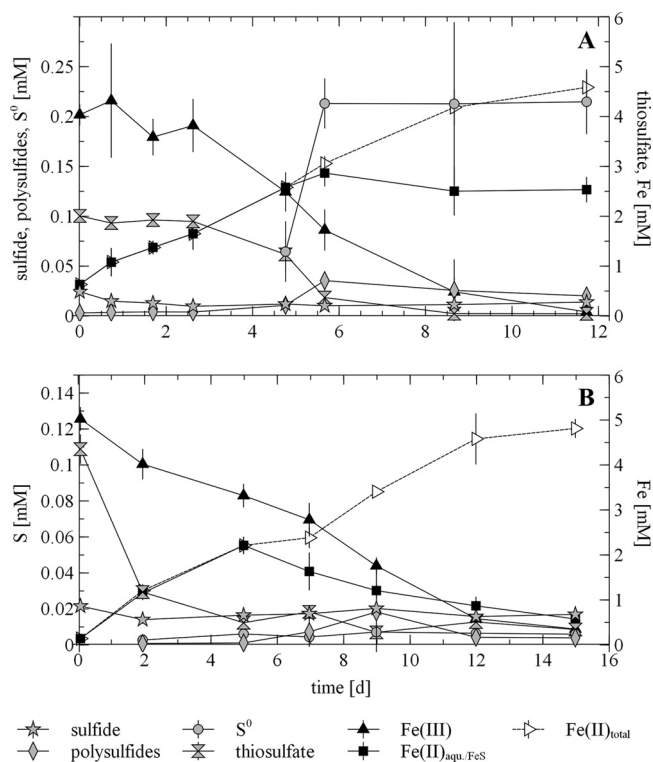


FIG 3 Reduction of Fe(III) in ferrihydrite in incubations of *S. deleyianum* supplied with 5 mM acetate as a carbon source, 10 mM formate as an electron donor, and 2 mM (A) or 0.1 mM (B) thiosulfate as an electron acceptor. Error bars represent standard deviations based on three replicates.

iron(III) mineral reduction took 15 days. After depletion of the initially added amount of thiosulfate, no reincrease of the thiosulfate concentration was measurable. As shown before, thiosulfate was only a minor oxidation product. Therefore, either no thiosulfate was produced during sulfide oxidation or thiosulfate reduction by the microorganisms was faster than abiotic sulfide oxidation. Again, almost no sulfide was detectable in solution but seems to have immediately precipitated as FeS, since the suspension was already black on day 2. Hence, a dynamic equilibrium between abiotic sulfide oxidation and microbial reduction of the oxidized sulfur species seemed to have been established. The hypothesis that sulfide from FeS precipitates was reused (reaction 2b in Fig. 1) is also supported by the finding that Fe(II) concentrations in suspension decreased from day 5 on, when all of the initially added thiosulfate was reduced. The residual Fe(II) was then precipitated as vivianite or siderite (reaction 2c, Fig. 1). Elemental sulfur was measurable in unfiltered samples from day 2 on in much smaller amounts than in the experiment with 2 mM thiosulfate. Concentrations remained stable until the end of the experiment. Polysulfides also occurred in much smaller amounts than in the experiment with 2 mM thiosulfate. Overall, significant amounts of polysulfides and different species were detectable only in experiments with 2 mM thiosulfate.

(ii) **The roles of other sulfur species as electron shuttles.**

Apart from thiosulfate, also sulfide, polysulfides, sulfite, tetrathionate, and cystine were tested as initiators of the process of electron shuttling between *S. deleyianum* and ferrihydrite (Fig. 4). The fact that the rates of iron(III) mineral reduction were very comparable in the experiments with the reduced sulfur species (sulfide) and the oxidized sulfur species (thiosulfate, sulfite, and tetrathionate) revealed the rapid kinetics of microbial reduction of the different sulfur species. Thus, not the reductive part of the electron-shuttling process but rather the abiotic oxidation of sulfide seems to be rate limiting.

(a) **Sulfide or polysulfides.** The addition of sulfide or polysulfides to the bottles led to an immediate blackening of the suspensions and hence the formation of FeS. Abiotically, 0.5 and 1.4 mM Fe(II) were measurable directly at the beginning of the experiments with ferrihydrite amended with 0.1 mM sulfide and polysulfides, respectively. Nevertheless, not more than 2 mM Fe(III) was reduced in any of the abiotic experiments. In all biotic experiments, complete Fe(III) reduction was observable, with the fastest reaction kinetics for polysulfides, followed by thiosulfate, tetrathionate, sulfide, sulfite, and finally cystine. The reduction of polysulfides was expected, since according to IMG genome annotation (31), dissimilatory sulfur or polysulfide reduction to hydrogen sulfide is mediated by a sulfur reductase complex containing a NrfD-like subunit C (gene loci Sdel_0265, Sdel_0266, and Sdel_0267). The particularly fast reduction of polysulfides (reaction 3a in Fig. 1) can either be triggered by additional elemental sulfur impurities (up to 0.1 mM) in the commercial K_2S_x standard or be linked to their apparent association with the microorganisms as described before, facilitating electron transfer processes.

(b) **Sulfite.** Sulfite could be used as efficiently as thiosulfate (reaction 3b in Fig. 1), which is in accordance with earlier studies (19, 20). However, this observation is in contrast to the study of Straub and Schink (17), who could not detect any assimilation or dissimilation of sulfite. Comparative genome analyses revealed the presence of a *mccA*-type gene encoding a new emerging type of terminal sulfite reductase (Sdel_703) with high sequence similar-

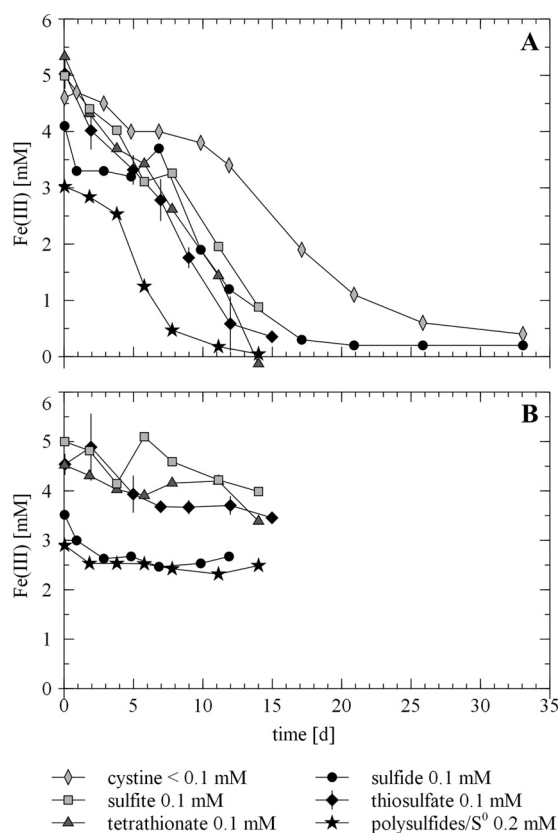


FIG 4 Reduction of Fe(III) in ferrihydrite in incubations of *S. deleyianum* (A) supplied with 5 mM acetate as a carbon source, 2 mM cysteine as a sulfur source and reductant, 10 mM formate as an electron donor, and different sulfur species as electron acceptors and in an abiotic control experiment (B). Error bars for the experiments with 2 mM cysteine and 0.1 mM thiosulfate represent standard deviations based on three replicates.

ity to *Wolinella succinogenes* MccA (blastp: 94% positives). Sulfite reduction activity of MccA was shown *in vitro* and/or *in vivo* for *W. succinogenes* and *Shewanella oneidensis* MR-1 (recently renamed SirA) (38, 39). The entire *mcc* gene cluster is present in the *S. deleyianum* genome (gene loci Sdel_0697 through Sdel_705), including the genes *mccABCD* and *ccsA1*, the genes for a two-component regulatory system named MccR/MccS located upstream, and two genes encoding hypothetical proteins downstream. In addition to the octaheme cytochrome *c* sulfite reductase MccA (gene locus Sdel_703), the genes for the following are essential for sulfite respiration, as shown for *W. succinogenes*: the predicted iron-sulfur protein MccC (gene locus Sdel_701), the putative quinol dehydrogenase MccD (a member of the NrfD/PrsC family, gene locus Sdel_0700), and a peptidyl-prolyl *cis-trans* isomerase named MccB (gene locus Sdel_702).

(c) **Tetrathionate.** Apparently, tetrathionate can also serve as an electron acceptor for *S. deleyianum* (reaction 3c in Fig. 1), which was, to the best of our knowledge, never shown before. On the basis of genome analysis, we would assume that tetrathionate is likely to be reduced to thiosulfate by a TsdA-type tetrathionate reductase in *S. deleyianum*. TsdA was first described in *Allochroamatium vinosum* as a novel diheme cytochrome *c* with thiosulfate dehydrogenase activity (40, 41). In *Campylobacter jejuni* 81116 (42), a homologue of TsdA shows

bifunctional activity, acting as both a thiosulfate dehydrogenase and a tetrathionate reductase. The similarity between the TsdA protein sequences of *S. deleyianum* (gene locus Sdel_0259) and *C. jejuni* (gene locus C8j_0815) was moderately high (blastp: 68% positives). Neither a homologue of the gene for tetrathionate reductase subunit A (TtrA) from *Salmonella enterica* serovar Typhimurium nor a homologue of the gene for octaheme tetrathionate reductase Otr from *Shewanella oneidensis* MR-1 is present in the genome of *S. deleyianum*.

(d) Cysteine. Cysteine was added to the medium as a sulfur source and a reducing agent as proposed by Straub and Schink (17). Nevertheless, genome analysis reveals that *S. deleyianum* is an L-cysteine prototroph that is able to convert L-serine via O-acetyl-L-serine (gene locus Sdel_1290 encoding a serine O-acetyltransferase) to L-cysteine (gene locus Sdel_1232 encoding a cysteine synthase). In *Escherichia coli*, this pathway is regulated by strong feedback inhibition of the final product, L-cysteine, and transcriptional regulation (43). Genes encoding L-cysteine oxidoreductases (EC 1.8.1.6) for the synthesis and degradation of L-cysteine could not be found in the *S. deleyianum* genome. Cysteine degradation to pyruvate is mediated by a putative C-S lyase (gene locus Sdel_1447) with high similarity to a PatB-like protein from *S. barnesii* SES-3 (accession no. YP_006404370 with 83% identical amino acid sites and 90% positives). The PatB protein of *Bacillus subtilis* is a proven C-S lyase that exhibits both cystathionine beta-lyase and cysteine desulfhydrase activities *in vitro* (44).

Concerning the electron-shuttling process, it has to be considered that cysteine is a redox-sensitive compound itself. Electron shuttling via cysteine and cystine has been shown for *Shewanella* species with the Fe(III)-containing clay mineral smectite (45) and for *Geobacter sulfurreducens* with ferrihydrite as a terminal electron acceptor (46). For *S. deleyianum*, Straub and Schink (17) excluded a shuttling mechanism via cysteine-cystine, as no ferrihydrite was reduced after the addition of cystine. Instead, they assumed that cysteine only served to protect the reduced sulfur species from oxidation.

We tested cystine, the oxidized form of cysteine, as a possible electron shuttle and found that cystine indeed could also serve as an electron acceptor for *S. deleyianum* (reaction 4a in Fig. 1) but showed the lowest rate of iron(III) mineral reduction. This might be attributable to a methodological problem. Because cystine is not readily soluble, when it is dissolved in pure water (graph in Fig. 4A), its true concentration might be lower than the nominal one. However, in another experiment, cystine was dissolved in 5 M NaOH prior to adjustment of the experimental pH, which led to complete dissolution. With 0.1 mM cystine and 0.1 mM cystine, 0.3 mM Fe(III) was reduced within 15 days, whereas 1.8 mM was reduced in the respective experiment with thiosulfate (see Table SI-2 in the supplemental material). This revealed that shuttling via cystine was not as efficient as that via thiosulfate.

(iii) The influence of cysteine on the process of electron shuttling between *S. deleyianum* and ferrihydrite. As discussed in the previous section, the presence of cystine seemed to have a certain influence on ferrihydrite reduction. Therefore, we also determined the effect of cysteine on ferrihydrite reduction by *S. deleyianum* in the presence of 0.1 mM thiosulfate (Fig. 5). Abiotically, up to 1.7 mM ferrihydrite was reduced when 2 mM cysteine was available. Either this could result from an abiotic reaction of cysteine with ferrihydrite (reaction 4b, Fig. 1), which would exclude any abiotic influence of thiosulfate, or cysteine reduced thiosulfate

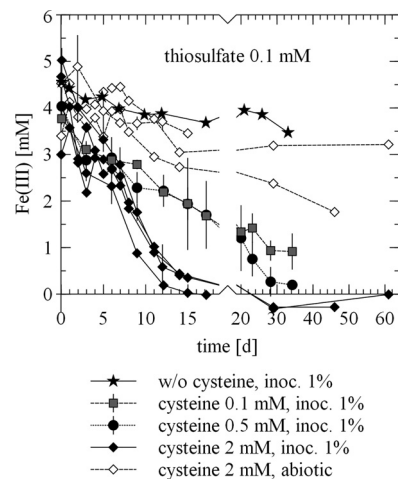


FIG 5 Reduction of Fe(III) in ferrihydrite in an abiotic control experiment and in incubations of *S. deleyianum* supplied with 5 mM acetate as a carbon source, 10 mM formate as an electron donor, and 0.1 mM thiosulfate as an electron acceptor. Error bars represent standard deviations based on three replicates. For the setup with 2 mM cysteine and a 1% inoculum, results of six experiments are shown, one experiment with three replicates and three additional independent experiments. For the abiotic setup with 2 mM cysteine, results of three independent experiments are shown. w/o, without; inoc., inoculum.

abiotically to sulfide (reaction 4c, Fig. 1), which then reacted with ferrihydrite. From the literature, it is known that sulfide can be produced by the reaction of thiosulfate with cysteine (47). On the basis of the experiments in this study, it cannot be decided whether, in the presence of thiosulfate, cysteine reduced ferrihydrite directly or indirectly via the reduction of thiosulfate. Without cysteine and with only 0.1 mM thiosulfate, 1.1 mM ferrihydrite was reduced in biotic experiments. Obviously, *S. deleyianum* could use thiosulfate as an electron acceptor, as was also confirmed by Straub and Schink (17). Since there was no cysteine in the system in the aforementioned experiment, thiosulfate must have also served as a sulfur source for the microorganisms. The addition of 0.1 mM cysteine increased the kinetics of ferrihydrite reduction significantly. A further increase was observable after the addition of 0.5 and 2 mM cysteine.

Finally, the effect of cysteine alone on ferrihydrite reduction by *S. deleyianum* was investigated. Straub and Schink (17) considered the abiotic reduction of ferrihydrite by cysteine negligible. In our control experiments without cysteine, we observed that no Fe(III) was reduced (Fig. 6). With 4 mM cysteine, complete reduction of 4 mM ferrihydrite was observed (Fig. 6). This could be attributed principally to the abiotic reaction of cysteine with ferrihydrite, since one electron is transferred per cysteine molecule in the oxidation of cysteine to cystine (reaction 4c in Fig. 1) and one electron per molecule is also needed for the reduction of ferrihydrite (reaction 1b in Fig. 1). In the two abiotic control experiments, 2 mM cysteine was able to reduce around 1.2 mM ferrihydrite within 46 and 61 days (Fig. 6). This is in line with previous studies in which iron was already shown to be reduced by cysteine under various conditions (48–50). In fact, even Straub and Schink (17) observed a reduction of 1 to 2 mM Fe(III) with 2 mM cysteine and a 0.01% inoculum over 35 days. In three experiments with 2 mM cysteine in the presence of *S. deleyianum* (1% inoculum), we determined an average ferrihydrite reduction of 2.33 ± 0.70 mM

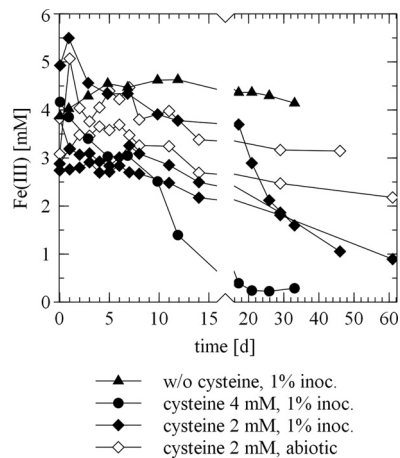


FIG 6 Reduction of Fe(III) in ferrihydrite in an abiotic control experiment and in incubations of *S. deleyianum* supplied with 5 mM acetate as a carbon source and 10 mM formate as an electron donor. The experiment with 2 mM cysteine and a 1% inoculum was done in triplicate, and the abiotic one with 2 mM cysteine was done in duplicate. w/o, without; inoc., inoculum.

within 33 to 61 days (Fig. 6). The fact that slightly more iron was reduced in the experiment with a 1% inoculum than in the abiotic experiment (Fig. 6) and the results of the experiment with cysteine described before indicate that the electron shuttling by the redox couple cysteine-cystine is possible but not very efficient compared to that by other sulfur species and thus plays a minor role in iron(III) reduction by *S. deleyianum*. Overall, the decisive effect of cysteine on ferrihydrite reduction is that it is an abiotic reductant of ferrihydrite itself or oxidized sulfur species that then can react with ferrihydrite.

Conclusions. The present study brings further insights into the role of sulfur species during ferrihydrite reduction specifically by *S. deleyianum* in the presence of reactive sulfur compounds. We observed complete microbial reduction of thiosulfate to sulfide with elemental sulfur and polysulfides as intermediate products. The main sulfur species, which formed during abiotic reoxidation of sulfide by iron reduction, was elemental sulfur attached to the surface of the iron mineral. Therefore, sulfur electron shuttling seems to be localized on the iron(III) mineral surface and direct physical contact between *S. deleyianum* and ferrihydrite seems to be necessary to complete the electron-shuttling cycle. No free sulfide could be detected in the presence of iron(III), because of both fast sulfide reoxidation by iron(III) and the formation of FeS, which acted as a recyclable sulfide reservoir.

Small amounts of sulfite, tetrathionate, thiosulfate, or polysulfides accelerated iron(III) mineral reduction considerably and reduced iron(III) to iron(II) in stoichiometric excess. Microbial sulfur reduction was so fast that no difference in iron reduction was observed whether sulfur species were initially applied in the oxidized (sulfite, tetrathionate, thiosulfate) or the reduced (sulfide) state.

Cysteine was found to have a significant influence on ferrihydrite reduction. It can react abiotically with ferrihydrite or oxidized sulfur species or may serve to a minor extent together with cystine as an electron shuttle between microorganisms and ferrihydrite. Cysteine should be eliminated from microbial experiments when sulfur redox reactions are to be investigated, espe-

cially since we found that *S. deleyianum* grows on thiosulfate as the only sulfur source as well.

ACKNOWLEDGMENTS

We acknowledge funding by the German Research Foundation for the research group etrap (electron transfer processes in anoxic aquifers) (FOR 580, PLA 302/7-1), as well as financial support for a Ph.D. scholarship to Regina Lohmayer from the State of Bavaria according to the Bayerisches Eliteförderungsgesetz (BayEFG).

REFERENCES

- Petersen W, Wallmann K, Schroer S, Schroeder F. 1993. Studies on the adsorption of cadmium on hydrous iron(III) oxides in oxic sediments. *Anal. Chim. Acta* 273:323–327. [http://dx.doi.org/10.1016/0003-2670\(93\)80172-H](http://dx.doi.org/10.1016/0003-2670(93)80172-H).
- Dong DM, Nelson YM, Lion LW, Shuler ML, Ghiorso WC. 2000. Adsorption of Pb and Cd onto metal oxides and organic material in natural surface coatings as determined by selective extractions: new evidence for the importance of Mn and Fe oxides. *Water Res.* 34:427–436. [http://dx.doi.org/10.1016/S0043-1354\(99\)00185-2](http://dx.doi.org/10.1016/S0043-1354(99)00185-2).
- Bennett B, Dudas MJ. 2003. Release of arsenic and molybdenum by reductive dissolution of iron oxides in a soil with enriched levels of native arsenic. *J. Environ. Eng. Sci.* 2:265–272. <http://dx.doi.org/10.1139/s03-028>.
- Phuengprasop T, Sittiwong J, Unob F. 2011. Removal of heavy metal ions by iron oxide coated sewage sludge. *J. Hazard. Mater.* 186:502–507. <http://dx.doi.org/10.1016/j.jhazmat.2010.11.065>.
- Hohmann C, Winkler E, Morin G, Kappler A. 2010. Anaerobic Fe(II)-oxidizing bacteria show As resistance and immobilize As during Fe(III) mineral precipitation. *Environ. Sci. Technol.* 44:94–101. <http://dx.doi.org/10.1021/es900708s>.
- Wang XM, Liu F, Tan WF, Li W, Feng XH, Sparks DL. 2013. Characteristics of phosphate adsorption-desorption onto ferrihydrite: comparison with well-crystalline Fe (hydr)oxides. *Soil Sci.* 178:1–11. <http://dx.doi.org/10.1097/SS.0b013e31828683f8>.
- Heckman K, Welty-Bernard A, Vazquez-Ortega A, Schwartz E, Chorover J, Rasmussen C. 2013. The influence of goethite and gibbsite on soluble nutrient dynamics and microbial community composition. *Biogeochemistry* 112:179–195. <http://dx.doi.org/10.1007/s10533-012-9715-2>.
- Nevin KP, Lovley DR. 2000. Lack of production of electron-shuttling compounds or solubilization of Fe(III) during reduction of insoluble Fe(III) oxide by *Geobacter metallireducens*. *Appl. Environ. Microbiol.* 66:2248–2251. <http://dx.doi.org/10.1128/AEM.66.5.2248-2251.2000>.
- von Canstein H, Ogawa J, Shimizu S, Lloyd JR. 2008. Secretion of flavins by *Shewanella* species and their role in extracellular electron transfer. *Appl. Environ. Microbiol.* 74:615–623. <http://dx.doi.org/10.1128/AEM.01387-07>.
- Kappler A, Benz M, Schink B, Brune A. 2004. Electron shuttling via humic acids in microbial iron(III) reduction in a freshwater sediment. *FEMS Microbiol. Ecol.* 47:85–92. [http://dx.doi.org/10.1016/S0168-6496\(03\)00245-9](http://dx.doi.org/10.1016/S0168-6496(03)00245-9).
- Roden EE, Kappler A, Bauer I, Jiang J, Paul A, Stoesser R, Konishi H, Xu HF. 2010. Extracellular electron transfer through microbial reduction of solid-phase humic substances. *Nat. Geosci.* 3:417–421. <http://dx.doi.org/10.1038/ngeo870>.
- Li XM, Liu L, Liu TX, Yuan T, Zhang W, Li FB, Zhou SG, Li YT. 2013. Electron transfer capacity dependence of quinone-mediated Fe(III) reduction and current generation by *Klebsiella pneumoniae* L17. *Chemosphere* 92:218–224. <http://dx.doi.org/10.1016/j.chemosphere.2013.01.098>.
- Afonso MD, Stumm W. 1992. Reductive dissolution of iron(III) (hydr)oxides by hydrogen sulfide. *Langmuir* 8:1671–1675. <http://dx.doi.org/10.1021/la00042a030>.
- Li YL, Vali H, Yang J, Phelps TJ, Zhang CL. 2006. Reduction of iron oxides enhanced by a sulfate-reducing bacterium and biogenic H₂S. *Geomicrobiol. J.* 23:103–117. <http://dx.doi.org/10.1080/01490450500533965>.
- Burton ED, Johnston SG, Bush RT. 2011. Microbial sulfidogenesis in ferrihydrite-rich environments: effects on iron mineralogy and arsenic mobility. *Geochim. Cosmochim. Acta* 75:3072–3087. <http://dx.doi.org/10.1016/j.gca.2011.03.001>.

16. Burton ED, Johnston SG, Planer-Friedrich B. 2013. Coupling of arsenic mobility to sulfur transformations during microbial sulfate reduction in the presence and absence of humic acid. *Chem. Geol.* 343:12–24. <http://dx.doi.org/10.1016/j.chemgeo.2013.02.005>.
17. Straub KL, Schink B. 2004. Ferrihydrite-dependent growth of *Sulfurospirillum deleyianum* through electron transfer via sulfur cycling. *Appl. Environ. Microbiol.* 70:5744–5749. <http://dx.doi.org/10.1128/AEM.70.10.5744-5749.2004>.
18. Luijten M, Weelink SAB, Godschalk B, Langenhoff AAM, van Eekert MHA, Schraa G, Stams AJM. 2004. Anaerobic reduction and oxidation of quinone moieties and the reduction of oxidized metals by halo-respiring and related organisms. *FEMS Microbiol. Ecol.* 49:145–150. <http://dx.doi.org/10.1016/j.femsec.2004.01.015>.
19. Schumacher W, Kroneck PMH, Pfennig N. 1992. Comparative systematic study on “spirillum” 5175, *Campylobacter* and *Wolinella* species—description of “spirillum” 5175 as *Sulfurospirillum deleyianum* gen. nov., spec. nov. *Arch. Microbiol.* 158:287–293. <http://dx.doi.org/10.1007/BF00245247>.
20. Wolfe RS, Pfennig N. 1977. Reduction of sulfur by spirillum 5175 and syntrophism with *Chlorobium*. *Appl. Environ. Microbiol.* 33:427–433.
21. Widdel F, Bak F. 1992. Gram-negative mesophilic sulfate-reducing bacteria, p 3352–3378. In Balows A, Trüper HG, Dworkin M, Harder W, Schleifer K.-H (ed), *The prokaryotes: a handbook on the biology of bacteria: ecophysiology, isolation, identification, applications*, 2nd ed, vol IV. Springer, Berlin, Germany.
22. Schwertmann U, Cornell RM. 2000. Iron oxides in the laboratory—preparation and characterization, 2nd ed. Wiley VCH Weinheim, Germany.
23. Raven KP, Jain A, Loeffert RH. 1998. Arsenite and arsenate adsorption on ferrihydrite: kinetics, equilibrium, and adsorption envelopes. *Environ. Sci. Technol.* 32:344–349. <http://dx.doi.org/10.1021/es970421p>.
24. Piepenbrock A, Dippon U, Porsch K, Appel E, Kappler A. 2011. Dependence of microbial magnetite formation on humic substance and ferrihydrite concentrations. *Geochim. Cosmochim. Acta* 75:6844–6858. <http://dx.doi.org/10.1016/j.gca.2011.09.007>.
25. Stookey LL. 1970. Ferrozine—a new spectrophotometric reagent for iron. *Anal. Chem.* 42:779–781. <http://dx.doi.org/10.1021/ac60289a016>.
26. Cline JD. 1969. Spectrophotometric determination of hydrogen sulfide in natural waters. *Limnol. Oceanogr.* 14:454–458. <http://dx.doi.org/10.4319/llo.1969.14.3.0454>.
27. Kamyshny A, Ekelchik I, Gun J, Lev O. 2006. Method for the determination of inorganic polysulfide distribution in aquatic systems. *Anal. Chem.* 78:2631–2639. <http://dx.doi.org/10.1021/ac051854a>.
28. Rizkov D, Lev O, Gun J, Anisimov B, Kuselman I. 2004. Development of in-house reference materials for determination of inorganic polysulfides in water. *Accredit. Qual. Assur.* 9:399–403. <http://dx.doi.org/10.1007/s00769-004-0788-z>.
29. Steudel R, Holdt G, Gobel T. 1989. Ion-pair chromatographic-separation of inorganic sulphur anions including polysulphide. *J. Chromatogr.* 475:442–446. [http://dx.doi.org/10.1016/S0021-9673\(01\)89701-6](http://dx.doi.org/10.1016/S0021-9673(01)89701-6).
30. Planer-Friedrich B, London J, McCleskey RB, Nordstrom DK, Wallschläger D. 2007. Thioarsenates in geothermal waters of Yellowstone National Park: determination, preservation, and geochemical importance. *Environ. Sci. Technol.* 41:5245–5251. <http://dx.doi.org/10.1021/es070273v>.
31. Markowitz VM, Chen IMA, Palaniappan K, Chu K, Szeto E, Grechkin Y, Ratner A, Jacob B, Huang JH, Williams P, Huntemann M, Anderson I, Mavromatis K, Ivanova NN, Kyrpides NC. 2012. IMG: the integrated microbial genomes database and comparative analysis system. *Nucleic Acids Res.* 40:D115–D122. <http://dx.doi.org/10.1093/nar/gkr1044>.
32. Hedderich R, Klimmek O, Kroger A, Dirmeier R, Keller M, Stetter KO. 1998. Anaerobic respiration with elemental sulfur and with disulfides. *FEMS Microbiol. Rev.* 22:353–381. <http://dx.doi.org/10.1111/j.1574-6976.1998.tb00376.x>.
33. Cantrell KJ, Yabusaki SB, Engelhard MH, Mitroshkov AV, Thornton EC. 2003. Oxidation of H₂S by iron oxides in unsaturated conditions. *Environ. Sci. Technol.* 37:2192–2199. <http://dx.doi.org/10.1021/es020994o>.
34. Poulton SW. 2003. Sulfide oxidation and iron dissolution kinetics during the reaction of dissolved sulfide with ferrihydrite. *Chem. Geol.* 202:79–94. [http://dx.doi.org/10.1016/S0009-2541\(03\)00237-7](http://dx.doi.org/10.1016/S0009-2541(03)00237-7).
35. Pyzik AJ, Sommer SE. 1981. Sedimentary iron monosulfides: kinetics and mechanism of formation. *Geochim. Cosmochim. Acta* 45:687–698. [http://dx.doi.org/10.1016/0016-7037\(81\)90042-9](http://dx.doi.org/10.1016/0016-7037(81)90042-9).
36. Saalfeld SL, Bostick BC. 2009. Changes in iron, sulfur, and arsenic speciation associated with bacterial sulfate reduction in ferrihydrite-rich systems. *Environ. Sci. Technol.* 43:8787–8793. <http://dx.doi.org/10.1021/es901651k>.
37. Peiffer S, Gade W. 2007. Reactivity of ferric oxides toward H₂S at low pH. *Environ. Sci. Technol.* 41:3159–3164. <http://dx.doi.org/10.1021/es062282d>.
38. Kern M, Klotz MG, Simon J. 2011. The *Wolinella succinogenes* mcc gene cluster encodes an unconventional respiratory sulphite reduction system. *Mol. Microbiol.* 82:1515–1530. <http://dx.doi.org/10.1111/j.1365-2958.2011.07906.x>.
39. Shirodkar S, Reed S, Romine M, Saffarini D. 2011. The octahaem SirA catalyses dissimilatory sulfite reduction in *Shewanella oneidensis* MR-13:1. *Environ. Microbiol.* 13:108–115. <http://dx.doi.org/10.1111/j.1462-2920.2010.02313.x>.
40. Hensen D, Sperling D, Truper HG, Brune DC, Dahl C. 2006. Thiosulphate oxidation in the phototrophic sulphur bacterium *Allochroamatium vinosum*. *Mol. Microbiol.* 62:794–810. <http://dx.doi.org/10.1111/j.1365-2958.2006.05408.x>.
41. Denkmann K, Grein F, Zigann R, Siemen A, Bergmann J, van Helmont S, Nicolai A, Pereira IAC, Dahl C. 2012. Thiosulfate dehydrogenase: a widespread unusual acidophilic c-type cytochrome. *Environ. Microbiol.* 14:2673–2688. <http://dx.doi.org/10.1111/j.1462-2920.2012.02820.x>.
42. Liu YW, Denkmann K, Kosciow K, Dahl C, Kelly DJ. 2013. Tetrathionate stimulated growth of *Campylobacter jejuni* identifies a new type of bi-functional tetrathionate reductase (TsdA) that is widely distributed in bacteria. *Mol. Microbiol.* 88:173–188. <http://dx.doi.org/10.1111/mmi.12176>.
43. Kredich NM. 1992. The molecular basis for positive regulation of *cys* promoters in *Salmonella typhimurium* and *Escherichia coli*. *Mol. Microbiol.* 6:2747–2753. <http://dx.doi.org/10.1111/j.1365-2958.1992.tb01453.x>.
44. Auger S, Gomez MP, Danchin A, Martin-Verstraete I. 2005. The PatB protein of *Bacillus subtilis* is a C-S-lyase. *Biochimie* 87:231–238. <http://dx.doi.org/10.1016/j.biochi.2004.09.007>.
45. Liu D, Dong H, Zhao L, Wang H. 2013. Smectite reduction by *Shewanella* species as facilitated by cystine and cysteine. *Geomicrobiol. J.* 31: 53–63. <http://dx.doi.org/10.1080/01490451.2013.806609>.
46. Doong RA, Schink B. 2002. Cysteine-mediated reductive dissolution of poorly crystalline iron(III) oxides by *Geobacter sulfurreducens*. *Environ. Sci. Technol.* 36:2939–2945. <http://dx.doi.org/10.1021/es0102235>.
47. Szczepkowski TW. 1958. Reactions of thiosulphate with cysteine. *Nature* 182:934–935. <http://dx.doi.org/10.1038/182934a0>.
48. Cornell RM, Schneider W, Giovanoli R. 1989. Phase-transformations in the ferrihydrite/cysteine system. *Polyhedron* 8:2829–2836. [http://dx.doi.org/10.1016/S0277-5387\(00\)80544-6](http://dx.doi.org/10.1016/S0277-5387(00)80544-6).
49. Morrison KD, Bristow TF, Kennedy MJ. 2013. The reduction of structural iron in ferruginous smectite via the amino acid cysteine: implications for an electron shuttling compound. *Geochim. Cosmochim. Acta* 106: 152–163. <http://dx.doi.org/10.1016/j.gca.2012.12.006>.
50. Amirbahman A, Sigg L, vonGunten U. 1997. Reductive dissolution of Fe(III) (hydr)oxides by cysteine: kinetics and mechanism. *J. Colloid Interface Sci.* 194:194–206. <http://dx.doi.org/10.1006/jcis.1997.5116>.
51. Wan M, Shchukarev A, Lohmayer R, Planer-Friedrich B, Peiffer S. The occurrence of surface polysulphides during the interaction between ferric (hydr)oxides and aqueous sulphide. *Environ. Sci. Technol.*, in press.

SUPPORTING INFORMATION

Role of sulfur species as redox partners and electron shuttles for ferrihydrite reduction by
Sulfurospirillum deleyianum

Regina Lohmayer^a, Andreas Kappler^b, Tina Lösekann-Behrens^b, Britta Planer-Friedrich^{a#}

Environmental Geochemistry Group, Bayreuth Center for Ecology and Environmental Research
(BayCEER), University of Bayreuth, Bayreuth, Germany^a;

Geomicrobiology, Center for Applied Geosciences, University of Tuebingen, Tuebingen,
Germany^b

Running Head: Sulfur electron shuttling to ferrihydrite

#Address correspondence to Britta Planer-Friedrich, b.planer-friedrich@uni-bayreuth.de

Table SI-1 Production of S_6^{2-} and S^0 from thiosulfate in incubations of *Sulfurospirillum deleyianum* supplied with 2 mM cysteine as sulfur source and reductant, 5 mM acetate as carbon source, and 10 mM formate as electron donor. The LOD (limit of detection) was derived from the smallest integrable peak and came to 0.1 μ M for S_6^{2-} and 0.5 μ M for S^0 .

[d]	2 mM thiosulfate, 1 % inoculum unfiltered		0.1 mM thiosulfate, 1 % inoculum unfiltered		2 mM thiosulfate, 1 % inoculum filtered		0.1 mM thiosulfate, 1 % inoculum filtered	
	S_6^{2-} [mM]	S^0 [mM]	S_6^{2-} [mM]	S^0 [mM]	S_6^{2-} [mM]	S^0 [mM]	S_6^{2-} [mM]	S^0 [mM]
0	< LOD	< LOD	< LOD	< LOD	< LOD	< LOD	< LOD	< LOD
2	0.002	0.009	< LOD	< LOD	< LOD	0.018	< LOD	< LOD
5	0.001	0.002	< LOD	< LOD	< LOD	0.012	< LOD	< LOD
7	0.012	< LOD	0.017	< LOD	< LOD	0.006	< LOD	< LOD
9	0.009	< LOD	0.009	< LOD	< LOD	< LOD	< LOD	< LOD
12	0.008	< LOD	0.007	< LOD	< LOD	< LOD	< LOD	< LOD
15	0.009	< LOD	0.016	< LOD	< LOD	< LOD	< LOD	< LOD

Table SI-2 Fe(II) total production from ferrihydrite in incubations of *Sulfurospirillum deleyianum* supplied with 5 mM acetate as carbon source, and 10 mM formate as electron donor.

Standard deviations are based on three replicates; n.d. means not determined.

[d]		0	3	6	9	12	15
Fe(II) total [mM]	cysteine 0.1 mM, thiosulfate 0.1 mM	0.02 ±	0.91 ±	1.12 ±	1.26 ±	1.79 ±	1.85 ±
		0.00	0.05	0.06	0.02	0.43	0.31
	cysteine 0.1 mM, cystine 0.1 mM	0.02 ±	0.19 ±	n.d.	0.28 ±	n.d.	0.30 ±
		0.00	0.25		0.32		0.23

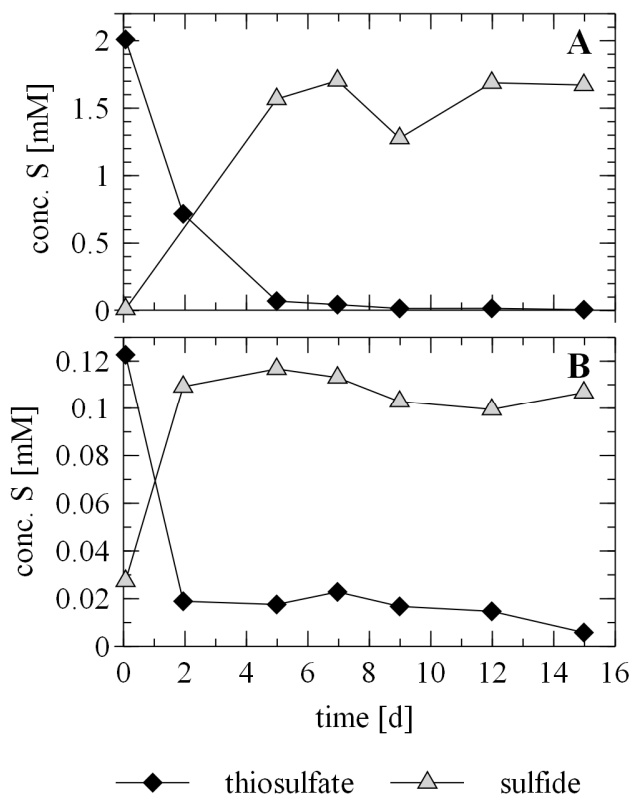


Fig. SI-1 Production of sulfide from thiosulfate (A: 2.0 mM, B: 0.1 mM) in incubations of *Sulfurospirillum deleyianum* supplied with 2 mM cysteine as sulfur source and reductant, 5 mM acetate as carbon source, and 10 mM formate as electron donor.

Study 4

Reproduced with permission from

Anaerobic chemolithotrophic growth of the haloalkaliphilic bacterium strain MLMS-1 by disproportionation of monothioarsenate

Britta Planer-Friedrich, Cornelia Härtig, Regina Lohmayer, Elke Suess, Shelley H. McCann,
Ronald Oremland

Environmental Science & Technology, 2015

Copyright 2015 American Chemical Society

Anaerobic Chemolithotrophic Growth of the Haloalkaliphilic Bacterium Strain MLMS-1 by Disproportionation of Monothioarsenate

B. Planer-Friedrich,^{*,†} C. Härtig,[†] R. Lohmayer,[†] E. Suess,^{‡,§} S. H. McCann,^{||} and R. Oremland^{||}

[†]Department of Environmental Geochemistry, Bayreuth Center for Ecology and Environmental Research (BayCEER), University of Bayreuth, Universitätsstraße 30, 95447 Bayreuth, Germany

[‡]Institute of Biogeochemistry and Pollutant Dynamics, Department of Environmental Systems Science, ETH Zürich, 8092 Zürich, Switzerland

[§]Department of Water Resources and Drinking Water, Swiss Federal Institute of Aquatic Science and Technology (EAWAG), 8600 Dübendorf, Switzerland

^{||}U.S. Geological Survey, Menlo Park, California, United States

Supporting Information

ABSTRACT: A novel chemolithotrophic metabolism based on a mixed arsenic–sulfur species has been discovered for the anaerobic deltaproteobacterium, strain MLMS-1, a haloalkaliphile isolated from Mono Lake, California, U.S. Strain MLMS-1 is the first reported obligate arsenate-respiring chemoautotroph which grows by coupling arsenate reduction to arsenite with the oxidation of sulfide to sulfate. In that pathway the formation of a mixed arsenic–sulfur species was reported. That species was assumed to be monothioarsenite ($[\text{H}_2\text{As}^{\text{III}}\text{S}^{-\text{II}}\text{O}_2]^-$), formed as an intermediate by abiotic reaction of arsenite with sulfide. We now report that this species is monothioarsenate ($[\text{HAS}^{\text{V}}\text{S}^{-\text{II}}\text{O}_3]^{2-}$) as revealed by X-ray absorption spectroscopy. Monothioarsenate forms by abiotic reaction of arsenite with zerovalent sulfur. Monothioarsenate is kinetically stable under a wide range of pH and redox conditions. However, it was metabolized rapidly by strain MLMS-1 when incubated with arsenate. Incubations using monothioarsenate confirmed that strain MLMS-1 was able to grow ($\mu = 0.017 \text{ h}^{-1}$) on this substrate via a disproportionation reaction by oxidizing the thio-group-sulfur ($\text{S}^{-\text{II}}$) to zerovalent sulfur or sulfate while concurrently reducing the central arsenic atom (As^{V}) to arsenite. Monothioarsenate disproportionation could be widespread in nature beyond the already studied arsenic and sulfide rich hot springs and soda lakes where it was discovered.



INTRODUCTION

Mono Lake is a closed-basin, alkaline, hypersaline lake, located in California, U.S. Its salinity increased significantly during the last century from 43 g/L TDS in 1941 to 91 g/L in 1982,¹ due to massive diversion of freshwater input.² The water column is characterized by periods of enduring chemical stratification (meromixis), which leads to sulfide enrichment at the lake bottom.³ Active hydrothermal springs discharging into the lake, volcanic rock weathering, and evaporation lead to high aqueous arsenic concentrations ($\sim 0.2 \text{ mM}$).^{3–5} While arsenate is the predominant arsenic species in the upper, oxic part of the lake, arsenite and thioarsenic species are abundant below the oxycline.³ In the anoxic zones of the lake, where sulfide concentrations can reach 3 mM during meromixis, a trithiolated thioarsenic species was determined as the most abundant aqueous arsenic species, accounting for $\sim 50\%$ of the total dissolved arsenic present.³

The actual redox state of the arsenic atom present in thioarsenic species has been subject of debate. Thioarsenic

species were first detected in sulfidic arsenite solutions by inductively coupled plasma-mass spectrometry (ICP-MS) following initial separation by ion chromatography (IC).⁶ An IC-ICP-MS analysis enables quantification of arsenic and sulfur concentrations, but does not reveal any structural characterization of thioarsenic molecules. Because the solutions were prepared under anoxic conditions, the thioarsenic species detected were assumed to be in the form of chemically reduced trivalent thioarsenites ($[\text{H}_2\text{As}^{\text{III}}\text{S}^{-\text{II}}\text{O}_{3-n}]^-$, $n = 1–3$).⁶ A number of studies adopted this terminology without carrying out their own species identifications. In this regard the thiolated species observed in Mono Lake water were originally termed “thioarsenites”,³ before follow-up studies using molecular identification from electrospray-MS⁷ and structural identifica-

Received: October 16, 2014

Revised: May 1, 2015

Accepted: May 5, 2015

tion by XAS⁸ correctly identified the peaks observed by IC-ICP-MS analysis as pentavalent “thioarsenates” ($[\text{HAS}^{\text{V}}\text{S}^{\text{-II}}\text{O}_{4-n}]^{2-}$, $n = 1-4$).

Thioarsenates are interesting molecules to investigate as substrates for microbial chemolithotrophic metabolism because they contain internally an electron donor ($\text{S}^{\text{-II}}$) and an electron acceptor (As^{V}). In Mono Lake, a variety of haloalkaliphiles use either arsenic or sulfur or both for energy conservation^{3-5,9-12} and arsenate- and sulfate-reduction contribute significantly to the mineralization of organic matter in the lake’s anoxic water column.¹³ The involvement of thioarsenates in this Mono Lake sulfur and arsenic biochemistry has not been elucidated.

Previous studies with Mono Lake enrichment cultures reported the detection of thioarsenates during oxidation of sulfide and arsenite,¹⁴ or inferred the involvement of “arsenic–thiol-complexes” as well as polysulfides in the metabolism of sulfide and arsenate.¹² Polysulfides are intermediate sulfur species where one S atom has a redox state of -II and n S atoms ($n = 1-7$) have a redox state of 0 ($[\text{S}^{\text{0}}\text{S}^{\text{-II}}]^{2-}$). They form readily under suboxic conditions from partial oxidation of sulfide. A thioarsenic intermediate was observed during growth of the obligate chemoautotrophic deltaproteobacterium strain MLMS-1 by dissimilatory arsenate reduction with sulfide as the electron donor.¹³ The thioarsenic species was termed “monothioarsenite” ($(\text{H}_2\text{As}^{\text{III}}\text{S}^{\text{-II}}\text{O}_2)^-$) following the original assignment by Wilkin et al.⁶ It was hypothesized that its intermediate occurrence was a chemical phenomenon rather than an intermediate in bacterial metabolism. A direct production and consumption of the thioarsenic intermediate by the metabolism of strain MLMS-1 was considered unlikely¹³ and no other publications existed at the time about microbial metabolism of thioarsenic species. Thioarsenates were subsequently found to serve as energy sources for *Aquificales* in the hydrothermal systems of Yellowstone National Park¹⁵ and monothioarsenate was confirmed as an electron donor for the aerobic growth of *Thermocrinis ruber* strain OC14/7/2¹⁶ as well as during anoxygenic photosynthesis by strains of the Ectothiorhodospiraceae family.¹⁷

Recognizing now that the IC-fractions were probably thioarsenates and not thioarsenites,⁸ we hypothesized that strain MLMS-1 could directly form and subsequently metabolize monothioarsenate ($[\text{HAS}^{\text{V}}\text{S}^{\text{-II}}\text{O}_3]^{2-}$) instead of the proposed monothioarsenite. Therefore, we (I) reinvestigated growth of strain MLMS-1 on arsenate and sulfide with the aim of identifying the intermediate thioarsenic species formed; (II) explored the relevance of sulfide vs polysulfide species with regard to formation and transformation of intermediate thioarsenic species under abiotic conditions as well as in the presence of strain MLMS-1; and (III) directly monitored growth of strain MLMS-1 on synthesized monothioarsenate with the goal to demonstrate that this compound can serve as a substrate for chemolithotrophy.

MATERIALS AND METHODS

Strain and Culture Conditions in Metabolic Experiments with Pentavalent Arsenic (Arsenate, Monothioarsenate). A pure culture of the previously¹³ characterized strain MLMS-1 was provided by the Oremland group (USGS, Menlo Park, CA) and was grown in the laboratories in Bayreuth at 28 °C in an anoxic inorganic mineral salts medium that lacked any organic electron donors (“ML-medium”).¹³ The initial pH was 9.8 and pH changes with time were less than 0.2 pH units. To remove oxygen from the medium, it was boiled

for >10 min, bubbled with nitrogen gas during cooling and immediately transferred into an anoxic chamber (95% N₂, 5% H₂, O₂ at 0 ppm; H₂ and O₂ monitored by a COY Anaerobic Monitor CAM-12) for dispensing into glass serum bottles which were sealed with rubber septa. Three different MLMS-1 experiments with the respective uninoculated (abiotic) controls ($n = 3$) were carried out by supplying: (I) 5 mM sulfide ($\text{Na}_2\text{S} \times 9 \text{H}_2\text{O}$, Sigma-Aldrich) as electron donor and 12.5 mM arsenate ($\text{Na}_2\text{HAS}^{\text{V}}\text{O}_4 \times 7 \text{H}_2\text{O}$, Fluka) as electron acceptor, (II) 7 mM sulfide and 8.5 mM arsenate, and (III) 5 mM sulfide and 7.6 mM monothioarsenate ($\text{Na}_3\text{As}^{\text{V}}\text{O}_3\text{S} \times 7 \text{H}_2\text{O}$, synthesized in our laboratory according to a previously described method¹⁸).

Abiotic experiments with arsenite, sulfide, and polysulfides. Abiotic experiments were conducted in ML-medium ($n = 1$) in the anoxic chamber. Different concentrations of arsenite (1 and 3 mM) were combined with varying concentrations of sulfide (1 mM, 3 mM, or 6 mM) or a mixture of polysulfides (10 mMeq). To facilitate comparability, all concentrations of polysulfides refer to the total sulfur concentrations in the respective compound and are reported in millimol equivalent (mMeq; with 1 mM S_n^{2-} being n times mMeq S). A polysulfide stock solution was prepared from 0.5 M sulfide ($\text{Na}_2\text{S} \times 9 \text{H}_2\text{O}$, Sigma-Aldrich) and 5 M elemental sulfur (S, reagent grade powder, purified by sublimation up to a 100 mesh particle size; Sigma-Aldrich) in deionized water. In sulfidic solutions elemental sulfur dissolves to form polysulfides.¹⁹ The chain lengths of polysulfides depend upon the sulfur concentration and the pH of the solution.²⁰ After filtration through 0.2 μm cellulose-acetate filters (Membrex, Membra Pure, Mannheim), the stock solution was diluted into ML-medium which thereafter contained approximately 10 mMeq polysulfides (predominantly S_4^{2-} (4.1 mMeq) and S_5^{2-} (4.1 mMeq)).

Sampling Procedure. All incubations were done in tightly sealed, 120 mL glass serum bottles, which were filled with 100 mL medium (for the first arsenate experiment) or 50 mL medium (in all other experiments) under nitrogen headspace. After sterilizing septa with 70% ethanol, liquid samples were obtained by penetration of the septa using sterile syringes fitted with metal cannulas. Sampling took place in the anoxic chamber to avoid oxidation. Removed liquid samples were replaced by an equivalent volume of sterile nitrogen. Directly after sampling, the samples (except for cell counts) were filtered through 0.2 μm cellulose-acetate filters to remove cells and precipitates. Subsequently, samples were immediately flash-frozen in liquid nitrogen and stored at -20 °C until analysis. It was previously shown that frozen storage does not change speciation.²¹ For analysis, samples were thawed in the anoxic chamber, filtered a second time, and diluted in nitrogen-purged deionized water for the respective analyses.

IC-ICP-MS. Arsenite, arsenate, and thioarsenate species were determined by IC (Dionex ICS-3000; AG/AS16 IonPac column, 20–100 mM NaOH at a flow rate of 1.2 mL/min) coupled to an ICP-MS (Thermo-Fisher XSeries2) as described previously.²¹ While all experiments and all samplings were conducted in the absence of oxygen, samples were in contact with atmospheric oxygen while sitting in capped, but not gastight vials on the IC autosampler waiting for analysis. We have previously shown by comparative X-ray absorption spectroscopy (XAS) and IC-ICP-MS measurements that thioarsenates survive this treatment, while thioarsenites oxidize to thioarsenates and cannot be analyzed by IC-ICP-MS.^{8,22}

Calibration standard solutions were made from sodium arsenate dibasic-heptahydrate ($\text{Na}_2\text{HAsO}_4 \times 7\text{H}_2\text{O}$, Fluka), sodium (meta)arsenite (NaAsO_2 , Fluka), ammonium sulfate ($(\text{NH}_4)_2\text{SO}_4$, Fluka), and sodium thiosulfate ($\text{Na}_2\text{S}_2\text{O}_3$, Sigma-Aldrich). Due to a lack of commercial standards, thioarsenates were quantified via the arsenate calibration curve. The validity of this approach has been shown in a previous publication.²¹

XAS. X-ray absorption near-edge spectroscopy (XANES) was done for the samples taken after 0, 5, 9, and 14 days of incubation with strain MLMS-1 and after 7 days from the abiotic control (experiment series I with 5 mM sulfide and 12.5 mM arsenate). After sample collection and filtration as described above, samples were pipetted into PE sample holders, capped with Kapton tape, and immediately flash-frozen in liquid nitrogen in the anoxic chamber. This method has previously been shown to exclude oxidation and conserve thioarsenates as well as thioarsenites.^{8,22} The As K-edge spectra were obtained at the ESRF (European Synchrotron Radiation Facility, Rossendorf-Beamline (BM-20)) in Grenoble, France. All flash-frozen samples were analyzed frozen in a closed-cycle He-cryostat to avoid oxidation and thermal vibrations. Beamline details and the analysis of reference spectra for arsenate, monothioarsenate, arsenite, and trithioarsenite have been described previously.^{8,22} Data evaluation was performed using SixPack²³ for dead-time correction, averaging of several scans and WINXAS for energy calibration. The XANES edge energy was determined by zero-crossing of the second order XANES derivatives in ATHENA.²⁴

Photometric Sulfide Determination. Sulfide was determined in filtered samples by the methylene blue method.²⁵ Absorption was measured at 660 nm with a spectrophotometer (HACH Lange DR 3800) after 2 h of reaction. The method determines acid-labile sulfides as H_2S , but not oxidized sulfur compounds (for example, thiosulfate, sulfite) or thiols (for example, glutathione, cysteine).²⁶ Based on its stability under acidic conditions,²⁷ the sulfur bound to monothioarsenate is not codetermined, while transformation of higher thiolated species to arsenite and sulfide upon acidification will lead to at least partial codetermination of their arsenic-bound sulfur. Polysulfides dissociate to S^0 and H_2S upon acidification,²⁸ suggesting the possibility of a quantitative determination of their terminal sulfide by the methylene blue method. However, while some researchers recovered up to 80% of the terminal polysulfide-bound $\text{S}^{-\text{II}}$ in solutions with Na_2S_4 ,²⁹ others reported only 3% recovery from K_2S_n .³⁰ In conclusion, the “sulfide” signal reported in the Results includes free sulfide, sulfur dissociated from higher thiolated arsenates (but not from monothioarsenate), and polysulfides to an unknown extent.

HPLC. For polysulfide analysis, a 100 μL aliquot of filtered sample was added simultaneously with 15 μL methyl trifluoromethanesulfonate ($\text{CF}_3\text{SO}_3\text{CH}_3$, Sigma-Aldrich) to 800 μL methanol (H_3COH , VWR) immediately after sampling. This derivatization transforms unstable polysulfides to stable dimethylpolysulfanes,³¹ which were then analyzed on a Merck Hitachi high-pressure liquid chromatography (HPLC) using a reversed phase C18 column (Waters-Spherisorb, ODS2, 5 μm , 250 \times 4.6 mm) and gradient elution.³² Detection was achieved with a L-2420 UV-vis detector at 230 nm wavelength. In pretests we tried to determine whether sulfur in monothioarsenate is codetermined using this derivatization method. In solutions containing 1 to 10 mM monothioarsenate and 0, 4, or 8 mM sulfide in ML-medium, we detected 0.3 to 1.6 mMeq polysulfides, mainly as disulfide (S_2^{2-} ; Supporting Information

Figure SI-1). Disulfide contains one S atom in the redox state -II, the second S atom in the redox state 0 (zerovalent sulfur). We were not able to differentiate whether the disulfide was a remnant of monothioarsenate synthesis from the reaction of elemental sulfur with As_2O_3 or resulted from (partial) monothioarsenate transformation during derivatization and its recombination as released sulfur within polysulfides. In conclusion, this means that the “polysulfide” signal reported in the Results includes polysulfides formed directly by the reaction, but potentially also sulfur, which originates from monothioarsenate (roughly 10–26% according to our pretests). A qualitative way of differentiating the two sources is the color of the frozen samples: solutions containing zerovalent sulfur bound in polysulfides are yellow, while solutions containing monothioarsenate-bound sulfur in the redox state -II are colorless.

Growth Monitoring. MLMS-1 cell counts were obtained by direct counting using a Neubauer improved counting chamber (0.02 mm depth) and a ZEISS Axioplan fluorescence microscope at 400 \times magnification. MLMS-1 cells were stained with SYBR Gold (Invitrogen).³³

RESULTS AND DISCUSSION

Identification of the Intermediate Thioarsenic Species Formed during Growth of Strain MLMS-1 on Arsenate and Sulfide. To better identify the transient thioarsenic species previously reported, we reproduced the experiment of Hoeft et al.¹³ using arsenate (12.5 mM) as electron acceptor and sulfide (5 mM) as electron donor (Figure 1, Supporting

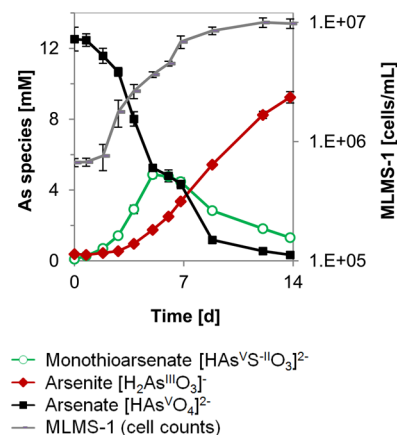


Figure 1. Cell growth and arsenic speciation (determined by IC-ICP-MS) in an incubation experiment of MLMS-1 on 12.5 mM arsenate and 5 mM sulfide (error bars represent standard deviation of triplicate experiments).

Information Table SI-1). No loss of arsenate or significant production of arsenite occurred in sterile controls (arsenite ≤ 0.07 mM (0.8%); Supporting Information Figure SI-2, Table SI-1), as chemical reduction of arsenate with sulfide is only relevant at $\text{pH} < 4$.³⁴ In the experiments with strain MLMS-1 growth occurred at a rate of 0.016 h^{-1} (generation time 42 h) and reached maximum cell numbers of $(9.98 \pm 0.91) \times 10^6$ cells/mL after 12 days. Previously reported growth rates were in a similar range (0.022 h^{-1}).¹³ With the decrease of arsenate, we observed the formation of arsenite (maximum 9.3 mM, 82%, after 14 days) and the appearance of an intermediate thioarsenic species. The dominant thioarsenic species (maximum 4.9 mM, 40%, after 5 days) had sulfur:arsenic ratios of

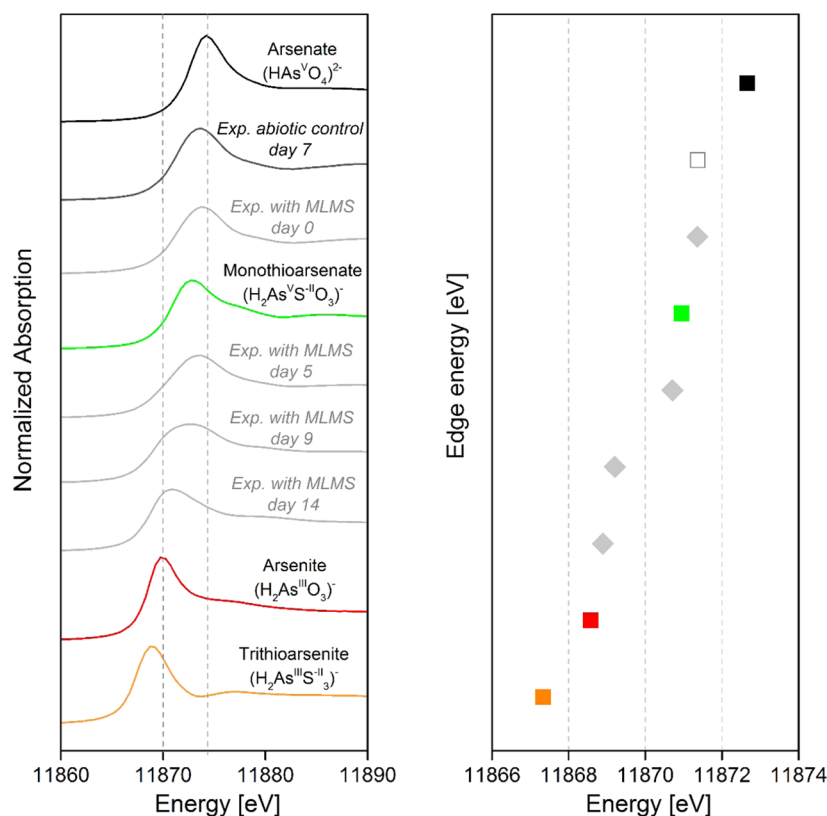


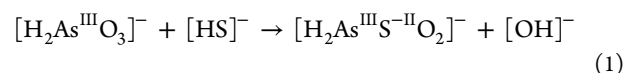
Figure 2. X-ray absorption edge energies of solutions from the incubation experiment of MLMS-1 on 12.5 mM arsenate and 5 mM sulfide (shown in Figure 1) and one abiotic control (shown in Supporting Information Figure SI-2) compared to references of arsenate, monothioarsenate, arsenite, and trithioarsenite.

1:1 and its chromatographic retention time matched that of our synthesized monothioarsenate. Only minor quantities of trithioarsenate (max. 0.5 mM, 4%, after 0.8 days), dithioarsenate (max. 0.3 mM, 2.8%, after 14 days), and tetrathioarsenate (max. 0.1 mM, 0.9%, 0 days) were observed (Supporting Information Table SI-1).

To exclude the possibility that the observed thioarsenic species was trivalent monothioarsenate that was oxidized to monothioarsenate during analysis by IC-ICP-MS, we obtained XANES spectra of samples that were flash-frozen in the anoxic chamber and analyzed using a cryostat without exposition to oxygen. These XANES analyses confirmed identification of the transient thioarsenic species detected in the biotic samples as monothioarsenate (Figure 2). With time, edge energies in the biotic experiments decreased from 11871.4 to 11870.7 eV, 11869.2 eV, and finally 11868.9 eV (Figure 2). This is in line with an initial dominance of arsenate (reference spectra 11872.7 eV²²), transient formation of monothioarsenate (reference spectra 11871 eV²²) along with arsenite, and finally complete transformation to arsenite (reference spectra 11868.6 eV²²). To date, there are no published XANES reference spectra for monothioarsenate. Its formation has been speculated to occur in an arsenite-sulfide mix (As:S, 1:1), but was of minor importance.⁸ By analogy to existing reference spectra of thioarsenates, where each addition of an SH⁻-group decreases the absorption edge by 0.5 to 1 eV,²² monothioarsenate should have an absorption edge between arsenite (11868.6 eV) and trithioarsenite (11867.4 eV). Since the XANES signals never dropped below the absorption edge of arsenite, we exclude the presence of monothioarsenate and confirm that the transient

thioarsenic species that formed during growth of MLMS-1 on arsenate and sulfide was monothioarsenate.

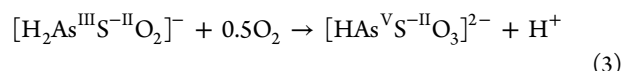
Abiotic Formation of Monothioarsenate. Details of the transient formation of a thioarsenic species during growth of strain MLMS-1 (Figure 1) were not investigated previously¹³ and it was assumed that anoxic chemistry promoted formation of monothioarsenite from the electron donor sulfide and arsenite produced from microbial reduction of arsenate (eq 1).



However, our previous XAS analyses have shown that the only species detected in arsenite-sulfide mixes were trithioarsenite and the unreacted, residual arsenite.⁸ Decreasing the experimental sulfide to arsenite ratios shifted the equilibrium toward more arsenite and less trithioarsenite, but did not yield a dominance of mono- or dithioarsenite. In the previous study,⁸ Extended X-ray absorption fine spectroscopy (EXAFS) data were interpreted as showing traces of monothioarsenite (<10% of total arsenic) in solutions with a sulfide to arsenite ratio of 1:1, but it was never observed as the dominant species. Thus, even though spontaneous formation of monothioarsenite is possible, this reaction seems kinetically unfavored and is thus unlikely to have occurred in the published strain MLMS-1 experiment.¹³

The present study now shows that the intermediate species formed during growth of MLMS-1 is a pentavalent monothioarsenate rather than trivalent monothioarsenite. Formation of monothioarsenate could occur either from the pentavalent arsenate via ligand exchange of an OH⁻ versus SH⁻

group (eq 2) or by oxidation of trivalent monothioarsenite (eq 3).



However, arsenate only reacts spontaneously with sulfide at $\text{pH} < 4$,³⁴ so monothioarsenate in our experiments ($\text{pH} 9.8$) did not form by $\text{OH}^{-}\text{-SH}^{-}$ ligand exchange from arsenate. With regard to thioarsenate formation by oxidation of thioarsenites, previous analyses by XAS have shown that trithioarsenite quickly transforms to di- and trithioarsenate when exposed to atmospheric oxygen, for example, while waiting on the autosampler for IC-ICP-MS analysis.^{8,22} However, monothioarsenate was never observed as dominant species. Direct oxidation of monothioarsenite could not be tested because it was never the dominant species in any mix and no commercial standard exists.

In the present study, we conducted numerous abiotic experiments with mixes of arsenite and sulfide at different ratios in anoxic ML-medium in the anoxic chamber, allowing formation of thioarsenites, and then willingly exposed those solutions for a few minutes to atmospheric oxygen while waiting on the autosampler for IC-ICP-MS analysis. As expected, we found different thioarsenates (Figure 3a, b, Supporting Information Table SI-2, Figure SI-3). However, again, we were not able to create a solution where monothioarsenate was the predominant species detected.

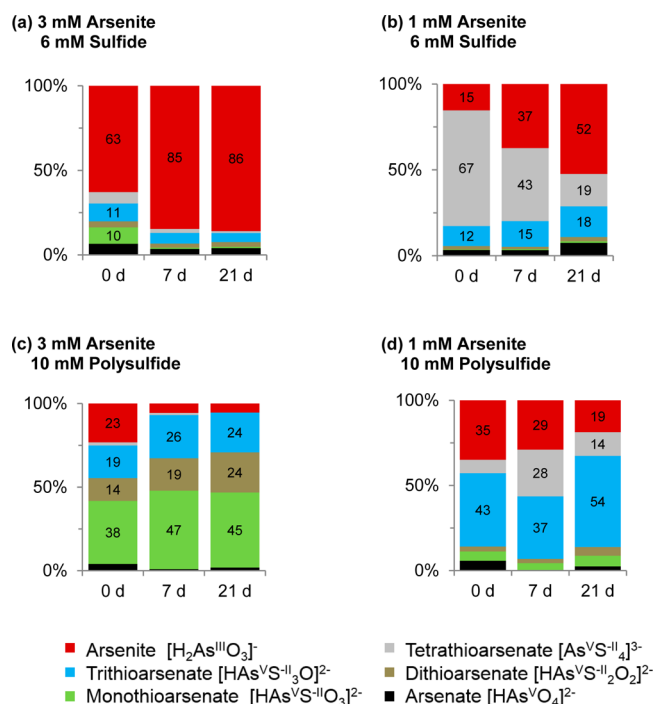


Figure 3. Arsenic speciation (determined by IC-ICP-MS) in abiotic solutions of arsenite with excess sulfide (a, b) or polysulfides (c, d) at different As/S ratios in ML-medium. Formation of thioarsenates was induced by exposing solutions briefly to atmospheric oxygen, while waiting in capped, but not gastight vials for analysis on the IC-autosampler. Y-axis shows relative percentage of As-species (%) (for species with percentages of less than 10% no numbers are displayed in columns for better readability), X-axis shows sampling time in days.

High sulfide to arsenite ratios (6:1) yielded large percentage of thioarsenates with a dominance of higher thiolated arsenic species (67% tetrathioarsenate, 12% trithioarsenate) and less than 1% monothioarsenate (Figure 3b, Supporting Information Table SI-2, Figure SI-3). Decreasing the sulfide to arsenite ratio resulted in smaller percentage of all thioarsenates and a clear dominance of arsenite (Figure 3a, Supporting Information Table SI-2, Figure SI-3). In contrast to the experiments with strain MLMS-1 (Figure 1), none of the abiotic arsenite-sulfide oxidation experiments showed monothioarsenate as the dominant thioarsenic species (max. 0.3–10%, Figure 3, Supporting Information Table SI-2, Figure SI-3). A clear dominance of monothioarsenate was, however, observed when using polysulfides instead of sulfide for the reaction with arsenite. At a polysulfide to arsenite ratio of 3:1 we found immediate formation of 38% monothioarsenate as the dominant species (Figure 3c). At a ratio of 10:1, only 5% monothioarsenate formed and higher thiolated arsenates were the dominant species (Figure 3d).

These experiments suggest that the direct abiotic formation of monothioarsenate from arsenite requires sulfur in the redox state S^0 rather than $\text{S}^{-\text{II}}$ (eq 4). Thioarsenate formation by addition of zerovalent sulfur to arsenite also fits previously published theoretical considerations.^{35–37} Only if sulfide concentrations are low ($\text{OH}^{-} > \text{SH}^{-}$) is the arsenite-trithioarsenite equilibrium shifted toward arsenite dominance⁸ and addition of S^0 leads to formation of monothioarsenate from arsenite. High sulfide concentrations prevent formation of monothioarsenate but lead to rapid ligand exchange between OH^{-} and SH^{-} , forming trithioarsenite from arsenite.⁸ Addition of S^0 then leads to spontaneous formation of dominantly tetrathioarsenate (eq 5). Therefore, mono- and tetrathioarsenate are the end-products of the proposed reaction, with di- and trithioarsenate forming as transient intermediate species. The observation that the share of thioarsenates increased with time (Figure 3c, 3d) indicates that zerovalent sulfur pushes the chemical equilibrium toward thioarsenate formation.

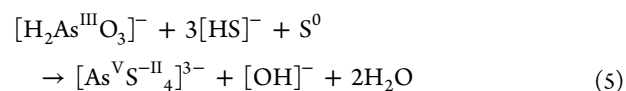


Figure 4 summarizes the described pathways of thioarsenite and thioarsenate formation. It is important to note that the different reactions for thioarsenite and thioarsenate formation and transformation seem to have very different kinetics. Formation of trithioarsenite from arsenite and transformation of trithioarsenite back to arsenite occur spontaneously.⁸ Previous⁸ and present experiments have shown that thioarsenates also form spontaneously from arsenite or thioarsenites in the presence of zerovalent sulfur (Figure 3). However, once formed, thioarsenates are kinetically stable, even in the absence of arsenite, thioarsenites, and zerovalent sulfur. Higher thiolated arsenates transform to arsenite when sulfide is removed, for example, by purging solutions with air³⁸ or when addition of protons forces the formation of SH^{-} -groups.^{27,39} Transformation to arsenate only occurs in the presence of a strong oxidizing agent such as H_2O_2 .³⁸ Monothioarsenate with its double-bound sulfur is kinetically stable even upon aeration³⁸ and acidification²⁷ and chemically only transforms to arsenate when exposed to a strong oxidizing agent such as H_2O_2 .³⁸

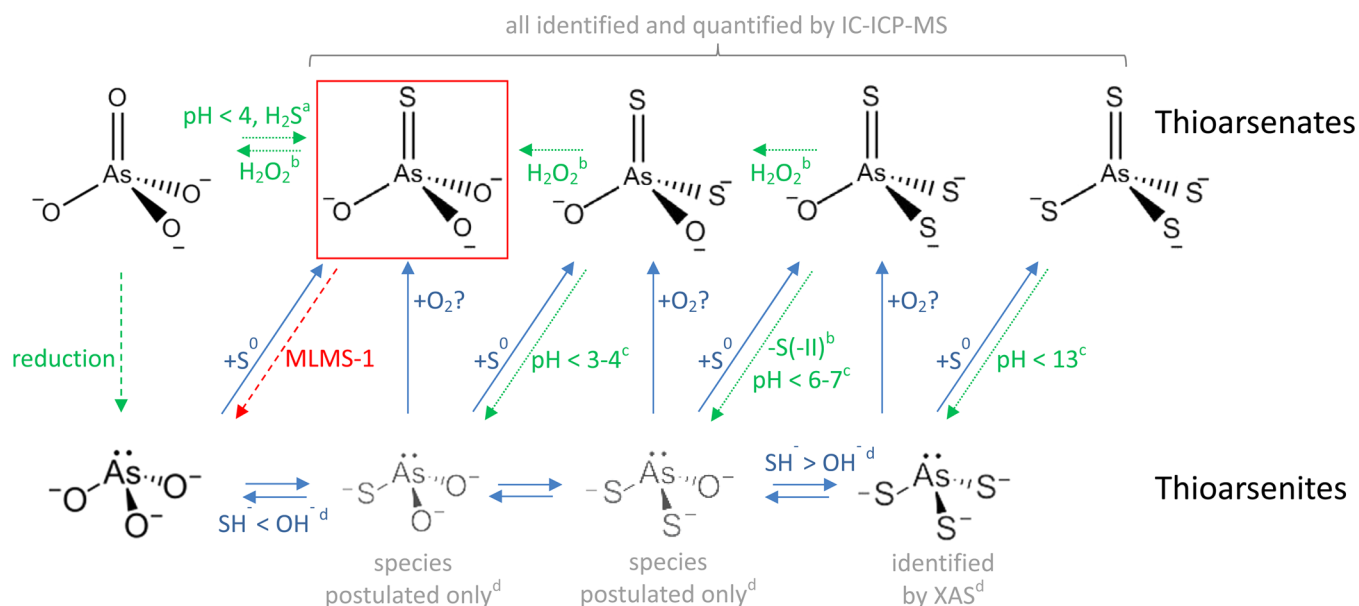


Figure 4. Reaction pathway of thioarsenite and thioarsenate formation; blue solid arrows indicate that reactions occur spontaneously, green dashed lines indicate that reaction is slow and needs an additional reactant like O_2 , H_2O_2 , H^+ ; -S(-II) refers to an experiment where trithioarsenate was partially converted to arsenite by purging the solution with air, presumably S(-II) was either oxidized or degassed; monothioarsenate forms spontaneously from arsenite by addition of zerovalent sulfur at low SH^- versus OH^- concentrations (conditions that are closest met with the experimental results from Figure 3c) and is kinetically stable; it only transforms spontaneously with a strong oxidizing agent to arsenate or (red line) in the presence of MLMS-1 to arsenite (superscript letters refer to reactions shown in (a) Rochette et al. 2000,³⁴ (b) Planer-Friedrich et al. (2009),³⁸ (c) Planer-Friedrich and Wallschläger (2009),²⁷ and (d) Planer-Friedrich et al. (2010)⁸ and Suess et al. (2009)²²).

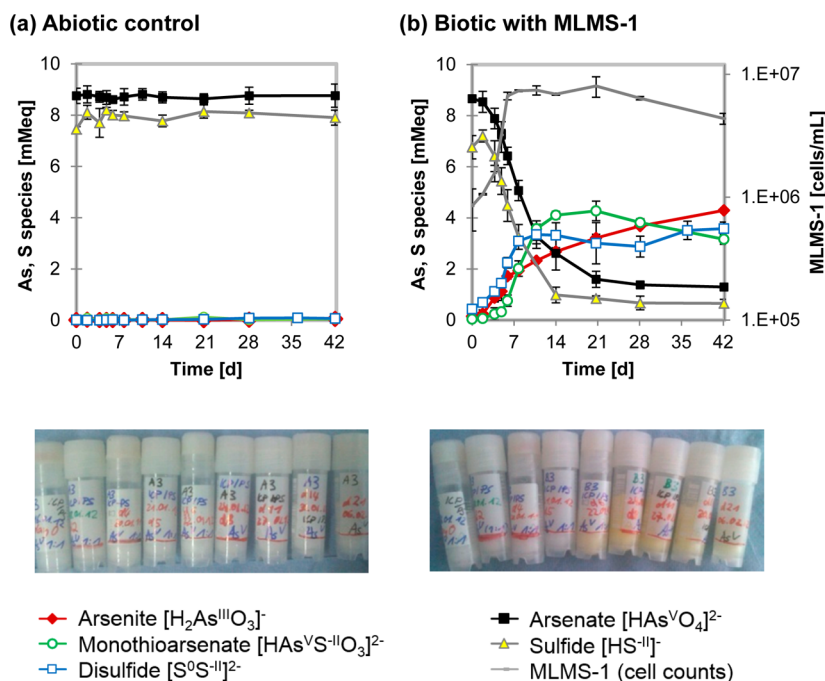


Figure 5. Reaction of 8.5 mM arsenate with 7 mM sulfide in (a) an abiotic control and (b) the presence of MLMS-1. Error bars represent standard deviation of triplicate experiments. Photographs include the frozen samples from day 0 to 21 and show yellow color in Figure 5b from day 6 on.

Formation of Monothioarsenate and Polysulfides in the Presence of Strain MLMS-1. Samples from a growth experiment with strain MLMS-1 using nearly equimolar concentrations of arsenate (8.5 mM) and sulfide (7 mM), were analyzed for thioarsenate and polysulfide formation (Figure 5). Neither arsenate or sulfide degradation, nor thioarsenate or polysulfide formation were detectable in the abiotic controls (Figure 5a). For the biotic experiments,

MLMS-1 growth rates (0.018 h^{-1}) and generation time (38 h) were comparable to the first experiment. During the microbially catalyzed transformation of arsenate and sulfide by strain MLMS-1 up to 4.3 mM arsenite (44%) formed after 42 days (Figure 5b) along with 5.0 mMeq polysulfides, mainly as disulfide S_2^{2-} (3.6 mMeq or 39% of the originally applied sulfur). Note that the “sulfide” depicted in Figure 5b was determined by the methylene-blue method which also measures

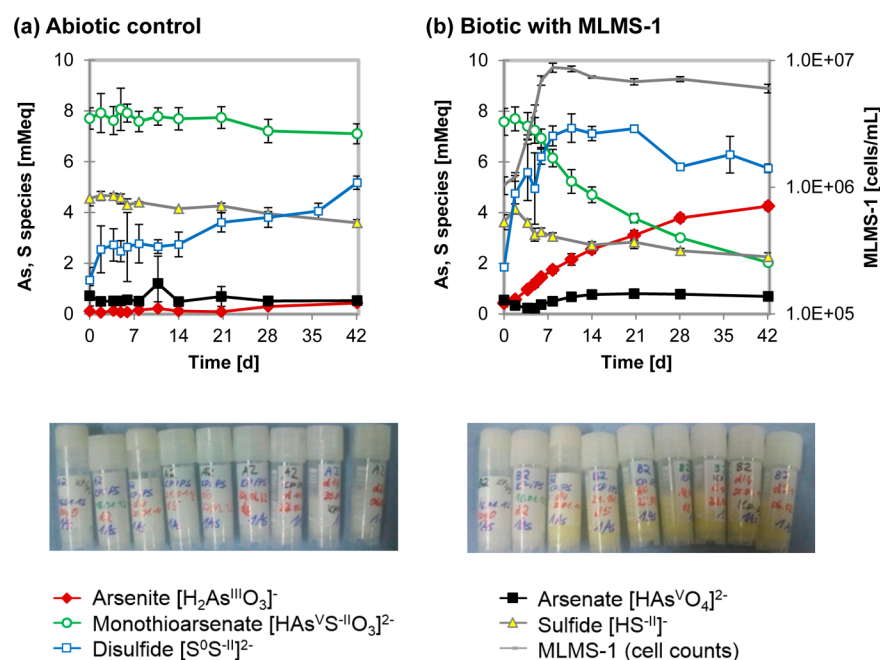
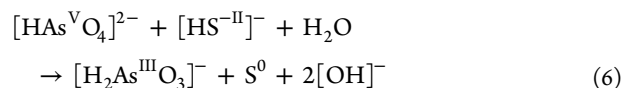


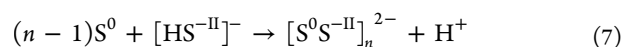
Figure 6. Reaction of 7.5 mM monothioarsenate with 5 mM sulfide in (a) an abiotic control and (b) the presence of MLMS-1. Error bars represent standard deviation of triplicate experiments. Photographs include frozen samples of day 0 to 21 and show yellow color in Figure 6b from day 4 on.

disulfide-bound sulfide. It is thus not possible to say whether there was truly any free sulfide left in solution after 14 days.

The dissimilatory reduction of arsenate to arsenite requires two electrons, so it is plausible that the primary oxidation product of sulfide is zerovalent sulfur (eq 6).

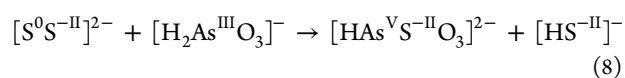


Zerovalent sulfur then reacts quickly with remaining sulfide in the ML-medium⁴⁰ (eq 2) to form polysulfides (eq 7).



Polysulfide formation rates are relatively slow ($\sim 3\text{--}4\text{ h}$)⁴¹ while in contrast disproportionation of different polysulfides into other polymeric forms only takes seconds.⁴²

The increase in disulfide concentrations in our experiment preceded that of monothioarsenate (maximum 4.3 mMeq, 44%, after 21 days). Thus, zerovalent sulfur in disulfide most likely reacted with arsenite to form monothioarsenate (eq 8). As mentioned, pretests showed that 10–26% of the monothioarsenate is codetermined as disulfide artifact using derivatization (Supporting Information Figure SI-1). The exact concentration of “true” disulfide thus might be lower (2.5–3.2 mMeq). However, the fact that the disulfide concentrations increased before those of monothioarsenate coupled with the observation of the yellow color in the frozen samples confirmed the original presence of disulfide. The observed dominance of the short disulfide polymer over longer-chained polysulfides ($\text{S}_3^{2-} < 1.6\text{ mMeq}$; $\text{S}_4^{2-} < 0.4\text{ mMeq}$; S_5^{2-} , S_6^{2-} , S_7^{2-} and $\text{S}_8^{2-} < 0.1\text{ mMeq}$; Supporting Information Table SI-3, Figure SI-4) is consistent with previous observations at low elemental sulfur concentrations,⁴³ high pH, and in a salt-rich medium.^{20,44}



The limited available concentrations of free sulfide relative to those of arsenite did not allow for the formation of higher thiolated arsenates (Figure 5b). This is similar to what we observed in the abiotic experiments conducted with low polysulfide excess in comparison to arsenite (Figure 3c). An active involvement of strain MLMS-1 in monothioarsenate formation does not seem likely in comparison to rapid abiotic formation (Figure 3c, d).

When compared with oxidation of sulfide to zerovalent sulfur, oxidation of sulfide to sulfate was of minor significance during growth of strain MLMS-1. While the measured initial concentrations of arsenate ($\sim 8.5\text{ mM}$) and sulfide ($\sim 7\text{ mM}$) were nearly equimolar, sulfate concentrations did not increase significantly ($< 1\text{ mM}$, Supporting Information Table SI-3) within 42 days. A complete microbial redox transformation from $\text{S}^{-\text{II}}$ to $\text{S}^{+\text{VI}}$ was reported earlier for experiments employing lower initial sulfide concentrations (3.3 mM) in the presence of $\sim 9\text{ mM}$ arsenate, when sulfate was detected as the main sulfur product.¹³

Disproportionation of Monothioarsenate by strain MLMS-1. To determine whether strain MLMS-1 can directly metabolize monothioarsenate as a substrate for growth, a third experiment was performed. Sterile controls confirmed that no chemical monothioarsenate transformation occurred (Figure 6a). Variations in concentrations between different days were within the standard deviation of triplicate analyses from the same day (Supporting Information Table SI-4). This lack of transformation is in accordance with earlier findings of its kinetic stability toward aeration³⁸ and acidification.²⁷ The “disulfide” signal likely is an artifact of codetermined monothioarsenate, because no yellow color was observed in the original solutions (Figure 6a). From day 21 on, monothioarsenate and sulfide decreased slightly and the corresponding increase in disulfide is likely a true signal of polysulfide formation from monothioarsenate transformation.

In biotic experiments, strain MLMS-1 showed an exponential growth rate of 0.017 h^{-1} (generation time 40 h) and reached

maximum cell numbers of $(8.80 \pm 0.72) \times 10^6$ cells/mL (Supporting Information Table SI-1), which is comparable to what was observed for growth on arsenate with sulfide in the present (Figure 1) and the previous experiment.¹³ The monothioarsenate concentrations decreased during the exponential and later stationary growth phase of strain MLMS-1. The major products were arsenite and disulfide (Figure 6b). Again, the actual disulfide concentrations were probably lower than depicted because of partial monothioarsenate codetermination, especially at the onset of the incubation when monothioarsenate concentrations were highest. However, the assumption of true formation of disulfide is supported by the yellow color that all frozen biotic samples showed after day 4 (Figure 6b), in contrast to the abiotic samples, which lacked this hue (Figure 6a).

Three possibilities could explain the observed decrease of monothioarsenate in the biotic experiments. First is that monothioarsenate chemically transforms into arsenate and sulfide; hence, we would have the same growth scenario as in the arsenate experiments in the present (Figure 1) and the previous study.¹³ However, both biotic (Figure 1) and abiotic experiments (Figure 3) have shown that monothioarsenate is formed from arsenite and zerovalent sulfur (eq 4), not from arsenate and sulfide. A second theoretical possibility is the abiotic transformation of monothioarsenate to arsenite and zerovalent sulfur. However, then the observed microbial growth could only have been achieved by using the zerovalent sulfur, for example, by disproportionation to sulfide and sulfate, thereby decreasing zerovalent sulfur concentration. However, this idea is contradicted by our observations: only small increases of sulfate, minor loss of sulfide and increasing disulfide concentrations. Thus, the third and only plausible explanation is a microbially catalyzed disproportionation of monothioarsenate, with the central arsenate (As^{V}) serving as electron acceptor (upon reduction yielding arsenite) and the sulfur in the thio-group ligand ($\text{S}^{-\text{II}}$) serving as electron donor (upon oxidation yielding zerovalent sulfur).

Sulfide was added to the monothioarsenate experiment to yield comparable conditions to the two previous experiments with arsenate and to guarantee reducing conditions. Biotic transformation of free sulfide ($[\text{HS}^-]$) in this experiment was negligible. Sulfide showed a slight decrease in the presence of strain MLMS-1 (Figure 6b) but that was comparable to the decrease observed in the abiotic control (Figure 6a). Small increases in sulfate concentrations were also observed in the biotic and abiotic experiments (Supporting Information Table SI-4). Hence, the small decrease of sulfide (~ 1.3 mM) in the biotic experiments cannot explain the large increase in disulfide (5 mMeq, which would be the product of sulfide oxidation) nor the large decrease of monothioarsenate (5.6 mM, which would be the compound to be reduced concurrently to sulfide oxidation). Compared to oxidation of monothioarsenate-bound sulfide to S^0 (coupled to arsenate reduction to arsenite), oxidation of free sulfide to S^{VI} was subordinate.

The Relevance of Arsenic and Sulfur Stoichiometry for Microbial Transformation of Arsenate and Monothioarsenate. Comparing our three biotic experiments conducted at different arsenic to sulfide ratios (Figures 1, 5b, and 6b) and earlier findings¹³ indicates that the arsenic to sulfide stoichiometry influences which oxidized sulfur species forms. The first oxidation product is zerovalent sulfur, which makes it a closed 2-electron transfer at equimolar arsenate and sulfide concentrations. Equal concentrations of arsenite,

monothioarsenate, and disulfide remained at the end of the experiment when all arsenate was transformed (Figure 5b). Further oxidation of zerovalent sulfur to sulfate occurs when arsenate concentrations exceed those of sulfide (previous experiment¹³ and Figure 1). In this experiment, monothioarsenate was almost completely transformed (Figure 1). Considering the kinetic stability of monothioarsenate in the absence of zerovalent sulfur (Figure 6a), a purely chemical transformation of the monothioarsenate seems unlikely. However, it seems that the microbial oxidative removal of zerovalent sulfur also facilitated or accelerated microbial disproportionation of monothioarsenate.

Relevance of Monothioarsenate for Microbial Ecology. Recently, thioarsenates have been shown to play an important role in the microbial ecology of (micro)aerophilic hyperthermophiles at hot springs^{15,16} as well as during anoxygenic photosynthesis by purple sulfur bacteria in alkaline environment.¹⁷ Our results with strain MLMS-1 give another example for the ecological relevance of thioarsenates in anoxic environments and highlight the importance of considering thioarsenates in future studies. We have shown that monothioarsenate, though kinetically stable under a wide range of abiotic conditions, can serve as substrate for the metabolism of strain MLMS-1 and can be transformed by disproportionation to arsenite and zerovalent sulfur. Other microorganisms in Mono Lake or similar sulfidic environments might have similar capabilities. Microorganisms could therefore play a significant role in determining which thioarsenic species occur in nature, often in contrast to thermodynamic equilibrium predictions.

■ ASSOCIATED CONTENT

📄 Supporting Information

As and S species concentrations for microbial and abiotic experiments, monothioarsenate artifact determination during polysulfide analysis after triflate derivatization, kinetics of abiotic reaction of arsenate with sulfide, reaction of arsenite with 1 and 3 mM sulfide and polysulfides, formation of individual polysulfides during abiotic and biotic reaction of arsenate and monothioarsenate with sulfide. The Supporting Information is available free of charge on the ACS Publications website at DOI: 10.1021/acs.est.5b01165.

■ AUTHOR INFORMATION

Corresponding Author

*Phone +49 921 553999; fax +49 921 52334; e-mail: b.planer-friedrich@uni-bayreuth.de.

Notes

The authors declare no competing financial interest.

■ ACKNOWLEDGMENTS

We acknowledge generous funding by the German Research Foundation within the Emmy Noether program to Britta Planer-Friedrich (Grant No. PL 302/3-1). We thank Carolin Kerl, Linda Schneider, Sinikka Hinrichsen, Frank Thomas, Stefan Will, Harold Drake, Steffen Kolb, and Marcus Horn for help with experiments, standard synthesis, sample analysis and/or brainstorming.

REFERENCES

- (1) Dana, G. L.; Lenz, P. H. Effects of increasing salinity on an artemia population from Mono-Lake, California. *Oecologia* **1986**, *68* (3), 428–436.
- (2) Ficklin, D. L.; Stewart, I. T.; Maurer, E. P. Effects of projected climate change on the hydrology in the Mono Lake Basin, California. *Clim. Change* **2013**, *116* (1), 111–131.
- (3) Hollibaugh, J. T.; Carini, S.; Gürleyük, H.; Jellison, R.; Joye, S. B.; LeClerc, G.; Meile, C.; Vasquez, L.; Wallschläger, D. Arsenic speciation in Mono Lake, California: Response to seasonal stratification and anoxia. *Geochim. Cosmochim. Acta* **2005**, *69* (8), 1925–1937.
- (4) Oremland, R. S.; Stolz, J. F.; Hollibaugh, J. T. The microbial arsenic cycle in Mono Lake, California. *FEMS Microbiol. Ecol.* **2004**, *48* (1), 15–27.
- (5) Oremland, R.; Dowdle, P.; Hoeft, S.; Sharp, J.; Schaefer, J.; Miller, L.; Blum, J.; Smith, R.; Bloom, N.; Wallschläger, D. Bacterial dissimilatory reduction of arsenate and sulfate in meromictic Mono Lake, California. *Geochim. Cosmochim. Acta* **2000**, *64* (18), 3073–3084.
- (6) Wilkin, R.; Wallschläger, D.; Ford, R. Speciation of arsenic in sulfidic waters. *Geochem. T.* **2003**, *4* (1), 1–7.
- (7) Wallschläger, D.; Stadey, C. J. Determination of (Oxy)-thioarsenates in Sulfidic Waters. *Anal. Chem.* **2007**, *79*, 3873–3880.
- (8) Planer-Friedrich, B.; Suess, E.; Scheinost, A. C.; Wallschläger, D. Arsenic speciation in sulfidic waters: Reconciling contradictory spectroscopic and chromatographic evidence. *Anal. Chem.* **2010**, *82*, 10228–10235.
- (9) Oremland, R.; Hoeft, S.; Santini, J.; Bano, N.; Hollibaugh, R.; Hollibaugh, J. Anaerobic oxidation of arsenite in Mono Lake Water and by a facultative, arsenite-oxidizing chemoautotroph, strain MLHE-1. *Appl. Environ. Microbiol.* **2002**, *68* (10), 4795–4802.
- (10) Kulp, T. R.; Hoeft, S. E.; Asao, M.; Madigan, M. T.; Hollibaugh, J. T.; Fisher, J. C.; Stolz, J. F.; Culbertson, C. W.; Miller, L. G.; Oremland, R. S. Arsenic(III) fuels anoxygenic photosynthesis in hot spring biofilms from Mono Lake, California. *Science* **2008**, *321* (5891), 967–970.
- (11) Kulp, T. R.; Hoeft, S. E.; Miller, L. G.; Saltikov, C.; Murphy, J. N.; Han, S.; Lanoil, B.; Oremland, R. S. Dissimilatory arsenate and sulfate reduction in sediments of two hypersaline, arsenic-rich soda lakes: Mono and Searles lakes, California. *Appl. Environ. Microbiol.* **2006**, *72* (10), 6514–6526.
- (12) Hollibaugh, J. T.; Budinoff, C.; Hollibaugh, R. A.; Ransom, B.; Bano, N. Sulfide oxidation coupled to arsenate reduction by a diverse microbial community in a soda lake. *Appl. Environ. Microbiol.* **2006**, *72* (3), 2043–2049.
- (13) Hoeft, S. E.; Kulp, T. R.; Stolz, J. F.; Hollibaugh, J. T.; Oremland, R. S. Dissimilatory arsenate reduction with sulfide as electron donor: Experiments with mono lake water and isolation of strain MLMS-1, a chemoautotrophic arsenate respirer. *Appl. Environ. Microbiol.* **2004**, *70* (5), 2741–2747.
- (14) Fisher, J. C.; Wallschläger, D.; Planer-Friedrich, B.; Hollibaugh, J. T. A new role for sulfur in arsenic cycling. *Environ. Sci. Technol.* **2008**, *42*, 81–85.
- (15) Haertig, C.; Planer-Friedrich, B. Thioarsenate transformation by filamentous microbial mats thriving in an alkaline, sulfidic hot spring. *Environ. Sci. Technol.* **2012**, *46* (8), 4348–4356.
- (16) Haertig, C.; Lohmayer, R.; Kolb, S.; Horn, M. A.; Inskeep, W. P.; Planer-Friedrich, B. Chemolithotrophic growth of the aerobic hyperthermophilic bacterium *Thermocrinis ruber* OC 14/7/2 on monothioarsenate and arsenite. *FEMS Microbiol. Ecol.* **2014**, *90*, 747–760.
- (17) Edwardson, C.; Planer-Friedrich, B.; Hollibaugh, J. Transformation of monothioarsenate by haloalkaliphilic, anoxygenic photosynthetic purple sulfur bacteria. *FEMS Microbiol. Ecol.* **2014**, *90*, 858–868.
- (18) Schwedt, G.; Rieckhoff, M. Separation of thio- and oxothioarsenates by capillary zone electrophoresis and ion chromatography. *J. Chromatogr. A* **1996**, *736* (1–2), 341–350.
- (19) Chen, K. Y.; Gupta, S. K. Formation of polysulfides in aqueous-solution. *Environ. Lett.* **1973**, *4* (3), 187–200.
- (20) Giggenbach, W. Optical-spectra and equilibrium distribution of polysulfide ions in aqueous-solution at 20 degrees. *Inorg. Chem.* **1972**, *11* (6), 1201–8.
- (21) Planer-Friedrich, B.; London, J.; McCleskey, R. B.; Nordstrom, D. K.; Wallschläger, D. Thioarsenates in geothermal waters of Yellowstone National Park: Determination, preservation, and geochemical role. *Environ. Sci. Technol.* **2007**, *41* (15), S245–S251.
- (22) Suess, E.; Scheinost, A. C.; Bostick, B. C.; Merkel, B. J.; Wallschläger, D.; Planer-Friedrich, B. Discrimination of thioarsenites and thioarsenates by X-ray absorption spectroscopy. *Anal. Chem.* **2009**, *81*, 8318–8326.
- (23) Webb, S. M. SIXpack: A graphical user interface for XAS analysis using IFEFFIT. *Phys. Scr.* **2005**, *T115*, 1011–1014.
- (24) Ravel, B.; Newville, M. ATHENA, ARTEMIS, HEPHAESTUS: Data analysis for X-ray absorption spectroscopy using IFEFFIT. *J. Synchrotron. Radiat.* **2005**, *12*, 537–541.
- (25) Cline, J. D. Spectrophotometric determination of hydrogen sulfide in natural waters. *Limnol. Oceanogr.* **1969**, *14*, 454–458.
- (26) Mylon, S. E.; Benoit, G. Subnanomolar detection of acid-labile sulfides by the classical methylene blue method coupled to HPLC. *Environ. Sci. Technol.* **2001**, *35* (22), 4544–4548.
- (27) Planer-Friedrich, B.; Wallschläger, D. A critical investigation of hydride generation-based arsenic speciation in sulfidic waters. *Environ. Sci. Technol.* **2009**, *43*, 5007–5013.
- (28) Fossing, H.; Jorgensen, B. B. Measurement of bacterial sulfate reduction in sediments—Evaluation of a single-step chromium reduction method. *Biogeochemistry* **1989**, *8* (3), 205–222.
- (29) Wu, F.; Kramer, J. R. Assessment of the AVS Method and “Cline’s” Method with respect to Reactive Sulfide, Transport, Fate and Effects of Silver in the Environment; Andren, A.; Bober, T. W., Eds.; Sea Grant Institute, University of Wisconsin, 1997; pp 109–114.
- (30) Small, J. M.; Hintelmann, H. Methylene blue derivatization then LC-MS analysis for measurement of trace levels of sulfide in aquatic samples. *Anal. Bioanal. Chem.* **2007**, *387* (8), 2881–2886.
- (31) Kamyschny, A.; Ekeltchik, I.; Gun, J.; Lev, O. Method for the determination of inorganic polysulfide distribution in aquatic systems. *Anal. Chem.* **2006**, *78* (8), 2631–2639.
- (32) Rizkov, D.; Lev, O.; Gun, J.; Anisimov, B.; Kuselman, I. Development of in-house reference materials for determination of inorganic polysulfides in water. *Accredit. Qual. Assur.* **2004**, *9* (7), 399–403.
- (33) Wegley, L.; Mosier-Boss, P.; Lieberman, S.; Andrews, J.; Graff-Baker, A.; Rohwer, F. Rapid estimation of microbial numbers in water using bulk fluorescence. *Environ. Microbiol.* **2006**, *8* (10), 1775–1782.
- (34) Rochette, E.; Bostick, B.; Li, G.; Fendorf, S. Kinetics of arsenate reduction by dissolved sulfide. *Environ. Sci. Technol.* **2000**, *34*, 4714–4720.
- (35) Stauder, S.; Raue, B.; Sacher, F. Thioarsenates in sulfidic waters. *Environ. Sci. Technol.* **2005**, *39* (16), 5933–5939.
- (36) Nilson, H. Über die Sulfüre des Arsens und deren Verbindungen. *J. Prakt. Chem.* **1876**, *14*, 1–61.
- (37) Weinland, R. F.; Lehmann, P. Über die Einwirkung von Natriumäthylat und Alkalien auf Arsenpentasulfid. *Z. Anorg. Chem.* **1901**, *26*, 322–344.
- (38) Planer-Friedrich, B.; Fisher, J. C.; Hollibaugh, J. T.; Süß, E.; Wallschläger, D. Oxidative transformation of trithioarsenate along alkaline geothermal drainages—Abiotic versus microbially mediated processes. *Geomicrobiology* **2009**, *26*, 339–350.
- (39) Thilo, E.; Hertzog, K.; Winkler, A. Über Vorgänge bei der Bildung des Arsen(V)-sulfids beim Ansäuern von Tetrathioarsenatlösungen. *Z. Anorg. Allg. Chem.* **1970**, *373*, 111–121.
- (40) Fossing, H.; Jorgensen, B. B. Isotope Exchange-Reactions with Radiolabeled Sulfur-Compounds in Anoxic Seawater. *Biogeochemistry* **1990**, *9* (3), 223–245.
- (41) Boulégue, J.; Michard, G. Dissolution du soufre élémentaire dans les solutions aqueuses diluées d’hydrogène sulfure. *C. R. Acad. Sci. Paris* **1977**, *284*, 713–716.

(42) Kamyshny, A.; Goifman, A.; Rizkov, D.; Lev, O. Kinetics of disproportionation of inorganic polysulfides in undersaturated aqueous solutions at environmentally relevant conditions. *Aquat. Geochem.* **2003**, *9* (4), 291–304.

(43) Rickard, D.; Luther, G. W. Chemistry of iron sulfides. *Chem. Rev.* **2007**, *107* (2), 514–562.

(44) Giggenbach, W. Optical spectra of highly alkaline sulfide solutions and second dissociation constant of hydrogen sulfide. *Inorg. Chem.* **1971**, *10* (7), 1333–1138.

Supporting Information to

**Anaerobic chemolithotrophic growth
of the haloalkaliphilic bacterium strain MLMS-1
by disproportionation of monothioarsenate**

Authors: B. Planer-Friedrich^{1*}, C. Härtig¹, R. Lohmayer¹, E. Suess², S. H. McCann³, R. Oremland³

¹*Department of Environmental Geochemistry, Bayreuth Center for Ecology and Environmental Research (BayCEER), University of Bayreuth, Universitätsstraße 30, 95447 Bayreuth, Germany*

²*Institute of Biogeochemistry and Pollutant Dynamics, Department of Environmental Systems Science, ETH Zurich, 8092 Zurich, Switzerland and Department of Water Resources and Drinking Water, Swiss Federal Institute of Aquatic Science and Technology (EAWAG), 8600 Dübendorf, Switzerland*

³*US Geological Survey, Menlo Park, California, USA*

- 10 pages
- 4 Tables
- 4 Figures

* corresponding author: phone +49 921 553999, fax +49 921 52334; email: b.planer-friedrich@uni-bayreuth.de.

Table SI-1 Arsenic species during growth of MLMS-1 on 10 mM Arsenate + 5 mM Sulfide. Experiment was reproduced after Hoefft et al. 2004.

Time [d]	Arsenite [mM]	Arsenate [mM]	Monothio-arsenate [mM]	Dithio-arsenate [mM]	Trithio-arsenate [mM]	Tetrathio-arsenate [mM]	Sum of As [mM]	MLMS-1 [$\times 10^6$ cells/mL]
Biotic experiment with MLMS-1 (refers to Figure 1)								
0.0	0.38 \pm 0.07	12.52 \pm 0.67	0.10 \pm 0.02	0.03 \pm 0.01	0.37 \pm 0.10	0.12 \pm 0.13	13.53 \pm 0.97	0.67 \pm 0.05
0.8	0.34 \pm 0.07	12.47 \pm 0.36	0.28 \pm 0.01	0.04 \pm 0.01	0.51 \pm 0.08	0.01 \pm 0.01	13.64 \pm 0.35	0.67 \pm 0.05
1.8	0.45 \pm 0.06	11.58 \pm 0.42	0.70 \pm 0.05	0.07 \pm 0.01	0.41 \pm 0.05	<0.01	13.22 \pm 0.43	0.76 \pm 0.19
2.8	0.55 \pm 0.07	10.67 \pm 0.24	1.42 \pm 0.11	0.11 \pm 0.02	0.28 \pm 0.06	<0.01	13.05 \pm 0.14	1.77 \pm 0.45
3.8	0.96 \pm 0.03	8.01 \pm 0.41	2.91 \pm 0.24	0.13 \pm 0.01	0.12 \pm 0.01	<0.01	12.14 \pm 0.34	2.65 \pm 0.36
5.0	1.75 \pm 0.10	5.26 \pm 0.07	4.87 \pm 0.20	0.11 \pm 0.01	0.14 \pm 0.01	<0.01	12.14 \pm 0.13	3.65 \pm 0.20
6.0	2.50 \pm 0.04	4.80 \pm 0.34	4.77 \pm 0.16	0.09 \pm 0.004	0.13 \pm 0.01	<0.01	12.30 \pm 0.43	4.51 \pm 0.21
6.8	3.35 \pm 0.07	4.35 \pm 0.27	4.47 \pm 0.21	0.10 \pm 0.01	0.13 \pm 0.01	<0.01	12.42 \pm 0.20	6.87 \pm 0.83
8.8	5.43 \pm 0.08	1.19 \pm 0.05	2.84 \pm 0.18	0.17 \pm 0.02	0.14 \pm 0.02	<0.01	9.77 \pm 0.22	8.51 \pm 0.62
12.1	8.24 \pm 0.20	0.55 \pm 0.10	1.82 \pm 0.08	0.25 \pm 0.02	0.14 \pm 0.02	<0.01	11.02 \pm 0.08	9.98 \pm 0.91
13.8	9.24 \pm 0.32	0.34 \pm 0.15	1.31 \pm 0.12	0.32 \pm 0.02	0.12 \pm 0.01	<0.01	11.33 \pm 0.46	9.79 \pm 0.88
Sterile abiotic control (refers to Figure SI-2)								
0.0	0.02 \pm 0.01	11.58 \pm 1.14	<0.01	<0.01	<0.01	<0.01	11.62 \pm 1.14	abiotic control
0.8	0.01 \pm 0.01	12.16 \pm 0.88	<0.01	<0.01	0.01 \pm 0.01	<0.01	12.19 \pm 0.87	abiotic control
1.8	0.04 \pm 0.05	12.27 \pm 0.70	<0.01	<0.01	<0.01	<0.01	12.32 \pm 0.74	abiotic control
2.8	<0.01	12.30	<0.01	<0.01	<0.01	<0.01	12.32 \pm 0.00	abiotic control
3.8	0.01 \pm 0.003	10.80 \pm 0.83	<0.01	<0.01	<0.01	<0.01	10.82 \pm 0.83	abiotic control
6.8	0.02 \pm 0.01	11.54 \pm 0.53	0.01 \pm 0.01	<0.01	<0.01	0.01 \pm 0.01	11.58 \pm 0.52	abiotic control
13.8	0.07 \pm 0.07	8.67 \pm 0.92	0.02 \pm 0.00	0.01 \pm 0.01	<0.01	0.01 \pm 0.01	8.78 \pm 0.86	abiotic control

Table SI-2 Sterilized experiments with Arsenite plus Sulfide or Polysulfides (refers to Figure 3 + Figure SI-3) in ML-medium (pH 9.8).

Time [days]	Arsenite [mM]	Arsenate [mM]	Monothio-arsenat [mM]	Dithio-arsenat [mM]	Trithio-arsenate [mM]	Tetrathio-arsenat [mM]	Sum of As [mM]
1 mM Arsenite plus 6 mM Sulfide							
0	0.13	0.03	0.00	0.02	0.10	0.57	0.85
7	0.32	0.03	0.00	0.01	0.13	0.37	0.86
21	0.48	0.07	0.01	0.02	0.16	0.17	0.92
3 mM Arsenite plus 6 mM Sulfide							
0	2.11	0.22	0.32	0.12	0.35	0.23	3.36
7	2.63	0.11	0.02	0.08	0.20	0.07	3.11
21	2.53	0.12	0.02	0.08	0.16	0.03	2.95
1 mM Arsenite plus 3 mM Sulfide							
0	0.20	0.03	0.04	0.05	0.27	0.20	0.79
7	0.31	0.03	0.03	0.09	0.29	0.14	0.88
21	0.45	0.08	0.01	0.05	0.18	0.08	0.86
3 mM Arsenite plus 3 mM Sulfide							
0	2.61	0.12	0.05	0.09	0.15	0.02	3.04
7	2.90	0.11	0.04	0.07	0.09	0.00	3.21
21	3.10	0.12	0.03	0.06	0.08	0.00	3.39
1 mM Arsenite plus 1 mM Sulfide							
0	0.51	0.05	0.08	0.10	0.10	0.02	0.85
7	0.77	0.04	0.06	0.09	0.09	0.01	1.05
21	0.87	0.00	0.04	0.07	0.09	0.00	1.06
3 mM Arsenite plus 1 mM Sulfide							
0	2.91	0.10	0.12	0.13	0.08	0.00	3.34
7	3.25	0.07	0.05	0.05	0.05	0.00	3.48
21	3.14	0.08	0.05	0.06	0.07	0.01	3.41
1 mM Arsenite plus 10 mM Polysulfide							
0	0.30	0.05	0.05	0.02	0.37	0.07	0.85
7	0.26	0.00	0.04	0.02	0.32	0.24	0.88
21	0.18	0.02	0.06	0.05	0.51	0.13	0.96
3 mM Arsenite plus 10 mM Polysulfide							
0	0.69	0.12	1.12	0.41	0.58	0.06	2.98
7	0.17	0.03	1.46	0.60	0.80	0.04	3.11
21	0.17	0.06	1.44	0.77	0.76	0.00	3.21

Table SI-3 Arsenic species during growth of MLMS-1 on 8.5 mM Arsenate + 7 mM Sulfide (refers to Figure 5).

Time [d]	Arsenite [mM]	Arsenate [mM]	Monothio-arsenate [mM]	Dithio-arsenate [mM]	Trithio-arsenate [mM]	Tetrathio-arsenate [mM]	Sum of As [mM]	MLMS-1 [$\times 10^6$ cells/mL]
Sterilized abiotic control (refers to Figure 5a)								
0.0	<0.01	8.76 \pm 0.30	0.02 \pm 0.01	<0.01	<0.01	<0.01	8.79 \pm 0.28	abiotic control
1.8	0.02 \pm 0.02	8.81 \pm 0.33	0.08 \pm 0.07	0.01 \pm 0.02	<0.01	<0.01	8.93 \pm 0.35	abiotic control
3.8	0.01 \pm 0.00	8.72 \pm 0.21	0.02 \pm 0.02	<0.01	<0.01	<0.01	8.75 \pm 0.23	abiotic control
4.9	<0.01	8.69 \pm 0.27	0.07 \pm 0.08	<0.01	0.01 \pm 0.00	<0.01	8.78 \pm 0.34	abiotic control
5.9	0.01 \pm 0.01	8.61 \pm 0.07	0.05 \pm 0.06	<0.01	0.02 \pm 0.03	<0.01	8.69 \pm 0.15	abiotic control
7.8	0.01 \pm 0.01	8.71 \pm 0.32	0.02 \pm 0.01	<0.01	<0.01	<0.01	8.75 \pm 0.32	abiotic control
10.8	0.01 \pm 0.01	8.81 \pm 0.22	0.03 \pm 0.02	<0.01	0.01 \pm 0.00	<0.01	8.86 \pm 0.22	abiotic control
14.0	0.01 \pm 0.00	8.70 \pm 0.21	0.02 \pm 0.00	<0.01	<0.01	<0.01	8.73 \pm 0.21	abiotic control
20.7	<0.01	8.64 \pm 0.19	0.12 \pm 0.18	<0.01	<0.01	<0.01	8.77 \pm 0.20	abiotic control
28.1	0.02 \pm 0.01	8.76 \pm 0.33	0.02 \pm 0.002	<0.01	<0.01	<0.01	8.81 \pm 0.33	abiotic control
42.1	0.05 \pm 0.03	8.76 \pm 0.45	0.05 \pm 0.03	<0.01	0.02 \pm 0.02	<0.01	8.89 \pm 0.42	abiotic control
Biotic experiment with MLMS-1 (refers to Figure 5b)								
0.0	0.15 \pm 0.05	8.66 \pm 0.11	0.04 \pm 0.01	0.01 \pm 0.01	0.47 \pm 0.20	0.10 \pm 0.15	9.43 \pm 0.02	0.85 \pm 0.32
1.8	0.24 \pm 0.16	8.54 \pm 0.41	0.06 \pm 0.02	0.03 \pm 0.01	0.62 \pm 0.24	0.13 \pm 0.18	9.63 \pm 0.42	1.06 \pm 0.01
3.8	0.88 \pm 0.17	7.89 \pm 0.40	0.24 \pm 0.25	0.04 \pm 0.00	0.67 \pm 0.16	0.13 \pm 0.13	9.84 \pm 0.28	1.58 \pm 0.24
4.9	1.13 \pm 0.36	7.28 \pm 0.19	0.32 \pm 0.04	0.10 \pm 0.10	0.91 \pm 0.32	0.07 \pm 0.09	9.82 \pm 0.19	3.22 \pm 0.90
5.9	1.72 \pm 0.10	6.42 \pm 0.34	0.76 \pm 0.22	0.04 \pm 0.005	0.71 \pm 0.03	0.03 \pm 0.03	9.68 \pm 0.36	6.68 \pm 0.48
7.8	1.94 \pm 0.04	5.07 \pm 0.40	2.02 \pm 0.30	0.10 \pm 0.01	0.55 \pm 0.08	0.01 \pm 0.01	9.69 \pm 0.36	7.34 \pm 0.13
10.8	2.33 \pm 0.02	3.28 \pm 0.29	3.57 \pm 0.18	0.16 \pm 0.01	0.42 \pm 0.05	0.01 \pm 0.01	9.77 \pm 0.36	7.43 \pm 0.64
14.0	2.68 \pm 0.06	2.62 \pm 0.66	4.11 \pm 0.15	0.16 \pm 0.02	0.44 \pm 0.02	< 0.01	10.01 \pm 0.78	6.89 \pm 0.14
20.7	3.21 \pm 0.15	1.60 \pm 0.32	4.27 \pm 0.38	0.21 \pm 0.01	0.49 \pm 0.02	0.01 \pm 0.02	9.80 \pm 0.86	8.03 \pm 1.52
28.1	3.68 \pm 0.20	1.38 \pm 0.16	3.82 \pm 0.15	0.34 \pm 0.02	0.34 \pm 0.02	0.11 \pm 0.05	9.67 \pm 0.31	6.39 \pm 0.20
42.1	4.30 \pm 0.16	1.30 \pm 0.17	3.16 \pm 0.19	0.37 \pm 0.04	0.43 \pm 0.02	0.13 \pm 0.04	9.67 \pm 0.42	4.37 \pm 0.44

Table SI-3 (continued): Sulfur species during growth of MLMS-1 on 8.5 mM Arsenate + 7 mM Sulfide (refers to Figure 5).

	HS ⁻ , H ₂ S [mM]	S ₂ ²⁻ [mMeq]	S ₃ ²⁻ [mMeq]	S ₄ ²⁻ [mMeq]	S ₅ ²⁻ [mMeq]	S ₆ ²⁻ [mMeq]	S ₇ ²⁻ [mMeq]	S ₈ ²⁻ [mMeq]	Sum of Polysulfide [mMeq]	Sulfate [mM]	Thiosulfate [mMeq]	Sum of Sulfur (including ThioAs) [mM]
Sterilized abiotic control (refers to Figure 5a)												
0	7.5 ± 0.10	< 0.1	< 0.1	< 0.1	< 0.1	< 0.1	< 0.1	< 0.1	< 0.1	1.9 ± 0.1	0.09 ± 0.05	9.5 ± 0.2
2	8.1 ± 0.27	< 0.1	< 0.1	< 0.1	< 0.1	< 0.1	< 0.1	< 0.1	< 0.1	2.1 ± 0.1	0.08 ± 0.05	10.4 ± 0.3
4	7.7 ± 0.56	< 0.1	< 0.1	< 0.1	< 0.1	< 0.1	< 0.1	< 0.1	< 0.1	1.7 ± 0.3	0.11 ± 0.02	9.6 ± 0.3
5	8.2 ± 0.11	< 0.1	< 0.1	< 0.1	< 0.1	< 0.1	< 0.1	< 0.1	< 0.1	1.9 ± 0.1	0.06 ± 0.02	10.2 ± 0.1
6	8.0 ± 0.18	< 0.1	< 0.1	< 0.1	< 0.1	< 0.1	< 0.1	< 0.1	< 0.1	1.9 ± 0.2	0.12 ± 0.10	10.2 ± 0.2
8	8.0 ± 0.16	< 0.1	< 0.1	< 0.1	< 0.1	< 0.1	< 0.1	< 0.1	< 0.1	1.9 ± 0.2	0.09 ± 0.05	10.0 ± 0.2
11	n.d.	< 0.1	< 0.1	< 0.1	< 0.1	< 0.1	< 0.1	< 0.1	< 0.1	2.0 ± 0.1	0.13 ± 0.05	n.d.
14	7.8 ± 0.23	< 0.1	< 0.1	< 0.1	< 0.1	< 0.1	< 0.1	< 0.1	< 0.1	1.8 ± 0.2	0.14 ± 0.04	9.8 ± 1.1
21	8.1 ± 0.26	< 0.1	< 0.1	< 0.1	< 0.1	< 0.1	< 0.1	< 0.1	0.1 ± 0.05	1.9 ± 0.3	0.11 ± 0.08	10.4 ± 0.4
28	8.1 ± 0.11	0.1 ± 0.05	< 0.1	< 0.1	< 0.1	< 0.1	< 0.1	< 0.1	0.1 ± 0.04	2.3 ± 0.7	0.14 ± 0.05	10.8 ± 0.8
36	n.d.	0.1 ± 0.02	< 0.1	< 0.1	< 0.1	< 0.1	< 0.1	< 0.1	0.1 ± 0.02	n.d.	n.d.	n.d.
42	7.9 ± 0.29	0.1 ± 0.02	< 0.1	< 0.1	< 0.1	< 0.1	< 0.1	< 0.1	0.1 ± 0.02	2.0 ± 0.5	0.14 ± 0.09	10.3 ± 0.8
Biotic experiment with MLMS-1 (refers to Figure 5b)												
0	6.8 ± 0.5	0.4 ± 0.1	< 0.1	< 0.1	< 0.1	< 0.1	< 0.1	< 0.1	0.5 ± 0.05	1.9 ± 0.2	0.07 ± 0.02	11.1 ± 0.7
2	7.2 ± 0.2	0.7 ± 0.04	< 0.1	< 0.1	< 0.1	< 0.1	< 0.1	< 0.1	0.8 ± 0.1	2.0 ± 0.2	0.05 ± 0.03	12.6 ± 0.5
4	6.4 ± 0.6	1.1 ± 0.2	0.2 ± 0.1	0.1 ± 0.1	< 0.1	< 0.1	< 0.1	< 0.1	1.5 ± 0.1	2.1 ± 0.2	0.07 ± 0.03	12.9 ± 0.9
5	5.4 ± 0.5	1.4 ± 0.3	0.4 ± 0.1	0.1 ± 0.1	< 0.1	< 0.1	< 0.1	< 0.1	2.0 ± 0.1	2.3 ± 0.1	0.09 ± 0.08	13.4 ± 1.0
6	4.5 ± 0.6	2.2 ± 0.2	0.4 ± 0.1	< 0.1	< 0.1	< 0.1	< 0.1	< 0.1	2.7 ± 0.2	2.4 ± 0.2	0.06 ± 0.004	12.7 ± 0.6
8	3.3 ± 0.5	3.1 ± 0.3	0.6 ± 0.1	0.1 ± 0.1	< 0.1	< 0.1	< 0.1	< 0.1	3.8 ± 0.1	2.4 ± 0.1	0.08 ± 0.02	13.4 ± 0.6
11	n.d.	3.3 ± 0.5	0.8 ± 0.03	< 0.1	< 0.1	< 0.1	< 0.1	< 0.1	4.2 ± 0.5	2.6 ± 0.2	0.05 ± 0.01	n.d.
14	1.0 ± 0.3	3.3 ± 0.4	0.8 ± 0.1	0.2 ± 0.01	< 0.1	< 0.1	< 0.1	< 0.1	4.3 ± 0.5	2.9 ± 0.3	0.13 ± 0.01	14.0 ± 0.9
21	0.8 ± 0.1	3.0 ± 0.4	0.6 ± 0.5	0.2 ± 0.04	< 0.1	< 0.1	< 0.1	< 0.1	3.8 ± 0.8	2.9 ± 0.2	0.10 ± 0.07	13.8 ± 0.7
28	0.7 ± 0.3	2.9 ± 0.4	1.3 ± 0.1	0.4 ± 0.1	< 0.1	< 0.1	< 0.1	< 0.1	4.6 ± 0.4	2.5 ± 0.2	0.03 ± 0.001	13.8 ± 1.0
36	n.d.	3.5 ± 0.4	1.1 ± 0.1	0.3 ± 0.1	< 0.1	< 0.1	< 0.1	< 0.1	4.9 ± 0.4	n.d.	n.d.	n.d.
42	0.7 ± 0.2	3.6 ± 0.4	1.1 ± 0.1	0.3 ± 0.1	< 0.1	< 0.1	< 0.1	< 0.1	5.0 ± 0.3	3.0 ± 0.2	0.11 ± 0.08	14.5 ± 0.5

Table SI-4 As and As-S species during growth of MLMS-1 on 7.6 mM Monothioarsenate + 4 mM Sulfide (refers to Figure 6).

Time [d]	Arsenite [mM]	Arsenate [mM]	Monothioarsenate [mM]	Dithioarsenate [mM]	Trithioarsenate [mM]	Tetrathioarsenate [mM]	Sum of As [mM]	MLMS-1 [$\times 10^6$ cells/mL]
Sterilized abiotic control (refers to Figure 6a)								
0.0	0.12 \pm 0.08	0.72 \pm 0.40	7.70 \pm 0.42	0.05 \pm 0.01	0.26 \pm 0.14	0.15 \pm 0.11	9.01 \pm 0.53	abiotic control
1.8	0.06 \pm 0.04	0.50 \pm 0.07	7.92 \pm 0.77	0.03 \pm 0.01	0.26 \pm 0.16	0.08 \pm 0.08	8.85 \pm 0.97	abiotic control
3.8	0.14 \pm 0.05	0.52 \pm 0.04	7.62 \pm 0.55	0.05 \pm 0.01	0.37 \pm 0.12	0.08 \pm 0.11	8.78 \pm 0.61	abiotic control
4.9	0.07 \pm 0.02	0.52 \pm 0.04	8.06 \pm 0.83	0.03 \pm 0.01	0.43 \pm 0.14	0.04 \pm 0.06	9.15 \pm 0.88	abiotic control
5.9	0.08 \pm 0.02	0.56 \pm 0.11	7.92 \pm 0.35	0.04 \pm 0.002	0.36 \pm 0.07	0.03 \pm 0.02	8.98 \pm 0.33	abiotic control
7.8	0.16 \pm 0.03	0.51 \pm 0.04	7.58 \pm 0.40	0.04 \pm 0.004	0.60 \pm 0.06	0.02 \pm 0.02	8.93 \pm 0.36	abiotic control
10.8	0.22 \pm 0.26	1.21 \pm 1.07	7.78 \pm 0.34	0.06 \pm 0.01	0.43 \pm 0.15	0.05 \pm 0.09	9.75 \pm 1.45	abiotic control
14.0	0.12 \pm 0.05	0.49 \pm 0.04	7.69 \pm 0.44	0.06 \pm 0.01	0.47 \pm 0.05	0.03 \pm 0.06	8.87 \pm 0.50	abiotic control
20.7	0.09 \pm 0.03	0.69 \pm 0.39	7.74 \pm 0.43	0.04 \pm 0.01	0.44 \pm 0.04	0.01 \pm 0.02	9.02 \pm 0.88	abiotic control
28.1	0.30 \pm 0.04	0.52 \pm 0.04	7.21 \pm 0.46	0.04 \pm 0.002	0.54 \pm 0.04	0.02 \pm 0.004	8.63 \pm 0.47	abiotic control
42.1	0.43 \pm 0.08	0.53 \pm 0.03	7.10 \pm 0.39	0.06 \pm 0.01	0.59 \pm 0.04	0.05 \pm 0.01	8.77 \pm 0.39	abiotic control
Biotic experiment with MLMS-1 (refers to Figure 6b)								
0.0	0.43 \pm 0.15	0.55 \pm 0.04	7.6 \pm 0.5	0.06 \pm 0.02	0.59 \pm 0.20	0.26 \pm 0.33	9.47 \pm 0.62	1.04 \pm 0.17
1.8	0.57 \pm 0.00	0.33 \pm 0.02	7.7 \pm 0.5	0.05 \pm 0.01	0.64 \pm 0.32	0.17 \pm 0.24	9.47 \pm 0.58	1.21 \pm 0.09
3.8	0.97 \pm 0.10	0.23 \pm 0.08	7.4 \pm 0.5	0.11 \pm 0.03	0.68 \pm 0.24	0.12 \pm 0.19	9.52 \pm 0.69	2.49 \pm 0.09
4.9	1.20 \pm 0.16	0.23 \pm 0.03	7.2 \pm 0.5	0.16 \pm 0.03	0.65 \pm 0.14	0.05 \pm 0.06	9.52 \pm 0.76	4.00 \pm 0.46
5.9	1.45 \pm 0.06	0.37 \pm 0.07	6.9 \pm 0.4	0.28 \pm 0.08	0.60 \pm 0.24	0.02 \pm 0.02	9.65 \pm 0.52	6.97 \pm 0.59
7.8	1.74 \pm 0.15	0.50 \pm 0.05	6.1 \pm 0.3	0.37 \pm 0.03	0.89 \pm 0.06	0.02 \pm 0.03	9.67 \pm 0.61	8.80 \pm 0.72
10.8	2.15 \pm 0.23	0.68 \pm 0.08	5.2 \pm 0.5	0.52 \pm 0.08	0.94 \pm 0.06	0.01 \pm 0.01	9.52 \pm 0.90	8.59 \pm 0.44
14.0	2.55 \pm 0.16	0.77 \pm 0.06	4.7 \pm 0.3	0.65 \pm 0.06	1.07 \pm 0.05	< 0.01	9.75 \pm 0.58	7.40 \pm 0.14
20.7	3.10 \pm 0.19	0.80 \pm 0.05	3.8 \pm 0.2	0.81 \pm 0.08	1.24 \pm 0.16	0.07 \pm 0.11	9.80 \pm 0.49	6.80 \pm 0.38
28.1	3.79 \pm 0.16	0.78 \pm 0.07	3.0 \pm 0.1	0.81 \pm 0.01	0.89 \pm 0.07	0.12 \pm 0.04	9.40 \pm 0.17	7.13 \pm 0.32
42.1	4.26 \pm 0.16	0.69 \pm 0.06	2.0 \pm 0.1	0.89 \pm 0.02	1.14 \pm 0.11	0.18 \pm 0.03	9.18 \pm 0.30	6.02 \pm 0.46

Table SI-4 (continued): S species during growth of MLMS-1 on 7.6 mM Monothioarsenate + 4 mM Sulfide (refers to Figure 6).

	HS ⁻ , H ₂ S [mM]	S ₂ ²⁻ [mMeq]	S ₃ ²⁻ [mMeq]	S ₄ ²⁻ [mMeq]	S ₅ ²⁻ [mMeq]	S ₆ ²⁻ [mM eq]	S ₇ ²⁻ [mM eq]	S ₈ ²⁻ [mM eq]	Sum of Polysulfide [mMeq]	Sulfate [mM]	Thiosulfate [mMeq]	Sum of Sulfur (including ThioAs) [mM]
Sterilized abiotic control (refers to Figure 6a)												
0	4.6 ± 0.04	1.3 ± 0.1	0.7 ± 0.3	0.2 ± 0.1	< 0.1	< 0.1	< 0.1	< 0.1	2.2 ± 0.5	1.7 ± 0.03	0.09 ± 0.07	17.8 ± 0.9
2	4.7 ± 0.2	2.5 ± 0.3	0.8 ± 0.3	0.3 ± 0.2	< 0.1	< 0.1	< 0.1	< 0.1	3.7 ± 0.9	1.7 ± 0.1	0.06 ± 0.04	19.2 ± 1.6
4	4.7 ± 0.1	2.7 ± 0.3	0.9 ± 0.2	0.3 ± 0.1	< 0.1	< 0.1	< 0.1	< 0.1	3.9 ± 0.6	1.6 ± 0.1	0.15 ± 0.10	19.5 ± 0.2
5	4.6 ± 0.1	2.5 ± 0.2	0.7 ± 0.2	0.2 ± 0.1	< 0.1	< 0.1	< 0.1	< 0.1	3.3 ± 0.4	1.7 ± 0.2	0.08 ± 0.01	19.3 ± 1.3
6	4.3 ± 0.2	2.6 ± 0.6	0.9 ± 0.5	0.3 ± 0.2	< 0.1	< 0.1	< 0.1	< 0.1	3.9 ± 1.4	1.7 ± 0.2	0.06 ± 0.005	19.1 ± 1.4
8	4.4 ± 0.02	2.8 ± 0.4	0.8 ± 0.3	0.2 ± 0.1	< 0.1	< 0.1	< 0.1	< 0.1	3.7 ± 0.8	1.7 ± 0.2	0.05 ± 0.01	n.d.
11	n.d.	2.7 ± 0.1	0.9 ± 0.1	0.2 ± 0.04	< 0.1	< 0.1	< 0.1	< 0.1	3.8 ± 0.3	1.7 ± 0.1	0.69 ± 1.03	n.d.
14	4.2 ± 0.03	2.7 ± 0.1	1.2 ± 0.2	0.3 ± 0.1	< 0.1	< 0.1	< 0.1	< 0.1	4.2 ± 0.5	1.7 ± 0.1	0.10 ± 0.06	19.6 ± 1.0
21	4.3 ± 0.1	3.6 ± 0.2	1.2 ± 0.2	0.5 ± 0.2	0.1 ± 0.1	< 0.1	< 0.1	< 0.1	5.4 ± 0.4	1.8 ± 0.1	0.07 ± 0.03	20.8 ± 0.6
28	4.0 ± 0.1	3.8 ± 0.4	1.7 ± 0.1	0.6 ± 0.1	< 0.1	< 0.1	< 0.1	< 0.1	6.2 ± 0.4	2.2 ± 0.6	0.11 ± 0.04	21.4 ± 0.6
36	n.d.	4.1 ± 0.2	1.4 ± 0.1	0.4 ± 0.03	< 0.1	< 0.1	< 0.1	< 0.1	6.0 ± 0.3	n.d.	n.d.	n.d.
42	3.6 ± 0.1	5.2 ± 0.1	1.6 ± 0.2	0.5 ± 0.1	< 0.1	< 0.1	< 0.1	< 0.1	7.4 ± 0.3	2.2 ± 0.2	0.17 ± 0.04	22.5 ± 0.7
Biotic experiment with MLMS-1 (refers to Figure 6b)												
0	3.6 ± 0.3	1.9 ± 0.1	0.4 ± 0.1	< 0.1	< 0.1	< 0.1	< 0.1	< 0.1	2.3 ± 0.1	1.7 ± 0.2	0.07 ± 0.04	18.2 ± 0.9
2	4.1 ± 0.2	4.8 ± 0.3	0.8 ± 0.3	0.2 ± 0.1	< 0.1	< 0.1	< 0.1	< 0.1	5.8 ± 0.7	1.9 ± 0.1	0.05 ± 0.02	22.3 ± 0.8
4	3.6 ± 0.1	5.6 ± 0.8	0.9 ± 0.3	0.2 ± 0.1	< 0.1	< 0.1	< 0.1	< 0.1	6.8 ± 1.1	2.0 ± 0.1	0.10 ± 0.07	22.7 ± 1.1
5	3.1 ± 0.3	4.9 ± 0.8	0.8 ± 0.5	0.2 ± 0.1	< 0.1	< 0.1	< 0.1	< 0.1	5.9 ± 1.4	2.1 ± 0.1	0.07 ± 0.04	20.9 ± 1.3
6	3.2 ± 0.2	6.2 ± 0.2	1.1 ± 0.1	0.2 ± 0.04	< 0.1	< 0.1	< 0.1	< 0.1	7.5 ± 0.3	2.2 ± 0.05	0.10 ± 0.04	21.7 ± 1.8
8	3.1 ± 0.1	7.0 ± 0.2	1.3 ± 0.2	0.3 ± 0.1	< 0.1	< 0.1	< 0.1	< 0.1	8.6 ± 0.4	2.4 ± 0.1	0.08 ± 0.01	23.8 ± 0.2
11	n.d.	7.3 ± 0.4	1.4 ± 0.1	0.3 ± 0.1	< 0.1	< 0.1	< 0.1	< 0.1	9.0 ± 0.6	2.6 ± 0.1	0.05 ± 0.02	n.d.
14	2.7 ± 0.1	7.1 ± 0.3	1.6 ± 0.1	0.4 ± 0.1	< 0.1	< 0.1	< 0.1	< 0.1	9.2 ± 0.3	2.8 ± 0.2	0.13 ± 0.05	24.1 ± 0.5
21	2.8 ± 0.3	7.3 ± 0.1	1.4 ± 0.1	0.3 ± 0.03	< 0.1	< 0.1	< 0.1	< 0.1	9.0 ± 0.1	2.9 ± 0.3	0.07 ± 0.03	24.3 ± 0.4
28	2.5 ± 0.1	5.8 ± 0.1	1.4 ± 0.1	0.4 ± 0.1	< 0.1	< 0.1	< 0.1	< 0.1	7.7 ± 0.1	2.9 ± 0.5	0.18 ± 0.09	21.0 ± 0.6
36	n.d.	6.3 ± 1.0	1.4 ± 0.1	0.4 ± 0.1	< 0.1	< 0.1	< 0.1	< 0.1	8.1 ± 0.7	n.d.	n.d.	n.d.
42	2.3 ± 0.2	5.7 ± 0.1	1.3 ± 0.01	0.3 ± 0.02	< 0.1	< 0.1	< 0.1	< 0.1	7.4 ± 0.2	2.8 ± 0.2	0.10 ± 0.07	20.4 ± 0.9

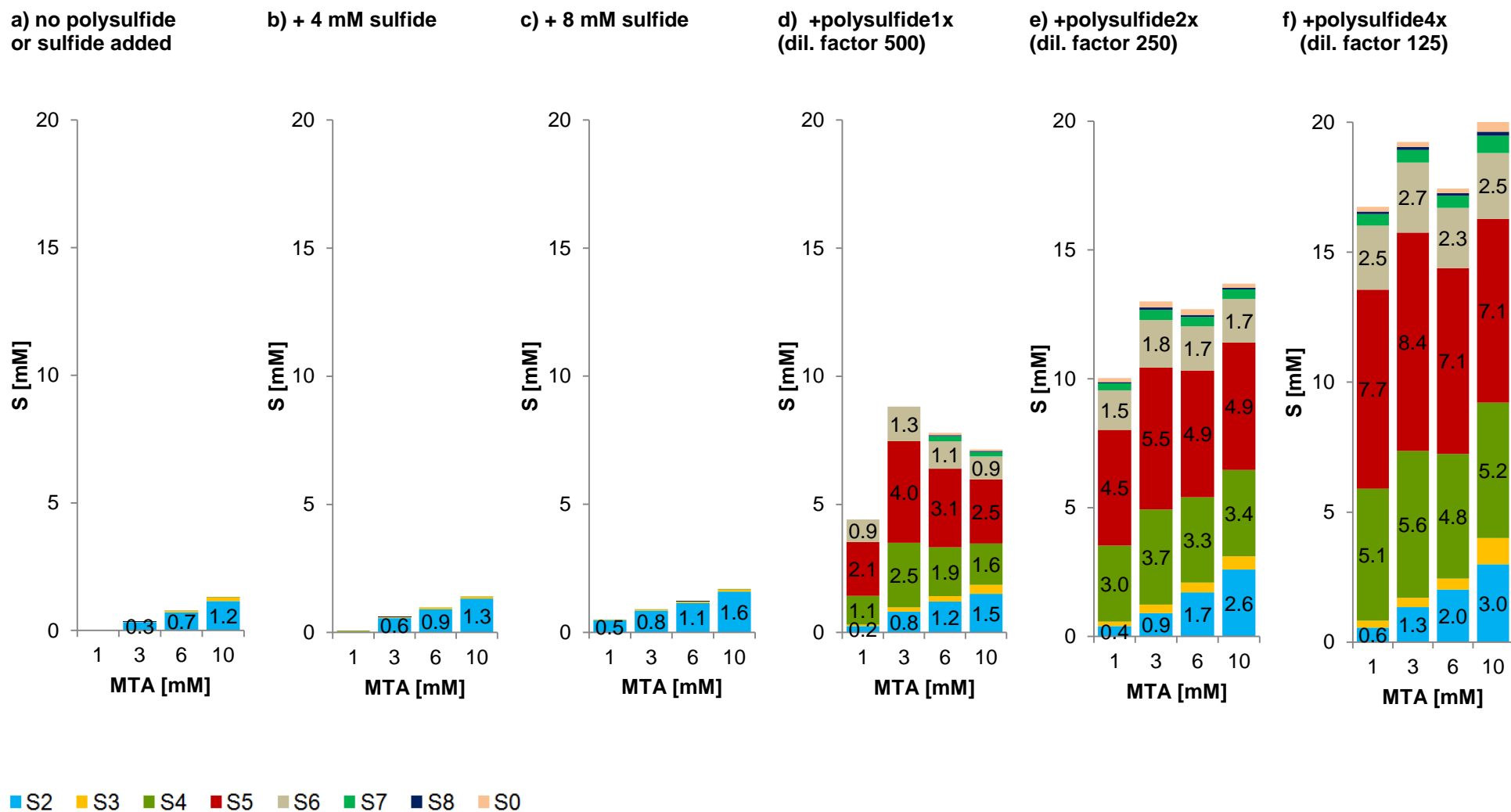


Figure SI-1 Comparison of results of polysulfide measurements in ML-medium having 1, 3, 6, and 10 mM monothioarsenate (MTA). Individual graphs display a) ML-medium without sulfide or polysulfide; ML-medium plus sulfide b) 4 mM and c) 8 mM; ML-medium plus polysulfide stock solution d) 1x = 500x diluted stock; e) 2x = 250x diluted stock; f) 4x = 125x diluted stock. The corresponding polysulfide stock solution was prepared by adding 0.5 M sulfide plus 5 M elemental sulfur and was filtered prior to its dilution; the percentage of disulfide codetermination with monothioarsenate was calculated from these data (excluding the 1 mM data because they were often below detection limit) to be 10-26%.

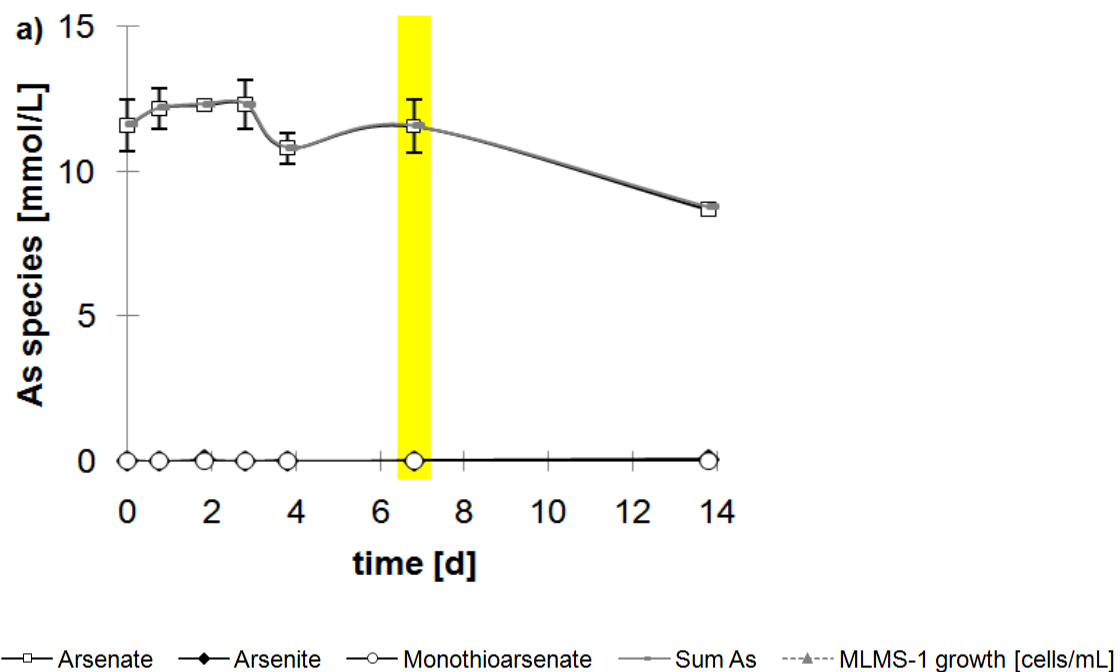


Figure SI-2 Abiotic control experiment applying 12.5 mM arsenate and 5 mM sulfide, referring to the biotic experiment with *MLMS-1* in Figure 1 in the manuscript. Displayed are results of As-S species analyses by IC-ICP-MS (n=3). Sample d7, highlighted by yellow color, was investigated by XAS in this study, referring to data in Figure 2 of the manuscript.

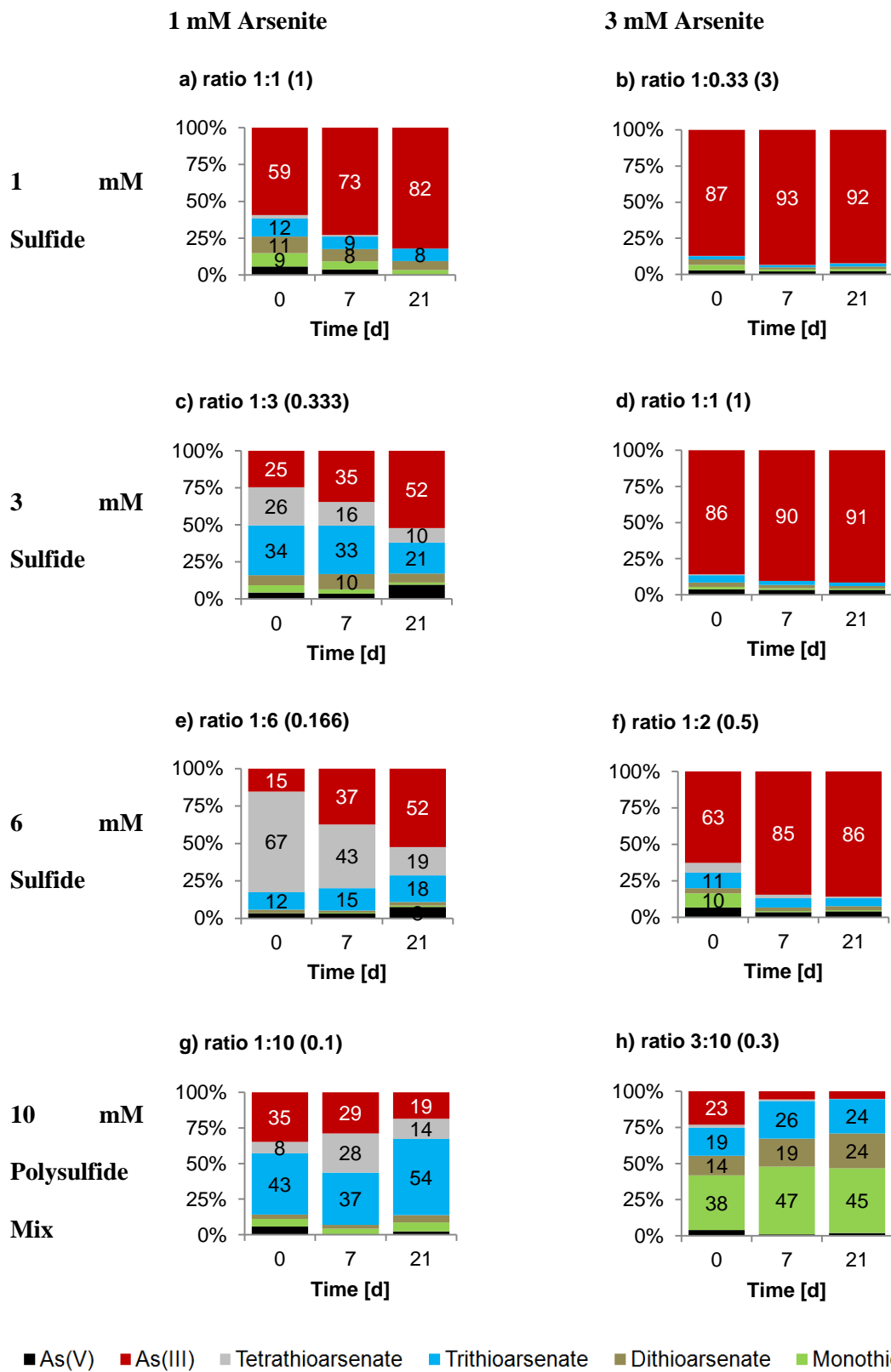
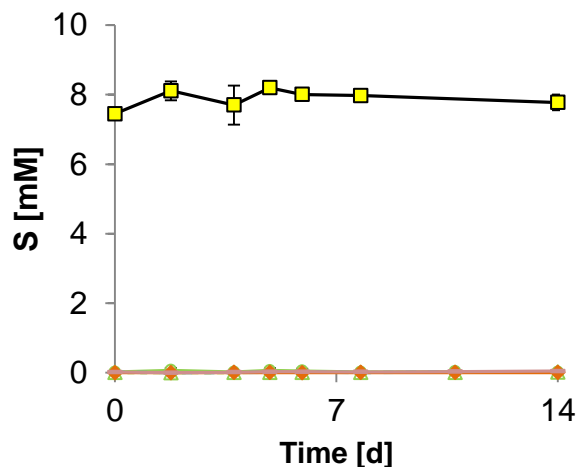
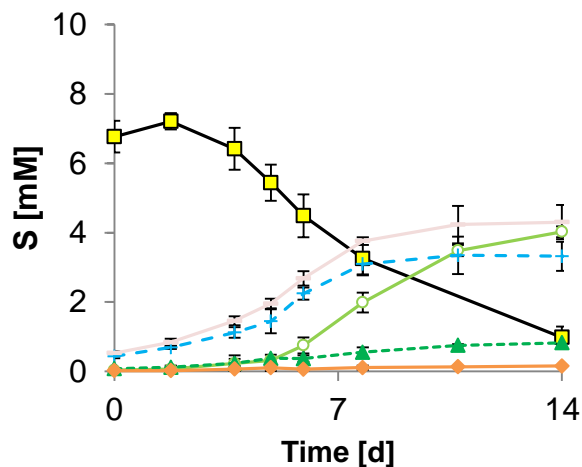


Figure SI-3 Experiments in sterilized, anaerobic ML-Medium, applying different concentrations of arsenite vs sulfide or a polysulfide mix, measured by IC-ICP-MS. Single species were normalized relative [%] to the sum of As-species.

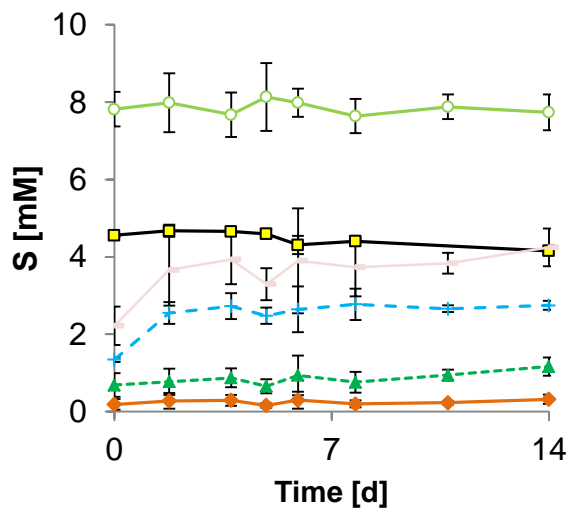
(a) Abiotic Sulfide + Arsenate



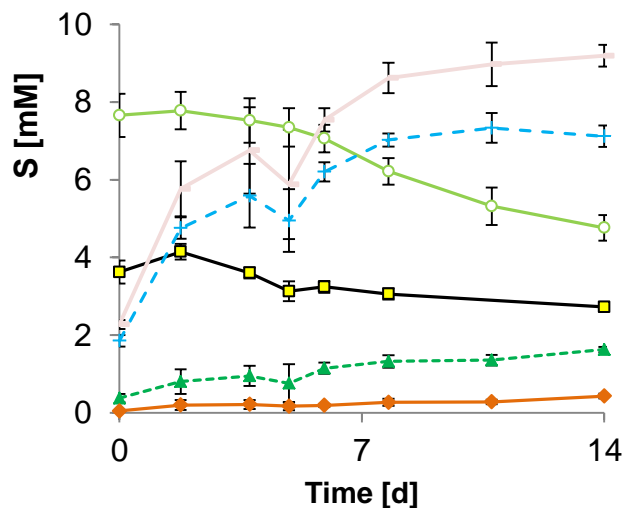
(b) Biotic Sulfide + Arsenate



(c) Abiotic Sulfide + Monothioarsenate



(d) Biotic Sulfide + Monothioarsenate



—■— sulfide —○— monothioarsenate -+-+ polysulfide S2
- -▲- polysulfide S3 —◆— polysulfide S4 — — sum of polysulfides

Figure SI-4 Comparison of the detected polysulfide species S_2^{2-} , S_3^{2-} and S_4^{2-} and the sum of polysulfides with measured concentrations of monothioarsenate and sulfide in biotic (b, d) and abiotic (a, c) experiments with 10 mM arsenate plus nominally 10 mM sulfide (a, b) and with 10 mM monothioarsenate plus 5 mM sulfide (c, d), respectively. Higher polysulfide-sum concentrations than initial monothioarsenate concentrations (d) could indicate that the measured concentrations for polysulfide-species are over-estimated. This is a known problem during HPLC-polysulfide-speciation, especially regarding S_2 (and S_3), since the UV-detector is not so sensitive towards these species and may also result in relatively high standard deviations between multiple measurements (Reference: Kamysny, A.; Goifman, A.; Gun, J.; Rizkov, D.; Lev, O. Equilibrium Distribution of Polysulfide Ions in Aqueous Solutions at 25 °C: A New Approach for the Study of Polysulfides' Equilibria. *Environ. Sci. Technol.* **2004**, 38 (24), 6633–6644).

Study 5

Chemolithotrophic growth of the aerobic hyperthermophilic bacterium *Thermocrinis ruber* OC 14/7/2 on monothioarsenate and arsenite

Cornelia Härtig, Regina Lohmayer, Steffen Kolb, Marcus A. Horn, William P. Inskeep,
Britta Planer-Friedrich

FEMS Microbiology Ecology, 2014, 90, pp 747-760

Copyright 2014 Federation of European Microbiological Societies

This is a pre-copy-editing, author-produced PDF of an article accepted for publication in FEMS Microbiology Ecology following peer review. The definitive publisher-authenticated version is available online at:

<http://femsec.oxfordjournals.org/content/90/3/747>

Chemolithotrophic Growth of the Aerobic Hyperthermophilic Bacterium *Thermocrinis ruber* OC 14/7/2 on Monothioarsenate and Arsenite

Cornelia Härtig¹, Regina Lohmayer¹, Steffen Kolb², Marcus A. Horn², William P. Inskeep³, Britta Planer-Friedrich*¹

¹Department of Environmental Geochemistry, Bayreuth Center for Ecology and Environmental Research (BayCEER), University of Bayreuth, Universitätsstraße 30, 95447 Bayreuth, Germany

²Department of Ecological Microbiology, Bayreuth Center for Ecology and Environmental Research (BayCEER), University of Bayreuth, Dr. Hans-Frisch-Strasse 1-3, 95440 Bayreuth, Germany

³Department of Land Resources and Environmental Sciences and Thermal Biology Institute (TBI), 805 Leon-Johnson Hall, Montana State University, Bozeman, MT 59717, USA

Abstract Novel insights are provided regarding aerobic chemolithotrophic growth of *Thermocrinis ruber* OC14/7/2 on the electron donors arsenite and monothioarsenate. *T. ruber* is a hyperthermophilic bacterium that thrives in pH-neutral to alkaline hot springs and grows on hydrogen, elemental sulfur, and thiosulfate. Our study showed that *T. ruber* can also utilize arsenite as sole electron donor producing arsenate. Growth rates of 0.024 h⁻¹ were lower than for oxidation of thiosulfate to sulfate ($\mu=0.247$ h⁻¹). Fast growth was observed on monothioarsenate ($\mu=0.359$ h⁻¹), comprising different abiotic and biotic redox interactions. The initial dominant process was abiotic transformation of monothioarsenate to arsenate and elemental sulfur, followed by microbial oxidation of sulfur to sulfate. Elevated microbial activity during stationary growth of *T. ruber* might be explained by microbial oxidation of thiosulfate and arsenite, both also products of abiotic monothioarsenate transformation. However, the observed rapid decrease of monothioarsenate, exceeding concentrations in equilibrium with its products, also indicates direct microbial oxidation of arsenic-bond S(-II) to sulfate. Free sulfide was oxidized abiotically too fast to play a role as electron donor for *T. ruber*. Our present laboratory and previous field studies suggest that thioarsenates can either indirectly or directly be used by (hyper)thermophiles in arsenic-sulfidic environments.

Introduction

The high affinity of arsenic and sulfur has been known for over a century to lead to formation of thioarsenic species and their chemistry has been well studied (Brauner & Tomicek, 1888; McCay, 1902; McCay & Foster, 1904; Thilo *et al.*, 1970; Schwedt & Rieckhoff, 1996a, 1996b; Wilkin *et al.*, 2003; Stauder *et al.*, 2005; Wallschläger & Stadey, 2007; Planer-Friedrich *et al.*, 2009; Planer-Friedrich & Wallschläger, 2009; Suess *et al.*, 2009; Planer-Friedrich *et al.*, 2010). Recently, pentavalent thioarsenates have been shown to occur in different environments, e.g., hypersaline anoxic lake water (Hollibaugh *et al.*, 2005; Wallschläger & Stadey, 2007), reduced contaminated groundwater (Stauder *et al.*, 2005; Wallschläger & Stadey, 2007), polluted marina sediments (Mamindy-Pajany *et al.*, 2013), landfill leachate (Zhang *et al.*, 2014), and repeatedly in hydrothermal waters (Planer-Friedrich *et al.*, 2007; Planer-Friedrich *et al.*, 2009; Härtig & Planer-Friedrich, 2012; Ullrich *et al.*, 2013). Yet, little is known about the fate of thioarsenates in the environment, especially about the role of microorganisms in thioarsenate transformation.

Our previous research has focused on thioarsenate transformation in hot springs of Yellowstone National Park (YNP), USA. Trithioarsenate ($\text{HAs}^{\text{V}}\text{OS}_3^{2-}$) has been identified as the dominant arsenic species at the sources of several alkaline-sulfidic hot springs (Planer-Friedrich *et al.*, 2007). However, along their drainage channels, trithioarsenate is rapidly transformed to monothioarsenate ($\text{HAs}^{\text{V}}\text{O}_3\text{S}^{2-}$) and arsenite ($\text{H}_3\text{As}^{\text{III}}\text{O}_3$), followed by appearance of arsenate ($\text{HAs}^{\text{V}}\text{O}_4^{2-}$) as the final product (Planer-Friedrich *et al.*, 2009; Härtig & Planer-Friedrich, 2012). Hyperthermophilic microorganisms (specifically *Thermocrinis ruber*, a member of the *Aquificales* bacterial order) were hypothesized to catalyze these stepwise transformation processes of thioarsenates and arsenite (Planer-Friedrich *et al.*, 2009). On-site bio-assays (at 78°C) at one selected spring, called Conch-Spring, in the Lower Geyser Basin of Yellowstone National Park, using the native, pink-brownish microbial streamer communities (Härtig & Planer-Friedrich, 2012) showed biotic transformation of arsenite and monothioarsenate, in addition to transformation of sulfide and thiosulfate.

For trithioarsenate, differentiation between abiotic and biotic processes was more difficult, because it is already subject to rapid abiotic transformation to sulfide and arsenate. Consequently, it was difficult to differentiate whether the microbial community transformed trithioarsenate directly, or just accelerated abiotic trithioarsenate decomposition via microbial sulfide oxidation.

Thermocrinis ruber (strain OC 1/4) is a gram negative hyperthermophile, isolated from Octopus Spring (YNP), capable of microaerophilic chemotrophic growth on hydrogen and on reduced sulfur species like elemental sulfur or thiosulfate, as well as chemoorganoheterotrophic growth on formate and formamide (Huber *et al.*, 1998; Jahnke *et al.*, 2001). Optimal growth occurs at 80 °C, with growth being observed within the range 44 to 89 °C (Huber *et al.*, 1998). *T. ruber* grows at pH 7 and 8.5 (Huber *et al.*, 1998). *Thermocrinis* spp. probably fix inorganic carbon via the reductive tricarboxylic acid cycle (rTCA) (Jahnke *et al.*, 2001; Hügler *et al.*, 2007; Hall *et al.*, 2008; Takacs-Vesbach *et al.*, 2013).

Temporally resolved speciation data on how reduced sulfur species are transformed by *T. ruber* are lacking to date. It has been shown that the ancient sulfide:quinone reductase (SQR) (Theissen *et al.*, 2003) catalyzes the oxidation of sulfide to elemental sulfur (S^0) or polysulfides ($S_n^{2-} = [S_{n-1}^0 S^-]^{2-}$) (Cherney *et al.*, 2010; Takacs-Vesbach *et al.*, 2013). Genes encoding SQR were present *in-situ* in different *Aquificales* streamer populations (*Thermocrinis* spp., *Sulfurihydrogenibium* spp., *Hydrogenobaculum* spp. Takacs-Vesbach *et al.*, 2013) and activity of SQR is verified for *Aquifex aeolicus* (Nübel *et al.*, 2000; Marcia *et al.*, 2009). Though not confirmed for *T. ruber* to date, other *Aquificales* contain genes encoding parts of the Sox multienzyme complex (e.g. *Aquifex aeolicus* (Friedrich *et al.*, 2001; Meyer *et al.*, 2007; Dahl & Friedrich, 2008; Braakman *et al.*, 2014); *Sulfurihydrogenibium* spp. (Takacs-Vesbach *et al.*, 2013)). The Sox enzyme complex regulates oxidation of thiosulfate, sulfite, and sulfur (Friedrich *et al.*, 2001; Dahl & Friedrich, 2008). The Sox complex is widespread among sulfur-oxidizing *Bacteria* (Meyer *et al.*, 2007); respective Sox genes putatively derive from common ancestors of *Aquificae* and *Epsilonproteobacteria* (Ghosh & Dam, 2009; Ghosh *et al.*, 2009). Such findings suggest that the capability to utilize sulfide, thiosulfate, sulfite, and sulfur occurs among diverse members of the *Aquificales*. Though previous work has already demonstrated the importance of *in-situ* arsenite oxidation via *Thermocrinis*-like organisms in alkaline hot springs (Hamamura *et al.*, 2009;

Härtig & Planer-Friedrich, 2012), successful cultivation of a pure *Thermocrinis* culture on arsenite was not reported to date. Culture-based studies with other strains of *Aquificales* revealed that *Sulfurihydrogenibium azorense* and *S. subterraneum* are capable of utilization of arsenite as the sole electron donor (Takai *et al.*, 2003; Aguiar *et al.*, 2004), whereas *Venenivibrio stagnispumatis* tolerated up to 8 mM arsenite during growth on hydrogen (Hetzer *et al.*, 2008).

Evidence for microbial transformation of thioarsenates in pure culture by chemolithotrophs like *T. ruber* or their role as potential electron donors in prokaryotic chemolithotrophy as well as identification of potential transformation pathways is lacking to date despite the importance of *Thermocrinis*-like organisms for streamer communities in thioarsenate-dominated environments (Planer-Friedrich *et al.*, 2009). Thus, our objectives were to (I) investigate the utilization of a thioarsenate as electron donor for aerobic growth of *T. ruber*, (II) clarify the transformation pathways of the thioarsenate and (III) determine the growth potential of *T. ruber* on sulfur and arsenic species that form during abiotic thioarsenate transformation, namely sulfide, thiosulfate, and arsenite. We selected monothioarsenate due to its greater abiotic stability in comparison to higher thiolated thioarsenates to enhance chances for a better separation between biotic and abiotic reactions.

Materials and Methods

Strain and culture conditions

Thermocrinis ruber strain OC14/7/2 (DSM No. 23557, AJ005640), isolated from Octopus Spring, Yellowstone National Park, was obtained from the DSMZ (Huber *et al.*, 1998). Note that we did not use the other available isolate (OC1/4, DSM No. 12173), which was recently shown to have only little 16S rRNA gene similarity to the originally published *T. ruber* sequence (Wirth *et al.*, 2010). *T. ruber* OC14/7/2 was cultivated in liquid Octopus Spring (OS) medium (Huber *et al.*, 1998), supplemented with 10 mM TrisHCl (pH 7 or 8) as pH buffer (personal recommendation by Prof. R. Wirth, Institute for Microbiology, University of Regensburg). The OS medium (20 or 40 mL), gassed with N₂ for 45 min, was filled into glass septum bottles (120 mL, #102046, Glasgerätebau Ochs, Bovenden, Germany), and tightly closed with black butyl rubber stoppers (#102049, Glasgerätebau Ochs, Bovenden, Germany) in an anaerobic chamber. These bottles were gassed for 20 min with N₂, finally pressurized to 2.5 bar

(TensioCheck TC03S, #1701, Bambach GbR, Geisenheim, Germany). After autoclaving, the carbon source (NaHCO_3), the electron acceptor (oxygen), the different electron donors, and the inoculum were added to the medium. Either 3% (100 mL headspace, 20 mL OS medium) or 8% (80 mL headspace, 40 mL OS medium) of oxygen were applied. Experiments using thiosulfate ($\text{Na}_2\text{S}_2\text{O}_3 \times 5 \text{H}_2\text{O}$), monothioarsenate ($\text{Na}_3\text{AsSO}_3 \times 7 \text{H}_2\text{O}$, synthesized according to Schwedt & Rieckhoff, 1996a) or sulfide ($\text{Na}_2\text{S} \times 9 \text{H}_2\text{O}$) as the electron donors were performed with 40 mL OS media (pH 8). Experiments with arsenite (2 mM) were run with 20 mL OS-media at pH 7, because growth was more easily achieved than with pH 8 media. The concentration of the applied, freshly grown inoculum was 1% in all biotic experiments; except 2.5% in the arsenite experiment "Biotic I". The *T. ruber*-inoculated vs. abiotic triplicates were incubated (no shaking) at *T. ruber*'s optimum growth temperature of 80 °C (Huber *et al.*, 1998). Biotic control experiments without supplemental electron donors were carried out at pH 7 and pH 8 under otherwise similar conditions.

Sample collection

Syringes, firmly connected to a canula (both sterile), were used to draw samples from the incubation bottles, avoiding loss of the pressurized gas phase. Removed medium volumes were replaced by fresh sterile gas phase. All samples (except for cell counts) were filtered through 0.2 μm cellulose acetate filters (DIAFIL CA, #5123280D, DIA-Nielsen, Düren, Germany), removing bacteria and any potential colloids > 0.2 μm or precipitates.

Bacterial cell counts

The samples were stained with SYBRGold (#S-11494, Invitrogen; Noble & Fuhrman, 1998; Breitbart *et al.*, 2004; Wegley *et al.*, 2006). Growth was determined by direct counting, using a Neubauer Improved counting chamber (0.02 mm depth) and epifluorescent microscopy (400x magnification, Zeiss Axioplan).

Analytical Methods

Samples for As-S-speciation by anion exchange chromatography coupled to inductively-coupled plasma mass spectrometry (AEC-ICP-MS) were immediately flash-frozen in liquid nitrogen after sampling and filtration and were stored at -20 °C. Prior to analysis, samples were thawed in an anaerobic chamber (95% N_2 , 5% H_2) and diluted in N_2 -purged ultra-pure water (MQ). Thioarsenates, arsenite, arsenate, sulfate, and thiosulfate were

measured by AEC-ICP-MS (AEC Dionex ICS-3000 SP coupled to ICP-MS XSeries2, Thermo-Fisher) as published previously (Planer-Friedrich *et al.*, 2007). Standard solutions for calibrations were made from sodium arsenate dibasic heptahydrate ($\text{Na}_2\text{HAsO}_4 \cdot 7 \text{H}_2\text{O}$, Fluka #71625), sodium(meta)arsenite (NaAsO_2 , Fluka #71287), ammonium sulfate [$(\text{NH}_4)_2\text{SO}_4$, Fluka #09979] and sodium thiosulfate ($\text{Na}_2\text{S}_2\text{O}_3$, Aldrich #563188). The matrix for calibration standards was OS-medium, diluted in MQ according to the sample dilution. Quantification of thioarsenates was based upon the arsenate calibration curve.

Filtered samples were analyzed for sulfide using the methylene blue method (Cline, 1969), measuring the absorption after 2 hours of color development with a spectrophotometer (HACH Lange DR 3800) at 660 nm.

For analysis of polysulfides ($[\text{S}^0_{n-1}\text{S}^{-II}]^{2-}$), a 100 μL aliquot of 0.2 μm -filtered sample was added simultaneously with 15 μL methyl trifluoromethanesulfonate ($\text{CF}_3\text{SO}_3\text{CH}_3$, Sigma-Aldrich) to 800 μL methanol immediately after sampling. This derivatization according to (Kamysny *et al.*, 2006) transforms unstable polysulfides to stable dimethylpolysulfanes, which were then analyzed on a Merck Hitachi high-pressure liquid chromatography (HPLC) using a reversed phase C18 column (Waters-Spherisorb, ODS2, 5 μm , 250 x 4.6 mm) and gradient elution after (Rizkov *et al.*, 2004). Detection was done with a L-2420 UV-VIS detector at 230 nm wavelength.

Colloids larger than 0.2 μm filter-cutoff size or precipitates of elemental sulfur were not determined analytically. To get an estimate on their potential role for sulfur redox reactions during the experiments, the difference between initially applied sulfur concentration and sum of all other analytically determined sulfur species in solution was calculated. This delta value is referred to in the following as $\text{S}^0_{\text{calc}}(\text{s})$. Note that this calculated value is of course subject to larger variations because analytical uncertainties of all sulfur species sum up here.

The pH was measured with a PHC101 gel electrode connected to a HACH HQ40d digital multimeter. All pH measurements were carried out at room temperature.

All concentrations in the following are given in moles As or S or for polysulfides and thiosulfate in moles equivalent S, e.g. 8 mMeq of thiosulfate-S (4 mM $\text{Na}_2\text{S}_2\text{O}_3 \times 5 \text{H}_2\text{O}$) contain 4 mM S^{-1} plus 4 mM S^{+V} .

Results

Monothioarsenate

In the presence of *T. ruber*, monothioarsenate transformed completely (< 1%) within 2.6 days (Fig. 1A, S1, Table S1). Two phases can be differentiated: A slower decrease until day 0.8 with a transformation rate of 0.5 mM/day, followed by a steeper decrease with transformation of 1.6 mM/day until day 2.6. Polysulfides were observed from the beginning on in the experiment and decreased concurrently to monothioarsenate (Fig. 1G). They showed the same acceleration of transformation rate after day 0.8 (Fig. 1G). The dominant polysulfide species was tetrasulfide (Fig. S4). Arsenate (99%) was the major arsenic-containing product (Fig. 1C). Sulfate (89%, including 16% medium background) constituted the main sulfur product (Fig. 1F), besides 10% thiosulfate (Fig. 1E) after 6.6 d. The very first decrease of monothioarsenate until 0.4 days was not accompanied by a corresponding increase of any measured sulfur species (Fig. 1, Table S1). On the contrary, both sulfide (Fig. S3A) and polysulfide (Fig. 1G, S4) concentrations in solution decreased, too, and left a deficit in the

sulfur mass balance, which we attribute to $S^0_{\text{calc}}(s)$ (Fig. 1H). The biotic $S^0_{\text{calc}}(s)$ curve showed large variations with a maximum of 1.5 mM after 1.9 days. At the end of the experiment (11.7 d, Table S1), almost all the sulfur was recovered in measurable dissolved sulfur species again ($S^0_{\text{calc}}(s) = 0.4$ mM; Fig. S1). Maximum concentrations of arsenite (< 0.3 mM) were comparatively low with less than 7% of the total As after 1.4 days (Fig. 1B). *T. ruber* grew up with an exponential growth rate of 0.359 h^{-1} (1.9 h generation time) during day 0.3 to 0.8 (Fig. 1D). The cell numbers after exponential growth were $(2.52 \pm 0.56) \times 10^7$ cells/mL at day 0.8 (Table S1). The cell numbers further increased to $(3.71 \pm 0.38) \times 10^7$ cells/mL between 0.8 to 2.6 d, which indicates an elevated microbial activity of *T. ruber* at this time and concurred with the observed steeper decrease of monothioarsenate transformation (Fig. 1A). No growth was observed in pure OS medium controls, without any donor (Fig. S5).

In the abiotic experiments, monothioarsenate was transformed, too, but transformation was slower, incomplete, and a different dominant sulfur product was measured (Fig. 1, Table S1). The initial

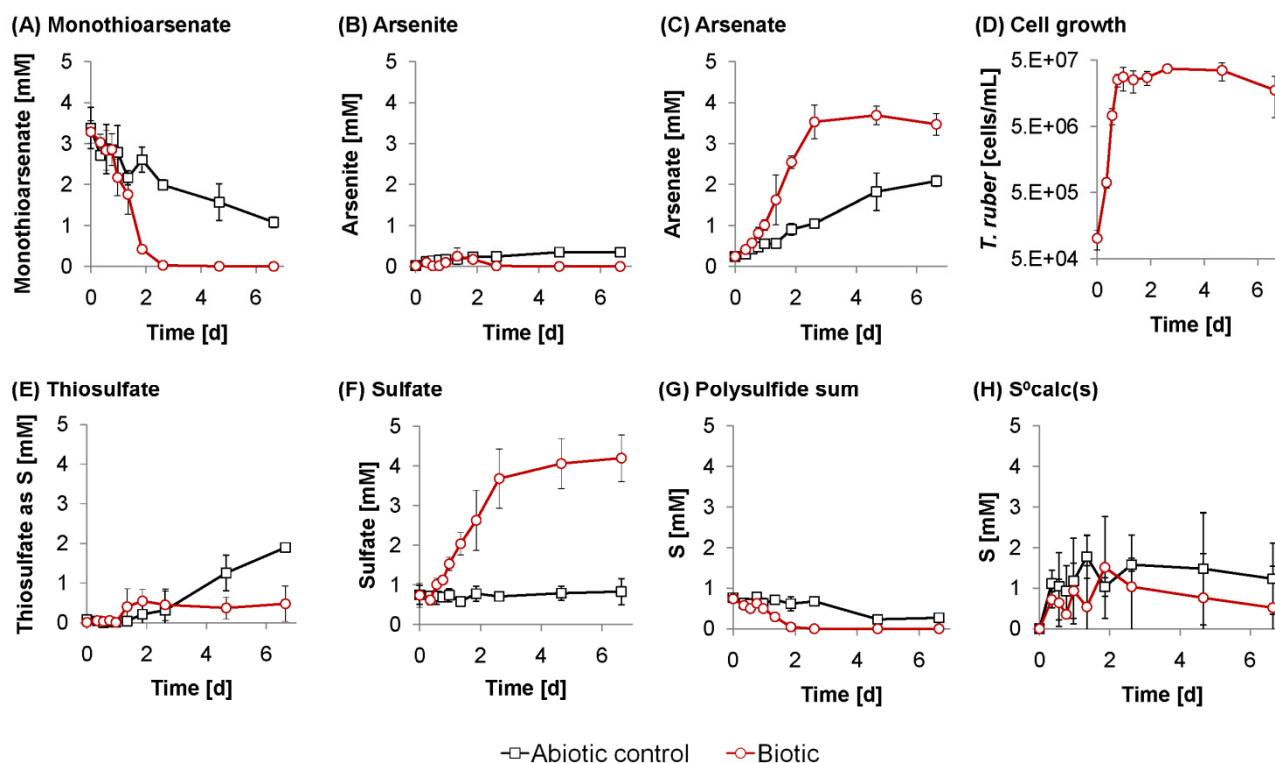


Fig. 1: Oxidation of monothioarsenate ($\text{Na}_3\text{As}^{\text{V}}\text{SO}_3 \times 7 \text{H}_2\text{O}$) during growth of *T. ruber* with 8% O_2 in the gas phase in a medium of pH 8. The biotic set-ups received 1% of a *T. ruber* pre-culture actively growing on monothioarsenate as inoculum. Graphs show average concentrations \pm standard deviation ($n=3$), displayed by error bars (Table S1). For better visibility, only results up to day 6.6 are displayed, all data including those of day 11.7 can be found in Table S1, as a compilation of all species data and time steps in one diagram in Fig. S1 or as summary of species production with reference to day 0 in Fig. S2.

decreases in monothioarsenate (Fig. 1A), sulfide (Fig. S3A), and polysulfides (Fig. 1G) were comparable to those in the biotic experiments. Concentrations of elemental sulfur ($S^0_{\text{calc}}(s)$) increased to a maximum of 1.8 mM (1.4 d). After 6.6 days, 30% of initial arsenic remained as monothioarsenate (Fig. 1A), while 59% arsenate (Fig. 1C) plus 10% arsenite (Fig. 1B) had formed. The main sulfur product was thiosulfate (46% after 6.6 days; Fig. 1E), while sulfate showed only a slight increase towards the end of the experiment (< 2%; Fig. 1F). At the end of the abiotic experiment (11.7 d, Table S1, Fig. S1), the deficit in the sulfur balance was higher ($S^0_{\text{calc}}(s) = 1.0$ mM) than in the biotic experiment ($S^0_{\text{calc}}(s) = 0.4$ mM). The pH in the abiotic control was 8.32 ± 0.04 , while in biotic essays it was distinctly lower (7.57 ± 0.05).

Arsenite

In the presence of 2 mM arsenite and 3% oxygen *T. ruber* grew reproducibly at pH 7 (Fig. 2, Table S2). Experiments using 4 mM arsenite under otherwise similar conditions did not support growth. Occasionally, growth was observed at pH 8 plus 2 mM arsenite (data not shown). No growth was observed at pH 9 (data not shown). Results of three

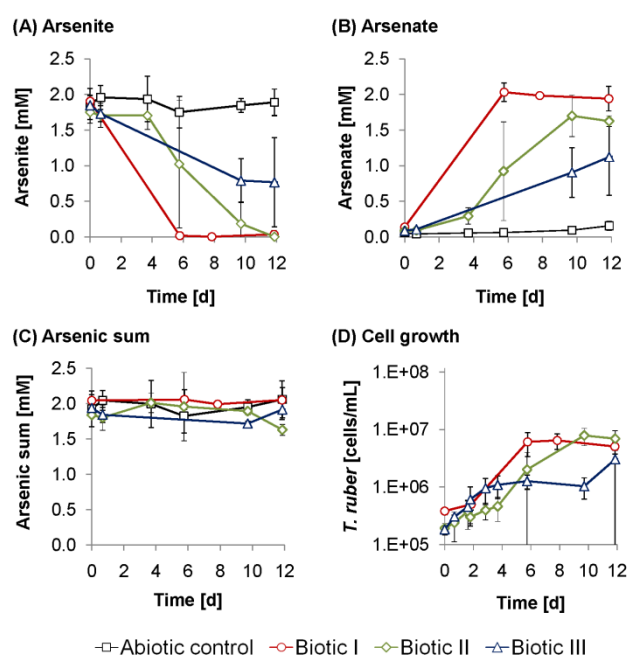


Fig. 2: Oxidation of arsenite ($\text{NaAs}^{\text{III}}\text{O}_2$) during growth of *T. ruber* with 3% O_2 (v/v) in the gas phase in a medium of pH 7. One abiotic and three different biotic experiments (Biotic I-III) are displayed. The biotic set-ups were inoculated with a *T. ruber* pre-culture actively growing on arsenite. Biotic I and II/III received 2.5% and 1% inoculum, respectively. Graphs show average concentrations \pm standard deviation ($n=3$), displayed by error bars (Table S2).

triplicate experiments (Biotic I-III) versus abiotic controls at pH 7 confirmed the biotic conversion of arsenite to arsenate (Fig. 2, Table S2). Under abiotic conditions, arsenite remained stable for up to 12 days at 1.8 ± 0.1 mM (Fig. 2A). No substantial loss of total arsenic was observed during abiotic or biotic experiments (Fig. 2C). The microbial arsenite oxidation rates developed slightly different over time, corresponding to the increase in cell numbers in the three individual experiments (Biotic I-III, Table S2). The fastest arsenite oxidation rate was achieved by $(0.79 \pm 0.35) \times 10^7$ cells mL^{-1} within 5.8 days, producing 2.03 ± 0.13 mM arsenate (Biotic I, Table S2). From the exponential slopes of the three individual experiments, an average growth rate of 0.024 ± 0.003 h^{-1} and an average generation time of 29.0 ± 4.3 h were calculated. Biotic experiments revealed a lower final pH (7.64 ± 0.03) than abiotic controls (7.86 ± 0.04).

Thiosulfate

Thermocrinis ruber grew well in the presence of thiosulfate at pH 7 and pH 8, but not at pH 9 (data not shown). Thiosulfate was completely oxidized within 2.6 days (pH 8, Fig. 3A). No changes in sulfur species were detected in abiotic thiosulfate controls at 80 °C over 6.6 days (Fig. 3A, Table S3). Initial thiosulfate concentrations of 8.3 ± 1.5 mEq

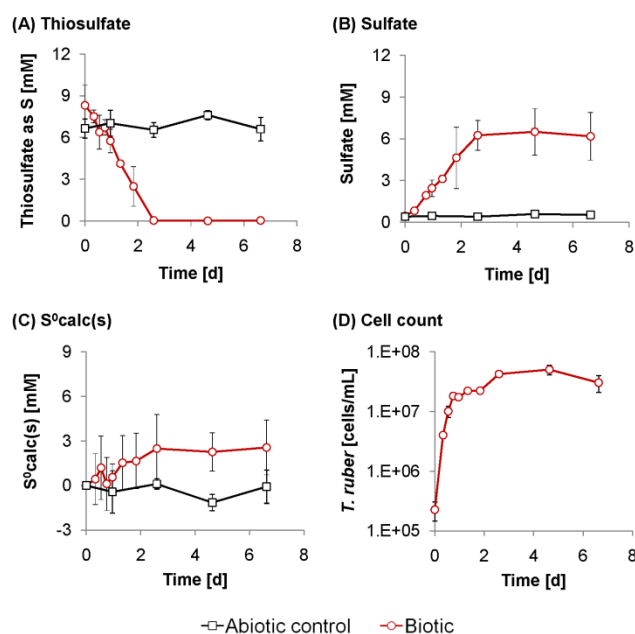


Fig. 3: Oxidation of thiosulfate ($\text{Na}_2\text{S}_2\text{O}_3 \times 5 \text{H}_2\text{O}$) during growth of *T. ruber* with 8% O_2 in the gas phase in a medium of pH 8. The biotic set-ups received 1% of a *T. ruber* pre-culture actively growing on thiosulfate as inoculum. The graphs show average concentrations \pm standard deviation ($n=3$), displayed by error bars (Table S3).

(Fig. 3A) resulted in the formation of up to 6.3 ± 1.1 mM sulfate (Fig. 3B). The sulfur deficit of ~ 2 mM (Table S3) is again attributed to $S^0_{\text{calc}(s)}$ (Fig. 3C) and in fact visual inspection revealed some beige precipitate during the biotic experiment, which probably was removed by sample filtration. Abiotic controls did not show such a decline in the sum of sulfur species (Table S3), nor a beige precipitate. Cell numbers reached a first plateau with $(1.82 \pm 0.05) \times 10^7$ cells mL^{-1} after 0.8 days. Based on these data, an exponential growth rate of 0.247 h^{-1} and a generation time of 2.8 h (168 min) were calculated. A further rise in cell numbers occurred after 0.8 days, and resulted in $(4.25 \pm 0.90) \times 10^7$ cells mL^{-1} after 2.6 days. At the end of the experiments, the pH in the abiotic controls was 7.97 ± 0.01 , while in biotic essays it was distinctly lower (7.15 ± 0.03).

Sulfide

Biotic and abiotic control experiments using sulfide as the sole electron donor (Fig. 4; Table S4) were conducted under conditions similar to the experiments with monothioarsenate and thiosulfate. Abiotic oxidation of sulfide was rapid, i.e. 4.2 mM transformed and less than 7% of initial sulfide remained after 25 hours (Fig. 4). The sulfur deficit was 36% of the initial sulfide ($S^0_{\text{calc}(s)} = 1.7 \text{ mM}$) (Table S4). The dominant oxidized species was thiosulfate with approximately 39%. Sulfate accounted for 19%. The oxidation pattern of sulfide revealed no difference between abiotic controls and inoculated samples (Fig. 4). Growth of *T. ruber* was not detectable under these conditions (data not shown).

Discussion

Various previous studies demonstrated microbial oxidation of arsenite and/or reduced sulfur species in diverse hydrothermal ecosystems which host, among others, Aquificales spp. (Gehring *et al.*, 2001; Jackson *et al.*, 2001; Langner *et al.*, 2001; Macur *et al.*, 2004; Inskeep *et al.*, 2007; Connon *et al.*, 2008; Hamamura *et al.*, 2009; Kubo *et al.*, 2011; Takacs-Vesbach *et al.*, 2013). Recent reports on the dominance of thioarsenates in natural arsenic-rich, sulfidic environments (Stauder *et al.*, 2005; Planer-Friedrich *et al.*, 2007; Planer-Friedrich *et al.*, 2009; Härtig & Planer-Friedrich, 2012; Ullrich *et al.*, 2013) raised the question how microorganisms transform such mixed arsenic-sulfur species. Specifically for *Thermocrinis ruber* only growth on elemental sulfur and thiosulfate had been shown before, not on any arsenic or mixed arsenic-sulfur species. In the following, we first discuss growth of *T. ruber* on arsenite and thiosulfate as sole electron donors, then show the various pathways of abiotic

Sulfide (80 °C, OS-Medium)

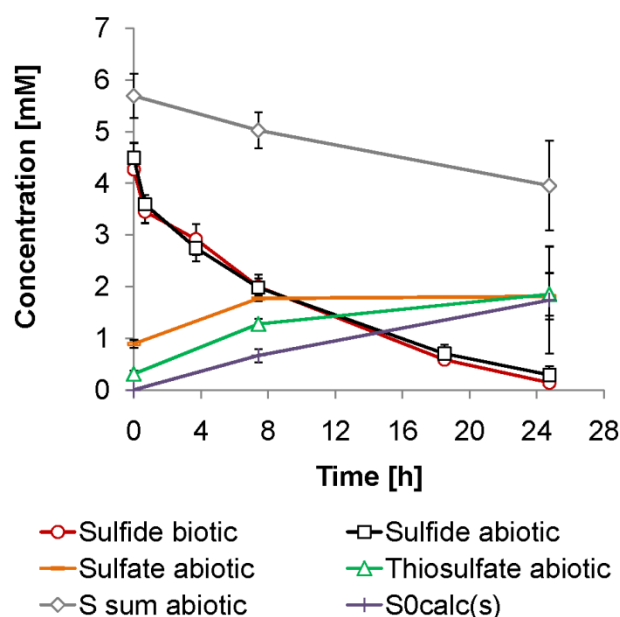


Fig. 4: Transformation of **sulfide** ($\text{Na}_2\text{S} \times 9 \text{ H}_2\text{O}$) in abiotic sulfide controls and *T. ruber*-inoculated sulfide experiments (that showed no cell growth). Sulfide experiments were run without thiosulfate or monothioarsenate, but otherwise had similar experimental conditions - OS-medium, pH 8, 80 °C, with 8 % O_2 . The graphs show average concentrations \pm standard deviation ($n=3$), displayed by error bars (Table S4). (Please note: Since *T. ruber*-inoculated and abiotic sulfide experiments showed no differences in the rate of sulfide transformation, we did not measure S-species in biotic samples by IC-ICP-MS.)

and biotic monothioarsenate transformation. All equations mentioned in the following text are also listed in Table 1, together with the electron transfer of these reactions, and (where information was available) Gibbs' free energies.

Growth of *T. ruber* OC14/7/2 on arsenite

Growth of *T. ruber* on arsenite in cultivation studies has not been reported before, though other members of the order *Aquificales* are known to use arsenite as sole electron donor (Takai *et al.*, 2003; Aguiar *et al.*, 2004). We had recognized arsenite oxidation by streamer communities in field incubations, earlier (Härtig & Planer-Friedrich, 2012). We thus tested growth of *T. ruber* on arsenite in cultivation studies and found that growth was coupled to aerobic oxidation of arsenite, when no other potential electron donor was present (Fig. 2). These findings provide evidence that arsenite represents an important hitherto unknown energy source for *T. ruber*. The aerobic oxidation of arsenite, yielding two mole electrons per mole of arsenite oxidized (Equation 1), is highly exergonic (Inskeep *et al.*,

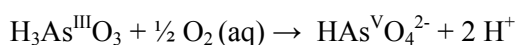
Table 1: Comparison of electron transfer and Gibbs free energies (so far available in literature) in known (Equation 1, 2, 3, 4) and proposed (Equation 7) microbially catalyzed reactions that could explain growth of *Thermocrinis ruber* (strain OC14/7/2) on the electron donor's arsenite, thiosulfate, elemental sulfur, and monothioarsenate.

No.	Reactions	Transfer of electrons per reaction [per mol of donor] [e ⁻]	ΔG_r^0 Standard molal Gibbs Free Energy of reaction (literature) [kJ mol ⁻¹]	ΔG_r^0 Standard molal Gibbs Free Energy/mol e ⁻ (calculated) [kJ (mol e ⁻) ⁻¹]	ΔG_r Gibbs Free Energy/mol e ⁻ 'hydrothermal waters' (literature) [kJ (mol e ⁻) ⁻¹]
Eq. 1	$\text{H}_3\text{As}^{\text{III}}\text{O}_3 + \frac{1}{2} \text{O}_2(\text{aq}) \rightarrow \text{HAs}^{\text{V}}\text{O}_4^{2-} + 2 \text{H}^+$ [1][2]	2 [2]	-115.6 (70 °C) ^[1]	-58	-50 to -80 ^[1] -75 ^[2]
Eq. 2	$\text{S}_2\text{O}_3^{2-} + 2 \text{O}_2(\text{aq}) + \text{H}_2\text{O} \rightarrow 2 \text{SO}_4^{2-} + 2 \text{H}^+$ [3]	8 [8]	-739.0 (85 °C) ^[3] -738.7 (? °C) ^[4]	-92	n.a.
Eq. 3a	$\text{S}_2\text{O}_3^{2-} + \frac{1}{2} \text{O}_2(\text{aq}) \rightarrow \text{SO}_4^{2-} + \text{S}^0(\text{s})$	2 [2]	n.a.	n.a.	n.a.
Eq. 3b	$5 \text{S}_2\text{O}_3^{2-} + \text{H}_2\text{O} + 4 \text{O}_2(\text{aq}) \rightarrow 6 \text{SO}_4^{2-} + 4 \text{S}^0(\text{s}) + 2 \text{H}^+$ [3]	16 [3.2]	-1640.3 (85 °C) ^[3]	-103	n.a.
Eq. 4	$\text{S}^0(\text{s}) + 1.5 \text{O}_2(\text{aq}) + \text{H}_2\text{O} \rightarrow \text{SO}_4^{2-} + 2 \text{H}^+$ [3]	6 [6]	-513.7 (85 °C) ^[3] -518.9 (70 °C) ^[1]	-86	n.a.
Eq. 7	$\text{HAs}^{\text{V}}\text{S}^{\text{II}}\text{O}_3^{2-} + 2 \text{O}_2(\text{aq}) + \text{H}_2\text{O} \rightarrow \text{HAs}^{\text{V}}\text{O}_4^{2-} + \text{SO}_4^{2-} + 2 \text{H}^+$	8 [8]	n.a.	n.a.	n.a.

References: [1] Inskeep *et al.* 2005; [2] Akerman *et al.* 2011; [3] Amend *et al.* 2001; [4] Kelly *et al.* 1999;

Remarks: The overall Gibbs free energy of reaction (ΔG_r) is calculated by $\Delta G_r = \Delta G_r^0 + RT \ln(Q_r)$ with ΔG_r^0 – standard molal free energy of reaction, R – gas constant, T – temperature, Q_r – activity product, based on geochemical analyses in hydrothermal waters (for further details see: Amend *et al.* 2001, Inskeep *et al.* 2005). (n.a. = data not available)

2005; Takacs-Vesbach *et al.*, 2013). The Gibbs free energies (ΔG_r) as determined in Yellowstone hot springs (temperature range 75 to 90 °C), ranged from -50 to -80 kJ mol⁻¹ e⁻ (Inskeep *et al.*, 2005; Table 1).



(Equation 1)

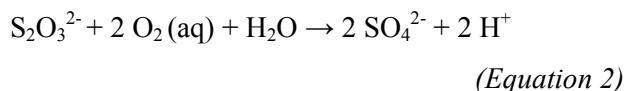
These findings likely explain the rapid oxidation of arsenite observed in neutral and alkaline hot spring drainage channels, where *Thermocrinis*-like populations thrive (Connon *et al.*, 2008; Hamamura *et al.*, 2009; Planer-Friedrich *et al.*, 2009; Takacs-Vesbach *et al.*, 2013). Earlier gene expression studies (Hamamura *et al.*, 2009) linked *aroA*-like bacterial arsenite oxidase genes (new unified nomenclature: *aioA* Lett *et al.*, 2012) with in-situ arsenite oxidation in pH-neutral Yellowstone hot springs to members of the *Aquificales*, including *Thermocrinis* spp. A concurrent cultivation study showed that other *Aquificales* isolates (i.e. *Sulfurihydrogenibium* and *Hydrogenobaculum* spp.)

expressed *aioA* and oxidized arsenite, but these organisms do not appear to conserve energy from arsenite oxidation (Hamamura *et al.*, 2010). Although *aioA* genes could not be amplified in a related strain of *T. ruber* (str. OC1/4; DSM No. 12173) (Hamamura *et al.*, 2010), the current strain (str. OC14/7/2; DSM No. 23557) exhibited growth on arsenite as the sole electron donor under laboratory conditions. Further studies are needed to investigate the molecular and biochemical mechanisms responsible for arsenite oxidation in *Thermocrinis* spp. However, to date, the *Thermocrinis*-dominated communities present in outflow channels of alkaline hot springs all contain *aioA* genes (Hamamura *et al.*, 2009; Takacs-Vesbach *et al.*, 2013). Our current *T. ruber*-based results suggest that arsenite is a potential energy source for chemolithotrophic *Aquificales* as primary producers in hydrothermal systems.

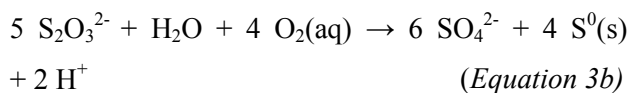
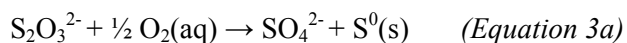
Growth of *T. ruber* OC14/7/2 on thiosulfate

It was previously shown that *T. ruber* grows aerobically on thiosulfate plus hydrogen (Huber *et*

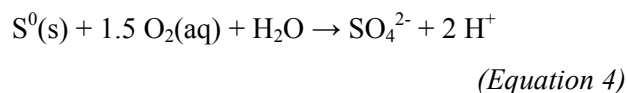
al., 1998). However, neither oxidation products nor growth rates were published. In our experiments without adding hydrogen, we observed generation times of 168 min (80 °C) for aerobic growth of *T. ruber* on thiosulfate (Fig. 3A), resulting in the formation of sulfate (Fig. 3B) and protons, as indicated by a drop in pH. The nominal oxidation states of sulfur in thiosulfate are S⁻¹ and S^{+V} (Vairavamurthy *et al.*, 1993), thus 8 electrons are transferred per mole of thiosulfate converted to sulfate (Equation 2, Table 1).



However, the microbial oxidation of thiosulfate to sulfate does not necessarily need to occur in one step (e.g., when catalyzed by specific bacterial Sox enzymes (Friedrich *et al.*, 2001; Friedrich *et al.*, 2005; Hensen *et al.*, 2006; Meyer *et al.*, 2007; Dahl & Friedrich, 2008; Ghosh & Dam, 2009)). Indeed, several of our pure culture observations (Fig. 3) are consistent with a two-step thiosulfate oxidation process. The observation of a beige precipitate as well as a deficit in the mass balance of aqueous sulfur species (Table S3) in our study suggested that elemental sulfur formed (S⁰calc(s), Fig. 3C) during the disappearance of thiosulfate (Fig. 3A). The cell numbers further increased between 1.8 and 2.6 days (Fig. 3D), which is also consistent with the oxidation of elemental sulfur as subsequent step in thiosulfate oxidation. It has been established earlier that *T. ruber* can aerobically oxidize elemental sulfur (at least in the presence of hydrogen) (Huber *et al.*, 1998). Thus, in a first step, thiosulfate is likely oxidized to sulfate and elemental sulfur. Different ratios of the products, sulfate and elemental sulfur, are possible (e.g., 1:1, Equation 3a or 3:2, Equation 3b Amend & Shock, 2001).



In a second step (Equation 4), microbial oxidation of elemental sulfur leads to further cell growth. Six electrons per mol S are transferred during formation of additional sulfate (Equation 4, Table 1). The concurrent formation of protons (Equation 3b, 4) was confirmed by a drop in pH. Increasing acidification of the medium, decreases in carbonate, and/or decreases in oxygen below critical levels may explain why further growth (Fig. 3D) or sulfate formation (Fig. 3B) could not be observed after 2.6 days.



The oxidative transformation of thiosulfate by *T. ruber* (Equations 2, 3) was in accordance with the previous observation of rapid microbial transformation of thiosulfate by a mixed pink-brownish streamer community (Härtig & Planer-Friedrich, 2012) from a spring hosting *Thermocrinis* spp. (Planer-Friedrich *et al.*, 2009). In contrast to *T. ruber* strain OC1/4 that grew on thiosulfate in the presence of hydrogen (Huber *et al.*, 1998), thiosulfate served as the sole electron donor for *T. ruber* strain OC14/7/2 in our study.

Growth of *T. ruber* OC14/7/2 on monothioarsenate

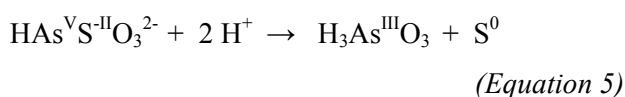
Our data established that *T. ruber* grew well in the presence of monothioarsenate (Fig. 1D). *T. ruber* accelerated the transformation process of monothioarsenate (Fig. 1A) substantially (3.3 mM transformed in 2.6 days) when compared to the slower decline in abiotic controls (1.3 mM transformed in 2.6 days). Sulfate (Fig. 1F) was the predominant biotic product, instead of thiosulfate (Fig. 1E) in abiotic controls. However, at the high temperature and oxic conditions used in our experiments, we also observed significant abiotic transformation. Instead of a direct microbial usage of the compound monothioarsenate, microbial oxidation of the products from abiotic transformation could have just shifted the monothioarsenate equilibrium towards further abiotic transformation. The fact that we observed an initial exponential growth phase until day 0.8 with a growth rate of 0.359 h⁻¹ that resulted in (2.52 ± 0.56) × 10⁷ cells/mL, and afterwards a further rise in cell numbers, reaching (3.71 ± 0.38) × 10⁷ cells/mL until day 2.6 (Fig. 1D, Table S1), already indicates that the transformation was governed by more than one process, similar to what was discussed for thiosulfate before. We discuss in the following potential abiotic and biotic pathways and their contribution to the observed transformation of monothioarsenate.

Mechanisms and products of abiotic monothioarsenate transformation

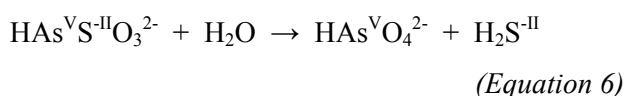
In earlier *on-site* experiments (Härtig & Planer-Friedrich, 2012), monothioarsenate had shown no substantial abiotic transformation within 4h under sulfide-deficient conditions, but was transformed almost exclusively microbially (Fig. S6). Due to its abiotic stability, monothioarsenate was considered suitable for growth experiments with *T. ruber*. However, over the longer time frame in the

laboratory (11.7 d, Fig. S1, Table S1), nearly 79% of the initial 3.3 mM monothioarsenate (Fig. 1A) transformed abiotically under the high-temperature, oxic conditions to arsenate (Fig. 1C) and thiosulfate (Fig. 1E), as well as small quantities of arsenite (Fig. 1B).

During synthesis, monothioarsenate is formed from arsenite and elemental sulfur. It thus appeared likely that it will also disproportionate in these two species (Equation 5).



However, at the high-temperature, oxic conditions of the present experiment, this abiotic pathway seemed to be of minor importance. The major abiotic reaction was transformation to arsenate and thiosulfate. However, while arsenate production was observed from day 0.3 on (Fig. 1C), formation of thiosulfate (Fig. 1E) only began after 1.9 days. This lag along with the observed immediate increase in $\text{S}^0_{\text{calc}}(\text{s})$ (Fig. 1H) indicates that elemental sulfur is the precursor species of thiosulfate. The original reaction might even have been desulfidation of monothioarsenate leading to formation of arsenate and hydrogen sulfide (Equation 6).



However, sulfide never accumulated in the abiotic monothioarsenate experiments (Fig. S3A). Its concentration (max. 0.3 mM) decreased from the beginning on and was below 0.1 mM after 1 day (Table S1). The experiment with a pure sulfide standard confirmed that sulfide (HS^-) undergoes rapid abiotic oxidation to elemental sulfur ($\text{S}^0_{\text{calc}}(\text{s})$), thiosulfate and sulfate (Fig. 4). All three products were observed in the abiotic monothioarsenate experiment as well (Fig. 1). Polysulfides were measured in the monothioarsenate experiment (Fig. 1G, Fig. S4). Apparently both, polysulfides (0.7 mM) and arsenate (0.3 mM) form immediately in an equilibrium reaction upon dissolution of the monothioarsenate standard in the medium at the beginning of the experiment (Table S1).

The observed redox transformations of monothioarsenate under abiotic conditions in the laboratory experiments were unexpected based on earlier field observations (Härtig & Planer-Friedrich, 2012) and are unfortunate because they render interpretation of the microbial influence on thioarsenate transformation more difficult. However, the two parameters – high temperature and oxygen – that are detrimental to

monothioarsenate stability over longer times were required for growth of *T. ruber*. In the following, we thus interpret the likeliness of different pathways of monothioarsenate transformation in relation to the abiotic results.

Relevance of individual microbial processes behind growth of *T. ruber* on monothioarsenate

Possible transformation pathways supporting the growth of *T. ruber* in the presence of monothioarsenate could be (I) abiotic transformation to arsenate, sulfide, elemental sulfur and thiosulfate and growth on only the S-products, or (II) abiotic disproportionation of monothioarsenate and growth on both products, arsenite and elemental sulfur, or (III) direct growth on the arsenic-bound sulfur of monothioarsenate. We discuss the relevance of the individual species for microbial oxidation in increasing order of oxidation state for the sulfur species sulfide (S^{II}), elemental sulfur (S^0), thiosulfate ($\text{S}^{\text{I}}\text{S}^{\text{V}}$), then arsenite (As^{III}), and finally monothioarsenate ($\text{As}^{\text{V}}\text{S}^{\text{II}}$).

Relevance of growth on sulfide

The presence of SQR (sulfide:quinone reductase) had been reported in several *Aquificales* species, including *Thermocrinis* spp., before (Nübel *et al.*, 2000; Marcia *et al.*, 2009; Takacs-Vesbach *et al.*, 2013) and microbial sulfide oxidation had been observed in *on-site* incubations with pink-brownish streamers (Härtig & Planer-Friedrich, 2012). However, the applied cultivation conditions in sulfide experiments, which were equivalent to those in monothioarsenate experiments, neither allowed faster than abiotic oxidation of sulfide (Fig. 4), nor showed growth of *T. ruber* OC14/7/2 (data not shown). Whether the applied strain cannot grow with sulfide as sole donor at all, or only the applied concentrations were already in a toxic range, is not clear at present. The decline of sulfide occurred comparably rapid in abiotic controls and *T. ruber*-inoculated sulfide experiments (Fig. 4), indicating that its abiotic oxidation was the dominant process. In summary, for the observed transformation of monothioarsenate, microbial sulfide oxidation did not play a role.

Relevance of growth on elemental sulfur

Elemental sulfur was observed in the monothioarsenate experiments in two forms: (I) measured as dissolved polysulfides (Fig. 1G) and (II) calculated as the difference of total sulfur applied and the measured dissolved sulfur species ($\text{S}^0_{\text{calc}}(\text{s})$; Fig. 1H). While polysulfides mimicked in

transformation the temporal behavior of monothioarsenate, $S^0_{\text{calc}}(s)$ showed a different behavior. Unfortunately, the data is (due to the nature of its calculation) also subject to large variations both in the abiotic and biotic experiments. Two trends are obvious despite variations: (I) the initial decrease of monothioarsenate both in the abiotic and biotic experiment from day 0 to 0.3 was not explained by the behavior of any other dissolved sulfur species but only by the increase of $S^0_{\text{calc}}(s)$ and (II) the deficit in sulfur mass balance was larger in the abiotic compared to the biotic experiment. It can thus be deduced that $S^0_{\text{calc}}(s)$ was initially produced abiotically by transformation of monothioarsenate and then oxidized not only abiotically but also by *T. ruber*. Furthermore, during the initial fast cell growth ($\mu=0.359 \text{ h}^{-1}$) up to day 0.8 monothioarsenate (Fig. 1A), thiosulfate (Fig. 1E) and sulfide (Fig. S3A), behaved similar in the abiotic and the biotic experiment. Differences were observed for polysulfides (Fig. 1G) and $S^0_{\text{calc}}(s)$ (Fig. 1H) with a more pronounced decrease in the biotic than abiotic experiments between day 0.3 and 0.8. The corresponding increase that was only observed in the biotic experiments was in sulfate (Fig. 1F). We thus postulate that initial cell growth was based on oxidation of elemental sulfur (bond in polysulfides or present as colloidal or precipitated form) to sulfate. By transfer of 6 electrons this reaction is energetically attractive (Equation 4, Table 1). Growth of *T. ruber* OC1/4 on elemental sulfur had previously been observed, but only in the presence of hydrogen (Huber *et al.*, 1998). According to our experiments, *T. ruber* OC14/7/2 is able to also grow on elemental sulfur as electron donor. Elemental sulfur caused the observed initial exponential cell growth in the monothioarsenate experiment and its oxidation to sulfate was the major initial pathway for increasing abiotic transformation of monothioarsenate as a follow-up reaction.

Relevance of growth on thiosulfate

As our experiments (Fig. 3) and Huber *et al.* (1998) had shown, thiosulfate can support growth of *T. ruber*. Thiosulfate (Fig. 1E) was the major product of abiotic monothioarsenate transformation (Fig. 1A) and its subsequent microbial transformation to sulfate could have accelerated abiotic monothioarsenate transformation. Thiosulfate did, however, not contribute to the exponential growth of *T. ruber* from day 0.3 to 0.8 because abiotic thiosulfate production only started after 1.3 days (Fig. 1E). It could have contributed to the observed increase of microbial activity until day 2.6. The

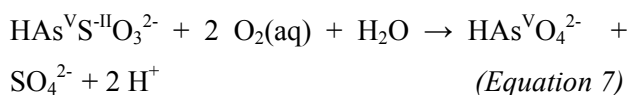
abiotic monothioarsenate experiment showed that a decrease of 2 mM monothioarsenate from day 0.8 to 11.7 (plus 0.9 mM $S^0_{\text{calc}}(s)$ at day 0.8) resulted in the production of 2.4 mMeq thiosulfate (plus 0.4 mM sulfate) (Fig. S1, Table S1). The faster decrease of the same amount of 2 mM monothioarsenate in the biotic experiment from day 0.8 to roughly day 1.8 left only 0.5 mMeq thiosulfate and correspondingly more sulfate (1.5 mM; Fig. S1, Table S1). This observation could either be interpreted as direct microbial oxidation of arsenic-bond S(-II) to sulfate, which then would have had proceeded faster than abiotic production of thiosulfate. However, it can neither be excluded that thiosulfate was further oxidized to sulfate by *T. ruber*, increasing abiotic monothioarsenate transformation indirectly.

Relevance of growth on arsenite

T. ruber was also shown to be able to grow on arsenite (Fig. 2, Equation 1). However, generation times determined for arsenite in pure cultures (29 h, Fig. 2D) were significantly longer than those observed for growth on monothioarsenate (2.2 h, Fig. 1D). The much slower growth rates determined on arsenite ($\mu = 0.024 \text{ h}^{-1}$) compared to monothioarsenate ($\mu = 0.331 \text{ h}^{-1}$) can thus not explain the exponential growth phase from day 0.3 to 0.8. Arsenite might have contributed to the observed increase of microbial activity until day 2.6. In fact, the small amount of arsenite detected under abiotic conditions until the end of the monothioarsenate experiment (0.3 mM), disappeared in the biotic experiments after 2.6 days, likely due to oxidation to arsenate by *T. ruber*. The amount of oxidized arsenite, however, was insufficient to have supported the observed microbial activity alone. An amount of 2 mM arsenite (Fig. 2A) were needed to support growth of at best $(1.02 \pm 0.34) \times 10^7$ cells/mL in pure arsenite experiments ("Biotic II", Fig. 2D), while in the monothioarsenate experiment, growth of further 1.19×10^7 cells/mL (Fig. 1D) between 0.8 d ($(2.52 \pm 0.56) \times 10^7$) and 2.6 d ($(3.71 \pm 0.38) \times 10^7$) was observed. Thus, while microbial arsenite oxidation could have contributed to indirect monothioarsenate transformation, it is not sufficient as only explanation.

Direct microbial oxidation of monothioarsenate

Direct microbial oxidation of the arsenic-bound sulfur of monothioarsenate (thiogroup, S^{II}) to sulfate would provide 8 electrons per mole of monothioarsenate and is thus energetically highly attractive (Equation 7; Table 1).



We observed that S(-II) in form of free sulfide was oxidized too quickly in our abiotic experiments to serve as electron donor (Fig 4). However, monothioarsenate was more stable than free sulfide and could thus have provided a reservoir of S(-II) for direct microbial oxidation without prior abiotic transformation.

Due to the significant abiotic monothioarsenate transformation to arsenate, elemental sulfur and thiosulfate over the time of the experiment, as well as the exponential growth on elemental sulfur by oxidation to sulfate, and a later linear increase of cell numbers during the stationary phase potentially caused by growth on arsenite and especially thiosulfate as described above it is difficult to clearly identify whether there is also direct microbial transformation of monothioarsenate. However, if the monothioarsenate transformation was purely an abiotic reaction due to microbial oxidation of the products elemental sulfur and thiosulfate, then the ratios of monothioarsenate to $\text{S}_{\text{calc}}^0(\text{s})$ and to thiosulfate should be similar to the abiotic experiment or, if microbial transformation was much faster than the abiotic monothioarsenate transformation, less monothioarsenate should have transformed compared to the abiotic experiment. Complete abiotic transformation of monothioarsenate could have only occurred once the main products (elemental sulfur and thiosulfate) were completely microbially oxidized. However, in the biotic experiments, monothioarsenate decreased significantly faster than expected based on the respective $\text{S}_{\text{calc}}^0(\text{s})$ concentrations, e.g. after 4.7 days we observed 1.5 mM $\text{S}_{\text{calc}}^0(\text{s})$ in the abiotic experiment together with 1.6 mM monothioarsenate, while biotically we still observed 0.8 mM $\text{S}_{\text{calc}}^0(\text{s})$, but already no more monothioarsenate (< 0.005 mM; Fig. 1, Table S1). Standard deviations for the elemental sulfur data are large because they were only calculated as difference of other measured species concentrations. However, the same observation was made for thiosulfate. We observed 1.6 mM monothioarsenate at 1.3 mEq thiosulfate after 4.7 days in the abiotic experiment, but no more monothioarsenate (< 0.005 mM) in the biotic experiment, even though there still 0.4 mEq thiosulfate was left (Fig. 1, Table S1). We take this as an indication that monothioarsenate was, at least “also”, directly microbially transformed in our culture experiments between day 0.8 and 2.6.

Conclusions

In the present study, we investigated the transformation of a mixed arsenic-sulfur species, monothioarsenate, as well as arsenite and thiosulfate under high-temperature, oxic conditions in the presence of a hyperthermophilic microorganism of the *Aquificales* bacterial order (*Thermocrinis ruber* OC14/7/2) previously known for its ability to grow on elemental sulfur and thiosulfate. Complete monothioarsenate transformation with formation of arsenate and sulfate was observed in the presence of *T. ruber* within 2.6 days. A major motivation was to follow the underlying different arsenic and sulfur redox reactions, differentiating which species are only transformed abiotically due to a shift in chemical equilibrium by removal of products by microorganisms and which are substrates for microbial growth.

The initial reaction was abiotic transformation of monothioarsenate to arsenate and elemental sulfur. Elemental sulfur was then microbially oxidized to sulfate, providing fast growth for *T. ruber* ($\mu=0.359 \text{ h}^{-1}$) until day 0.8. The following rapid decrease of monothioarsenate concentrations from day 0.8 to 2.6 was linked with a further increase of the cell numbers (plus 1.19×10^7 cells/mL), and could be abiotic transformation of monothioarsenate due to microbial oxidation of arsenite or thiosulfate. Arsenite was proven in a pure culture experiment to serve as a hitherto unknown electron donor with growth rates of 0.024 h^{-1} . However, in the monothioarsenate experiment, its concentrations were too low to explain significant growth and transformation. Thiosulfate oxidation - a two-step reaction to sulfate and elemental sulfur which is then also oxidized to sulfate - yielded growth rates of 0.247 h^{-1} in a pure culture experiment and concentrations in the monothioarsenate experiments would have been high enough to explain the elevated microbial activity during the stationary phase. However, actually more monothioarsenate was transformed than what was in equilibrium with its products. We attribute this to direct microbial oxidation of arsenic-bond S(-II) to sulfate. Free sulfide, on the contrary, did not play a role as electron donor for *T. ruber* because it was oxidized abiotically too fast.

Thioarsenates were lately reported to dominate in a number of different arsenic-rich sulfidic environments. Based on our previous field and the current laboratory experiments, we postulate that their role for microbial transformation is important. If conditions are unfavorable for their abiotic stability due to e.g. high temperature, presence of oxygen, or long reaction times, they provide

different arsenic and sulfur species that can be used by microorganisms upon abiotic transformation. In systems with lower temperature, limited oxygen or short reaction times, as observed e.g. in our previous field study (Härtig & Planer-Friedrich, 2012), thioarsenates are at least meta-stable (stability decreases with increasing number of thio-groups) and could serve directly as substrate for microbial metabolisms. An advantage then is that by oxidation of their As-bond S(-II) they provide the same electron yield as oxidation of free sulfide, but their stability is higher than that of sulfide.

Acknowledgements

Britta Planer-Friedrich dedicates this article to Gerhard Roewer, her early chemistry mentor at Freiberg University, on the occasion of his 75th birthday. We acknowledge generous funding by the German Research Foundation within the Emmy Noether program to Britta Planer-Friedrich (grant # PL 302/3-1). We like to thank Reinhardt Wirth and Yvonne Bilek from University of Regensburg for their support regarding the handling of *T. ruber*. We thank Harold Drake, Frank Thomas, Sinikka Hinrichsen, Stefan Will, Rita Schubert, and Linda Schneider from University of Bayreuth for brainstorming and/or for help during microbial experiments and/or chemical analyses.

References

- Aguiar P, Beveridge TJ & Reysenbach AL (2004) *Sulfurihydrogenibium azorense*, sp nov., a thermophilic hydrogen-oxidizing microaerophile from terrestrial hot springs in the Azores. *Int J Syst Evol Microbiol* **54**: 33–39.
- Amend JP & Shock EL (2001) Energetics of overall metabolic reactions of thermophilic and hyperthermophilic *Archaea* and *Bacteria*. *FEMS Microbiol Rev* **25**: 175–243.
- Braakman R, Smith E & Crécy-Lagard V de (2014) Metabolic evolution of a deep-branching hyperthermophilic chemoautotrophic bacterium. *Plos One* **9**: e87950.
- Brauner B & Tomicek F (1888) Ueber die Einwirkung von Schwefelwasserstoff auf Arsensäure. *Fresenius - Zeitschrift für Anal Chem* **27**: 508–513.
- Breitbart M, Wegley L, Leeds S, Schoenfeld T & Rohwer F (2004) Phage community dynamics in hot springs. *Appl Environ Microbiol* **70**: 1633–1640.
- Cherney MM, Zhang Y, Solomonson M, Weiner JH & James MNG (2010) Crystal structure of sulfide:quinone oxidoreductase from *Acidithiobacillus ferrooxidans*: Insights into sulfidrotrophic respiration and detoxification. *J. Mol. Biol.* **398**: 292–305.
- Cline JD (1969) Spectrophotometric determination of hydrogen sulfide in natural waters. *Limnology and Oceanography* **14**: 454–459.
- Connon SA, Koski AK, Neal AL, Wood SA & Magnuson TS (2008) Ecophysiology and geochemistry of microbial arsenic oxidation within a high arsenic, circumneutral hot spring system of the Alvord Desert. *FEMS Microbiology Ecology* **64**: 117–128.
- Dahl C & Friedrich CG (2008) *Microbial sulfur metabolism*, 1st edn. Springer, Berlin, New York.
- Friedrich CG, Bardischewsky F, Rother D, Quentmeier A & Fischer J (2005) Prokaryotic sulfur oxidation. *Current Opinion in Microbiology* **8**: 253–259.
- Friedrich CG, Rother D, Bardischewsky F, Quentmeier A & Fischer J (2001) Oxidation of reduced inorganic sulfur compounds by *Bacteria*: Emergence of a common mechanism? *Appl Environ Microbiol* **67**: 2873–2882.
- Ghosh W & Dam B (2009) Biochemistry and molecular biology of lithotrophic sulfur oxidation by taxonomically and ecologically diverse *Bacteria* and *Archaea*. *FEMS Microbiology Reviews* **33**: 999–1043.
- Ghosh W, Mallick S & DasGupta SK (2009) Origin of the Sox multienzyme complex system in ancient thermophilic *Bacteria* and coevolution of its constituent proteins. *Res Microbiol* **160**: 409–420.
- Gihring TM, Druschel GK, McCleskey RB, Hamers RJ & Banfield JF (2001) Rapid arsenite oxidation by *Thermus aquaticus* and *Thermus thermophilus*: Field and laboratory investigations. *Environ Sci Technol* **35**: 3857–3862.
- Hall JR, Mitchell KR, Jackson-Weaver O, Kooser AS, Cron BR, Crossey LJ & Takacs-Vesbach CD (2008) Molecular characterization of the diversity and distribution of a thermal spring microbial community using rRNA and Metabolic Genes. *Appl Environ Microbiol* **74**: 4910–4922.
- Hamamura N, Macur RE, Korf S, Ackerman G, Taylor WP, Kozubal M, Reysenbach A & Inskeep WP (2009) Linking microbial oxidation of arsenic with detection and phylogenetic analysis of arsenite oxidase genes in diverse geothermal environments. *Environ Microbiol* **11**: 421–431.
- Hamamura N, Macur RE, Liu Y, Inskeep WP & Reysenbach A (2010a) Distribution of aerobic arsenite oxidase genes within the Aquificales. *Interdisciplinary Studies on Environmental Chemistry, Volume 3*. Biological responses to contaminants: From molecular to community level (Hamamura, N., Suzuki, S., Mendo, S., Barroso, C. M., Iwata, H. & Tanabe, S., eds), pp. 47–55, Terrapub, Tokyo. http://www.terrapub.co.jp/onlineproceedings/ec/03/pdf/BR_03047.pdf.
- Härtig C & Planer-Friedrich B (2012) Thioarsenate transformation by filamentous microbial mats thriving in an alkaline, sulfidic hot spring. *Environ Sci Technol* **46**: 4348–4356.
- Hensen D, Sperling D, Trüper HG, Brune DC & Dahl C (2006) Thiosulphate oxidation in the phototrophic sulphur bacterium *Allochrochromatium vinosum*. *Mol Microbiol* **62**: 794–810.

- Hetzer A, McDonald IR & Morgan HW (2008) *Venenivibrio stagnispumantis* gen. nov., sp. nov., a thermophilic hydrogen-oxidizing bacterium isolated from Champagne Pool, Waiotapu, New Zealand. *Int J Syst Evol Microbiol* **58**: 398–403.
- Hollibaugh JT, Carini S, Gürleyük H, Jellison R, Joye SB, LeClerc G, Meile C, Vasquez L & Wallschläger D (2005) Arsenic speciation in Mono Lake, California: Response to seasonal stratification and anoxia. *Geochim Cosmochim Acta* **69**: 1925–1937.
- Huber R, Eder W, Heldwein S, Wanner G, Huber H, Rachel R & Stetter KO (1998) *Thermocrinis ruber* gen. nov., sp. nov., a pink-filament-forming hyperthermophilic bacterium isolated from Yellowstone National Park. *Appl Environ Microbiol* **64**: 3576–3583.
- Hügler M, Huber H, Molyneaux SJ, Vetrani C & Sievert SM (2007) Autotrophic CO₂ fixation via the reductive tricarboxylic acid cycle in different lineages within the phylum *Aquificae*: evidence for two ways of citrate cleavage. *Environ Microbiol* **9**: 81–92.
- Inskeep WP, Ackerman G, Taylor KG, Kozubal M, Korf S & Macur RE (2005) On the energetics of chemolithotrophy in non-equilibrium systems: case studies of geothermal springs in Yellowstone National Park. *Geobiology* **3**: 297–317.
- Inskeep WP, Macur RE, Hamamura N, Warelow TP, Ward SA & Santini JM (2007) Detection, diversity and expression of aerobic bacterial arsenite oxidase genes. *Environ Microbiol* **9**: 934–943.
- Jackson CR, Langner HW, Donahoe-Christiansen J, Inskeep WP & McDermott TR (2001) Molecular analysis of microbial community structure in an arsenite-oxidizing acidic thermal spring. *Environ Microbiol* **3**: 532–542.
- Jahnke LL, Eder W, Huber R, Hope JM, Hinrichs KU, Hayes JM, Des Marais DJ, Cady SL & Summons RE (2001) Signature lipids and stable carbon isotope analyses of Octopus Spring hyperthermophilic communities compared with those of *Aquificales* representatives. *Appl Environ Microbiol* **67**: 5179–5189.
- Kamyshny A, Ekeltchik I, Gun J & Lev O (2006) Method for the determination of inorganic polysulfide distribution in aquatic systems. *J Anal Chem* **78**: 2631–2639.
- Kubo K, Knittel K, Amann R, Fukui M & Matsuura K (2011) Sulfur-metabolizing bacterial populations in microbial mats of the Nakabusa hot spring, Japan. *Syst Appl Microbiol* **34**: 293–302.
- Langner HW, Jackson CR, McDermott TR & Inskeep WP (2001) Rapid oxidation of arsenite in a hot spring ecosystem, Yellowstone National Park. *Environ Sci Technol* **35**: 3302–3309.
- Lett M, Muller D, Lièvreumont D, Silver S & Santini J (2012) Unified nomenclature for genes involved in prokaryotic aerobic arsenite oxidation. *J Bacteriol* **194**: 207–208.
- Macur RE, Langner HW, Kocar BD & Inskeep WP (2004) Linking geochemical processes with microbial community analysis: successional dynamics in an arsenic-rich, acid-sulphate-chloride geothermal spring. *Geobiology* **2**: 163–177.
- Mamindy-Pajany Y, Bataillard P, Séby F, Crouzet C, Moulin A, Guezennec A, Hurel C, Marmier N & Battaglia-Brunet F (2013) Arsenic in marina sediments from the mediterranean coast: Speciation in the solid phase and occurrence of thioarsenates. *Soil and Sediment Contamination* **22**: 984–1002.
- Marcia M, Ermler U, Peng G & Michel H (2009) The structure of *Aquifex aeolicus* sulfide:quinone oxidoreductase, a basis to understand sulfide detoxification and respiration. *PNAS* **106**: 9625–9630.
- McCay LW (1902) Die Einwirkung von Schwefelwasserstoff auf Arsensäure. *Z Anorg Chem* **29**: 36–50.
- McCay LW & Foster W (1904) Über die Trisulfoxyarsensäure. *Z Anorg Chem* **41**: 452–473.
- Meyer B, Imhoff JF & Kuever J (2007) Molecular analysis of the distribution and phylogeny of the *soxB* gene among sulfur-oxidizing *Bacteria* – evolution of the Sox sulfur oxidation enzyme system. *Environ Microbiol* **9**: 2957–2977.
- Noble RT & Fuhrman JA (1998) Use of SYBR Green I for rapid epifluorescence counts of marine viruses and bacteria. *Aquat Microb Ecol* **14**: 113–118.
- Nübel T, Klughammer C, Huber R, Hauska G & Schütz M (2000) Sulfide:quinone oxidoreductase in membranes of the hyperthermophilic bacterium *Aquifex aeolicus* (VF5). *Arch Microbiol* **173**: 233–244.
- Planer-Friedrich B, Fisher JC, Hollibaugh JT, Süß E & Wallschläger D (2009) Oxidative transformation of trithioarsenate along alkaline geothermal drainages - abiotic versus microbially mediated processes. *Geomicrobiol J* **26**: 339–350.
- Planer-Friedrich B, London J, McCleskey RB, Nordstrom DK & Wallschläger D (2007) Thioarsenates in geothermal waters of Yellowstone National Park: Determination, preservation, and geochemical importance. *Environ Sci Technol* **41**: 5245–5251.
- Planer-Friedrich B, Suess E, Scheinost AC & Wallschläger D (2010) Arsenic speciation in sulfidic waters: Reconciling contradictory spectroscopic and chromatographic evidence. *J Anal Chem* **82**: 10228–10235.
- Planer-Friedrich B & Wallschläger D (2009) A critical investigation of hydride generation-based arsenic speciation in sulfidic waters. *Environ Sci Technol* **43**: 5007–5013.
- Rizkov D, Lev O, Gun J, Anisimov B & Kuselman I (2004) Development of in-house reference materials for determination of inorganic polysulfides in water. *Accreditation and Quality Assurance* **9**: 399–403.
- Schwedt G & Rieckhoff M (1996a) Separation of thio- and oxothioarsenates by capillary zone electrophoresis and ion chromatography. *J Chromatography A* **736**: 341–350.
- Schwedt G & Rieckhoff M (1996b) Zur Analytik von Oxothioarsen-Species in Schlacken und Grubenwässern. *J Praktische Chemie* **338**: 55–59.

- Stauder S, Raue B & Sacher F (2005) Thioarsenates in sulfidic waters. *Environ Sci Technol* **39**: 5933–5939.
- Suess E, Scheinost AC, Bostick BC, Merkel BJ, Wallschläger D & Planer-Friedrich B (2009) Discrimination of thioarsenites and thioarsenates by X-ray absorption spectroscopy. *J Anal Chem* **81**: 8318–8326.
- Takacs-Vesbach C, Inskeep WP & Jay ZJ *et al.* (2013) Metagenome sequence analysis of filamentous microbial communities obtained from geochemically distinct geothermal channels reveals specialization of three *Aquificales* lineages. *Front Microbiol* **4**.
- Takai K, Kobayashi H, Nealson KH & Horikoshi K (2003) *Sulfurihydrogenibium subterraneum* gen. nov., sp nov., from a subsurface hot aquifer. *Int J Syst Evol Microbiol* **53**: 823–827.
- Theissen U, Hoffmeister M, Grieshaber M & Martin W (2003) Single eubacterial origin of eukaryotic sulfide:quinone oxidoreductase, a mitochondrial enzyme conserved from the early evolution of eukaryotes during anoxic and sulfidic times. *Mol Biol Evol* **20**: 1564–1574.
- Thilo E, Hertzog K & Winkler A (1970) Über Vorgänge bei der Bildung des Arsen(V)-Sulfids beim Ansäuern von Tetrathioarsenatlösungen. *Z anorg allg Chem* **373**: 111–121.
- Ullrich MK, Pope JG, Seward TM, Wilson N & Planer-Friedrich B (2013) Sulfur redox chemistry governs diurnal antimony and arsenic cycles at Champagne Pool, Waiotapu, New Zealand. *J Volcanol Geotherm Res* **262**: 164–177.
- Vairavamurthy A, Manowitz B, Luther G & Jeon Y (1993) Oxidation state of sulfur in thiosulfate and implications for anaerobic energy metabolism. *Geochim Cosmochim Acta* **57**: 1619–1623.
- Wallschläger D & Stadey CJ (2007) Determination of (oxy)thioarsenates in sulfidic waters. *J Anal Chem* **79**: 3873–3880.
- Wegley L, Mosier-Boss P, Lieberman S, Andrews J, Graff-Baker A & Rohwer F (2006) Rapid estimation of microbial numbers in water using bulk fluorescence. *Environ Microbiol* **8**: 1775–1782.
- Wilkin RT, Wallschläger D & Ford RG (2003) Speciation of arsenic in sulfidic waters. *Geochem Transact* **4**: 1–7.
- Wirth R, Sikorski J & Brambilla E *et al.* (2010) Complete genome sequence of *Thermocrinis albus* type strain (HI 11/12T). *Stand Genomic Sci* **2**: 194–202.
- Zhang J, Kim H & Townsend T (2014) Methodology for assessing thioarsenic formation potential in sulfidic landfill environments. *Chemosphere* **107**: 311–318.

Supporting Information

Monothioarsenate as Hitherto Unknown Electron Donor for Chemolithotrophic Growth of the Aerobic Hyperthermophilic Bacterium *Thermocrinis ruber* OC 14/7/2

Cornelia Härtig¹, Regina Lohmayer¹, Steffen Kolb², Marcus A. Horn², William P. Inskeep³, Britta Planer-Friedrich*¹

¹Department of Environmental Geochemistry, Bayreuth Center for Ecology and Environmental Research (BayCEER), University of Bayreuth, Universitätsstraße 30, 95447 Bayreuth, Germany

²Department of Ecological Microbiology, Bayreuth Center for Ecology and Environmental Research (BayCEER), University of Bayreuth, Dr. Hans-Frisch-Strasse 1-3, 95440 Bayreuth, Germany

³Department of Land Resources and Environmental Sciences and Thermal Biology Institute (TBI), 805 Leon-Johnson Hall, Montana State University, Bozeman, MT 59717, USA

* corresponding author: phone +49 921 552370, e-mail: b.planer-friedrich@uni-bayreuth.de

This file contains supplementary data further supporting our study and is meant for online publication. The data and their descriptions are displayed in:

- **4 Supplementary Tables** (designated as Table S1, S2, S3, S4)
- **6 Supplementary Figures** (designated as Figure S1, S2, S3, S4, S5, S6)

Table S1: Oxidation of **monothioarsenate** ($\text{Na}_3\text{AsSO}_3 \times 7 \text{H}_2\text{O}$) during growth of *T. ruber* with 8 % O_2 (v/v) in the gas phase at 80 °C. Initial medium pH was 8. Arsenic and sulfur speciation data show average concentrations \pm standard deviation (n=3). The biotic set-up was inoculated with 1 % of a *T. ruber* pre-culture actively growing on monothioarsenate.

Monothioarsenate BIOTIC As, As-S species	Incubation time	Arsenite	Arsenate	Mono- thioarsenate	Dithio- arsenate	Trithio- arsenate	Tetrathio- arsenate	Sum of Arsenic species	<i>Thermocrinis ruber</i>
Unit	days	mM	mM	mM	mM	mM	mM	mM	Cells/mL
Method	-	IC-ICP-MS	IC-ICP-MS	IC-ICP-MS	IC-ICP-MS	IC-ICP-MS	IC-ICP-MS	Calculated	Neubauer Chamber
BIOTIC t0	0.0	0.020 \pm 0.004	0.246 \pm 0.029	3.285 \pm 0.271	0.021 \pm 0.002	0.025 \pm 0.003	0.001 \pm 0.0001	3.655 \pm 0.291	(0.01 \pm 0.003) $\times 10^7$
BIOTIC t1	0.4	0.096 \pm 0.014	0.416 \pm 0.029	3.029 \pm 0.205	0.024 \pm 0.002	0.001 \pm 0.0003	0.001 \pm 0.0005	3.601 \pm 0.203	(0.07 \pm 0.01) $\times 10^7$
BIOTIC t2	0.6	0.015 \pm 0.005	0.573 \pm 0.098	2.835 \pm 0.485	0.021 \pm 0.002	0.001 \pm 0.0001	0.001 \pm 0.0008	3.472 \pm 0.598	(0.73 \pm 0.20) $\times 10^7$
BIOTIC t3	0.8	0.019 \pm 0.026	0.813 \pm 0.146	2.856 \pm 0.386	0.025 \pm 0.005	0.001 \pm 0.0002	0.001 \pm 0.0004	3.737 \pm 0.524	(2.52 \pm 0.56) $\times 10^7$
BIOTIC t4	1.0	0.097 \pm 0.069	1.011 \pm 0.127	2.174 \pm 0.445	0.027 \pm 0.018	0.001 \pm 0.0001	0.001 \pm 0.0002	3.324 \pm 0.488	(2.79 \pm 1.09) $\times 10^7$
BIOTIC t5	1.4	0.248 \pm 0.201	1.626 \pm 0.604	1.760 \pm 0.488	0.062 \pm 0.052	0.001 \pm 0.001	0.001 \pm 0.0002	3.706 \pm 0.488	(2.52 \pm 0.93) $\times 10^7$
BIOTIC t6	1.9	0.172 \pm 0.070	2.549 \pm 0.155	0.422 \pm 0.036	0.014 \pm 0.007	0.001 \pm 0.0003	0.001 \pm 0.0004	3.159 \pm 0.088	(2.73 \pm 0.66) $\times 10^7$
BIOTIC t7	2.6	0.013 \pm 0.009	3.531 \pm 0.413	0.029 \pm 0.007	0.001 \pm 0.0001	0.001 \pm 0.001	0.001 \pm 0.0005	3.577 \pm 0.400	(3.71 \pm 0.38) $\times 10^7$
BIOTIC t8	4.7	0.001 \pm 0.001	3.690 \pm 0.225	0.004 \pm 0.002	0.001 \pm 0.001	0.001 \pm 0.0001	0.001 \pm 0.0002	3.698 \pm 0.225	(3.50 \pm 1.07) $\times 10^7$
BIOTIC t9	6.6	0.001 \pm 0.001	3.472 \pm 0.264	0.002 \pm 0.0004	0.001 \pm 0.0003	0.001 \pm 0.0004	0.001 \pm 0.0004	3.477 \pm 0.264	(1.76 \pm 1.08) $\times 10^7$
BIOTIC t10^(a)	11.7	0.001 \pm 0.001	3.951 \pm 0.220	0.002 \pm 0.0016	0.001 \pm 0.0008	0.001 \pm 0.0002	0.001 \pm 0.0004	3.958 \pm 0.2225	n.d.

(a) data of day 11.7 were not displayed in Fig. 1 of the manuscript;

Further comments: A not further specified arsenic-peak (retention times 354013 ms - 363714 ms) was detected during IC-ICP-MS analysis. However, its concentration range (based on the arsenate calibration curve) was very low with 0.01 ± 0.02 mM in biotic and 0.02 ± 0.02 mM in abiotic monothioarsenate experiments.

Table S1 continued:

Monothioarsenate S-Species BIOTIC	Incubation time	Sulfate	Thiosulfate	Sulfide	Polysulfide Sum	Sum of Sulfur species (incl. S in thioarsenates)	S-Deficit 'S⁰_{calc(s)}'^(b)	<i>Thermocrinis ruber</i>
Unit	d	mM	mM	mM	mM	mM	mM	cells/mL
Method	-	IC-ICP-MS	IC-ICP-MS	Methylene Blue	HPLC	Calculated	Calculated	Neubauer Chamber
BIOTIC t0	0.0	0.73 ± 0.30	0.01 ± 0.01	0.31 ± 0.02	0.74 ± 0.02	5.20 ± 0.36	0.00 ± 0.00	(0.01 ± 0.003) × 10 ⁷
BIOTIC t1	0.4	0.61 ± 0.13	0.05 ± 0.08	0.16 ± 0.01	0.57 ± 0.05	4.48 ± 0.18	0.72 ± 0.20	(0.07 ± 0.01) × 10 ⁷
BIOTIC t2	0.6	1.01 ± 0.16	0.03 ± 0.04	0.14 ± 0.01	0.50 ± 0.05	4.56 ± 0.45	0.64 ± 0.58	(0.73 ± 0.20) × 10 ⁷
BIOTIC t3	0.8	1.12 ± 0.09	0.06 ± 0.06	0.13 ± 0.02	0.63 ± 0.08	4.85 ± 0.45	0.35 ± 0.09	(2.52 ± 0.56) × 10 ⁷
BIOTIC t4	1.0	1.53 ± 0.17	0.01 ± 0.00	n.d.	0.50 ± 0.03	(4.27 ± 0.54)	(0.93 ± 0.68)	(2.79 ± 1.09) × 10 ⁷
BIOTIC t5	1.4	2.03 ± 0.28	0.40 ± 0.46	0.04 ± 0.03	0.29 ± 0.03	4.66 ± 0.74	0.54 ± 1.01	(2.52 ± 0.93) × 10 ⁷
BIOTIC t6	1.9	2.62 ± 0.76	0.55 ± 0.30	0.02 ± 0.01	0.04 ± 0.03	3.69 ± 1.12	1.51 ± 1.26	(2.73 ± 0.66) × 10 ⁷
BIOTIC t7	2.6	3.68 ± 0.75	0.45 ± 0.40	< 0.01	< 0.01	4.16 ± 0.94	1.04 ± 1.28	(3.71 ± 0.38) × 10 ⁷
BIOTIC t8	4.7	4.06 ± 0.63	0.37 ± 0.27	< 0.01	< 0.01	4.44 ± 0.73	0.76 ± 1.09	(3.50 ± 1.07) × 10 ⁷
BIOTIC t9	6.6	4.19 ± 0.59	0.48 ± 0.44	< 0.01	< 0.01	4.68 ± 0.72	0.52 ± 1.03	(1.76 ± 1.08) × 10 ⁷
BIOTIC t10^(a)	11.7	4.45 ± 0.65	0.34 ± 0.15	< 0.01	< 0.01	4.80 ± 0.58	0.40 ± 0.94	n.d.

(a) data of day 11.7 were not displayed in Fig. 1 of the manuscript;

(b) Calculation of the S-deficit $S^0_{calc(s)}$: $S^0_{calc(s)}(t_x) = \text{Sum of sulfur species}(t_x) - \text{Sum of sulfur species}(t_0)$

Table S1 continued:

Monothioarsenate ABIOTIC As, As-S species	Incubation time	Arsenite	Arsenate	Mono- thioarsenate	Dithio- arsenate	Trithio- arsenate	Tetrathio- arsenate	Sum of Arsenic species	<i>Thermocrinis ruber</i>
Unit	days	mM	mM	mM	mM	mM	mM	mM	Cells/mL
Method	-	IC-ICP-MS	IC-ICP-MS	IC-ICP-MS	IC-ICP-MS	IC-ICP-MS	IC-ICP-MS	Calculated	Neubauer Chamber
ABIOTIC t0	0.0	0.020 ± 0.002	0.241 ± 0.038	3.381 ± 0.503	0.021 ± 0.007	0.017 ± 0.008	< 0.001	3.732 ± 0.583	-
ABIOTIC t1	0.4	0.117 ± 0.018	0.304 ± 0.017	2.716 ± 0.115	0.020 ± 0.004	0.001 ± 0.0004	0.001 ± 0.001	3.188 ± 0.120	-
ABIOTIC t2	0.6	0.140 ± 0.035	0.423 ± 0.067	2.869 ± 0.602	0.023 ± 0.007	0.001 ± 0.0003	0.001 ± 0.0002	3.479 ± 0.702	-
ABIOTIC t3	0.8	0.154 ± 0.006	0.478 ± 0.021	2.844 ± 0.092	0.025 ± 0.0002	0.001 ± 0.0004	0.001 ± 0.0002	3.522 ± 0.120	-
ABIOTIC t4	1.0	0.172 ± 0.048	0.554 ± 0.112	2.786 ± 0.654	0.031 ± 0.007	0.001 ± 0.001	0.001 ± 0.0004	3.553 ± 0.824	-
ABIOTIC t5	1.4	0.173 ± 0.012	0.564 ± 0.043	2.166 ± 0.168	0.024 ± 0.001	0.001 ± 0.0003	0.001 ± 0.0004	2.938 ± 0.215	-
ABIOTIC t6	1.9	0.232 ± 0.045	0.906 ± 0.145	2.608 ± 0.306	0.038 ± 0.008	0.001 ± 0.0005	0.001 ± 0.0003	3.796 ± 0.503	-
ABIOTIC t7	2.6	0.242 ± 0.011	1.046 ± 0.023	1.989 ± 0.123	0.035 ± 0.002	0.001 ± 0.001	0.003 ± 0.004	3.319 ± 0.154	-
ABIOTIC t8	4.7	0.349 ± 0.065	1.825 ± 0.459	1.567 ± 0.448	0.020 ± 0.014	0.001 ± 0.0004	0.001 ± 0.0004	3.764 ± 0.959	-
ABIOTIC t9	6.6	0.348 ± 0.010	2.085 ± 0.126	1.081 ± 0.132	0.029 ± 0.005	0.001 ± 0.001	0.002 ± 0.002	3.550 ± 0.239	-
ABIOTIC t10^(a)	11.7	0.337 ± 0.064	2.889 ± 0.687	0.716 ± 0.213	0.017 ± 0.005	0.001 ± 0.001	0.001 ± 0.001	3.963 ± 0.967	-

(a) data of day 11.7 were not displayed in Fig. 1 of the manuscript;

Further comments: A not further specified arsenic-peak (retention times 354013 ms - 363714 ms) was detected during IC-ICP-MS analysis. However, its concentration range (based on the arsenate calibration curve) was very low with 0.01 ± 0.02 mM in biotic and 0.02 ± 0.02 mM in abiotic monothioarsenate experiments.

Table S1 continued:

Monothioarsenate S-Species ABIOTIC	Incubation time	Sulfate	Thiosulfate	Sulfide	Polysulfide Sum	Sum of Sulfur species (incl. S in thioarsenates)	S-Deficit 'S⁰_{calc(s)}'^(b)	<i>Thermocrinis ruber</i>
Unit	d	mM	mM	mM	mM	mM	mM	cells/mL
Method	-	IC-ICP-MS	IC-ICP-MS	Methylene Blue	HPLC	Calculated	Calculated	Neubauer Chamber
ABIOTIC t0	0.0	0.75 ± 0.24	0.08 ± 0.10	0.33 ± 0.01	0.76 ± 0.04	5.40 ± 0.47	0.00 ± 0.00	-
ABIOTIC t1	0.4	0.72 ± 0.12	0.04 ± 0.05	0.13 ± 0.01	0.63 ± 0.07	4.28 ± 0.19	1.11 ± 0.33	-
ABIOTIC t2	0.6	0.71 ± 0.21	<0.01	0.10 ± 0.01	0.61 ± 0.13	4.35 ± 0.74	1.05 ± 0.83	-
ABIOTIC t3	0.8	0.69 ± 0.07	0.02 ± 0.03	0.08 ± 0.01	0.78 ± 0.10	4.47 ± 0.16	0.93 ± 0.62	-
ABIOTIC t4	1.0	0.74 ± 0.17	0.01 ± 0.01	n.d.	0.62 ± 0.12	(4.22 ± 0.90)	(1.18 ± 1.05)	-
ABIOTIC t5	1.4	0.58 ± 0.04	0.04 ± 0.±03	0.07 ± 0.01	0.71 ± 0.05	3.62 ± 0.24	1.78 ± 0.53	-
ABIOTIC t6	1.9	0.77 ± 0.19	0.21 ± 0.36	0.07 ± 0.01	0.62 ± 0.17	4.36 ± 0.51	1.03 ± 0.23	-
ABIOTIC t7	2.6	0.70 ± 0.08	0.31 ± 0.49	0.05 ± 0.004	0.68 ± 0.09	3.82 ± 0.34	1.58 ± 0.16	-
ABIOTIC t8	4.7	0.79 ± 0.18	1.25 ± 0.45	0.03 ± 0.01	0.23 ± 0.01	3.92 ± 1.05	1.48 ± 1.38	-
ABIOTIC t9	6.6	0.83 ± 0.33	1.90 ± 0.09	0.02 ± 0.0004	0.27 ± 0.09	4.17 ± 0.41	1.23 ± 0.88	-
ABIOTIC t10^(a)	11.7	1.05 ± 0.37	2.39 ± 0.91	0.01 ± 0.001	0.18 ± 0.01	4.38 ± 1.43	1.01 1.70	-

(a) data of day 11.7 were not displayed in Fig. 1 of the manuscript;

(b) Calculation of the S-deficit $S^0_{calc(s)}$: $S^0_{calc(s)}(t_x) = \text{Sum of sulfur species}(t_x) - \text{Sum of sulfur species}(t_0)$

Table S2: Oxidation of arsenite ($\text{NaAs}^{\text{III}}\text{O}_2$) during growth of *T. ruber* with 3% O_2 (v/v) in the gas phase at 80 °C. Initial medium pH was 7. Data show average concentrations \pm standard deviation (n=3) of one abiotic and three different biotic experiments (Biotic I-III). The biotic set-ups were inoculated with a *T. ruber* pre-culture actively growing on arsenite. Biotic I and II/III received 2.5 % and 1 % inoculum, respectively.

Arsenite ABIOTIC Control	Incubation time	Arsenite	Arsenate	Mono- thioarsenate	Dithio- arsenate	Trithio- arsenate	Tetrathio- arsenate	Sumof Arsenic species	<i>Thermocrinis ruber</i> OC 14/7/2
Unit	days	mM	mM	mM	mM	mM	mM	mM	Cells/mL
Method	-	IC-ICP-MS	IC-ICP-MS	IC-ICP-MS	IC-ICP-MS	IC-ICP-MS	IC-ICP-MS	Calculated	Neubauer Chamber
ABIOTIC t0	0.0	1.866 \pm 0.221	0.059 \pm 0.055	0.001 \pm 0.0002	< 0.001	< 0.001	< 0.001	1.927 \pm 0.252	-
ABIOTIC t1	0.7	1.959 \pm 0.170	0.043 \pm 0.010	0.043 \pm 0.070	< 0.001	0.001 \pm 0.001	< 0.001	2.047 \pm 0.139	-
ABIOTIC t2	3.7	1.935 \pm 0.319	0.056 \pm 0.016	0.005 \pm 0.001	< 0.001	< 0.001	< 0.001	1.997 \pm 0.335	-
ABIOTIC t3	5.7	1.751 \pm 0.220	0.062 \pm 0.011	0.011 \pm 0.010	< 0.001	< 0.001	< 0.001	1.825 \pm 0.241	-
ABIOTIC t4	9.7	1.847 \pm 0.099	0.095 \pm 0.004	0.009 \pm 0.002	< 0.001	< 0.001	< 0.001	1.951 \pm 0.103	-
ABIOTIC t5	11.9	1.890 \pm 0.186	0.156 \pm 0.062	0.014 \pm 0.001	< 0.001	< 0.001	< 0.001	2.062 \pm 0.168	-
Arsenite BIOTIC I									
BIOTIC t0	0.00	1.904 \pm 0.084	0.139 \pm 0.019	< 0.001	< 0.001	< 0.001	< 0.001	2.046 \pm 0.081	(0.05 \pm 0.01) E+07
BIOTIC t1	1.9	n.d.	n.d.	n.d.	n.d.	n.d.	n.d.	n.d.	(0.07 \pm 0.01) E+07
BIOTIC t2	5.8	0.018 \pm 0.016	2.032 \pm 0.132	< 0.001	< 0.001	< 0.001	< 0.001	2.059 \pm 0.142	(0.79 \pm 0.35) E+07
BIOTIC t3	7.8	0.003 \pm 0.004	1.984 \pm 0.020	< 0.001	< 0.001	< 0.001	< 0.001	1.993 \pm 0.017	(0.84 \pm 0.25) E+07
BIOTIC t4	11.9	0.036 \pm 0.056	1.941 \pm 0.172	0.050 \pm 0.043	< 0.001	0.022 \pm 0.037	< 0.001	2.052 \pm 0.274	(0.66 \pm 0.17) E+07

Table S2 continued:

Arsenite BIOTIC II	Incubation time	Arsenite	Arsenate	Mono- thioarsenate	Dithio- arsenate	Trithio- arsenate	Tetrathio- arsenate	Sum of Arsenic species	<i>Thermocrinis ruber</i> OC 14/7/2
Unit	days	mM	mM	mM	mM	mM	mM	mM	Cells/mL
Method	-	IC-ICP-MS	IC-ICP-MS	IC-ICP-MS	IC-ICP-MS	IC-ICP-MS	IC-ICP-MS	Calculated	Neubauer Chamber
BIOTIC t0	0.0	1.751 ± 0.153	0.086 ± 0.010	< 0.001	< 0.001	< 0.001	< 0.001	1.839 ± 0.161	(0.02 ± 0.01) E+07
BIOTIC t1	0.7	1.706 ± 0.169	0.093 ± 0.011	< 0.001	< 0.001	< 0.001	< 0.001	1.803 ± 0.179	(0.03 ± 0.02) E+07
BIOTIC t2	1.6	n.d.	n.d.	n.d.	n.d.	n.d.	n.d.	n.d.	(0.05 ± 0.03) E+07
BIOTIC t3	1.8	n.d.	n.d.	n.d.	n.d.	n.d.	n.d.	n.d.	(0.04 ± 0.01) E+07
BIOTIC t4	2.9	n.d.	n.d.	n.d.	n.d.	n.d.	n.d.	n.d.	(0.05 ± 0.02) E+07
BIOTIC t5	3.7	1.704 ± 0.195	0.294 ± 0.115	0.008 ± 0.003	< 0.001	0.005 ± 0.007	< 0.001	2.012 ± 0.139	(0.06 ± 0.03) E+07
BIOTIC t6	5.7	1.023 ± 0.896	0.923 ± 0.692	0.010 ± 0.008	< 0.001	< 0.001	< 0.001	1.958 ± 0.484	(0.26 ± 0.39) E+07
BIOTIC t7	9.7	0.186 ± 0.311	1.700 ± 0.291	0.008 ± 0.007	< 0.001	< 0.001	< 0.001	1.895 ± 0.028	(1.02 ± 0.34) E+07
BIOTIC t8	11.9	0.002 ± 0.001	1.626 ± 0.076	< 0.001	< 0.001	< 0.001	< 0.001	1.630 ± 0.078	(0.90 ± 0.35) E+07
Arsenite BIOTIC III									
BIOTIC t0	0.0	1.848 ± 0.093	0.088 ± 0.004	0.001 ± 0.001	0.000 ± 0.000	0.000 ± 0.000	0.000 ± 0.000	1.938 ± 0.096	(0.02 ± 0.004) × 10 ⁷
BIOTIC t1	0.7	1.730 ± 0.111	0.107 ± 0.005	0.003 ± 0.001	0.000 ± 0.000	0.001 ± 0.001	0.000 ± 0.000	1.842 ± 0.107	(0.04 ± 0.003) × 10 ⁷
BIOTIC t2	1.6	n.d.	n.d.	n.d.	n.d.	n.d.	n.d.	n.d.	(0.06 ± 0.02) × 10 ⁷
BIOTIC t3	1.8	n.d.	n.d.	n.d.	n.d.	n.d.	n.d.	n.d.	(0.08 ± 0.05) × 10 ⁷
BIOTIC t4	2.9	n.d.	n.d.	n.d.	n.d.	n.d.	n.d.	n.d.	(0.12 ± 0.06) × 10 ⁷
BIOTIC t5	3.7	n.d.	n.d.	n.d.	n.d.	n.d.	n.d.	n.d.	(0.14 ± 0.06) × 10 ⁷
BIOTIC t6	5.7	n.d.	n.d.	n.d.	n.d.	n.d.	n.d.	n.d.	(0.16 ± 0.05) × 10 ⁷
BIOTIC t7	9.7	0.792 ± 0.308	0.905 ± 0.348	0.019 ± 0.005	0.001 ± 0.001	0.000 ± 0.000	0.001 ± 0.000	1.718 ± 0.034	(0.13 ± 0.05) × 10 ⁷
BIOTIC t8	11.9	0.768 ± 0.627	1.122 ± 0.536	0.023 ± 0.011	0.002 ± 0.000	0.002 ± 0.001	0.000 ± 0.000	1.917 ± 0.116	(0.40 ± 0.52) × 10 ⁷

Table S3: Oxidation of thiosulfate ($\text{Na}_2\text{S}_2\text{O}_3 \times 5 \text{H}_2\text{O}$) during growth of *T. ruber* with 8 % O_2 (v/v) in the gas phase at 80 °C. Initial medium pH was 8. Data show average concentrations \pm standard deviation (n=3). The biotic set-up was inoculated with 1 % of a *T. ruber* pre-culture actively growing on thiosulfate.

Thiosulfate BIOTIC vs. ABIOTIC	Incubation time	Sulfate	Thiosulfate	Sum of sulfur species	S-Deficit „$S^0_{\text{calc}}(\text{s})$“^(a)	<i>Thermocrinis ruber</i> OC 14/7/2
Unit	d	mM	mM	mM	mM	Cells/mL
Method	-	IC-ICP-MS	IC-ICP-MS	IC-ICP-MS	calculated	Neubauer Chamber
BIOTIC t0	0.0	0.46 \pm 0.17	8.32 \pm 1.45	8.77 \pm 1.60	0.00 \pm 0.00	(0.02 \pm 0.01) $\times 10^7$
BIOTIC t1	0.3	0.83 \pm 0.13	7.52 \pm 0.46	8.35 \pm 0.48	0.43 \pm 1.71	(0.40 \pm 0.03) $\times 10^7$
BIOTIC t2	0.5	1.19 \pm 0.43	6.39 \pm 1.21	7.58 \pm 1.61	1.19 \pm 2.14	(1.01 \pm 0.21) $\times 10^7$
BIOTIC t3	0.8	1.94 \pm 0.23	6.73 \pm 0.56	8.66 \pm 0.79	0.11 \pm 1.78	(1.82 \pm 0.05) $\times 10^7$
BIOTIC t4	1.0	2.45 \pm 0.59	5.76 \pm 0.85	8.22 \pm 1.44	0.56 \pm 0.89	(1.74 \pm 0.17) $\times 10^7$
BIOTIC t5	1.3	3.12 \pm 0.25	4.13 \pm 0.12	7.25 \pm 0.30	1.53 \pm 1.84	(2.23 \pm 0.16) $\times 10^7$
BIOTIC t6	1.8	4.64 \pm 2.21	2.49 \pm 1.43	7.13 \pm 3.45	1.65 \pm 1.86	(2.24 \pm 0.25) $\times 10^7$
BIOTIC t7	2.6	6.25 \pm 1.06	0.04 \pm 0.05	6.29 \pm 1.01	2.48 \pm 2.29	(4.25 \pm 0.30) $\times 10^7$
BIOTIC t8	4.6	6.50 \pm 1.66	0.01 \pm 0.01	6.51 \pm 1.66	2.26 \pm 1.28	(5.05 \pm 0.90) $\times 10^7$
BIOTIC t9	6.6	6.18 \pm 1.71	0.04 \pm 0.04	6.22 \pm 1.75	2.56 \pm 1.84	(3.05 \pm 0.96) $\times 10^7$
ABIOTIC t0	0.0	0.40 \pm 0.07	6.65 \pm 0.69	7.05 \pm 0.76	0.00 \pm 0.00	-
ABIOTIC t4	1.0	0.45 \pm 0.14	7.03 \pm 0.93	7.48 \pm 1.07	-0.43 \pm 1.43	-
ABIOTIC t7	2.6	0.40 \pm 0.04	6.55 \pm 0.53	6.95 \pm 0.56	0.10 \pm 0.34	-
ABIOTIC t8	4.6	0.59 \pm 0.06	7.61 \pm 0.33	8.21 \pm 0.28	-1.15 \pm 0.55	-
ABIOTIC t9	6.6	0.53 \pm 0.20	6.61 \pm 0.85	7.13 \pm 1.01	-0.08 \pm 1.12	-

(a) Calculation of the S-deficit $S^0_{\text{calc}}(\text{s})$: $S^0_{\text{calc}}(\text{s})(t_x) = \text{Sum of sulfur species}(t_x) - \text{Sum of sulfur species}(t_0)$

Table S4: Oxidation of sulfide ($\text{Na}_2\text{S} \times 9 \text{H}_2\text{O}$) in abiotic controls with 8 % O_2 (v/v) in the gas phase at 80 °C. Initial medium pH was 8. Data show average concentrations \pm standard deviation (n=3). Analogous biotic set-ups, inoculated with 1 % of a *T. ruber* pre-culture actively growing on thiosulfate, showed no growth, but similar abiotic sulfide oxidation and thus were not analyzed by IC-ICP-MS.

Time step	Time [d]	Time [h]	Sulfide (inoculated with <i>T. ruber</i> , but no growth) [mM]	Sulfide abiotic [mM]	Sulfate abiotic [mM]	Thiosulfate abiotic [mM]	Sum of measured sulfur species abiotic [mM]	S-Deficit „ $S^0_{\text{calc}(s)}$ “ ^(c) abiotic [mM]
Method			Methylene blue	Methylene blue	IC-ICP-MS	IC-ICP-MS	Calculated	Calculated
t0	0.0	0.0	4.3 \pm 0.1	4.5 \pm 0.3	0.9 \pm 0.1 ^(a)	0.31 \pm 0.06 ^(b)	5.7 \pm 0.4	0 \pm 0
t1	0.0	0.7	3.5 \pm 0.2	3.6 \pm 0.2	n.d.	n.d.	n.d.	n.d.
t2	0.2	3.7	2.9 \pm 0.3	2.7 \pm 0.3	n.d.	n.d.	n.d.	n.d.
t3	0.3	7.4	2.0 \pm 0.2	2.0 \pm 0.3	1.8 \pm 0.1	1.28 \pm 0.09	5.0 \pm 0.3	\sim 0.7 \pm 0.1
t4	0.8	18.5	0.6 \pm 0.1	0.7 \pm 0.2	n.d.	n.d.	n.d.	n.d.
t5	1.0	24.8	0.1 \pm 0.04	0.3 \pm 0.2	1.8 \pm 0.4	1.85 \pm 0.41	4.0 \pm 0.9	\sim 1.7 \pm 1.0

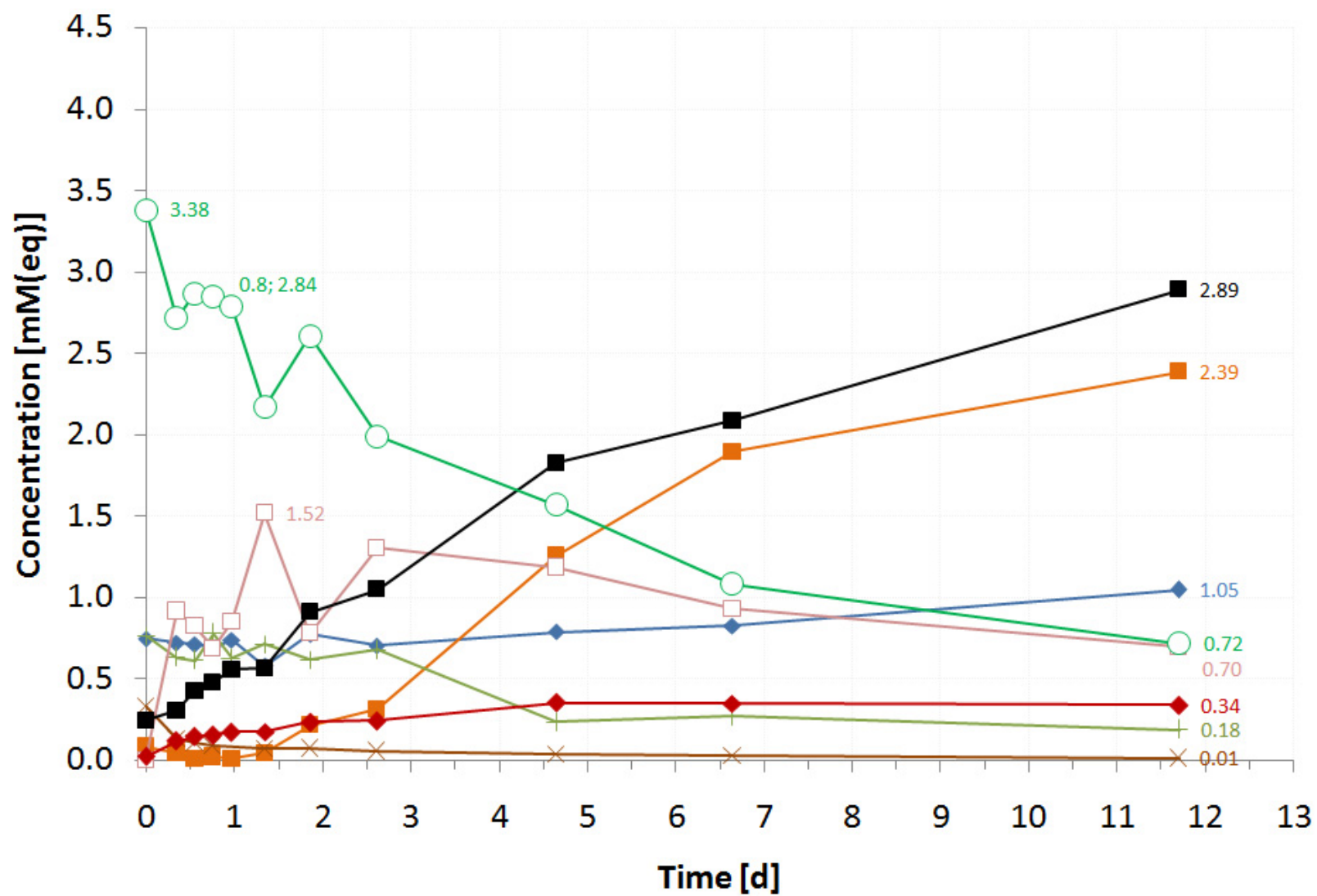
(a) Initial sulfate concentrations constitute background concentrations of OS-Medium;

(b) initial thiosulfate concentrations probably are the result of a spontaneous sulfide oxidation (prior to start of incubation at 80 °C).

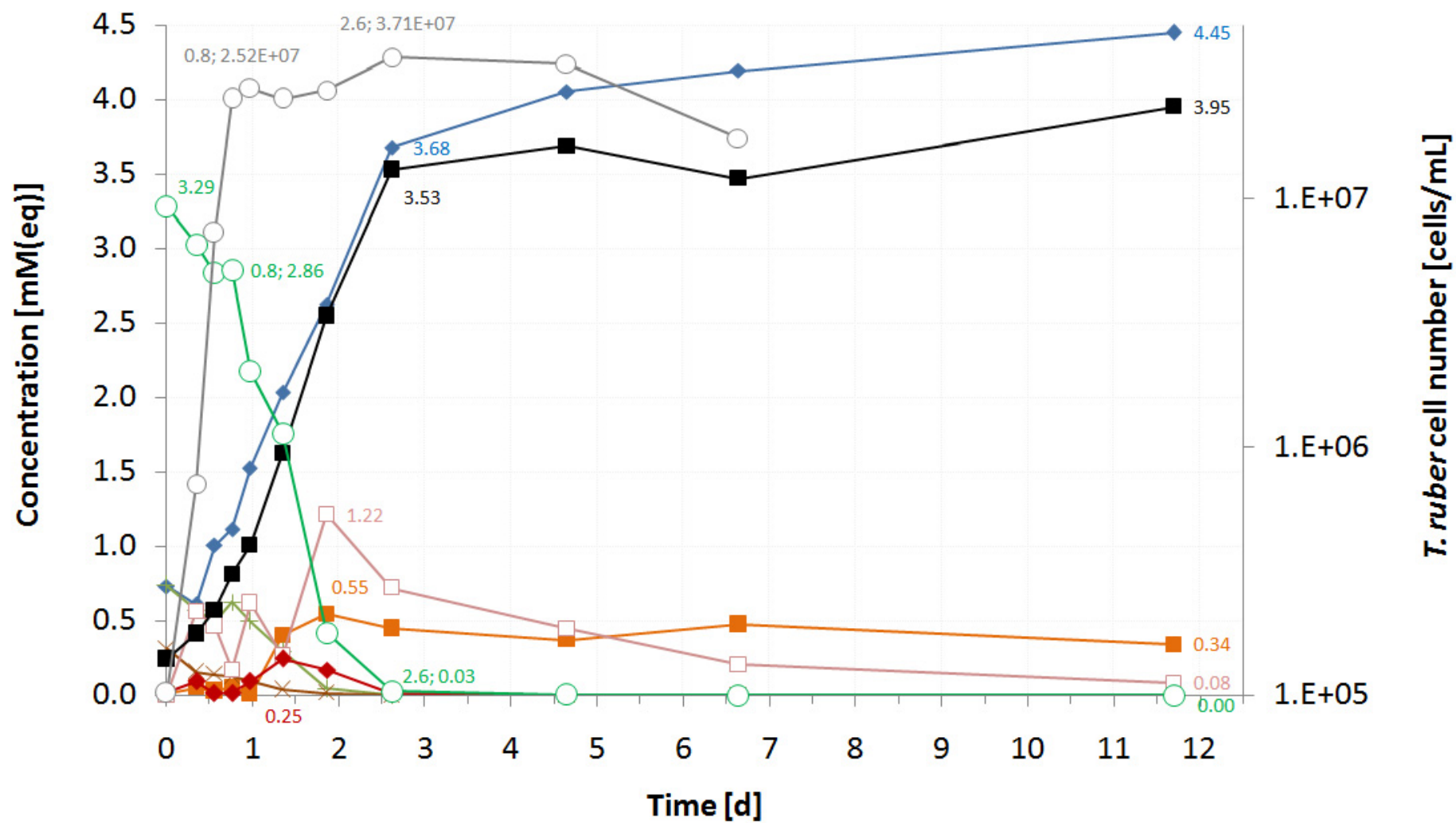
(c) Calculation of the S-deficit $S^0_{\text{calc}(s)}$: $S^0_{\text{calc}(s)}(t_x) = \text{Sum of sulfur species}(t_x) - \text{Sum of sulfur species}(t_0)$

Further Comments: Final percentage of sulfur species (after correction of sulfate data with initial sulfate medium background) **within 25 hours (t5):** \sim 36 % of sulfur deficit due to formation of elemental sulfur; \sim 39 % thiosulfate and \sim 19 % sulfate formed by sulfide oxidation; whereas $<$ 7 % of sulfide remained.

(S1a) ABIOTIC Monothioarsenate all data and time steps



(S1b) BIOTIC (*T. ruber*) Monothioarsenate all data and time steps



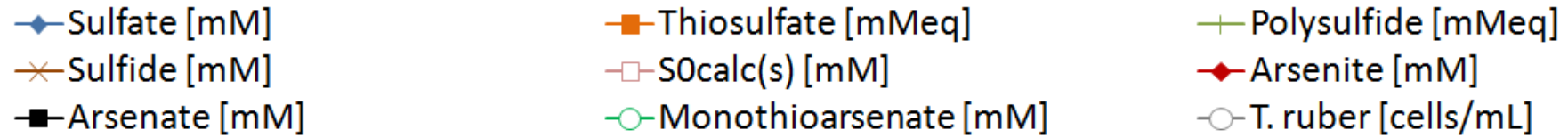
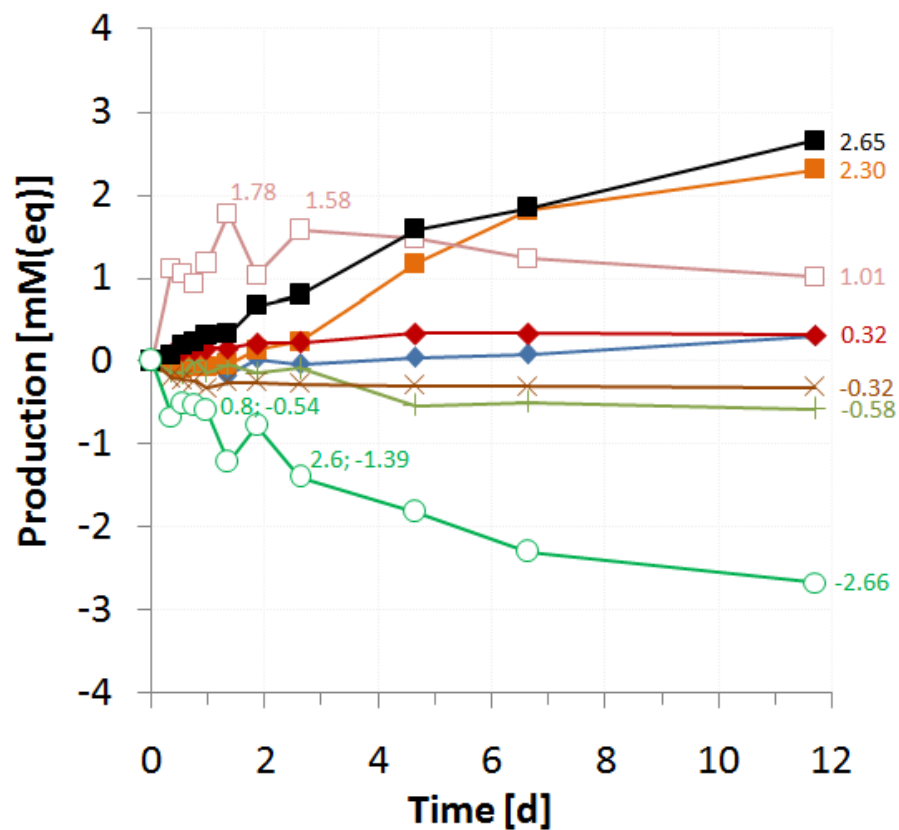
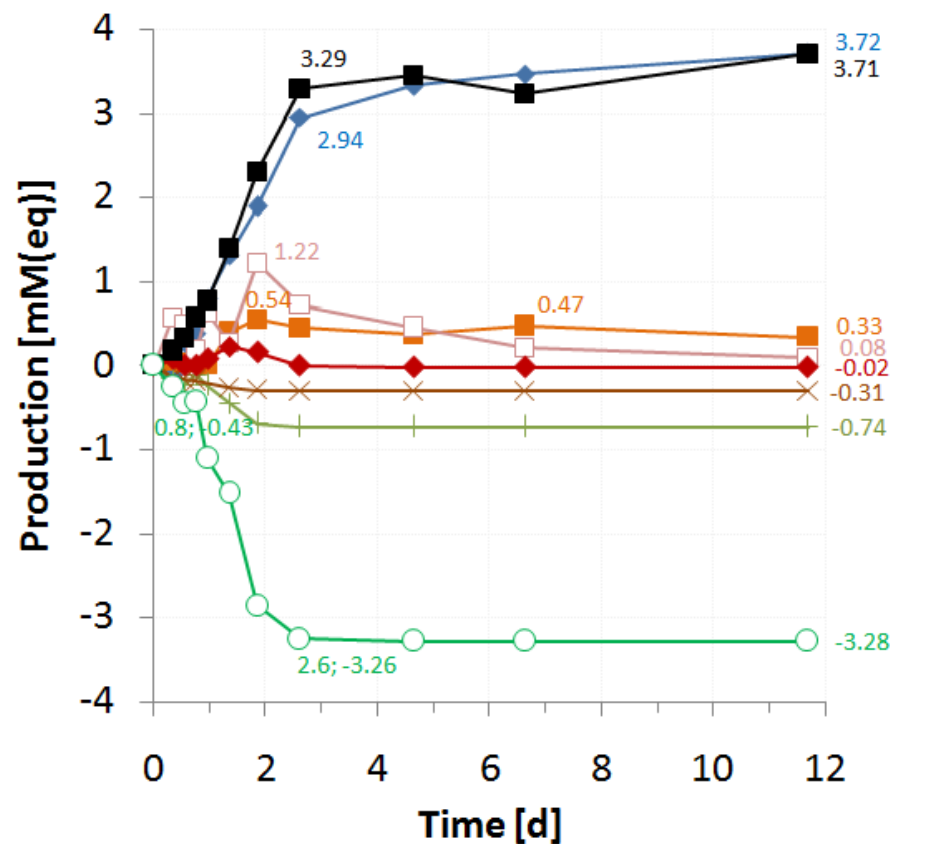


Figure S1: Diagrams of (a) abiotic controls and (b) biotic, *T. ruber* inoculated experiments, supplied with monothioarsenate (n=3). All available data and sampling time steps measured in monothioarsenate experiments are represented in one diagram. These data correspond to the data represented in Figure 1 of the manuscript. Please note that the data for day 11.7 were not shown in Fig.1, for better visibility of the early, more important processes.

(S2a) ABIOTIC Production



(S2b) BIOTIC Production



◆ Sulfate [mM]
□ S0calc(s) [mM]

■ Thiosulfate [mM]
◆ Arsenite [mM]

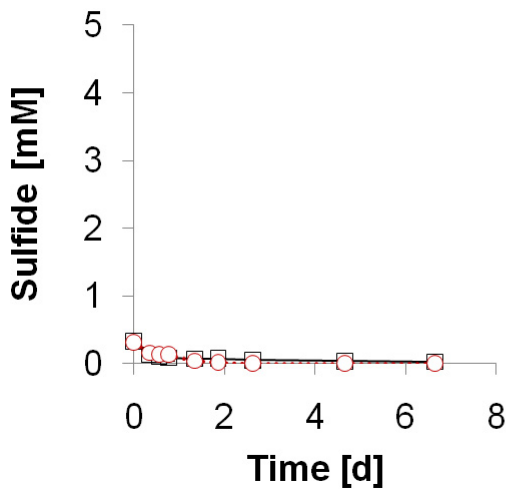
+ Polysulfide [mM]
■ Arsenate [mM]

× Sulfide [mM]
○ Monothioarsenate [mM]

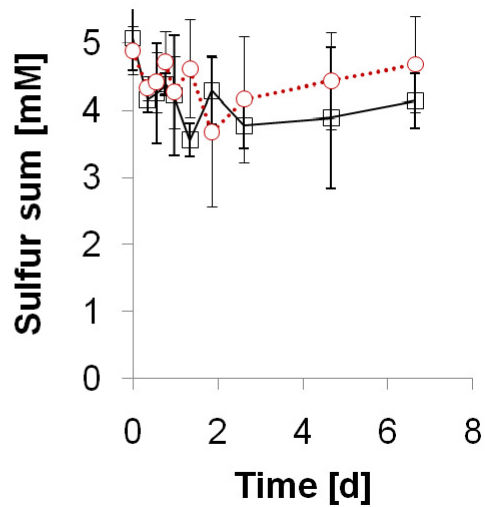
—◆— Sulfate [mM] —■— Thiosulfate [mMeq] —+— Polysulfide [mMeq] —×— Sulfide [mM]
—□— SO₄calc(s) [mM] —◆— Arsenite [mM] —■— Arsenate [mM] —○— Monothioarsenate [mM]

Figure S2: Production in (a) abiotic controls and (b) biotic, *T. ruber* inoculated experiments, supplied with monothioarsenate (n=3). For this graphical display, the available data for each sampling point were subtracted by their respective start concentration. These data refer to the experiment displayed in Figure 1 of the manuscript section. Please note that for better visibility of the early, more important processes the data for day 11.7 were not shown in Fig.1 of the manuscript (but were displayed in Fig S4, and listed in Table S1).

(S3a) Sulfide



(S3b) Sulfur sum



(S3c) Arsenic sum

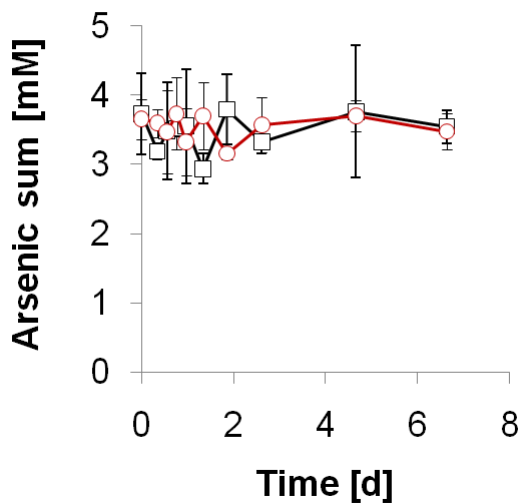
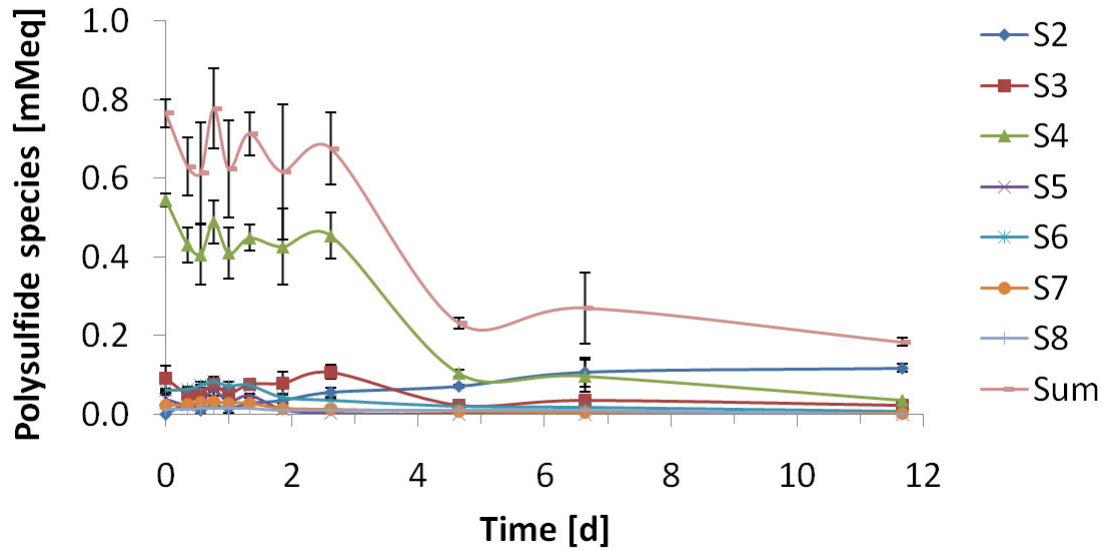


Figure S3: Graphical display of the results for the parameters (a) sulfide, (b) sulfur sum and (c) arsenic sum during oxidation of **monothioarsenate** ($\text{Na}_3\text{AsSO}_3 \times 7 \text{H}_2\text{O}$) and during growth of *T. ruber* with 8% O_2 in the gas phase in a medium of pH 8. The biotic set-ups received 1% of a *T. ruber* pre-culture actively growing on monothioarsenate as inoculum. Graphs show average concentrations \pm standard deviation ($n=3$), displayed by error bars. For better visibility, only results up to day 6.6 are displayed, all data including those of day 11.7 can be found in Table S1.

(S4a) Polysulfide Speciation during abiotic monothioarsenate transformation



(S4b) Polysulfide Speciation during biotic monothioarsenate transformation

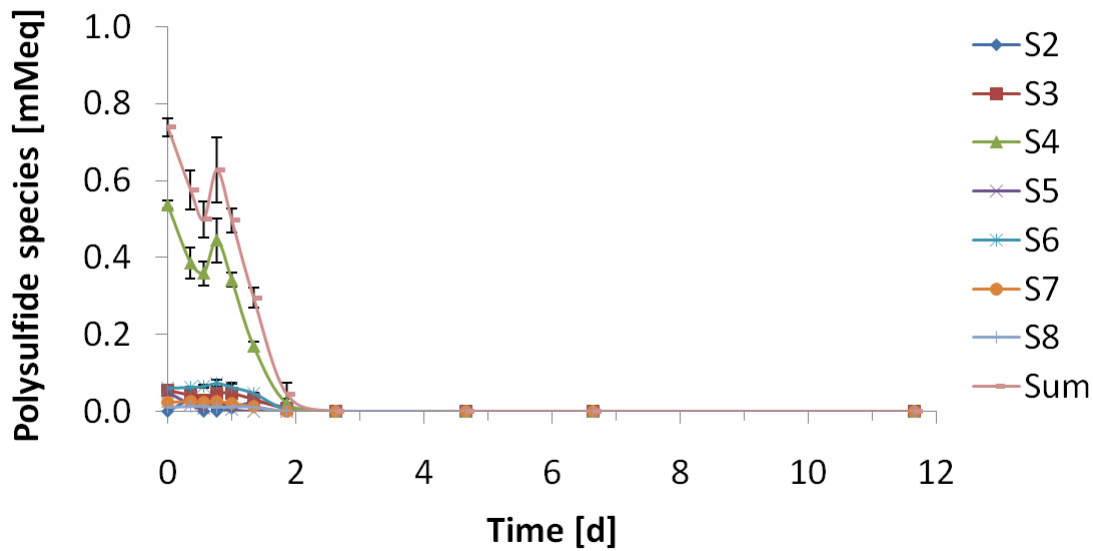


Figure S4: Polysulfide species and the sum of polysulfide species as detected in (a) abiotic controls and (b) biotic experiments (inoculated with *T. ruber* OC14/7/2) supplied with monothioarsenate (n=3). These data refer to the experiment displayed in Fig. 1 of the manuscript. Please note that the data for day 11.7 were not shown in Fig.1, for better visibility of the early, more important processes.

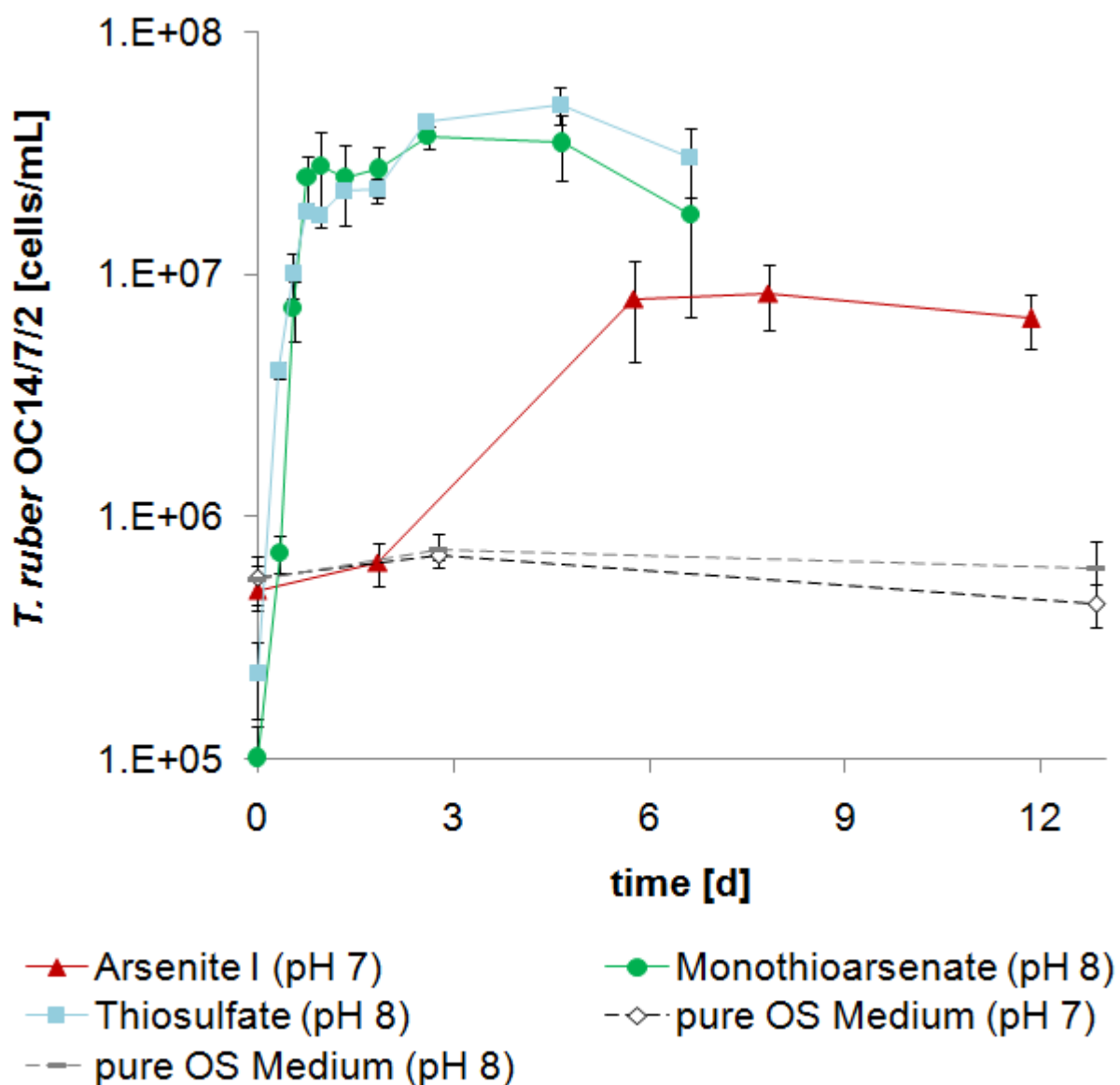
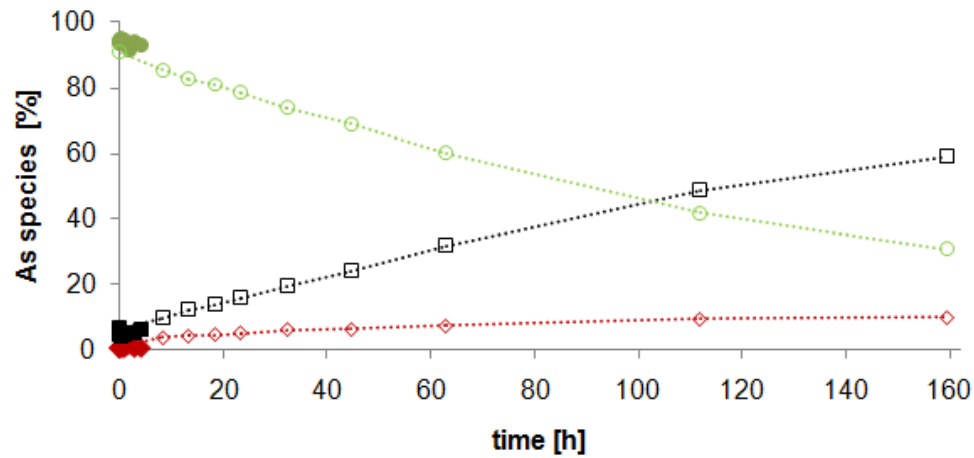
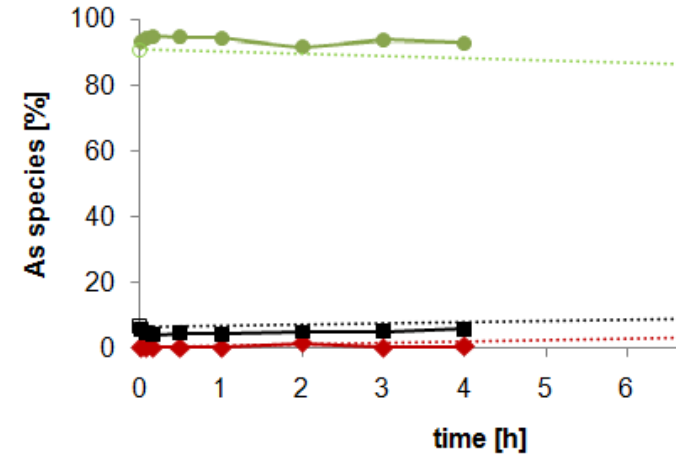


Figure S5: Cell counts during growth of *Thermocrinis ruber* OC14/7/2 in the presence of arsenite, monothioarsenate and thiosulfate as electron donors (Table S1-3; Fig. 1-3) vs. experiments using pure OS-Medium (pH 7 or pH 8) without addition of electron donors. Error bars indicate means of three replicates \pm standard deviation.

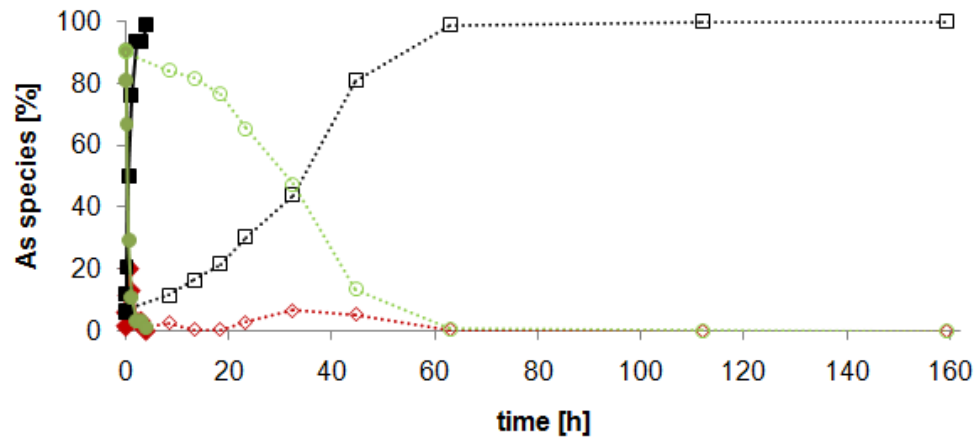
(S6a) ABIO (159 hours) - time scale laboratory experiments



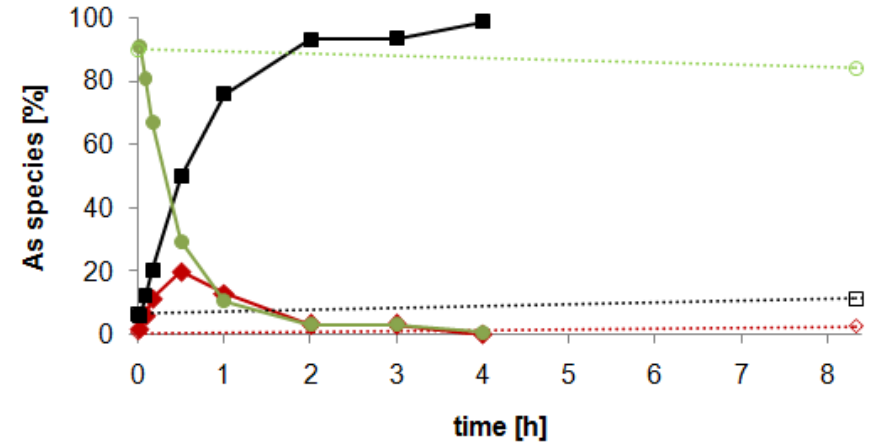
(S6b) ABIO (8.4 hours) - time scale field experiments



(S6c) BIO (159 hours) - time scale laboratory experiments



(S6d) BIO (8.4 hours) - time scale field experiments



—◆— on-site arsenite [% of As sum]
—■— on-site arsenate [% of As sum]
—●— on-site monothioarsenate [% of As sum]

—◆— lab arsenite [% of As sum]
—■— lab arsenate [% of As sum]
—●— lab monothioarsenate [% of As sum]

Figure S6: Comparison of results from laboratory batch experiments (this study) and earlier on-site incubation experiments at Conch Spring (YNP, USA; Härtig, Planer-Friedrich 2012) with supplemental monothioarsenate. Graphs (b) ABIOTIC and (d) BIOTIC highlight the first 8 h of the same incubations presented in graphs (a) ABIOTIC and (c) BIOTIC over a 159 hour (6.6 days) time interval, respectively. Since distinctly different start concentrations were used in the lab vs. field-site, respectively, we displayed relative percentages of single species [%] with respect to the sum of arsenic species. Please mind that microbial oxidation of ~ 3.3 mM monothioarsenate (lab experiment, sealed pressurized headspace with 8 % O₂ (v/v)) indeed took longer than oxidizing 60 μM (field-site, open headspace/atmospheric pressure). However, the observed products were similar. Note also that quantities of applied biomass were different. Start cell numbers of a pure *Thermocrinis ruber* culture were 1×10^5 cells/mL in the lab, facing 3.3 mM monothioarsenate. The field experiments applied 2 mL alive streamer biomass (diverse microbial community, containing *Thermocrinis* spp.; Planer-Friedrich *et al.* 2009), facing 60 μmol/L monothioarsenate. Though the exact cell number in the field experiments was unknown, the applied cell numbers presumably were far higher than lab cell numbers. Moreover, the gas-pressure and oxygen supply was different (lab: sealed pressurized headspace, 2.5 bar N₂ with 8% oxygen; field: open headspace, atmospheric pressure).

Study 6

Reproduced with permission from

Ion-Pair Chromatography Coupled to Inductively Coupled Plasma-Mass Spectrometry (IPC-ICP-MS) as a Method for Thiomolybdate Speciation in Natural Waters

Regina Lohmayer, Gloria Maria Susanne Reithmaier, Elvira Bura-Nakić,

Britta Planer-Friedrich

Analytical Chemistry, 2015, 87, pp 3388-3395

Copyright 2015 American Chemical Society

Ion-Pair Chromatography Coupled to Inductively Coupled Plasma–Mass Spectrometry (IPC-ICP-MS) as a Method for Thiomolybdate Speciation in Natural Waters

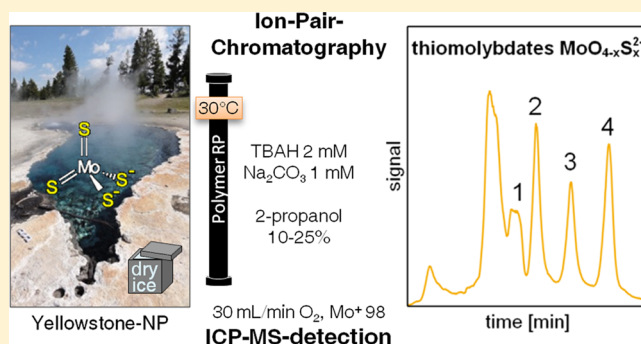
Regina Lohmayer,[†] Gloria Maria Susanne Reithmaier,[†] Elvira Bura-Nakić,[‡] and Britta Planer-Friedrich^{*†}

[†]Department of Environmental Geochemistry, Bayreuth Center for Ecology and Environmental Research (BayCEER), University of Bayreuth, Universitaetsstrasse 30, 95440 Bayreuth, Germany

[‡]Center for Marine and Environmental Research, Ruđer Bošković Institute, Bijenička 54, 10000 Zagreb, Croatia

ABSTRACT: Molybdenum precipitates preferentially under reducing conditions; therefore, its occurrence in sediment records is used as an indicator of paleoredox conditions. Although thiomolybdates ($\text{MoO}_{4-x}\text{S}_x^{2-}$ with $x = 1-4$) supposedly are necessary intermediates in the process of molybdenum precipitation under anoxic conditions, there is no information about their abundance in natural environments, because of a lack of element-specific methods with sufficiently low detection limits. Here, we optimized ion-pair chromatographic separation for coupling to an inductively coupled plasma–mass spectrometry detector (IPC-ICP-MS). 2-Propanol (10%–25% gradient) replaced the previously used acetonitrile (25%–75%) as the solvent, to reduce the carbon

load into the plasma. In synthetic solutions, formation of thiomolybdates was found to occur spontaneously in the presence of excess sulfide and the degree of thiolation was highest at pH 7. Excess hydroxyl led to a transformation of thiomolybdates to molybdate. Under acidic to neutral conditions, precipitation of molybdenum and hydrolysis of tetrathiomolybdate were observed. Flash-freezing was found to be suitable to stabilize tetrathiomolybdate, with <4% transformation over more than two months. High ionic strengths matrices (>2 mM) negatively affected the detection of molybdate, which eluted mainly in the dead volume, but had no negative effect on higher thiolated molybdates. Detection limits were ~10 nM. With the newly developed IPC-ICP-MS method, thiomolybdates were found to form spontaneously in euxinic marine waters after adding a molybdate spike and occur naturally in sulfidic geothermal waters.



The transition metal molybdenum (Mo) serves as an important paleo-proxy in the environment. Since Mo is mobile in its oxidic form as molybdate (MoO_4^{2-}), but precipitates preferentially under sulfidic conditions, the occurrence of Mo in sediments can provide information about the redox milieu during the time of deposition.¹ The exact mechanism of Mo burial in sediments is still unclear. Different possible pathways include reduction with subsequent adsorption and precipitation,² association with organic matter,³ precipitation within an iron mineral phase,⁴ and the reaction with polysulfides [$(\text{S}^0\text{S}^{2-})_n$] to Mo–S species, which can be scavenged, for example, by iron compounds.⁵ A summary has been provided by Chappaz et al.⁶

A crucial step in all these scenarios is assumed to be the formation of aqueous thiomolybdate species ($\text{MoO}_{4-x}\text{S}_x^{2-}$ with $x = 1-4$). In sulfidic solutions, a stepwise ligand exchange leads from molybdate (via the intermediate species monothiomolybdate, dithiomolybdate, and trithiomolybdate) to tetrathiomolybdate, which is the thermodynamically stable end-product.⁷ In natural systems, the occurrence of thiomolybdates was predicted based on thermodynamic calculations for Lake Rogoznica, which is a stratified saltwater lake on the Adriatic

coast of Croatia. Tetrathiomolybdate was found to be the predominant species in the euxinic waters below the chemocline.⁴

Despite their supposedly important role, thiomolybdates have never been measured in the environment. This can be attributed to environmentally low Mo concentrations in the nanomolar range⁸ and the lack of an analytical method, which is sensitive enough to detect nanomolar concentrations of thiomolybdates. Thiomolybdates can be determined by ultraviolet–visible (UV-Vis) spectroscopy.^{9–11} However, impurities in synthesized thiomolybdate standards and overlapping spectra constitute problems for quantification. Moreover, a low sensitivity and possible interferences by other trace elements or matrix components make UV-Vis spectroscopy unsuitable for the determination of thiomolybdates in natural samples.

Another possibility for analysis of thiomolybdates was published by Weiss et al.¹² They used a polymeric reversed-phase column and tetrabutylammonium hydroxide as an ion-

Received: December 14, 2014

Accepted: February 23, 2015

Published: February 23, 2015

pair reagent to separate the different Mo species. Isocratically, the eluent contained 25% acetonitrile. For gradient elution, the acetonitrile concentration was increased from 25% to 75%. Baseline separation of dithiomolybdate, trithiomolybdate, and tetrathiomolybdate could be achieved, while molybdate and monothiomolybdate were eluted as double peaks. Detection was performed using suppressed conductivity or a UV detector. Since this method is not element-specific and suffers from a low sensitivity, it is not suitable for the determination of thiomolybdates at environmentally relevant concentrations.

In order to determine thiomolybdates in the nanomolar concentration range, an element-specific detection is necessary to minimize the disturbing influence of matrix components. One detection system suitable for determining trace levels of elements is inductively coupled plasma–mass spectrometry (ICP-MS). In order to be able to use ICP-MS for detection, the chromatographic method of Weiss et al.¹² requires adaptation, because, at most ICP-MS instruments, the plasma is extinguished at acetonitrile concentrations of >10%.

In the present study, we therefore reproduced the ion-pair chromatography (IPC) method of Weiss et al.¹² initially with a UV detector and searched for alternative solvents that could be used with ICP-MS detection. We investigated the formation of thiomolybdates from molybdate and sulfide over time and the stability of tetrathiomolybdate during storage and at different pH values. Furthermore, the effect of salt concentrations on chromatographic separation was tested. Finally, the method was applied to analyze different natural samples for the occurrence of thiomolybdates.

■ MATERIALS AND METHODS

Analytical Methods. Determination of Mo Species by HPLC-UV. Mo species were analyzed using high-performance liquid chromatography (HPLC) (Merck Hitachi, Model L-2130 pump, Model L-2200 autosampler, and Model L-2420 UV-Vis detector) with separation by a reversed-phase polymeric column (Dionex, IonPac NS1, 10 μm , 250 \times 4 mm). The eluent contained 2 mM tetrabutylammonium hydroxide ($(\text{CH}_3\text{CH}_2\text{CH}_2\text{CH}_2)_4\text{N}(\text{OH})$, CAS No. 2052-49-5, Fluka), 1 mM sodium carbonate (Na_2CO_3 , CAS No. 497-19-8, Merck), and varying amounts of different solvents. Routinely, gradient elution by acetonitrile ($\text{C}_2\text{H}_5\text{N}$, HPLC gradient grade, CAS No. 75-05-8, Roth) was used. Initially, the solvent consisted of 25% acetonitrile and 75% ultrapure water (Merck, Millipore, 18.2 $\text{m}\Omega/\text{cm}$, 3 ppb total organic carbon at 25 $^\circ\text{C}$). Within 15 min, the acetonitrile concentration was increased up to 50%, decreased back to 25% within 0.1 min, and kept constant for the last 4.9 min. Alternatively, isocratic elution by 25% acetonitrile, 10% 1-propanol ($\text{CH}_3\text{CH}_2\text{CH}_2\text{OH}$, CAS No. 71-23-8, for analysis, Grüssing), and 13% 2-propanol ($(\text{CH}_3)_2\text{CHOH}$, CAS No. 67-63-0, AnalaR NORMAPUR, VWR) was tested. Gradient elution was performed with 1-propanol and 2-propanol, where the solvent concentration was increased from 10% to 25% within 10 min, kept constant for 5 min, decreased back to 10% within 1 min, and kept constant for the last 6 min. With 1-propanol and 2-propanol in the eluent, the column was heated to 30 $^\circ\text{C}$. The flow rate was 1 mL/min, the injection volume was 100 μL , and the detection wavelength was 254 nm.

Concentrations of molybdate and tetrathiomolybdate were determined by comparison with commercially available standards of ammonium molybdate ($(\text{NH}_4)_2\text{MoO}_4$, CAS No. 13106-76-8, Sigma–Aldrich) and ammonium tetrathiomolybdate

($(\text{NH}_4)_2\text{MoS}_4$, CAS No. 15060-55-6, Sigma–Aldrich). Since the tetrathiomolybdate salt for standard preparation was not completely soluble in water, the actual Mo concentration of the stock solution was determined by ICP-MS. Standards for monothiomolybdate, dithiomolybdate, and trithiomolybdate are not commercially available. Hence, the absorbance of the thio-intermediates at 254 nm was compared to that of molybdate, based on data from the literature.^{11,13,14} This comparison revealed that the absorbances of monothiomolybdate, dithiomolybdate, and trithiomolybdate were 2.3, 4.4, and 7.1 times higher, respectively, than that of molybdate. With these factors and the actual measured calibration data for molybdate, the respective calibration curves for the intermediate thiomolybdates could be calculated with some uncertainty. In the case of overlapping peaks, the unavoidable error in the assignment of peak areas to individual species and the different absorbances led to overestimation or underestimation of the respective species concentrations.

Determination of Mo Species by IPC-ICP-MS and Total Mo by ICP-MS. When using ICP-MS as a detection system for thiomolybdates, the same reversed-phase polymeric column (Dionex, IonPac NS1, 10 μm , 250 \times 4 mm) as that described for HPLC-UV was used with the ion chromatography (IC) system (Model ICS-3000 SP, Dionex). The eluent also contained 2 mM tetrabutylammonium hydroxide ($(\text{CH}_3\text{CH}_2\text{CH}_2\text{CH}_2)_4\text{N}(\text{OH})$, CAS No. 2052-49-5, Fluka) and 1 mM sodium carbonate (Na_2CO_3 , CAS No. 497-19-8, Merck). Gradient elution with 2-propanol from 10% to 25% was used as described previously. The column was heated to 30 $^\circ\text{C}$, the injection volume was 100 μL , and the flow rate was 1 mL/min. Mo species were detected by ICP-MS (XSeries2, Thermo-Fisher) as Mo^+ (m/z 98). A flow of 30 mL/min O_2 was added to the spray chamber to oxidize excess organic carbon from the eluent. All Mo species were quantified via the molybdate calibration curve. Total Mo concentrations were determined by ICP-MS as Mo^+ (m/z 98). Sensitivity changes of the instrument over time were corrected using an internal rhodium standard (Ultra Scientific Analytical Solutions, N. Kingstown, RI, USA).

Laboratory Experiments. Experiments concerning the formation and stability of thiomolybdates were conducted inside a glovebox (COY , N_2/H_2 95/5 (v/v)). Stock solutions of ammonium molybdate ($(\text{NH}_4)_2\text{MoO}_4$, CAS No. 13106-76-8, Sigma–Aldrich), ammonium tetrathiomolybdate ($(\text{NH}_4)_2\text{MoS}_4$, CAS No. 15060-55-6, Sigma–Aldrich), sodium sulfide nonahydrate ($\text{Na}_2\text{S}\cdot 9\text{H}_2\text{O}$, CAS No. 1313-84-4, Sigma–Aldrich), and potassium polysulfide (K_2S_x , CAS No. 37199-66-9, Sigma–Aldrich) were prepared in N_2 -purged ultrapure water inside the glovebox. From the polysulfide stock solution, samples were taken for the analysis of sulfide and polysulfides. Sulfide was determined using the methylene blue method,¹⁵ whereby the absorption was measured at 650 nm (Infinite 200 PRO, TECAN). Derivatization and determination of polysulfides was done according to Kamyshny et al.¹⁶ and Rizkov et al.,¹⁷ using the HPLC system mentioned above and a reversed-phase C18 column (Waters-Spherisorb, ODS2, 5 μm , 250 \times 4.6 mm) for analysis. With this method, elemental sulfur could also be detected.

A nominal Mo concentration of 200 μM was chosen for all experiments. Since the tetrathiomolybdate salt did not dissolve completely, the actual Mo concentration of the stock solution was determined by ICP-MS. Experimental solutions were prepared in 50-mL polypropylene (PP) vials with screw caps

(Sarstedt). The desired pH values were adjusted by NaOH, HCl, or HNO₃. Solutions for experiments to be conducted in darkness were protected from light by a light-tight box. To investigate the stability of tetrathiomolybdate after flash-freezing, the solution prepared inside the glovebox was aliquoted in 2-mL cryotubes, which were flash-frozen with liquid nitrogen at $-196\text{ }^{\circ}\text{C}$ and stored in a freezer at $-20\text{ }^{\circ}\text{C}$ until analysis. In the solutions stored at room temperature in the glovebox, pH values were measured by a Hach electrode (Model PHC101) connected to a Hach pH-meter (Model HQ40d). Solutions with macroscopically visible particles were filtered (200 nm, cellulose-acetate filter, Membrex) before analysis of Mo speciation.

To test the influence of matrix components on chromatographic separation, mixtures of 250 nM ammonium molybdate, 300 nM ammonium tetrathiomolybdate, and varying sodium chloride (NaCl, CAS No. 7647-14-5, Merck) concentrations were analyzed by IPC-ICP-MS. In addition, mixtures of 200 μM ammonium molybdate and varying concentrations of sodium sulfate (Na₂SO₄, CAS No. 7757-82-6, Merck) were analyzed by HPLC-UV.

Field Sampling. Lake Rogoznica, Croatia. To investigate thiomolybdate formation in natural samples, an incubation experiment was performed on-site at Lake Rogoznica on February 18, 2014. A water sample was obtained using a Niskin sampler from a depth of 12 m and was placed in a serum bottle to which 250 nM molybdate were added and then was sealed airtight with butyl rubber stoppers and aluminum caps. Sampling of the solution was performed after a reaction time of 60 min with a needle and a syringe. The presence of sulfide was determined immediately using the methylene blue method (Hach method 8131). Samples for the analysis of Mo species were filtered (200 nm, cellulose-acetate filter, Membrex), flash-frozen with liquid nitrogen, and stored frozen until analysis. For the analysis of total Mo concentrations in the lake, 10 mL of the sample taken by the Niskin sampler was filtered (200 nm, cellulose acetate filter, Membrex) and acidified with 100 μL of 8 M HNO₃ (CAS No. 7697-37-2, $\geq 65\%$, Sigma–Aldrich).

Yellowstone National Park. Sampling of 47 geothermal hot springs in Yellowstone National Park was performed in August and September 2014. From several hot springs, replicate samples were taken from the source or from different positions of the drainage channels. Sulfide was determined on-site by the methylene blue method (Hach method 8131). A WTW SenTix 41-3 and a WTW TetraCon 325 electrode connected to a WTW multimeter (Multi 340i) were used to measure pH and conductivity, respectively. Samples for Mo species analysis were filtered (200 nm, cellulose-acetate filter, Membrex) and flash-frozen with dry ice on-site. For the analysis of total Mo concentrations, 15 mL of sample were filtered (200 nm, cellulose-acetate filter, Membrex) and 375 μL of H₂O₂ (CAS No. 7722-84-1, 30%, VWR) and 375 μL of 8 M HNO₃ (CAS No. 7697-37-2, $\geq 65\%$, Sigma–Aldrich) were added.

RESULTS AND DISCUSSION

Development of an IPC-ICP-MS Method for Thiomolybdate Analysis. By reproducing the HPLC method previously published by Weiss et al.,¹² using an isocratic eluent of 25% acetonitrile on a mixture of molybdate and sulfide, peaks corresponding to monothiomolybdate, dithiomolybdate, trithiomolybdate, and mainly tetrathiomolybdate were observed (Figure 1a). In comparison to the chromatogram published by Weiss et al.,¹² retention of all species was higher, e.g.,

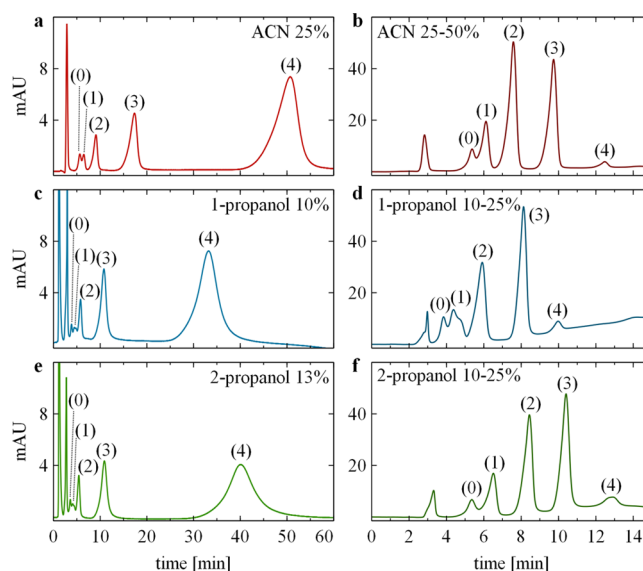


Figure 1. Separation of molybdate (denoted as peak “(0)”) and thiomolybdates (denoted as peaks “(1)–(4)”) by an IonPac NS1 column with an eluent composition of 2 mM tetrabutylammonium hydroxide, 1 mM Na₂CO₃, and different solvent compositions (determination by HPLC-UV); (thio)molybdate peaks are labeled by their number of S atoms. For isocratic elutions (panels (a), (c), and (e)), a thiomolybdate mixture with mainly tetrathiomolybdate was analyzed. For gradient elutions (panels (b), (d), and (f)), a solution with minor amounts of tetrathiomolybdate and larger shares of intermediate species was chosen.

tetrathiomolybdate eluted almost 30 min later, and the peaks were wider. This may partially be attributed to the fact that our column was 5 cm longer than that used by Weiss et al.¹²

In a further step, we used gradient elution with 25%–50% acetonitrile (Figure 1b). A gradient program (25%–75% acetonitrile) had already been suggested by Weiss et al.¹² for the analysis of poly(thiomolybdates), which bind stronger to the stationary phase than mononuclear molecules. We used a slightly different thiomolybdate mixture with higher amounts of intermediate species, to improve peak separation of molybdate and monothiomolybdate and to test whether minor amounts of tetrathiomolybdate still result in identifiable peaks at the end of the chromatogram. All thiomolybdates eluted within 13 min and the peaks became much narrower, in comparison to isocratic elution. Nevertheless, just as reported by Weiss et al.,¹² we were unable to achieve baseline separation of molybdate and monothiomolybdate with this method.

The next step was to test alternative solvents for acetonitrile, since acetonitrile extinguished the plasma at our ThermoFisher XSeries2 device at concentrations higher than 10%, even when adding oxygen as the plasma gas to oxidize excess organic carbon to CO₂. To reduce the amount of solvent needed, we tested 1-propanol and 2-propanol as solvents with higher elution strength than acetonitrile. Methanol was unsuitable as an alternative solvent, since its elution strength is lower. Because of the higher viscosity, in comparison to acetonitrile, the column was heated to 30 $^{\circ}\text{C}$ when using 1-propanol and 2-propanol. For isocratic and gradient elutions, the same mixtures as those analyzed with acetonitrile with mainly tetrathiomolybdate or high amounts of intermediate species were used, respectively. Isocratic elution with 10% 1-propanol shortened the necessary analysis time (Figure 1c) but separation of molybdate, monothiomolybdate, and dithiomolybdate was

poor. Also, gradient elution with 10%–25% 1-propanol (Figure 1d) resulted in poorer separation of molybdate, monothiomolybdate, and dithiomolybdate, in comparison to the use of acetonitrile. With 13% 2-propanol (Figure 1e), which has a higher elution strength than acetonitrile but a lower one than 1-propanol, the necessary analysis time resides between those for acetonitrile and 1-propanol. However, no separation of molybdate, monothiomolybdate, and dithiomolybdate could be achieved and the tetrathiomolybdate peak was almost 20 min wide. A gradient increase of 2-propanol from 10% to 25% within 10 min and then keeping 25% for the next 5 min (Figure 1f) led to a similar chromatogram than the one achieved with acetonitrile gradient. Yet, no baseline separation of molybdate and monothiomolybdate was obtained.

The last step was to try to adapt the 2-propanol gradient conditions and, hence, optimize peak separation. Several attempts were made (data not shown). A slower linear increase of 2-propanol in 12 min instead of 10 min had no effect on peak separation. A stronger increase of 2-propanol from 10% to 30% within 10 or 12 min led to poorer peak separation. An increase of 2-propanol from 5% to 25% or 30% led to a shift of all peaks to higher retention times and worse peak separation. A gradient from 15% to 25% within 12 min resulted in shorter retention times and poor peak separation. Consequently, gradient elution from 10% to 25% 2-propanol as described in the previous paragraph was the best achievable option for chromatographic thiomolybdate separation and selected for transfer to detection with ICP-MS. Quantification of all thiomolybdate species was done via the molybdate calibration curve. The lowest detectable molybdate concentration was dependent on different background levels; however, on average, the detection limit was ~ 10 nM.

Formation of Thiomolybdates from Molybdate and Sulfide or Polysulfides. To test the spontaneous formation of thiomolybdates in synthetic solutions, a first set of experiments was prepared at different sulfide:molybdate ratios with an initial pH of 7.3, keeping the solutions in darkness. These conditions were chosen to mimic the natural conditions in Lake Rogoznica for which the occurrence of thiomolybdates was previously predicted by modeling.⁴ At a 10-fold excess of sulfide to molybdate, successive sulfidation of molybdate was observed (Figure 2). Immediately after preparation of the mixture, the Mo speciation was dominated by 26% monothiomolybdate and 60% dithiomolybdate. Until day 20, the

concentrations of monothiomolybdate and dithiomolybdate decreased, whereas trithiomolybdate reached its maximum concentration. For tetrathiomolybdate, a continuous increase in concentration could be observed over 60 days. In a comparable experiment with a ~ 10 -fold excess of sulfide to molybdate, Erickson and Helz⁷ observed the stepwise formation of equilibrium concentrations of dithiomolybdate, trithiomolybdate, and tetrathiomolybdate within the time frame of minutes, hours, and days, respectively. In comparison, we observed almost constant levels of all four thiomolybdate species concurrently in solution after 60 days. In contrast to Erickson and Helz,⁷ who could not observe almost any molybdate, we determined increasing molybdate concentrations over time, with a final share of 19%. This might be an indication of gaseous hydrogen sulfide loss and re-equilibration of the solution. This assumption is also supported by the increase of pH from 7.3 to 8.4 over time. After 161 days, a last sample was taken, where a Mo concentration of only ~ 40 μM remained in solution (data not shown). The precipitation of particles was not observed. Instead, an additional peak appeared at the end of the chromatogram, which might be attributed to the formation of polymer thiomolybdates, as described by Weiss et al.¹² From the detectable Mo species, 53% were molybdate, 33% tetrathiomolybdate, 13% trithiomolybdate, and 1% dithiomolybdate. Therefore, tetrathiomolybdate seems to be the thermodynamically most stable thiomolybdenum species, as was also stated by Erickson and Helz.⁷ With a sulfide:molybdate ratio of 20:1, qualitatively, the same processes could be observed (Figure 2), whereby the sulfidation reactions proceeded faster and to a higher extent. Only minor amounts of monothiomolybdate could be observed, and after 60 days, the proportion of higher thiolated molybdates was greater, in comparison to the experiment with 10-fold sulfide excess. After 161 days, a Mo concentration of 138 μM could still be detected in solution, which contained mainly tetrathiomolybdate (63%), followed by molybdate (25%), trithiomolybdate (12%), and dithiomolybdate (1%) (data not shown).

Another set of experiments was conducted to test whether molybdate can react with elemental sulfur (data not shown). To offer elemental sulfur in dissolved form, polysulfides $[(\text{S}^0\text{S}^{-11})_n]^{2-}$ were mixed with molybdate in a nominal ratio of 10:1 and 20:1, respectively. As the molecular mass of the commercially available polysulfide standard was unknown, the sulfur to Mo excess could not be adjusted as exactly as in the sulfide experiments. Later analyses of the free sulfide, polysulfide, and elemental sulfur concentrations of the stock solution showed that the sulfur:molybdate ratio was about 8:1 and 17:1, respectively, and that the total sulfide amount (including sulfide of polysulfides) was about one-fourth in comparison to the molybdate-sulfide experiments. In the polysulfide experiments, molybdate accounted always for at least 60% of the sum of the Mo species. Because of the high amount of molybdate, there was a strong overlap of the molybdate and monothiomolybdate peak, which led to a relatively high error in quantification of the absolute concentrations of those two species. Nevertheless, it was obvious that the thiolation of molybdate proceeded to a much lesser extent in the presence of polysulfides than in the experiments with pure sulfide. After 59 days, only 0.45 and 2.7% of molybdate had transformed to tetrathiomolybdate in the experiments with an 8- and 17-fold excess of sulfur (including free sulfide, polysulfides, and elemental sulfur), respectively.

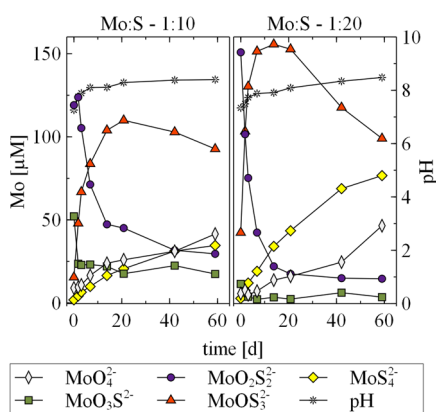


Figure 2. Formation of thiomolybdates in mixtures of 200 μM molybdate and 2 mM sulfide (Mo:S ratio of 1:10) or 4 mM sulfide (Mo:S ratio of 1:20) (determination by HPLC-UV).

In summary, these experiments showed that one decisive parameter for thiomolybdate formation is the sulfide availability or more specifically the sulfide to Mo excess, which influences not only the kinetic of the thiolation reaction but also the equilibrium concentrations of thiomolybdates. In the previously mentioned euxinic bottom waters of Lake Rogoznica for which tetrathiomolybdate was predicted to dominate,⁴ the sulfide to Mo excess is even higher than in our laboratory experiments ($\sim 1.3 \times 10^5$), rendering spontaneous complete transformation of molybdate very likely.

Dependency of Thiomolybdate Formation on pH.

Since the formation of thiomolybdates was described to be an acid-catalyzed process,⁷ mixtures with a 10-fold excess of sulfide versus molybdate were investigated at nominal pH values of 1, 3, 5, 7, 9, 11, and 13. At pH 1, immediate darkening of the solution and formation of black precipitates were observed after 2 days and attributed to the formation of amorphous Mo trisulfide MoS_3 , which precipitates under acidic conditions.^{18,19} At pH 3, the solution turned dark brown and black precipitates were visible after a few days. At pH 5, the solution also turned dark brown but no precipitates were visible. Nevertheless, only around 20 μM molybdate of the nominal 200 μM and minor amounts of thiomolybdates could be detected in solution (Figure 3). The formation of colloidal MoS_3 might explain the

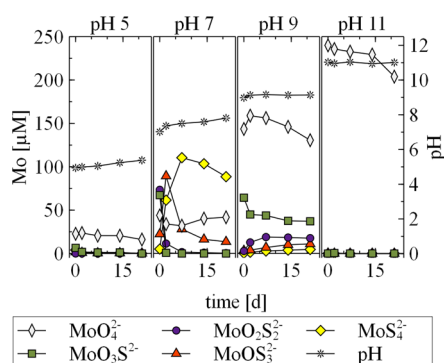


Figure 3. Formation of thiomolybdates in mixtures of 200 μM molybdate and 2 mM sulfide at different pH values (determination by HPLC-UV).

loss of Mo in solution. At pH 7 (Figure 3), the development of Mo speciation over time was comparable to the one described for the previous molybdate–sulfide experiment (Figure 2). The slightly lower initial pH of 7, in comparison to 7.3, led to a faster and higher sulfidation of molybdate. Already after 7 days, 64% of Mo in solution was present as tetrathiomolybdate and a continuous loss of Mo from solution was observable. After 21 days, only 144 μM Mo of the originally measured 212 μM remained in solution. This might again be due to the formation of MoS_3 colloids. At pH 9, a large amount of molybdate was not sulfidized at all (Figure 3). The dominating thiomolybdenum species was monothiomolybdate. At pH 11 (Figure 3) and pH 13 (data not shown), no formation of thiomolybdates could be observed. However, at pH 13, it was also not possible to quantify molybdate, because the alkaline matrix of the solution made peak identification or integration impossible (see also matrix effects discussed below).

Summarizing the pH experiment, we found the highest thiomolybdate formation at pH values in the neutral range. This pH range is in accordance with kinetic studies by Harner and Sykes,²⁰ who concluded that a pH value of ~ 7.3 is most

favorable for thiomolybdate formation, as a compromise between the availability of protons for loosening the Mo–O bond and the dominance of HS^- over H_2S , since HS^- has a higher nucleophilic tendency. Erickson and Helz⁷ determined thiomolybdate formation in ammonia-buffered solutions in the pH range of 7.9–8.5 and found no influence of pH on equilibrium concentrations. However, they found that the concentration of ammonia, which is an acid catalyst, had a high influence on thiomolybdate formation rates. In unbuffered solutions, where the pH increased from 8.0 to 9.0–9.6 over the course of the experiments, they detected only very small amounts of tetrathiomolybdate after four months. Moreover, they simulated Mo speciation for seasonally anoxic systems and found a significant occurrence of the thermodynamically unstable intermediate thiomolybdates. This implies that, especially for environmental systems that are not in equilibrium, parameters such as pH or the presence of catalysts are decisive for the actual prevailing Mo speciation. This again emphasizes the necessity of analyzing thiomolybdates in natural samples.

Stability of Tetrathiomolybdate. To determine the best preservation pH for natural samples, the stability of tetrathiomolybdate as the only commercially available thiomolybdenum species was determined at nominal pH values of 1, 3, 5, 7, 9, 11, and 13. For solutions at pH 1 and 3, black precipitates were again observed (at pH 1 immediately after acidification, and at pH 3 after 2 days), likely due to the formation of MoS_3 . Wildervanck and Jellinek¹⁸ described the immediate formation of MoS_3 precipitates in acidified thiomolybdate solutions for pH values of < 4 . Müller et al.⁹ determined increasing decomposition rates of tetrathiomolybdate with decreasing pH, and Quagraine et al.²¹ observed the formation of polynuclear thiomolybdates in tetrathiomolybdate solutions acidified to pH 2–3. In our case, the formation of polynuclear thiomolybdates would also result in a loss of detectable Mo species. At pH 5 and 7, we observed a decrease of the sum of Mo species in solution over time (Figure 4).

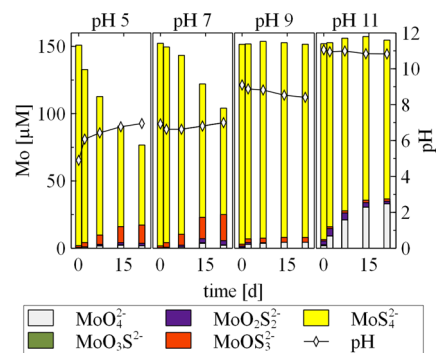


Figure 4. Stability of tetrathiomolybdate at different pH values over time (determination by HPLC-UV).

Wildervanck and Jellinek¹⁸ also described the slow formation of MoS_3 precipitates in thiomolybdate solutions in a pH range of 4–7. At pH 5, the loss of gaseous hydrogen sulfide, which could be linked to the observed pH increase from 5 to 7 (Figure 4), also might have contributed to the destabilization of tetrathiomolybdate. At pH 5 and 7, we observed that a certain amount of tetrathiomolybdate was subject to hydrolysis and mainly transformed back to trithiomolybdate (Figure 4). Clarke et al.¹⁰ studied thiomolybdate hydrolysis in the pH range of 6–

8 and observed an increasing rate with decreasing pH. In contrast to our study, they did not detect intermediate species during the hydrolysis of tetrathiomolybdate and attributed this to increasing reaction rates with proceeding hydrolysis. On the basis of data concerning thiometalate hydrolysis, Weiss et al.¹² concluded that those species are only stable under alkaline conditions. This was true for our experiment at pH 9, where 95% tetrathiomolybdate remained after 21 days (Figure 4). At pH 11, 21% of tetrathiomolybdate directly transformed back to molybdate within 21 days, whereby almost no intermediate thiomolybdate species occurred. This transformation might be attributed to the high amount of OH⁻ in solution and, consequently, the destabilization of thiomolybdate species. This phenomenon has previously been described for thioarsenites, which transform to arsenite at an excess of OH⁻ versus SH⁻.²² At pH 13, only 14 μM tetrathiomolybdate were detectable immediately after preparation of the solution and were already transformed after 2 days (data not shown). As no increase of intermediate thiomolybdate species could be observed in the completely clear solutions, we conclude that Mo was present as molybdate, which could not be detected due to a disturbing matrix effect at the highly alkaline conditions (see matrix effects discussed below). In summary, we conclude that tetrathiomolybdate is most stable under slightly alkaline conditions and acidification to pH <5, e.g., as routine species stabilization method is detrimental for species stability.

The stability of tetrathiomolybdate was tested upon flash-freezing versus storage at room temperature under light and dark conditions in the glovebox (Figure 5). A pH of 7 was

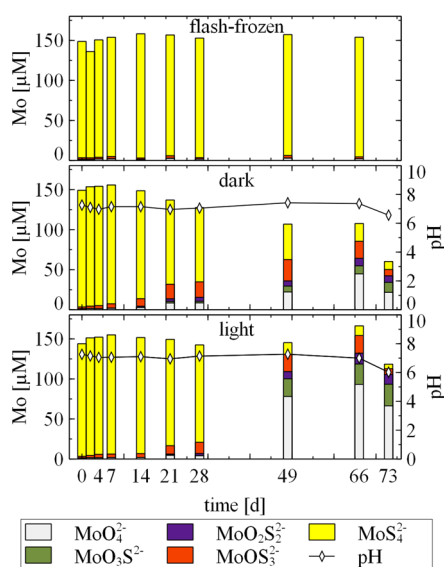


Figure 5. Stability of tetrathiomolybdate at pH 7 under different storage conditions over time (determination by HPLC-UV).

chosen because this approaches natural conditions, for example, in Lake Rogoznica and hydrolysis had been observed at pH 7 over time as described previously. In solutions stored at room temperature, the hydrolysis of tetrathiomolybdate could be observed over time (Figure 5). Up to day 28, hydrolysis seemed to be faster in darkness; after 28 days, it was faster in light. In solutions stored in darkness, the sum of dissolved Mo species seemed to decrease over time to a higher extent, in comparison to those stored in light (Figure 5). However, this difference was not reflected in the results of the total Mo analysis after 49 days,

which were 164 μM in darkness and 175 μM in light. In the flash-frozen samples, tetrathiomolybdate transformation was <4% over 66 days (Figure 5). The same preservation method had been suggested previously for systems with high arsenic and sulfide concentrations, where acidification leads to precipitation of AsS phases, while flash-freezing was found suitable to preserve thioarsenic speciation.²³ Conclusively, flash-freezing seems to be the best currently available method for preserving tetrathiomolybdate in solution.

Influence of Matrix Components on Chromatographic Separation. The effect of high ionic strength on the chromatographic separation was tested in two sets of experiments. While the peak of tetrathiomolybdate was not influenced at all up to NaCl concentrations of 50 mM, which is about one-tenth the NaCl concentration of seawater, the molybdate peak was only unaffected up to 0.2 mM NaCl (Figure 6a). With 2 mM, the formation of a small shoulder to

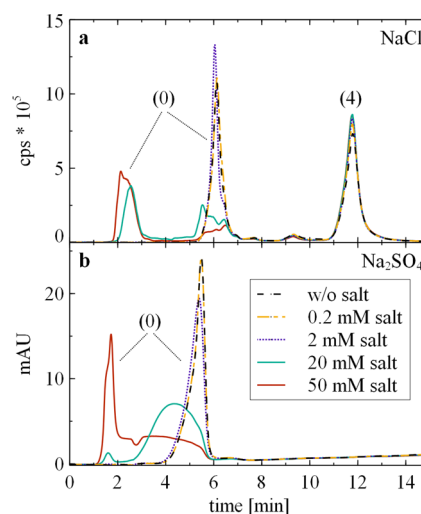


Figure 6. (a) Separation of 250 nM molybdate (denoted as peak “(0)”) and 300 nM tetrathiomolybdate (denoted as peak “(4)”) in the presence of sodium chloride (NaCl) (determination by IPC-ICP-MS). (b) Analysis of 200 μM molybdate (peak “(0)”) in the presence of sodium sulfate (Na₂SO₄) (determination by HPLC-UV).

the right of the molybdate peak was visible. At higher salt concentrations, a splitting of the molybdate peak and partial elution of molybdate in the void volume was observed. Since ICP-MS is an element-specific detector, it could be excluded that the void volume peak originated from NaCl. To investigate whether this disturbing effect was specifically related to the presence of Cl⁻ anions, another test was performed with sodium sulfate (Figure 6b). Since tetrathiomolybdate was not affected by NaCl, these experiments were done with molybdate only, and due to economic reasons with HPLC-UV instead of IPC-ICP-MS. In general, the retention time of molybdate was slightly different in comparison to the analysis with IPC-ICP-MS, because of the different tube lengths between the analytical column and the detector, but again, the presence of the salt had no influence at a concentration of 0.2 mM. With 2 mM sodium sulfate (Na₂SO₄), the Mo peak became somewhat smaller and broader, in comparison to the uninfluenced peak. At 20 and 50 mM, a complete deformation of the molybdate peak and partial shift to the void volume was observable. A similar lack of retention was described for inorganic selenium species in saline matrices, because of competition with matrix substances.²⁴ The

decisive parameter is not the absolute salt concentration but, rather, the similarity in retention of analyte and matrix substances. In our case, molybdate elutes shortly after the void volume. Therefore, all other substances, which are not or hardly retained, will have an influence on molybdate retention. Comparing the results of the NaCl and Na₂SO₄ experiments, it is obvious that the ratio of analyte to salt concentration had no influence, since disturbing matrix effects occurred at the same salt concentrations, regardless of whether Mo was present in nanomolar or micromolar concentrations. The obvious solution of diluting the sample is not a valid option, because Mo concentrations in the environment are in the nanomolar range (and, therefore, already close to the detection limit). For analysis of low concentrations in solutions with high matrix effects, separation of matrix components before analysis without changing Mo speciation would be required.

Determination of Thiomolybdates in Natural Samples. The optimized IPC-ICP-MS method was used to investigate spontaneous formation (Lake Rogoznica) and occurrence (Yellowstone National Park) of thiomolybdates in natural systems. In the euxinic saline bottom waters of Lake Rogoznica, sulfide concentrations were 1.7 mM but the natural total Mo concentration was 15 nM only, which was close to our minimum quantifiable concentration. In combination with the high salinity (35 g/L), including ~28 mM sulfate²⁵ and 600 mM chloride,²⁶ we were not able to get species information for the natural system with our current method. However, to understand generally whether thiomolybdate formation in nature works as spontaneously as shown for the laboratory experiments presented above, we spiked a bottom water sample from a depth of 12 m on-site with 250 nM molybdate, creating a natural sulfide to spiked Mo excess of 6600. After only 1 h, we already detected monothiomolybdate, dithiomolybdate, trithiomolybdate, and tetrathiomolybdate besides the originally spiked molybdate (Figure 7a). Tetrathiomolybdate was the dominant species. Unfortunately, the saline sample matrix caused splitting and shift of the molybdate peak, preventing a fully

quantitative interpretation. Despite the semiquantitative nature of the data, the findings of this spike experiment confirm the results of the laboratory experiments that sulfide excess is also a decisive parameter for thiomolybdate formation in natural systems. It is highly probable that thiomolybdates also occur naturally in the deep euxinic layers of Lake Rogoznica. Thermodynamic calculations predicted that intermediate thiomolybdates are of minor importance in Lake Rogoznica.⁴ This might be true most of the year, when an equilibrium between sulfide and Mo has established. However, especially after vertical mixing in the autumn and a subsequent increase of sulfide concentrations in the deep layers of the lake, intermediate thiomolybdates are expected to form, based on our laboratory results with molybdate-sulfide mixtures.

Direct application of our IPC-ICP-MS method to natural sample analysis (without spiking) was possible in the second natural environment we studied, 47 geothermal springs at Yellowstone National Park with sulfide concentrations up to 0.18 mM, Mo concentrations up to 2.4 μM, and a lower salinity (maximum of ~1.2 g/L). The occurrence of thiomolybdates had previously been predicted based on thermodynamic modeling for geothermal waters in Iceland.²⁷ For geothermal springs at Yellowstone National Park, thioarsenates²³ and thioantimonates²⁸ have already been determined to occur, constituting up to 83% of the total As and 30%–40% of the total Sb. For Mo, we detected dithiomolybdate, trithiomolybdate, or tetrathiomolybdate in approximately half of the springs, constituting a maximum of 20%, 12%, and 38%, respectively, of the total Mo. Again, the sample matrix disturbed molybdate elution and affected the adjacent monothiomolybdate peak. This is assumed to be caused by, among other factors, the presence of sulfate and chloride, as was also seen in synthetic solutions (Figure 6). At the discharge, Ojo Caliente contains 0.2 mM sulfate and 8.7 mM chloride,²⁹ Bath Spring contains 0.3 mM sulfate and 8.4 mM chloride.³⁰ The disturbing matrix effect prevented us from closing the mass balance between the sum of Mo species and the total Mo. For 87 analyzed samples, the average species recovery was 98.8% ± 16.4%. Two exemplary chromatograms are shown in Figure 7b. In contrast to Sb and As, thiomolybdates never became the dominant Mo species, which was molybdate in all hot springs. Tetrathiomolybdate was, by far, the most dominant and sometimes only thiomolybdate species, as shown, e.g., for the Ojo Caliente hot spring (Figure 7b). Significant shares of intermediate thiomolybdates were found only for two out of 47 springs, one of them being Bath Spring shown in Figure 7b. The location and basic chemistry of these two sites has been described previously.²³ Interestingly, sulfide concentrations were lower at Ojo Caliente (30 μM) than at Bath Spring (128 μM), yet the thiolation was higher. Since, in both cases, sulfide was available in excess (75- and 240-fold for Ojo Caliente and Bath Spring, respectively), the difference in absolute sulfide concentrations did not seem to be the decisive factor. The lower pH at Ojo Caliente (pH 7.6) compared to Bath Spring (pH 9.0) may have facilitated complete thiolation. Another factor might be the presence or absence of equilibrium conditions or the competition between Mo and other metals or metalloids in the reaction with sulfide.

The results both of our spike test at Lake Rogoznica and the detection of thiomolybdate natural occurrence at Yellowstone National Park clearly show that an investment in further method optimization for species-selective quantification of low concentrations in natural matrices, especially saline waters such

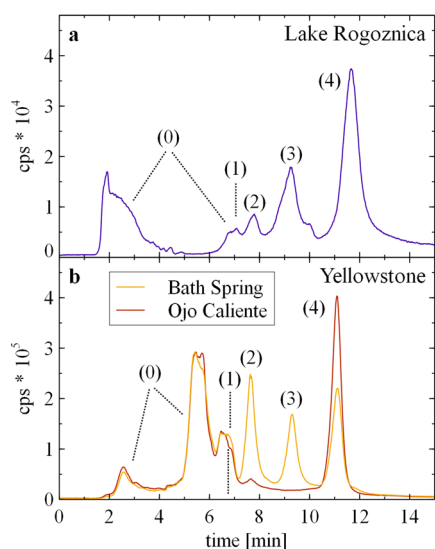


Figure 7. Molybdate (denoted as peak “(0)”) and thiomolybdates (denoted as peaks “(1)”–“(4)”) determined by IPC-ICP-MS (a) in Lake Rogoznica water at a depth of 12 m spiked with 250 nM molybdate and (b) in the hot springs of Yellowstone National Park. Thiomolybdate peaks are labeled based on their number of S atoms.

as Lake Rogoznica, will be rewarding, because thiomolybdates play an important role for Mo cycling in natural environments.

CONCLUSIONS

In the present study, we developed an analytical method for the element-specific determination of thiomolybdates in the nanomolar concentration range by IPC-ICP-MS using gradient elution with 10%–25% 2-propanol. This method is the basis for the analysis of thiomolybdates in the environment. Based on experiments in the laboratory, it can be predicted that, in natural systems with a high excess of sulfide to Mo and pH values in the neutral range, conditions for thiomolybdate formation are highly favorable. Samples for the analysis of thiomolybdates should not be acidified due to species transformation and loss of Mo by precipitation. Flash-freezing is the currently best available method for preserving thiomolybdates in solution.

We were able to provide the first evidence of thiomolybdate occurrence in nature, whereby dithiomolybdate, trithiomolybdate, and tetrathiomolybdate could be detected in considerable amounts concurrently in solution. Matrix components in natural samples were found to have a disturbing effect on analysis. Separating the matrix components without affecting the Mo speciation and lowering detection limits, e.g., by preconcentration will be important tasks for the future. However, our results show that the efforts will be necessary and rewarding, because thiomolybdates play an important role in the transformation of molybdate to Mo sulfide precipitates and Mo fixation in natural environments.

AUTHOR INFORMATION

Corresponding Author

*E-mail: b.planer-friedrich@uni-bayreuth.de.

Notes

The authors declare no competing financial interest.

ACKNOWLEDGMENTS

We acknowledge generous funding by the DAAD (Project ID No. 57051869 for Yellowstone and Project ID No. 56116854 for Croatia), as well as sampling permission at Yellowstone National Park (under Permit No. YELL-2014-SCI5372). We also thank Carolin Kerl, Maria Ullrich, and Julia Arndt for taking samples at Yellowstone National Park.

REFERENCES

- (1) Crusius, J.; Calvert, S.; Pedersen, T.; Sage, D. *Earth Planet. Sci. Lett.* **1996**, *145*, 65–78.
- (2) Wang, D. L.; Aller, R. C.; Sanudo-Wilhelmy, S. A. *Mar. Chem.* **2011**, *125*, 101–107.
- (3) Algeo, T. J.; Lyons, T. W. *Paleoceanography* **2006**, *21*, DOI: 10.1029/2004PA001112.
- (4) Helz, G. R.; Bura-Nakic, E.; Mikac, N.; Ciglenecki, I. *Chem. Geol.* **2011**, *284*, 323–332.
- (5) Dahl, T. W.; Chappaz, A.; Fitts, J. P.; Lyons, T. W. *Geochim. Cosmochim. Acta* **2013**, *103*, 213–231.
- (6) Chappaz, A.; Lyons, T. W.; Gregory, D. D.; Reinhard, C. T.; Gill, B. C.; Li, C.; Large, R. R. *Geochim. Cosmochim. Acta* **2014**, *126*, 112–122.
- (7) Erickson, B. E.; Helz, G. R. *Geochim. Cosmochim. Acta* **2000**, *64*, 1149–1158.
- (8) Pizarro, J.; Rubio, M. A.; Rios, E.; Vila, I. *Fresenius Environ. Bull.* **2014**, *23*, 159–168.
- (9) Müller, A.; Glemser, O.; Diemann, E.; Hofmeister, H. *Z. Anorg. Allg. Chem.* **1969**, *371*, 74–80.

(10) Clarke, N. J.; Laurie, S. H.; Blandamer, M. J.; Burgess, J.; Hakin, A. *Inorg. Chim. Acta* **1987**, *130*, 79–83.

(11) Reid, R. S.; Clark, R. J.; Quagrain, E. K. *Can. J. Chem.* **2007**, *85*, 1083–1089.

(12) Weiss, J.; Möckel, H. J.; Müller, A.; Diemann, E.; Walberg, H. J. *J. Chromatogr.* **1988**, *439*, 93–108.

(13) Quagrain, E. K.; Reid, R. S. *J. Inorg. Biochem.* **2001**, *85*, 53–60.

(14) Slamova, D. *Spectroscopic Studies of Copper-Thiomolybdate Interactions*. Ph.D. Dissertation, University of Saskatchewan, Saskatoon, Canada, 2009.

(15) Cline, J. D. *Limnol. Oceanogr.* **1969**, *14*, 454–458.

(16) Kamyshny, A.; Ekeltchik, I.; Gun, J.; Lev, O. *Anal. Chem.* **2006**, *78*, 2631–2639.

(17) Rizkov, D.; Lev, O.; Gun, J.; Anisimov, B.; Kuselman, I. *Accredit. Qual. Assur.* **2004**, *9*, 399–403.

(18) Wildervanck, J. C.; Jellinek, F. *Z. Anorg. Allg. Chem.* **1964**, *328*, 309–318.

(19) Weber, T.; Muijsers, J. C.; Niemantsverdriet, J. W. *J. Phys. Chem.* **1995**, *99*, 9194–9200.

(20) Harmer, M. A.; Sykes, A. G. *Inorg. Chem.* **1980**, *19*, 2881–2885.

(21) Quagrain, E. K.; Georgakaki, I.; Coucouvanis, D. *J. Inorg. Biochem.* **2009**, *103*, 143–155.

(22) Planer-Friedrich, B.; Suess, E.; Scheinost, A. C.; Wallschläger, D. *Anal. Chem.* **2010**, *82*, 10228–10235.

(23) Planer-Friedrich, B.; London, J.; McCleskey, R. B.; Nordstrom, D. K.; Wallschläger, D. *Environ. Sci. Technol.* **2007**, *41*, S245–S251.

(24) Wallschläger, D.; London, J. *J. Anal. At. Spectrom.* **2004**, *19*, 1119–1127.

(25) Kamyshny, A.; Zerkle, A. L.; Mansaray, Z. F.; Ciglenecki, I.; Bura-Nakic, E.; Farquhar, J.; Ferdelman, T. G. *Mar. Chem.* **2011**, *127*, 144–154.

(26) Furic, K.; Ciglenecki, I.; Cosovic, B. *J. Mol. Struct.* **2000**, *550*, 225–234.

(27) Kaasalainen, H.; Stefansson, A. *Chem. Geol.* **2012**, *330*, 60–85.

(28) Planer-Friedrich, B.; Scheinost, A. C. *Environ. Sci. Technol.* **2011**, *45*, 6855–6863.

(29) Ball, J. W.; McCleskey, R. B.; Nordstrom, D. K. *Water-Chemistry Data for Selected Springs, Geysers, and Streams in Yellowstone National Park, Wyoming, 2006–2008*; Open-File Report No. 2010-1192; U.S. Geological Survey: Reston, VA, 2010.

(30) McCleskey, R. B.; Ball, J. W.; Nordstrom, D. K.; Holloway, J. M.; Taylor, H. E. *Water-Chemistry Data for Selected Hot Springs, Geysers, and Streams in Yellowstone National Park, Wyoming, 2001–2002*; Open-File Report No. 2004-1316; U.S. Geological Survey: Boulder, CO, 2004.

(EIDESSTATTLICHE) VERSICHERUNGEN UND ERKLÄRUNGEN

(§ 8 S. 2 Nr. 6 PromO)

Hiermit erkläre ich mich damit einverstanden, dass die elektronische Fassung meiner Dissertation unter Wahrung meiner Urheberrechte und des Datenschutzes einer gesonderten Überprüfung hinsichtlich der eigenständigen Anfertigung der Dissertation unterzogen werden kann.

(§ 8 S. 2 Nr. 8 PromO)

Hiermit erkläre ich eidesstattlich, dass ich die Dissertation selbständig verfasst und keine anderen als die von mir angegebenen Quellen und Hilfsmittel benutzt habe.

(§ 8 S. 2 Nr. 9 PromO)

Ich habe die Dissertation nicht bereits zur Erlangung eines akademischen Grades anderweitig eingereicht und habe auch nicht bereits diese oder eine gleichartige Doktorprüfung endgültig nicht bestanden.

(§ 8 S. 2 Nr. 10 PromO)

Hiermit erkläre ich, dass ich keine Hilfe von gewerblichen Promotionsberatern bzw. -vermittlern in Anspruch genommen habe und auch künftig nicht nehmen werde.

Bayreuth, den 26.05.2015

Regina Lohmayer